Removal of Metal Ions from Wastewater using Adsorption: Experimental and Theoretical Studies

THESIS

Submitted in partial fulfillment
of the requirements for the degree of
DOCTOR OF PHILOSOPHY

by

UTKARSH MAHESHWARI

Under the Supervision of
Prof. Suresh Gupta

BITS Pilani
Pilani | Dubai | Goa | Hyderabad

BIRLA INSTITUTE OF TECHNOLOGY AND SCIENCE, PILANI
2015

Removal of Metal Ions from Wastewater using Adsorption: Experimental and Theoretical Studies

THESIS

Submitted in partial fulfillment
of the requirements for the degree of
DOCTOR OF PHILOSOPHY

by

UTKARSH MAHESHWARI

(2009PHXF441P)

Under the Supervision of
Prof. Suresh Gupta

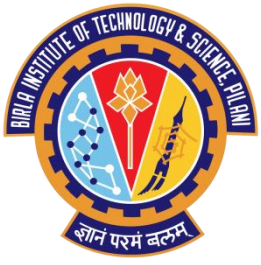

BITS Pilani
Pilani | Dubai | Goa | Hyderabad

BIRLA INSTITUTE OF TECHNOLOGY AND SCIENCE, PILANI
2015

Birla Institute of Technology & Science, Pilani
Pilani Campus
Dr. Suresh Gupta, Ph.D.,
Associate Professor & Head, Department of Chemical Engineering

CERTIFICATE

This is to certify that the thesis entitled "**Removal of Metal Ions from Wastewater using Adsorption: Experimental and Theoretical Studies**" submitted by **Utkarsh Maheshwari**, ID No. **2009PHXF441P** for the award of Ph.D. degree of the institute embodies the original work done by him under my supervision.

Signature in full of the supervisor _____

Name in capital block letters **Prof. SURESH GUPTA**

Date: 19.09.2015

Birla Institute of Technology & Science, Pilani
Pilani Campus, Vidya Vihar
Pilani 333031, Rajasthan, India

Tel: +91 1596 515224
Fax: +91 1596 244183
Email: sureshg@pilani.bits-pilani.ac.in;
Web: sureshg25@gmail.com
www.pilani.bits-pilani.ac.in

Dedicated to

My Parents

&

My Wife

ACKNOWLEDGMENTS

Henry Ford has rightly said, 'Failure is the opportunity to begin again more intelligently'. These words have kept me going and urged me to outdo myself whenever failures hauled me down. This research work has been a learning journey throughout with its occasional ups and downs, and would have been incomplete without people who have helped me make my way through. All contributions little or large have added immense value and shall be always appreciated.

At the onset, this work would have been impossible without my guide, **Prof. Suresh Gupta**, Associate Professor and Head, Department of Chemical Engineering, BITS, Pilani, Pilani Campus who provided me comprehensive direction, motivation and the much needed enthusiasm to complete my doctoral research work. I shall be indebted to him for his relentless efforts and encouragement that helped me work in spite of difficulties and challenges.

I wish to thank the members of the Doctoral Advisory Committee, Dr. Pradipta Chattopadhyay and Dr. Raman Sharma, Assistant Professors, Department of Chemical Engineering, BITS, Pilani, Pilani Campus for their valuable suggestions and constructive criticisms throughout. Their experience enriched my work and paved the way for further improvement. Also, I would express my gratitude to Dr. Hare Krishna Mohanta, Convener, Departmental Research Committee for his continued support and always lending a patient ear.

Special thanks to Prof. B.N.Jain, Vice Chancellor, BITS Pilani; for giving me the opportunity to be associated with a venerated and acclaimed Institute like BITS Pilani. I would also like to thank Prof. A.K. Sarkar, Director, Pilani Campus; Prof. G.Raghurama, Ex-Director, Pilani Campus; Prof. Sasikumar Punnekkat, Director, K.K.Birla Goa Campus; Prof. V.S.Rao, Director Hyderabad Campus; Prof. R.N.Saha, Director, Dubai Campus; and Prof. G.Sundar, Director, Off Campus & Industry Engagement for providing me the essential facility and infrastructure required. Also, thanks to Prof. S.K.Verma, Dean; and Prof. Hemant R.Jadhav, Associate Dean, Academic Research Division for providing the judicious information. My extended thanks to Prof. Anshuman Dalvi for agreeing to let me use the XRD facility of the Institute.

I would also like to thank Prof. Arvind Kr. Sharma, Dr. Pratik N. Sheth, Dr. Smita Raghuvanshi, Dr. Banasri Roy, Dr. Sonal Mazumder, Ms. Priya Sande, Mr. Amit Jain and Mr. Ajaya Kr. Pani, my fellow colleagues at Department of Chemical

Engineering, BITS, Pilani, Pilani Campus, for being supportive throughout. In particular, I would thank Mr. Subhajit Majumder for being a colleague, a friend and a helping hand always.

Besides the faculty members, I would like to thank the non-teaching staff at the Department, Mr. Babulal Saini, Mr. Jangvir Sheron and Mr. Jeevan Verma who went out of their way to help and channelize my work. I would like to specially mention Mr. Ashok Kr. Saini and Mr. Subodh Kr. Azad, who have extended their help in the experimental part of my research work. I would also thank all the research scholars in the Department for their support. Special thanks to my students at BITS Pilani, Pilani campus; Mr. Bhuvanesh Mathesan, Mr. Rajesh Silwant, Mr. Kuldeep Kuhar, Mr. Piyush Kumar and Mr. Arun (B.H.U.) who assisted in piloting some of the experiments.

A special thank-you to my friends and former colleagues, Dr. Nikhil Prakash, Dr. Sushil Kumar, Dr. Dipaloy Datta, Dr. Dipesh Patle, Dr. Ganesh Soni, Dr. Mohammad Sharique Khan, Mr. Karan Gupta, Mr. Abhishek Gupta, Mr. Pritesh Bansod and Dr. Pragati Yadav who stood by me and facilitated me by their opportune suggestions, counsels and vital research material.

Family is forever and thanks shall be too small a word to express my appreciation towards my parents, Dr. Shakuntala Maheshwari and Dr. Chandra Mohan Maheshwari for being such wonderful parents and providing unceasing love. My accomplishment would have been challenging without the encouragement of my in-laws Mrs. Chandrakala Bangad and Mr. Rameshwar Bangad; my sister Mrs. Dipti Maheshwari and my brother-in-law Mr. Nitin Maheshwari. Special thanks to Ar. Mahesh and Ashish who were there for me always!

Behind every successful man is a woman they say. I agree as my journey too would have been incomplete without my wife Snehal who has been my moral backing and an inspiration throughout. She always had an instinctive belief and worked in unison with me to make it all so achievable.

Utkarsh Maheshwari

2009PHXF441P

ABSTRACT

The present research work deals with the treatment of the synthetic wastewater samples containing various metal ions such as Cd(II), Cr(VI), Cu(II), Ni(II), Pb(II) and Zn(II) by adsorption. An easily available raw material, neem bark is used to develop six low cost adsorbent, activated neem barks (ANB1 to ANB6) for the adsorption of heavy metals at different activation conditions. The developed ANBs are characterized by FTIR to find the suitable functional groups available on the surface of adsorbents. The performance of the developed ANBs are tested for the adsorption of Cr(VI), Cu(II) and Zn(II) from aqueous solutions by performing equilibrium experiments. The ANB which is having relevant functional groups and demonstrated the maximum total adsorption capacity for Cr(VI), Cu(II) and Zn(II) adsorption is further tested for the removal of Cd(II), Ni(II) and Pb(II). The selected ANB is further characterized by SEM, EDS, BET Surface area, XRD and TGA techniques. The SEM images confirm the availability of nano pores on the surface of the ANB by which it is further named as nANB.

The batch experiments are conducted to study the effect of various parameters such as initial metal concentration, contact time, adsorbent dosage, pH, temperature and interference of other ions on the performance of nANB for metal adsorption. The equilibrium data obtained for the removal of Cd(II), Cr(VI), Cu(II), Ni(II), Pb(II) and Zn(II) are tested with the Langmuir isotherm model. The maximum adsorption capacity (q_m) of individual metal ions is obtained as 20.83, 26.95, 21.23, 29.41, 26.32 and 11.90 mg g^{-1} for the removal of Cd(II), Cr(VI), Cu(II), Ni(II), Pb(II) and Zn(II) respectively. The equilibrium data for Cr(VI), Cu(II) and Zn(II) adsorption are also fillted with Freundlich and Tempkin isotherm models. The removal of metal ions using nANB is better fitted using the Langmuir isotherm model and supports the monolayer adsorption of metals on the nANB surface. The experimental kinetic data are fitted with the pseudo-first order, second order and Elovich model. The removal kinetics of Cr(VI), Cu(II) and Zn(II) is well explained by the second order kinetic model. Weber & Moris and Boyd model are applied to propose the controlling mass transfer mechanism for the Cr(VI), Cu(II) and Zn(II) adsorption from aqueous phase to the nANB surface.

The interference of other ions on the adsorption of individual metal ions is studied. The total adsorption capacity of developed nANB for the simultaneous adsorption of Cr(VI), Cu(II) and Zn(II) is obtained as 38.95 mg g^{-1} which is much higher than the one evaluated for the adsorption of any individual metal ions. In the batch studies, the actual plating industry wastewater is also treated for the removal Cr(VI) using nANB. The saturated adsorbents are regenerated by thermal and chemical treatment methods. The mechanism of Cr(VI), Cu(II) and Zn(II) adsorption is proposed with the help of obtained experimental results, FTIR analysis and available reported studies. The obtained adsorption capacities of individual metal ions are also compared with the adsorption capacities of other low cost adsorbents available in the literature.

A generalized mathematical equation is developed using batch experimental data to correlate the adsorption capacity with the independent parameters. The developed equation is utilized to get the optimum parameter values using Differential Evolution (DE) as optimization technique. The cost analysis of the developed nANB is also done to check the economic viability of the adsorption process.

The continuous experiments are performed in fixed-bed adsorption column for the removal of Cr(VI), Cu(II) and Zn(II) from aqueous solutions. The effect of initial concentration, inlet flowrate, adsorbent dosage and the interference of other meal ions are studied on the continuous adsorption of metal ions using nANB. The developed adsorbent is also used to treat the synthetically developed pulp and paper industry effluent containing Cd(II), Cr(VI), Cu(II), Ni(II), Pb(II) and Zn(II). The various adsorption parameters are estimated to analyze the performance of fixed-bed adsorption process. The Yan and Yoon-Nelson models are used to fit the fixed-bed adsorption experimental data.

Keywords: *Heavy metal removal; Hexavalent chromium; Divalent Copper; Divalent Zinc; Low-cost adsorbent; Activated neem bark; Adsorption isotherms; Adsorption kinetics; Regeneration; Modeling; Optimization; Differential Evolution; Industrial effluent; Pulp and paper industry; Breakthrough curves; Intra-particle diffusion; Film diffusion; Mass transfer mechanism.*

TABLE OF CONTENTS

Contents **Page No.**

Contents **Page No.**

LIST OF TABLES

LIST OF FIGURES

LIST OF PLATES

NOMENCLATURE

Symbol	Details
A_c	The area underneath the curve is acquired by plotting a graph of the (C_{ad}, mg L^{-1}) with respect to the time (t, min).
a_i	Yan model parameters
A_T	Equilibrium binding constant (L min^{-1}) corresponding to the maximum binding energy
b	Langmuir constant (mg^{-1})
B	Boyd model constant
B_T	Tempkin isotherm constant (=RT/b_T)
b_T	Constant related to heat of adsorption
Cad	Adsorbed concentration (mg L^{-1})
C_0	Initial metal ion concentration in liquid phase (mg mL^{-1})
C_e	Final metal ion concentration in liquid phase at equilibrium (mg mL^{-1})
d_p	Average particle size
F	Fraction of solute adsorbed at time t
h	Initial sorption rate as t→0
k_1	Pseudo-first order kinetic constant
k_2	Second-order rate constant (g mg^{-1} min^{-1})
k_{ad}	Rate constant of the pseudo first-order adsorption process (min^{-1})
k_F	Freundlich constant
K_{id}	Intra particle diffusion rate constant (mg g^{-1} $min^{-1/2}$)
$K_{YN,i}$	Yoon-Nelson rate constant of ith component (h^{-1})
m_t	Total metal ion passed through the column
n_F	Heterogeneity factor
Q	The flow rate during the process (mL min^{-1})
q	Amount of Cr(VI) adsorbed by the adsorbent (mg g^{-1})
q_{calc}	Adsorption capacity obtained by varying individual parameters in DE
q_e	Solid phase concentration of metal ion on the adsorbent (mg g^{-1})
q_{exp}	Experimental adsorption capacity (mg g^{-1})

Symbol	Details
q_m	Maximum amount of metal adsorbed on the adsorbent surface (mg g^{-1})
$q_{0,i}$	Yan model parameter
q_{pre}	Predicted adsorption capacity (mg g^{-1})
q_t	Solid phase concentration in time, t , by the adsorbent (mg g^{-1})
R^2	Regression correlation coefficient
R_a	Adsorbent exhaustion rate
R_L	dimensionless equilibrium parameter
S	Total percentage removal
t	Contact time (h)
t_b	Breakthrough time (h)
t_f	Total time of the process (h)
t_t	Time equivalent to the total stoichiometric capacity of the fixed bed column (h)
V	Initial volume of metal solution (L)
W	Weight of the adsorbent (g)
y	Fraction of the unused bed length

Greek Symbols

α	Initial adsorption rate related to the extent of the surface coverage and activation energy for chemisorption (mg g^{-1} min^{-1})
β	Desorption constant related to the extent of the surface coverage and activation energy for chemisorption (g mg^{-1})
τi	Time required for 50% of i^{th} adsorbate breakthrough (h)

Subscripts

e	Equilibrium conditions
0	Initial conditions
t	Evaluated at time t

Symbol Details

Abbreviations

ANB	Activated Neem Bark
BCM	Billion Cubic Meters
BDST	Bed Depth Service Time
BET	Brunauer-Emmet-Teller
Ca(II)	Divalent Calcium ion
Cd(II)	Divalent Cadmium ion
Co(II)	Cobalt Divalent ion
CPCB	Central Pollution Control Board
Cr	Chromium
Cr(III)	Trivalent chromium ion
Cr(VI)	Hexavalent chromium ion
Cu(II)	Divalent copper ion
CWC	Central Water Commission
EBRT	Empty Bed Residence Time
EBCT	Empty Bed Contact Time
EDS	Energy Dispersive Spectroscopy
Fe(III)	Trivalent iron ion
FEG-SEM	Field Emission Gun-Scanning Electron Microscope
FTIR	Fourier Transform Infra-Red
HCl	Hydrochloric Acid
Hg(II)	Divalent Mercury Ion
HSDM	Homogeneous Surface Diffusion Model
ICMR	Indian Council of Medical Research
IDFC	IDFC – Infrastructure Finance Company
ISI	Indian Statistical Institute
K	Potassium
Mn(II)	Magnesium Divalent ion
nANB	Nano-porous Activated Neem Bark
NaOH	Sodium hydroxide

Symbol	Details
Ni(II)	Divalent Nickel Ion
Pb(II)	Divalent Lead Ion
SEM	Scanning Electron Microscope
TGA	Thermo-Gravimetric Analysis
USEPA	United Stated Environment Protection Agency
USIF	University Sophisticated Instruments Facility
WHO	World Health Organization
XPS	X-ray photoelectron spectroscope analysis
XRD	X-Ray Diffraction
Zn(II)	Divalent zinc ion

CHAPTER 1
INTRODUCTION

1.1 Water Crisis

Water is a primary natural resource. This is required for a number of purposes ranging from drinking, irrigation, industrial, construction, etc. (Perlman, 2014). In the present scenario, it is very hard to meet the growing demand with short supply and diverse claims on the water resources (Gupta, 2008a). According to 2012-13 annual report of Central Water Commission (CWC), India is having 24 river basins which along with ground water contribute to 1869 Billion Cubic Meters (BCM) of total water. Out of this amount, only 1121 BCM (690 BCM of surface water and 431 BCM of groundwater) is available for usage (Pandaya, 2013). According to the data published by CWC, the requirement of water for several applications such as industrial, domestic, irrigation, etc. will increase from 813 BCM in 2010 to 1093 BCM in 2025 (Jha, 2010). This growth in the demand of water will lead to the shortage of fresh water for drinking and industrial uses. According to India Infrastructure Report 2011 by IDFC, the requirement of the water for the industrial purpose was 41.4 BCM in 2010 which is estimated to increase up to 80 BCM by 2025 (Aggarwal and Kumar, 2011). This increased demand of fresh water for the industry as well as domestic purpose is not only limited to India, but also the similar situations are arising around the globe.

In the developing nations, particularly in India, the monitoring of the pollution is concentration based, which allows the industries to meet the pollutant discharge limit in the effluent by diluting it with the addition of fresh water. The industries prefer to

go for the dilution of the effluent streams to meet the standards in place of the treatment as the cost of water is quite low in India. This exercise leads to the utilization of more amount of fresh water and is leading to the discharge of higher quantity of pollutants to the water bodies. This is contributing to a more severe water pollution situation in India (Gupta, 2008b).

In the present scenario, the regulatory agencies are very much concerned about water pollution and its abatement techniques for controlling the water pollution. The most encouraging and well accepted method to achieve the discharge limits of various pollutants is to utilize cost effective effluent treatment technique. The proper treatment of effluent will lead to the large quantity of reusable water. This water may be reused by the industry itself or for the other utility purposes, such as cooling, steam generation, and so on. This will significantly reduce the use of fresh water and also help in reduction of the cost of fresh water utilized by the industries. The major pollutants present in the various industrial effluents ranges from metal pollutants, sludge, suspended solids, sulphates, halides, etc. Out of these pollutants, heavy metals are considered as most harmful and toxic for the living organisms.

1.2 Heavy Metal Ions in Wastewater

With an increase in the industrialization and urbanization, there is a tremendous rise in the usage of several heavy metals in the industrial operations. The various industries which are dealing with the heavy metals range from textile, pulp & paper, leather tanning, welding, chromate production, electroplating, pigments, fertilizers, metallurgical, metal cleaning, washing of brass units, mining drainage, etc. The range of these metals varies from Arsenic (As), Calcium (Ca), Cadmium (Cd), Chromium (Cr), Copper (Cu), Cobalt (Co), Lead (Pb), Iron (Fe), Manganese (Mn), Magnesium

(Mg), Mercury (Hg), Nickel (Ni), Molybdenum (Mo), Selenium (Se),Potassium (K), Tungsten (W), Vanadium (V) to Zinc (Zn). Many, among these metals such as Cr, Cu, Ni, Pb, Zn, etc. are being characterized as the priority pollutants from the various health organizations (Metcalf and Eddy, 2005). However, most of these metals such as Ca, Co, Cr, Cu, Fe, K, Pb, Mg, Mn, Mo, Ni, Se, Na, W, V and Zn are essential for the growth of the biological organisms on a macro or micro scale (Metcalf and Eddy, 2005). The trace amount of metals like Cu, Se and Zn is crucial to support the metabolism of the human beings. Although the metals are required in the micro/macro level. The excess of these metals can negatively affect the biological organisms by interfering with some of the body processes due to their toxic nature. The permissible range of various heavy metals in the water is given in Table 1.1.

The effluents coming out from the pulp & paper, tanning and textile industries are the principal source of heavy metal pollutions as they consist Cr, Cu, Zn, Ni, Pb, etc. in a significant amount. Disposing of these effluent streams to the outer water bodies like lakes, rivers, ponds, oceans, etc., lead to the significant increase of metal contamination in water. Sometimes, the metal content in discharge streams is very high which does not dissolve and settles down either on the surface or the bottom of the water bodies. This contributes to the significant water contamination and deterioration in the water quality.

The heavy metals are particularly non-degradable, highly toxic and having carcinogenic effects due to which it adversely affects the biological ecosystem. Out of all the available metals in the industrial effluents, Cr, Cu and Zn are primarily present among most of the metal industries. These metals have significant presence in the effluent streams of textile, tanning and pulp & paper industries. The properties, sources and harmful effects of Cr, Cu and Zn metals are illustrated in Table 1.2.

1.3 Treatment Methods

The effluents from the industries must be treated well before discharging the effluents to the outer water bodies. Identification of a proper method for the multiple metal ions removal is a matter of research today. There are several methods available for the metal ions removal and are tabulated in Table 1.3.

Most of these methods are having various drawbacks. The cost of the resin utilized in the ion-exchange process makes the process expensive (Dąbrowski et al., 2004; Mahmoud et al., 2015). Similarly the membranes used in the membrane separation, ultra-filtration, reverse osmosis process are very costly and are also found ineffective for the heavy metal removal at high concentrations (Ujang and Anderson, 1996; Cooper et al., 2004; Qiu and Mao, 2013). On the other hand, the methods like chemical precipitation and flotation are helpful in removal of high concentrations of heavy metals, however, they have associated problems like the disposal of the formed sludge and leads to a long term environmental problem (Meunier et al., 2006; Mahmoud et al., 2015). Other methods such as chemical coagulation, electro-coagulation and solvent extraction are not capable of complete removal of heavy metals from effluent streams and also require large amounts of reagents which make these processes cost intensive. The toxic sludge generated during the processes also lead to the negative impact on the environment (Aksu and Gönen, 2004; Aliabadi et al., 2006; Gupta, 2008b). Among all the above mentioned treatment methods, adsorption is a promising method for the removal of heavy metals in a simple, efficient and economical manner. This is a very effective method for the removal of heavy metals from the industrial effluents (Bailey et al., 1999; Babel and Kurniawan, 2003; Demirbas, 2008; Gupta, 2008b; Wan Ngah and Hanafiah, 2008; Ahmaruzzaman, 2011). Adsorption is a useful method for the removal of low and

high concentration heavy metals from industrial effluents. This method may be more economical, if low-cost adsorbents are utilized for the adsorption of heavy metals from the effluent streams.

1.4 Adsorption

Adsorption is one of the primary mass transfer operations which utilize the surface of the solid material to segregate out the liquid or gaseous molecules. One of the very important applications of the process is the removal of a variety of organic and inorganic chemicals from the industrial effluents. Suitable adsorbents are utilized for the removal of specific liquid and gaseous chemicals (Wan Ngah and Hanafiah, 2008; Wasewar, 2010; Xu et al., 2012). The properties of the material and their affinities towards pollutants are the determining factor for their usage as a suitable adsorbent. All the solid materials are having an adsorption affinity for one or other compound irrespective of their structure. The adsorption process is a surface phenomenon therefore the capacity of the adsorbent to adsorb the adsorbate depends on the surface area available for the process. The porous materials are certainly having a higher surface area leading to a higher adsorption capacity in comparison to a non-porous material. Hence, the selection of a suitable adsorbent is a primary task to be performed before using the adsorbent for the treatment of multiple metal ions from the industrial effluents (Cooney, 1999). There are a number of commercial adsorbents such as activated carbon, activated charcoal, activated alumina, etc. are available in the market for the adsorption of the pollutants. The higher costs of the commercial adsorbents lead to the further increase in the cost of the removal process. Hence, there is a dire need for a low-cost processing technique and material (low-cost adsorbent) which can be utilized for the simultaneous removal of multiple metal ions from the industrial effluents (Babu and Gupta, 2008a; 2008b; Gupta, 2008a; 2008b).

In the recent past, a number of researchers have reported the use of different solid materials as the adsorbent for the removal of heavy metals and other impurities (Table 1.4).

However, many of these adsorbents are having very low metal adsorption capacity and are also limited to the adsorption of single metal ions. The effluents from the industries are containing multiple metal ions. Very few adsorbents are reported in the literature for the adsorption of multiple metal ions (Moreno-Piraján et al., 2011; Sheela et al., 2012; Patel et al., 2013; Awual et al., 2014). These adsorbents are not showing the good adsorption capability when multiple metal ions are considered for adsorption. Therefore, there is a need to identify a low-cost material which can be utilized effectively for the adsorption of multiple metal ions from effluent streams.

Table 1.1: Permissible limits of heavy metals in waste water (WHO, 2008; USEPA, 2009; Kumar and Puri, 2012).

Metals	**Permissible Limit (mg L^{-1})**				
	USEPA	**WHO**	**ISI**	**ICMR**	**CPCB**
Arsenic	No Relaxation	0.05	0.05	0.05	No Relaxation
Cadmium	0.005	0.005	0.01	0.01	No Relaxation
Calcium	-	75	75	200	200
Chromium (Total)	0.1	-	0.05	-	No Relaxation
Copper	1.0	1.0	0.05	1.5	1.5
Iron	-	0.1	0.3	1.0	1.0
Lead	No Relaxation	0.05	0.1	0.05	No Relaxation
Magnesium	-	50	30	-	100
Mercury	0.002	0.001	0.001	0.001	No Relaxation
Nickel	0.1	-	-	-	-
Selenium	0.05	0.01	-	-	No Relaxation
Zinc	5.0	5.0	5.0	0.1	15.0

Table 1.2: Sources, properties and harmful effects of Cr, Cu and Zn.

Metal	State	Effect	Sources (Natural/Industrial)	Harmful Effects	References
Cr	III	Neutral	Fresh vegetables, fruits, meat, grains and yeast and is frequently added to vitamins as a dietary supplement	No effect	Tan et al. (1993); Namasivayam and Yamuna (1995); Labor (2006); Garg et al. (2007); Malkoc and Nuhoglu (2007); Mor et al. (2007); Suksabye et al. (2007); Babu and Gupta (2008); Namasivayam and Sureshkumar (2008); Orozco et al. (2008); Gupta and Babu (2009); Labor (2014)
	VI	Harmful	Rocks, as well as in various industrial processes such as welding, chromate production, electroplating, pigments, leather tanning, textile, pulp & paper, fertilizers, metallurgical, etc.	Non-biodegradable and having toxic, mutagenic and carcinogenic effect on the living organisms	
Cu	I	Neutral	Unstable in nature and react to form the stable Cu(II)	No effect	Kazemipour et al. (2008); Nadaroglu et al. (2010); SenthilKumar et al. (2011);

Metal	State	Effect	Sources (Natural/Industrial)	Harmful Effects	References
Cu	II	Harmful	Electroplating, metal cleaning, textile, pulp & paper, washing of brass units, boiler pipes and cooking utensils, fertilizer production, etc.	Carcinogenic and mutagenic properties, due to which one of the health problems associated with copper is lung cancer, which is common for the workers who are exposed to the copper containing spray	Shah et al. (2013); Rafiq et al. (2014); Kyzas et al. (2015)
Zn	II	Harmful	Galvanizing, pigments, mining drainage, textile, pulp & paper, etc.	Digestive problem, fever, cough, stomach upset, Lowered immune function, Reduced sense of taste or smell, etc.	Kazemipour et al. (2008); Plum et al. (2010); Senthil Kumar et al. (2010); Das et al. (2012); Lim et al. (2012); Pehlivan et al. (2012); Lassonde (2013)

Table 1.3: Abatement techniques for metal removal from wastewater.

S.No.	Techniques	References
1	Ion exchange	Juang et al. (2003); Dąbrowski et al. (2004)
2	Flotation	Polat and Erdogan (2007); Mahmoud et al. (2015)
3	Chemical precipitation	Charerntanyarak (1999); Meunier et al. (2006)
4	Membrane separation	Cooper et al. (2004); Walkowiak and Kozlowski (2009)
5	Chemical coagulation	Charerntanyarak (1999)
6	Ultra filtration	Camarillo et al. (2012); Qiu and Mao (2013)
7	Electro-coagulation	Meunier et al. (2006); Akbal and Camcı (2011)
8	Solvent extraction	Demopoulos and Gefvert (1984); Li et al. (2008a)
9	Reverse osmosis	Ujang and Anderson (1996); Sheikholeslami and Bright (2002)
10	Adsorption	Babu and Gupta (2008a); Gupta and Babu(2009a)

Table 1.4: List of various low-cost adsorbents utilized for metal removal.

S.No.	Adsorbent	Reference
1	Rice husk	Ajmal et al. (2003)
2	Sea nodule residue	Agrawal et al. (2004)
3	Immobilized activated sludge	Aksu and Gönen (2006)
4	Coconut shell	Alaerts et al. (1989)
5	Spent animal bones	Al-Asheh et al. (1999)
6	Lignocellulosic solid wastes	Aliabadi et al. (2006)
7	Shale oil ash	Al-Qodah (2000)
8	Walnut Shells	Altun and Pehlivan (2007)
9	Hazelnut Shells	
10	Almond Shells	
11	Prawn shell	Arulkumar et al. (2012)
12	Chitosan–clay	Auta and Hameed (2014)
13	Activated Neem Leaves	Babu and Gupta (2008b)
14	Activated Tamarind Seeds	Babu and Gupta (2008a)
15	Activated weed	Baral et al. (2009)
16	Sunflower leaves	Benaïssa and Elouchdi (2007)
17	Tunisian date stones	Bouhamed et al. (2012)
18	Wheat bran	Bulut and Baysal (2006)
19	Fly ash	Gupta and Babu (2010a)
20	De-oiled Allspice husk	Cruz-Olivares et al. (2010)
21	Soya cake	Daneshvar et al. (2002)
22	Pomegranate peel	El-Ashtoukhy et al. (2008)
23	Coir pith	Ewecharoen et al. (2008)
24	Rice husk	Kausar et al. (2013)

1.5 Motivation to Present Study

Adsorption of metal ions depends on the porosity, surface area and the nature of the surface available for the adsorption. A higher adsorption capacity of the adsorbent can be achieved by undergoing proper physical and chemical activation procedures. The chemical activation of the adsorbent enhances the surface property such as the positive charge on the surface which enhances the affinity for the metals to be adsorbed on the surface.

In the present scenario, nanotechnology has shown a great potential for the effluent treatment. Immense work has been conducted on the nano-structured materials due to their unusual physical and chemical properties. Nano-porous materials can meet the requirements for a good adsorbent due to the availability of large surface area for adsorption. A number of researchers are working on the production of nano-structured pure metal oxides and activated carbons for the removal of heavy metals from wastewater which are expensive (Deliyanni et al., 2007; Li et al., 2010; Rajiv Gandhi et al., 2011; Gong et al., 2012; Xu et al., 2012). Hence, there is a need to develop a nano-porous low-cost adsorbent from abundantly available raw material for the removal of various heavy metals from wastewater.

The adsorption of the metal ions depends on the various parameters such as initial concentration, pH of the solution, adsorbent dosage, temperature, contact time, particle size, etc. The efficiency of the adsorption process is also affected by the interference of other metal ions available during the adsorption process. The performance of the adsorbent is characterized using the adsorption capacity, which is estimated using the batch adsorption experiments. The effect of other parameters is also evaluated in the

batch experiments. The batch experiments will be further used to evaluate the design parameters such as adsorption rate constant, equilibrium constants, mass transfer coefficients, etc.

The applicability of the developed adsorbent is very much required for the industrial use. The batch experiments are ineffective and cost intensive process when the commercial scale operations are concerned. Hence, to treat a large amount of wastewater on a commercial scale, there is a need to carry out a cost effective adsorption operation in continuous mode. The fixed-bed adsorption process can be an efficient way of conducting the adsorption process for the wastewater treatment at the industrial scale (Liao and Shiau, 2000). Thus, a fixed-bed adsorption column for the removal of metal ions is required to be designed using the design parameters obtained from the batch experimental data. The design of the column depends on various factors such as flow rate, initial concentration, bed height, etc. The treated effluent from the adsorption column must be containing the metals in the allowable limits. The adsorption column is stopped when the treated effluent approaches the allowable limit. The design of the fixed-bed column is more complex when it is utilized to treat the effluent from industries containing multiple metal ions. Hence, there is a need to evaluate the performance of the developed adsorbent for the simultaneous removal of multiple metal ions in the continuous fixed-bed column.

The completion of the adsorption process leads to the metal loaded saturated adsorbent. This saturated adsorbent is considered to be toxic and hazardous when released into the environment. Hence, the prior treatment of saturated adsorbent is necessary to recover the adsorbed metal ions before it discharge into the environment. The environmental

constraints further emphasize the need to develop a suitable method for regeneration of the saturated adsorbent.

A thorough understanding of the adsorption phenomena and its mechanism is important. The break point time, the amount of solute treated, saturation loading, etc. are some of the parameters which need to be evaluated before the process scale-up. The effective utilization of the column can be very well explained by the modeling of the fixed-bed adsorption column. These models can be further utilized for the process scale-up.

The common trend followed by most of the researchers is that the effect of a parameter is examined by varying that parameter while keeping the other parameters constant. In the present scenario, there is a desperate need to optimize the process. The objective of the optimization can vary from the minimization of the cost and energy consumption to maximize the performance, profit or efficiency. Nowadays, optimization of the process becomes significantly vital due to the limitations on the time and resources. In a number of cases, even one has to gratify with the suboptimal or yet viable solutions which are safe enough and realistically attainable in a reasonable time scale. There are few studies, have been reported for estimating the maximum removal efficiency as a function of all the dependent parameters (Ahmadi et al.; Vázquez et al., 2009; Saadat and Karimi-Jashni, 2011; Maher et al., 2014; Vukčević et al., 2014). There is a need to propose a generalized mathematical equation which can be utilized to provide an optimal set of parameter values resulting in the maximum removal efficiency or adsorption capacity.

Modeling of the adsorption process will help the researchers to know well in advance the behavior of the adsorbent for the specific parameters. This also indicates the importance

of the process modeling which will later help in the process development, scaling up and optimization of the process parameters.

In summarizing the chapter, there is a need for the development of a low-cost nano-porous adsorbent which can be utilized for the removal of multiple metal ions from the industrial effluent. Extensive batch and continuous experimental studies are required to be performed to evaluate the performance of the developed adsorbent. The used adsorbent is required to be regenerated using proper technique to maximize the utilization of the developed adsorbent. The obtained experimental data are required to be modeled to get the optimum parametric values. Batch experiments are ineffective for the industrial effluent treatment. So, there is a need to check the applicability of the developed nano-porous adsorbent for the continuous removal of multiple metal ions. The continuous experimental data would also be helpful in estimating the design parameters required for the scale-up of the process.

1.6 Objectives

Thus the objectives of the present study are:

i. To develop the low-cost adsorbent using a biodegradable waste material and to characterize using various techniques.

ii. To carry out the batch and continuous experiments to determine the performance of developed low-cost adsorbents for removal of individual and multiple metal ions [Cd(II), Cr(VI), Cu(II), Ni(II), Pb(II), Zn(II), etc.] from wastewater.

iii. To apply various adsorption isotherms and rate kinetic models to estimate the adsorption parameters using batch experimental results.

iv. To model and optimize the batch experimental results to get the optimum parametric values.

v. To validate the mathematical models available in the literature with the obtained continuous experimental results to estimate the design parameters for further scale-up of the process.

1.7 Organization of the Thesis

The objectives of the present study are achieved by carrying out a thorough literature survey on the removal of metal ions using low-cost adsorbents and are given in the subsequent Chapter 2. The details of the experimental studies and setup are explained in Chapter 3. The batch and continuous experiments results are better analyzed with the use of various theoretical models which are presented in Chapter 4. The obtained experimental results for both, the batch and the continuous experiments are discussed and analyzed in Chapter 5. This chapter also includes the development and validation of existing mathematical models using the experimental results. Finally, Chapter 6 deals with the summary and conclusions of the overall work done during the study.

CHAPTER 2
LITERATURE REVIEW

Several studies were reported in literature for the removal of heavy metals using various commercial and low-cost adsorbents. The reported batch and continuous studies are discussed in subsequent sections.

2.1 Batch Studies

A number of studies reported the batch experiments for the removal of several metal ions using different adsorbents. Many of them have tried to utilize low-cost materials as the precursor to the adsorbents. The experiments were performed to examine the effect of few/several parameters such as initial concentration, pH, contact time, temperature, adsorbent dosage and particle size. Few of the recent studies, carried out for the removal of various metal ions, especially Cr(VI), Cu(II) and Zn(II), are being discussed in the subsequent paragraphs.

2.1.1 Cr(VI) Adsorption Studies

Gupta and Babu (2009b) and Itankar and Patil (2014) used saw dust as adsorbent for the removal of Cr(VI). Gupta and Babu (2009b) utilized fresh sawdust while Itankar and Patil had activated the sawdust using *L cysteine*. Itankar and Patil (2014) studied the variation of adsorbent dosage, initial concentration and pH of the solution while Gupta and Babu (2009b) studied the effect of initial concentration, pH, adsorbent dosage and contact time. The adsorption capacity for the fresh sawdust used by Gupta and Babu (2009b) was found to be 41.52 mg g^{-1} while for the activated sawdust used by Itankar and

Patil (2014) was obtained as 15.42 mg g^{-1}. Regeneration of saw dust was also studied and discussed briefly by Gupta and Babu (2009b) to estimate the overall utilization ability of the adsorbent.

Wang et al. (2010) utilized the black carbon isolated from the burning residuals of the wheat straw for the removal of Cr(VI). Batch experiments were performed to study the equilibrium and kinetic behavior of the process. The effect of parameters such as pH, temperature and supportive electrolyte concentration were also being investigated on the removal of Cr(VI). It was observed that the kinetic data of the adsorption process followed the pseudo-second order equation and equilibrium was well described by Freundlich isotherm. The Cr(VI) adsorption was temperature-dependent and almost independent on the sodium chloride concentrations.

Rao and Rehman (2010) studied the removal of Cr(VI) from wastewater using the fruits of *Ficus glomerata* as an adsorbent. The effect of various parameters such as temperature, pH, initial Cr(VI) concentration and time was investigated. The main objective of the work was to utilize the adsorbent for the removal of Cr(VI) from electroplating wastewater.

Suksabye and Thiravetyan (2012) used modified coir pith samples for the removal of Cr(VI) from electroplating wastewater. The maximum adsorption of 196 mg g^{-1} was achieved at pH 2, contact time of 22 h, temperature of 30°C, particle size of <150µm and 1171 mg L^{-1} of intial Cr(VI) concentration. This study showed that the adsorption capacity was found to be better for fresh coir pith as compared to modified coir pith. This may be due to the grafting of the coir pith with the acrylic acid, which enhanced the presence of carbonyl groups on the adsorbent surface.

Ali Khan Rao et al. (2012) utilized the fruit peel of *Litchi chinensis* for the removal of Cr(VI). The parameters investigated in this study were temperature, pH, initial Cr(VI) concentration and time. Fourier Transform Infra Red (FTIR) spectrophotometer was used in the study to identify the groups responsible for the adsorption of Cr(VI). The Langmuir isotherm model was found suitable to describe the equilibrium data.

Liang et al. (2013) studied the removal of Cr(VI) from wastewater using lignin based resin. The adsorbent was developed by the condensation polymerization. The effect of pH, initial metal ion concentration, adsorbent dose, contact time and temperature on the removal of Cr(VI) were studied. Freundlich isotherm model was found suitable to describe the adsorption phenomena for the Cr(VI) removal. The maximum adsorption capacity of the resin for the removal of Cr(VI) was obtained as 57.681 mg g^{-1}. The adsorption behavior was found to be spontaneous and endothermic in nature. The adsorption process was validated by the pseudo-first order kinetic model.

Kaya et al. (2014) used wheat barn and modified wheat barn for the removal of Cr(VI). This study reported the effect of initial concentration, contact time and pH for the removal of Cr(VI) using developed adsorbents. The equilibrium data for the study was very well explained by the Freundlich isotherm model. The maximum adsorption capacities of wheat barn and modified wheat barn as adsorbents for the removal of Cr(VI) were obtained as 4.53 and 5.28 mg g^{-1}.

Liang et al. (2014) used spruce bark for the removal of Cr(VI) ions from aqueous solutions. The three types of bark were prepared by treating it with the different chemicals i.e. formaldehyde, dilute and concentrated sulfuric acid. The study reported the increase in the percentage removal when the pH of the solution is decreased. It was also

found that the temperature increases the rate of adsorption. The adsorption capacity for the three adsorbents were found to be 423, 503 and 759 mg g^{-1} for the removal of Cr(VI).

Avila et al. (2014) in their study utilized functionalized Polyacrylonitrile nanofibers for the removal of Cr(VI). The effect of initial concentration, contact time and pH were studied. The adsorption capacity of functionalized polyacrylonitrile nano-fiber for the removal of Cr(VI) was obtained as 156.3 mg g^{-1}. Langmuir isotherm model explained well the adsorption behavior of the process. The pseudo-second order kinetic model explained the kinetic phenomena during the adsorption process. This study also emphasized the regeneration of adsorbent and recovery of Cr(VI) from regenerated solution.

2.1.2 Cu(II) Adsorption Studies

Benaïssa and Elouchdi (2007) studied the removal of Cu(II) using the sunflower leaves. The effect of various parameters such as contact time, initial metal concentration, initial pH of the solution and nature of copper salt on the metal removal kinetics were investigated. The pseudo-second order and Langmuir isotherm model were showing better agreement with the kinetic and equilibrium experimental data respectively. The maximum adsorption capacity obtained for the Cu(II) removal using sunflower leaves was 89.37 mg g^{-1}.

Liang et al. (2010) studied the removal of Cu(II) with the use of Mg^{2+}/K^{+} type orange peel adsorbents. In this study, the effect of pH, solid/liquid ratio, contact time and metal ion concentration on the Cu(II) adsorption were studied. Monolayer adsorption was suggested in both the adsorbents as the Langmuir model described well the adsorption process. Pseudo-second order kinetic model was found suitable to describe the adsorption

process. The thermodynamic studies showed that the adsorption of Cu(II) was spontaneous and exothermic in nature.

Senthil Kumar et al. (2010) investigated the efficiency of cashew nut shell as an adsorbent for the removal of Cu(II) by performing batch experiments. The effect of various parameters such as pH of the solution, initial concentration, contact time, temperature and adsorbent dosage were evaluated. It was found that the removal efficiency decreases with an increase in the temperature of the process. The equilibrium was attained in 30 minutes and the experimental kinetic data were following the pseudo-second order kinetic model.

Rafiq et al. (2014) studied the utilization of magnesium and zinc oxide nano-adsorbents as the potential materials for treatment of copper electroplating industry wastewater. The maximum adsorption capacities obtained were 226 and 593 mg g^{-1} for the removal of Cu(II) using ZnO and MgO respectively. The effect of initial concentration, pH, adsorbent dosage, contact time and temperature were studied. Freundlich isotherm model and pseudo-first order kinetic model well defined the adsorption of Cu(II) on ZnO and MgO adsorbents.

Cai et al. (2014) studied the removal of Cu(II) and nitrate from the kaolinite-Fe/Ni nanoparticles. The primary focus of this study was to simultaneously remove the heavy metals and inorganic pollutants from the wastewater. The adsorbent was found to have more affinity to reduce the metal contaminant in comparison to the inorganic pollutant. The adsorbent was characterized using surface area, XRD and SEM for better understanding of the adsorption mechanism.

Wen et al. (2015) used carbonaceous sulfur-containing chitosan as a novel material for the removal of Cu(II). This study found that the developed adsorbent shown a good performance in Cu(II) removal due to its fast kinetic behavior, high adsorption capacity and relatively good ability to resist acidic conditions. The adsorption capacity was found as 413.2 mg g^{-1} for the removal of Cu(II). This study confirmed the applicability of the Langmuir isotherm model in the adsorption process.

2.1.3 Zn(II) Adsorption Studies

Lim et. al. (2012) utilized the powdered fish bones as the adsorbent for the removal of Zn(II). The effects of selective parameters such as solution pH, adsorbent dose and contact time on the adsorption of Zn(II) were investigated by conducting batch experiments at room temperature. The results revealed that up to 98% of Zn(II) was removed at optimum adsorption conditions. The optimum values of pH, adsorbent dosage and contact time were obtained as 5.0, 18 g L^{-1} and 12 h respectively.

Kyzas et al. (2015) focused on the simultaneous removal of Zn(II) and cationic dye using the grafted Chitosan. The equilibrium and kinetic data for Zn(II) and dye removal were validated by the Langmuir & Freundlich isotherm models and the pseudo-second order kinetic model respectively. This study also demonstrated the reuse of the adsorbent by successive adsorption and desorption studies.

2.1.4 Multiple Metal Ions Adsorption Studies

El-Ashtoukhy et al. (2008) studied the utilization of raw and activated pomegranate as an adsorbent for the removal of Cu(II) and Pb(II). This study demonstrated the effect of activation of the adsorbent on the removal efficiency. The performance of activated

adsorbent was evaluated by performing batch adsorption experiments as a function of pH, contact time, solute concentration and adsorbent dose. The adsorption phenomena was well explained by the Langmuir model for the Pb(II) removal while the Cu(II) removal was better demonstrated by the Freundlich model. The kinetic study was well understood by the second order kinetic model for the removal of Cu(II) and Pb(II) ions.

Kazemipour et. al. (2008) utilized the activated forms of nutshells of walnut, hazelnut, pistachio, almond and apricot stone for the removal of Cu(II), Zn(II), Cd(II) and Pb(II). Selection of the metals was based on their presence in the industrial effluents. The removal efficiency was optimized with respect to the initial pH, flow rate and adsorbent dosage. The use of the developed adsorbent on the actual Cu(II) industrial effluent concluded that the removal efficiency was much more in real samples as compared to the aqueous samples.

Li et al. (2008b) used the orange peel cellulose as an adsorbent for the removal of Cd(II), Zn(II), Co(II) and Ni(II). The orange peel was chemically modified before being used as an adsorbent. This study incorporated the effect of various acid and alkali treatment on the orange peel for the metal removal. The equilibrium was attained in 60 minutes. The experimental kinetic data were fitted with the Lagergren first-order kinetics model. Both the Langmuir and Freundlich isotherm models describe well the equilibrium adsorption behavior of the orange peel.

Argun et. al. (2009) and Cutillas-Barreiro et.al. (2014) studied the utilization of modified pine bark and pine bark respectively. The developed adsorbent was utilized for the removal of Cd(II), Cu(II), Ni(II), Pb(II) and Zn(II) ions. The researchers had performed the stirred flow and the batch-type experiments. The rate of adsorption was found high at

the initial stages of the adsorption process. It was also observed that the uptake capacity was higher for Pb(II) followed by Cu, Cd, Ni and Zn. It was being deduced that the pine bark can be used effectively to remove Pb(II) and Cu(II) from polluted streams.

Pehlivan et al. (2009; 2012) studied the use of modified barley straw as an adsorbent for the removal of Pb(II) and Cu(II). The straw was first activated using citric acid and then utilized as an adsorbent. The batch experiments were performed by varying various parameters such as pH, contact time, initial concentration and adsorbent dosage. The maximum adsorption capacities for the Cu(II) and Pb(II) adsorption were obtained as 4.64 and 23.22 mg g^{-1} respectively. It was concluded that the carboxyl groups available on the surface of the modified barley straw were responsible for the better Cu(II) removal efficiency.

Ofomaja et al. (2010) studied the competition for the removal of Cu(II) and Pb(II) ions from the single and the binary mixtures. This study reported the utilization of the Mansonia wood sawdust as an adsorbent for the Cu(II) and Pb(II) adsorption. The equilibrium adsorption for Pb(II) was well described by the Langmuir isotherm model while the Cu(II) ion sorption was explained by the Freundlich and BET isotherms. It was observed that the removal of one metal in the presence of the other metal reduces the adsorption capacity of the either metal ion.

Moreno-Piraján et al. (2011) studied the use of activated carbon developed from the coconut shells for the removal of Mn, Fe, Ni and Cu ions. The effect of adsorbent dosage, contact time, solution pH and initial metal concentration on the metal removal were studied. It was noted that the Langmuir isotherm model well describes the equilibrium adsorption while the pseudo-second order kinetic model describes the kinetics of the

adsorption process. The solution pH was obtained as a determining factor during the adsorption process.

Lugo-Lugo et al. (2012) evaluated the performance of pretreated orange peel as an adsorbent for the removal of Cr(III) and Fe(III). The applicability of developed adsorbent was checked for single and simultaneous removal of both metal ions. It was observed that the rate of Cr(III) and Fe(III) adsorption in single and binary systems was significantly high and mutual interference effects in the competitive binary Cr(III)-Fe(III) adsorption system. The binary systems were well described by the multi-component Langmuir isotherm model. The maximum adsorption capacities of pretreated orange peel for Cr(III) and Fe(III) adsorption were estimated as 9.43 and 18.19 mg g^{-1} respectively.

Patel et al. (2013) investigated the two different types of husk (Rice and pigeon pea) for the removal of Cd(II) and Zn(II). It was observed that the percentage of adsorption for both, Cd(II) and Zn(II), was decreased with the increase in metal ion concentration while it increased with the increase in the solution pH (in acidic range). The developed adsorbents viz. pigeon pea and rice husks were characterized and confirmed to be excellent materials for treating wastewaters containing low concentrations of metal ions.

Morcali et al. (2014) studied the removal of Cu(II) and Zn(II) from sulfate media using commercial adsorbent. Various parameters such as sorbent quantity, contact time, temperature and acidity were studied by performing the batch experiments. The Langmuir isotherm model fitted well with the equilibrium adsorption data and the maximum adsorption capacities for Cu(II) and Zn(II) adsorption were estimated as 68.5 and 73.0 mg g^{-1} respectively.

Sikder et al. (2014) prepared Chitosan–carboxy-methyl-β-cyclodextrin entrapped nano-zero-valent iron composite for the removal of Cu(II) and Cr(VI) from wastewater. The rate of adsorption was expressed by pseudo-second order reaction kinetics. The equilibrium data were well described by both, Langmuir and Temkin isotherms. This confirmed the monolayer adsorption of Cu(II) and Cr(VI) and chemisorption nature of the processes. The application of film diffusion and intraparticle diffusion models indicated that the intraparticle diffusion may be the rate limiting steps.

Sankararamakrishnan et al. (2014) developed composite nano-floral clusters of carbon nano-tubes and activated alumina for the removal of Cr(VI) and Cd(II). Batch experiments were employed to examine the effect of pH and contact time on the Cr(VI) and Cd(II) removal. The saturation sorption capacities of nano-floral clusters for Cr(VI) and Cd(II) removal were obtained as 264.5 and 229.9 mg g^{-1} respectively.

Pumice-Supported Nanoscale Zero-Valent Iron was utilized by Liu et al. (2014) for the removal of Cr(VI) and Hg(II). The adsorption capacities of Hg(II) and Cr(VI) were evaluated as 332.4 mg g^{-1} and 306.6 mg g^{-1}, respectively. The removal of Hg(II) increased while the removal of Cr(VI) gradually decreased with an increase in the pH value. In this study, X-ray photoelectron spectroscope analysis (XPS) indicated that Hg(II) and Cr(VI) were removed by a quick physical adsorption in the initial stage of adsorption.

Zhong et al. (2014) utilized an amphoteric adsorbent based on the cellulose rich biomass for the removal of Cu(II) and Cr(VI). The adsorbent was prepared using the wheat straw which contains both cationic and anionic properties. In this study, kinetic and equilibrium experiments were performed to determine the performance of the adsorbent. This study

concluded that the removal of Cu(II) obeyed the Langmuir model while the Cr(VI) removal was well defined by the Freundlich model.

Water bamboo (Zizania caduciflora Turcz.) was utilized by Asberry et al. (2014) for the removal of five heavy metals ranging from Cu(II), Cr(III), Ni(II), Pb(II), and Fe(III). Adsorption isotherms were applied and breakthrough studies were conducted to evaluate the performance of water bamboo adsorbent for the removal of Fe(II) and Ni(II) at low metal concentrations. It was also observed that the adsorption capacity of water bamboo in continuous mode was 2-3 times higher than that of the adsorption capacity obtained from batch mode.

Arshadi et al. (2014) studied the utilization of barley straw ash as the adsorbent for the removal of Ni(II), Cd(II), Cu(II) and Co(II). The effect of initial concentration, contact time, temperature and initial pH was investigated on the metals removal. The various kinetic (Pseudo-first order, pseudo-second order) and equilibrium (Langmuir, Freundlich, and Langmuir-Freundlich) models were utilized for understanding the kinetic and equilibrium behavior of the adsorption process. This study concluded that the adsorption process was favorable, spontaneous and endothermic in nature.

Various other works for the removal of different metal ions are being reported in Table 2.1.

Table 2.1: List of various adsorbents available in the literature used for different metal removal.

Metal	Adsorbent	q_m (mg g^{-1})	Parameters Studied	Equilibrium Isotherm	Rate Kinetics	Reference
Cd(II)	Azadirachta indica (Neem) leaf powder	158	pH, adsorbent dosage, contact time, initial concentration, temperature	Langmuir, Freundlich	Pseudo-first order Lagergren equation, simple second order kinetics, Elovich equation, liquid film diffusion model, intraparticle diffusion mechanism	Sharma and Bhattacharyya (2005)
	Sawdust (Deciduous tree)	2.8	Process time, type of ion, initial metal concentration, pH, adsorbent concentration	Langmuir, Freundlich	Pseudo-second order	Božić et al. (2009)
	Annona squamosa shell	71	pH, adsorbent dosage, contact time, initial concentration, temperature	Langmuir, Freundlich	Pseudo-second order, pseudo-first order	Isaac and Sivakumar (2013)
	Electroactive polypyrrole (PPy) particles	71.4	Initial concentration, contact time, temperature	Langmuir	Pseudo-first order	Seid et al. (2014)

Metal	Adsorbent	q_m (mg g^{-1})	Parameters Studied	Equilibrium Isotherm	Rate Kinetics	Reference
Cd(II)	Modified magnetic mesoporous carbon	406.6	Initial concentration, pH, ionic strength	Langmuir, Freundlich	Pseudo-second order model, intraparticle diffusion model	Zeng et al. (2015)
	Chemically modified maize straw	196.1	pH, adsorbent dosage, contact time, initial concentration, Temperature	Langmuir, Freundlich	Pseudo-first order, pseudo-second order, Intraparticle diffusion model	Guo et al. (2015)
Cr(VI)	Tea factory waste	39.62	pH, initial concentration of Cr (VI) ion, temperature, agitating rate, adsorbent mass	Langmuir, Freundlich	First-order	Malkoc and Nuhoglu (2007)
	Oak(*Quercus coccifera*) sawdust	1.7	Shaking speed, adsorbent mass, contact time, pH	Langmuir, Dubinin-Radushkevich	Pseudo-second order	Argun et al. (2007)
	Activated Neem leaves	62.97	Contact time, pH, adsorbent dosage, initial Cr (VI) concentration	Langmuir, Freundlich	Pseudo-first order, second order	Babu and Gupta (2008b)

Metal	Adsorbent	q_m (mg g^{-1})	Parameters Studied	Equilibrium Isotherm	Rate Kinetics	Reference
Cr(VI)	Activated Tamarind seeds	29.08	Contact time, pH, adsorbent dosage, initial Cr (VI) concentration	Langmuir, Freundlich	Pseudo-first order, second order	Babu and Gupta (2008a)
	Activated Fly ash	21	pH, contact time, initial concentration, adsorbent dosage	Langmuir, Freundlich, Koble-Corrigan	Second order	Gupta and Babu (2010a)
Cu(II)	Oak (*Quercus coccifera*) sawdust	3.22	Shaking speed, adsorbent mass, contact time, pH	Langmuir, Dubinin-Radushkevich	Pseudo-second order	Argun et al. (2007)
	Sawdust(*Acacia arabica*)	5.64	pH, initial concentration, adsorbent dose, contact time, temperature	Langmuir, Freundlich	Lagergren pseudo-first order	Meena et al. (2008)
	Sphagnum peat	-	pH, initial concentration	Freundlich	Pseudo-second order	Kalmykova et al. (2008)
	Eucalyptus camaldulensis Dehn. bark	28.6	pH, contact time, initial metal concentration, temperature	Langmuir, Freundlich	Pseudo-second order	Patnukao et al. (2008)

Metal	Adsorbent	q_m (mg g^{-1})	Parameters Studied	Equilibrium Isotherm	Rate Kinetics	Reference
Cu(II)	Powdered activated carbon	19.2	Contact time, pH, adsorbate concentration	Langmuir	-	Terdkiatburana et al. (2009)
	Sawdust (Deciduous tree)	2	Process time, type of ion, initial metal concentration, adsorbent concentration, pH	Langmuir, Freundlich	Pseudo-second order	Božić et al. (2009)
	Chestnut shell	5.48	Initial cation concentration, temperature, pH	Langmuir, Freundlich and Redlich–Peterson isotherms	Thomas model, Clark model, Yoon - Nelson model	Vázquez et al. (2009)
	Date pits	35.9	pH, particle size, surface area	Langmuir, Freundlich	-	Al-Ghouti et al. (2010)
Ni(II)	Oak (*Quercus coccifera*) sawdust	3.29	Optimum shaking speed, adsorbent mass, contact time, pH	Langmuir, Dubinin-Radushkevich	Pseudo-second order	Argun et al. (2007)

Metal	Adsorbent	q_m (mg g^{-1})	Parameters Studied	Equilibrium Isotherm	Rate Kinetics	Reference
Ni(II)	Sphagnum peat	-	pH, initial concentration	Freundlich	Pseudo-second order	Kalmykova et al. (2008)
	Sawdust (Deciduous tree)	1.2	Time, type of ion, pH, initial metal, adsorbent concentration	Langmuir, Freundlich	Pseudo-second order	Božić et al. (2009)
	Alkaline-modified montmorillonite	200	pH, initial concentration, adsorbent dosage, particle size, contact time	Langmuir, Freundlich, Temkin, Dubinin–Radushkevich	Pseudo-first order, pseudo-second order, Elovich equation, intraparticle diffusion model	Akpomie and Dawodu (2014)
	Nigerian kaolinite clay	166.67	pH, initial metal ion concentration, sorbent dose, particle size, contact time, temperature, ligand	Langmuir, Freundlich, Temkin and Dubinin–Radushkevich (D–R)	Pseudo-first order, pseudo-second order, Elovich equation, intraparticle diffusion model	Dawodu and Akpomie (2014)

Metal	Adsorbent	q_m (mg g^{-1})	Parameters Studied	Equilibrium Isotherm	Rate Kinetics	Reference
Ni(II)	Scrap tire	25	pH, initial metal ion concentration, sorbent dose, particle size, contact time, temperature	Langmuir, Freundlich	Pseudo-first order, pseudo-second order	Gupta et al. (2014)
Pb(II)	Wheat bran	87	Initial concentration, adsorbent dose, particle size, agitation speed, temperature, contact time, solution pH	Langmuir, Freundlich	Pseudo-second order	Bulut and Baysal (2006)
	Sphagnum peat	-	pH, initial metal concentration	Freundlich	Pseudo-second order	Kalmykova et al. (2008)
	Chestnut shell	8.5	Initial cation concentration, temperature, pH	Langmuir, Freundlich and Redlich–Peterson isotherms	Thomas model, Clark model, Yoon - Nelson model	Vázquez et al. (2009)

Metal	Adsorbent	q_m (mg g^{-1})	Parameters Studied	Equilibrium Isotherm	Rate Kinetics	Reference
Pb(II)	Pine bark (Pinus brutia Ten.)	76.8	pH, adsorbent dosage, contact time, initial concentration, temperature, co-existing ions, desorption	Langmuir, Freundlich	Pseudo-first order, pseudo-second order, intraparticle diffusion models	Gundogdu et al. (2009)
	Corncobs	43.4	Contact time, initial metal concentration, pH	Langmuir	Lagergren-first order, Lagergren-second order	Tan et al. (2010)
	Annona squamosa shell	90.93	pH, adsorbent dosage, contact time, initial concentration, temperature	Langmuir, Freundlich	Pseudo-second order, pseudo-first order	Isaac and Sivakumar (2013)
	Carboxylated cellulose nanofibrils-filled magnetic chitosan hydrogel beads	171	pH, initial concentration, contact time	Langmuir, Freundlich	Pseudo-first order, pseudo-second order, intraparticle diffusion models	(Zhou et al. (2014)

Metal	Adsorbent	q_m (mg g^{-1})	Parameters Studied	Equilibrium Isotherm	Rate Kinetics	Reference
Pb(II)	Wheat straw pulp fine cellulose	248.64	pH, initial concentration, contact time	Langmuir, Freundlich	-	Suopajärvi et al. (2015)
	Cow bone	50.1	pH, initial concentration, contact time	Langmuir, Freundlich	Pseudo-second order	Cechinel et al. (2014)
Zn(II)	Sphagnum peat	-	pH, initial concentration	Freundlich	Pseudo-second order	Kalmykova et al. (2008)
	Sawdust (Deciduous tree)	1.6	Process time, type of ion, initial metal concentration, adsorbent concentration, pH	Langmuir, Freundlich	Pseudo-second order	Božić et al. (2009)
	Chestnut shell	2.41	Initial cation concentration, temperature, pH	Langmuir, Freundlich and Redlich–Peterson isotherms	Thomas model, Clark model, Yoon - Nelson model	Vázquez et al. (2009)

2.2 Continuous Studies

Very few researchers employed the low-cost adsorbent for the removal of heavy metals in a continuous mode. The following paragraphs discuss the work carried out by various researches for the continuous removal of different metal ions.

Goel et al. (2005) utilized the granular activated carbon prepared using the coconut shell for the Pb(II) adsorption. In this study, the performance of the activated carbon and treated activated carbon for the removal of Pb(II) was investigated by performing the batch and continuous experiments. The selection of the adsorbent for the column studies was done based on the results obtained from the batch experiments. Continuous experiments were performed to assess the effect of various process variables such as the bed height, hydraulic loading rate and initial feed concentration on the breakthrough time and the adsorption capacity. This study also included the regeneration of the used adsorbent using HNO_3.

Issabayeva et al. (2008) considered the removal of lead ions in the fixed-bed column using the commercial, granular and un-pretreated palm shell activated carbon. This study focused on the effect of pH and flow rates. Issabayeva used malonic and boric acids as the complexing agents. It was deduced from the study that the removal was more at the higher pH value of the solution. The increase in the flow rate was leading to a faster saturation of the adsorption bed. The model proposed by Wang et al. (2003) was validated with the obtained experimental results.

Pumice and Brown coal were used as an adsorbent for the removal of Cr(III) and Cr(VI) by Gode and Moral (2008). This study was conducted at room temperature with an initial

concentration of Cr(III) and Cr(VI) as $1x10^{-3}$ mol L^{-1}. The column study was performed as a function of pH, concentration of Cr(III) and Cr(VI) ions, volume of samples and flow rate. The dynamic breakthrough capacities of the adsorbents for Cr(III) and Cr(VI) were evaluated. It was observed that the maximum adsorption was taking place at a flow rate of 5 ml min^{-1}. This study provided a satisfactory result for the use of pumice and brown coal as an adsorbent for the removal of Cr(III) and Cr(VI).

Suksabye et al. (2008) studied the removal of Cr(VI) from the electroplating wastewater using coir pith as an adsorbent packed in the fixed-bed column. The effect of bed height and flow rate was investigated. It was found that the breakthrough volume was increased as the flow rate was decreased and the bed depth was increased due to an increase in the empty bed contact time (EBCT). Thomas model was found suitable to explain the experimental data. It was also observed that the adsorption capacity estimated from the bed depth service time model (BDST) model was reduced with increase in the flow rate. In this study, saturated adsorbent packed into the column was also regenerated with the use of 2M HNO_3. However, the obtained results had not confirmed the successful regeneration of the adsorbent.

Mohan and Sreelakshmi (2008) studied the performance of low-cost adsorbent such as raw rice husk (RRH) and phosphate treated rice husk (PRH) for the removal of different heavy metals (Pb, Cu, Zn and Mn). The materials adopted were found to be an efficient adsorbent for the removal of heavy metals in continuous mode using the fixed-bed column. The parameters evaluated during the study were the bed height and the flow rate. It was observed that the breakthrough time increased with an increase in the bed height. In this study, various column design parameters such as the adsorption rate, adsorption

capacity and depth of exchange zone were evaluated. It was found that there were increase in the adsorption capacity and the rate of adsorption with the decrease in the minimum column bed length by the use of phosphate treated rice husk.

Gupta and Babu (2009c; 2010b) had evaluated the performance of saw dust and activated tamarind seeds as the potential adsorbent for Cr(VI) removal by performing continuous experiments in a fixed-bed adsorption column. The effects of parameters such as flow rate, mass of adsorbent, initial Cr(VI) concentration were examined and the corresponding breakthrough curves were obtained. The process parameters such as breakthrough time, total percentage removal of Cr(VI), adsorption exhaustion rate and fraction of unused bed-length were estimated. This study also proposed a mathematical model for fixed-bed adsorption column by including the effect of velocity variation along the bed-length in the existing model. Pore and solid diffusion models were used to describe the intraparticle mechanism of Cr(VI) adsorption. The proposed mathematical model was validated with the literature data and the experimental data obtained in the present study. The improved model was found to be good for explaining the behavior of breakthrough curves.

Sousa et al. (2010) studied the use of green coconut shells as an adsorbent for the continuous removal of toxic metals (Cu, Pb, Cd, Zn and Ni). It was found that a flow rate of 2 mL min^{-1} and height of 10 cm may be the most feasible system for the metal removals. It was also concluded that the removal efficiency obtained for the different metal ions from the fixed-bed was in the order of Cu> Pb> Cd> Zn> Ni. Experimental results also confirmed that a larger quantity of the single ion effluent can be treated in comparison to a multiple ions effluent.

Escudero et al. (2013) investigated the applicability of the grape stalks waste as an adsorbent for the single and multiple ions [Cu(II), Cd(II), Ni(II) and Pb(II)] adsorption. It was observed that the adsorption of Pb(II) was not affected by the presence of other metal ions, while Cu(II) adsorption was affected by the presence of Pb(II), and was not by Cd(II) and Ni(II). Also, Ni(II) and Cd(II) adsorption was effected in the presence of Cu(II) and Pb(II). Homogeneous Surface Diffusion Model (HSDM) was also developed to describe the characteristics of breakthrough curves.

2.3 Gaps in Existing Research

The literature survey in the proposed research area revealed that in the present industrial era, the presence of toxic metals in the effluent streams of different industries is a growing environmental concern. There are various physical and chemical methods available for the removal of toxic metals from these effluent streams. It is also observed that few adsorption studies were reported for the purification of industrial effluent streams. However, economical treatment of effluent streams is the most important criteria. The reported low-cost materials used as adsorbents do not possess the higher adsorption capacity for the metal adsorption. In addition to that, most of the reported adsorbents were utilized for the removal of single metal ion. Very few adsorbents have been reported for the simultaneous removal of two metal ions. However, the actual industrial effluents contain multiple metal ions which are also required to be treated before discharging the effluent streams to the outer water bodies. Therefore, there is a need to develop a low-cost adsorbent prepared from biodegradable material capable of simultaneous adsorption of multiple metal ions with higher metal uptake. The removal of

single metal ion, with the use of specific adsorbent in the presence of other metals affects the adsorbent performance.

Very few studies have reported the regeneration of metal loaded adsorbent for the reutilization of adsorbent. The regeneration is very much required to make the adsorption process more economical and environmentally friendly. Most of the researchers follow a common trend of performing batch experiments to study the effect of a single parameter on the adsorption removal efficiency by keeping the other parameters constant. Only few studies have been reported for the estimation of the maximum removal efficiency as a function of all the independent parameters (Ahmadi et al.; Vázquez et al., 2009; Saadat and Karimi-Jashni, 2011; Maher et al., 2014; Vukčević et al., 2014). Whereas, no study is found where the researchers have performed experiments at the optimum parametric condition.

The literature survey also revealed that very few studies have reported the continuous adsorption experiments using the low-cost adsorbents. The lab/pilot scale continuous experiments are required to design/scale up the process to the industrial scale. The studies related to the removal of multiple metal ions using fixed-bed column are scarce. The mathematical models are used to scale-up the adsorption process from laboratory scale to pilot scale and subsequent to the industrial scale. There are a significant number of batch studies reported the use of various isotherm and kinetic model to fit the obtained experimental data and the estimation of model parameters. However, very few studies attempted the validation of available mathematical for the fixed-bed adsorption by the continuous experimental data.

2.4 Scope of Work

There is a need to develop a low-cost adsorbent from the naturally available waste material which can be utilized as a potential adsorbent for the removal of multiple metal ions. It is required to find the optimum activation conditions for the development of the suitable low-cost adsorbent having more surface area and higher adsorption capacity for the multiple metal ions. The batch experiments are needed to be performed at different parametric values to evaluate the performance of developed adsorbent. There is an ample scope of performing the continuous experiments using the developed low-cost adsorbent for the removal of Cu(II), Cr(VI) and Zn(II) to demonstrate the use of the developed adsorbent for the treatment of industrial effluent streams. A suitable method for the regeneration of metal loaded adsorbent is required to be developed to make the adsorption process more environmentally friendly.

The industrial effluents from pulp & paper and plating industries are mainly containing multiple metal ions ranging from Cu(II), Cr(VI), Cd(II), Pb(II), Ni(II) and Zn(II). Hence, there is a need to evaluate the application of the developed low-cost adsorbent for the simultaneous removal of multiple metal ions in a continuous column.

There is a need to propose a generalized mathematical equation which can be used by most of the reported studies in the literature to find an optimal set of parameters which results in the maximum removal efficiency or adsorption capacity. Batch and continuous experimental results are required to be analyzed by the use of appropriate mathematical models available in the literature. The obtained design parameters from the model validation can be further utilized to propose a design of adsorption column in pilot and industrial scale.

CHAPTER 3
MATERIALS AND METHODS

This chapter deals with the detailed description of the methodology applied to carry out the experimental studies and is discussed in the following sections.

3.1 Preparation of the Nano-porous Adsorbent

Neem is having its botanical name as *Azadirachta indica* and belongs to the mahogany family *Meliaceae.* It shows the similar property to its close family member, *Melia azederach*. The word *Azadirachta* is derived from the Persian 'azaddhirakt' which means 'noble tree'. The taxonomic positions of neem are as follows:

Order	:	Rutales
Suborder	:	Rutinae
Family	:	Meliaceae
Subfamily	:	Melioideae
Tribe	:	Melieae
Genus	:	Azadirachta
Specie	:	*Indica*
Latin	:	*Azadirachta indica*

It is a tough, fast-growing evergreen tree along with a straight stem, extended spreading branches and fairly thick, coarse, longitudinally fissured bark (Ogbuewu et al., 2011). The various parts of neem are used for different medicinal and other uses. The chemical composition of bark ranges from bitter principles, essential oils and polysaccharides. These inflammatory polysaccharides consist of glucose, arabinose and fructose which are water soluble in nature (Puri, 2006). The neem bark is used for the treatment of skin

infections, scabies, eczema, cancer, allergies, etc. (Hashmat et al., 2012). The proximate and ultimate analysis of neem bark (Table 3.1) support its carbonaceous and biodegradable nature. It is a well established fact that the carbonaceous materials are more suitable adsorbents for metals removal (Shen et al., 2010). The use of neem leaves for the Cr(VI) adsorption was established by Babu and Gupta (2008b). In the view of above mentioned factors, neem bark is selected as the raw material for the development of adsorbent for the heavy metals adsorption.

Neem bark, obtained from the trees of Birla Institute of Technology and Science, Pilani, Rajasthan, India is utilized for the preparation of the nano-porous adsorbent. The neem bark is repeatedly washed with distilled water for removing dust and other soluble impurities. Washed material is dried in a shade for 24 h. The dried neem bark is then crushed into smaller pieces by passing it through a roller crusher, jaw crusher and ball mill sequentially. The crushed material is then screened through 12-14 BSS mesh screens. The particles passed through 12 mesh and retained on 14 mesh are considered for the experiments. Therefore, the average size of 12 and 14 mesh screens [(d_p)≈ 1.20 mm] is considered as the average particle size of the developed adsorbent. The activated procedure reported by Babu and Gupta (2008b) is followed in the present study for the activation of neem bark. These particles are further activated by chemical and physical treatment at different activation conditions as given in Table 3.2. Finally, activated materials (ANB1 to ANB6) are repeatedly washed in distilled water for removing free acid and color impurities. Now the activated neem barks (ANBs) obtained from different activation procedures are ready as adsorbent for the adsorption process. The stepwise images of the evolution of ANB from neem bark are provided in Plate 3.1.

Table 3.1: Proximate and ultimate analysis of neem bark (Shen et al., 2010; Srivastava and Rupainwar, 2011).

Proximate Analysis (% by mass, dry basis)	
Fixed carbon	12.19
Volatile material	85.86
Ash	1.93
Ultimate Analysis (% by mass, dry basis)	
C	48.26
H	6.27
N	0.93
O	43.46

Table 3.2: Activation conditions for the preparation of activated neem bark.

S. No.	**ID**	**Neem Bark : H_2SO_4 (wt. %: wt. %)**	**Activation Temp. ($^{\circ}$C)**	**Time (h)**
1	ANB1	1:1	70	24
2.	ANB2	4:3	70	24
3.	ANB3	4:5	70	24
4.	ANB4	1:1	50	24
5.	ANB5	1:1	90	24
6.	ANB6	1:1	70	12

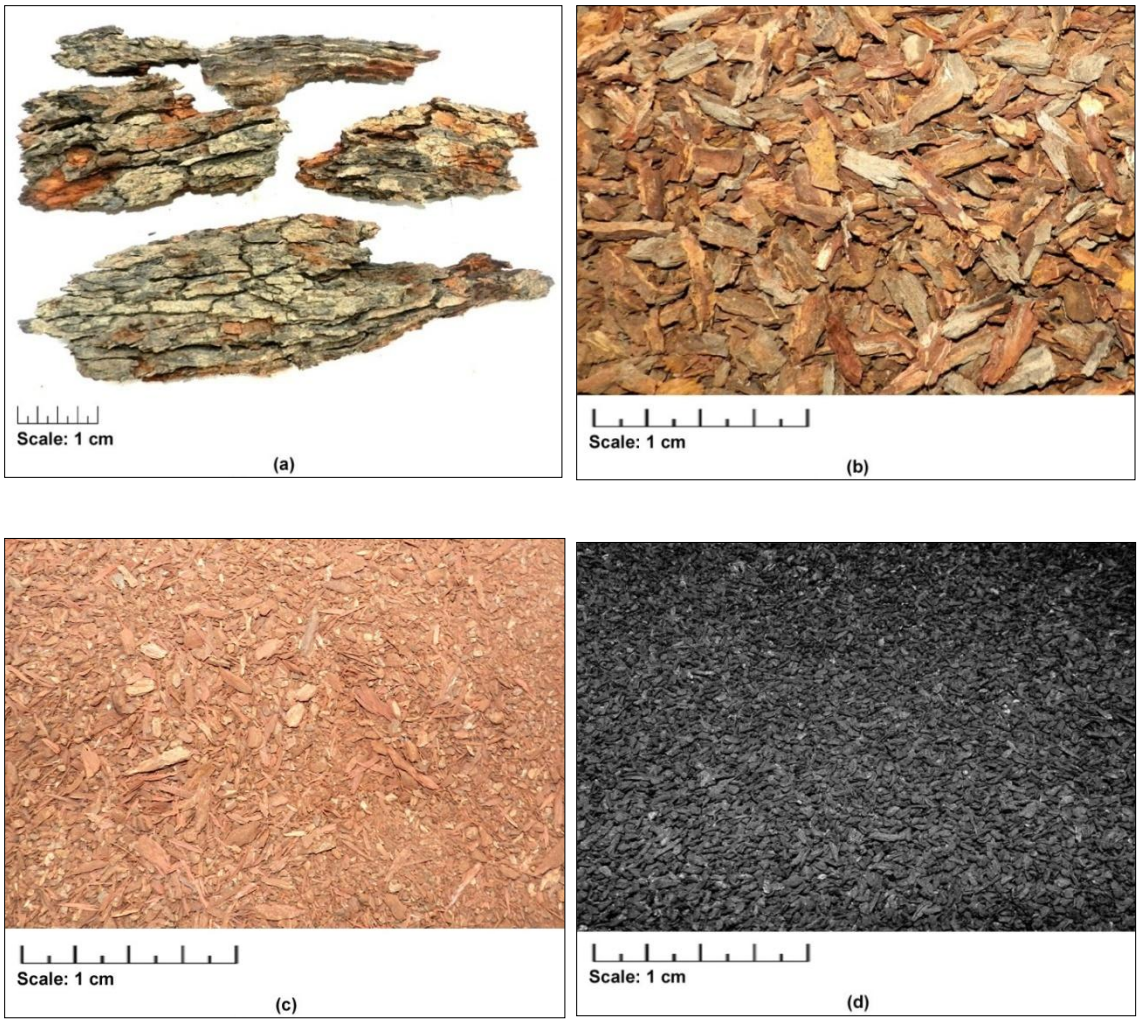

Plate 3.1: Photograph of (a) Fresh Neem Bark; (b) Neem bark after first crusher; (c) Neem bark after final crusher; (d) Neembark after activation; the different stages of preparation.

3.2 Characterization

Characterization is performed to study the various characteristics of the developed adsorbents from neem bark. The characterization is an important activity when a new material is developed as an adsorbent for the removal of specific pollutants.

The six developed ANBs (ANB1 to ANB6) are characterized using the Fourier Transform Infrared (FTIR) Spectroscopy (Frontier, Perkin Elmer) which is performed in a range of 4000 to 400 cm^{-1} to analyze the vibration mode of the available functional groups. Out of the six developed adsorbents, the one which is having the relevant functional groups on the surface and shows the maximum adsorption capacity for the removal of Cr(VI), Cu(II) and Zn(II) is being utilized for the further study and is termed as nANB.

The nANB is further characterized using five more techniques. The first characterization technique used is Scanning Electron Microscope (SEM) which captures various images by focusing a very high energy beam of electrons on the surface of nano-porous materials. Energy Dispersive Spectroscopy (EDS) is used to detect the specific elements present in the test material. This characterization technique provides the elemental composition of the materials in weight percent. The SEM and EDS analysis of fresh nANB, saturated nANB by Cr(VI), regenerated nANB from Cr(VI) and used nANB for plating industrial effluent are done using Field Emission Gun-Scanning Electron Microscopes (FEG-SEM, JSM-7600F, IIT Bombay). The SEM and EDS of nANB used on pure Cu(II), Zn(II) and combined solution of Cu(II), Cr(VI) & Zn(II) are performed using Scanning Electron Microscopes (JSM 6510LVat University Sophisticated Instruments Facility (USIF), Aligarh Muslim University). The SEM and EDS of the used

nANB on the synthetically prepared pulp & paper industrial effluent is done using ZEISS EVO Series SEM Model EVO 50 at Indian Institute of Technology (IIT), Delhi.

The available specific surface area is another important characteristic of developed adsorbent as the adsorption process is a surface phenomenon. Hence, the specific surface area of the nANB is determined using the Brunauer-Emmet-Teller (BET) surface analyzer (Smart Sorb 92/93, Smart instruments Co. Pvt. Ltd.). The X-ray diffraction (XRD) analysis of the developed nANB is carried out using Rigaku MiniFlex II desktop X-ray Diffractometer. The XRD analysis offers the phase analysis of the developed nANB. The developed nANB is also characterized by Thermo-Gravimetric Analysis (TGA) which is performed on TGA-4000, Perkin Elmer. This technique helps in determining the thermal stability of the newly developed nANB.

3.3 Preparation of Stock Solution

The 1000 mg L^{-1} of stock solutions are prepared by dissolving the specific amount of the respective metal complex salts in the distilled water and the volume of the solution is made upto 1000 mL. The details of the salts and the amount used are being tabulated in Table 3.3. All the chemicals used during the study are of analytical grade.

3.4 Batch Experiments

Equilibrium experiments are performed for the removal of different metal ions from aqueous solutions using developed ANB1 to ANB6. In this study, the initial concentration of different metal ions [Cr(VI), Cu(II) and Zn(II)] is varied from 5-200 mg L^{-1} by keeping other parameters constant (Table 3.4). Out of six developed adsorbents,

the one which is having more adsorption capacity for the removal of Cr(VI), Cu(II) and Zn(II) is being used for the further study.

Batch experiments are performed in 100 mL conical flask with working volume of 25 mL (Fig 3.1). The stock solutions are diluted using distilled water to prepare different metal ion concentration solutions ranging from 5-200 mg L^{-1}. The specified amount of adsorbent is added to the solutions and kept in agitation at a speed of 150 rpm on a rotary shaker (Julabo make, Plate 3.2) for a predetermined period. Parametric studies are performed to evaluate the effect of initial metal ion concentration, adsorbent dosage, contact time, pH and temperature on the removal of Cr(VI), Cu(II) and Zn(II) using nANB. The ranges of various parametric values are provided in Table 3.4. The batch equilibrium experiments are also conducted for the removal of Cd(II), Ni(II) and Pb(II) based on the composition of the pulp & paper industry effluent (Thippeswamy et al., 2012). All the experiments are performed twice and the averaged values are considered in the further evaluation.

3.5 Column Experiments

Continuous experiments are performed for the removal of heavy metals from aqueous solutions using nANB as a packing material in a fixed-bed column. The schematic diagram of the experimental setup is shown in Fig 3.2. The photograph of the experimental setup is provided in Plate 3.3. A glass column of 2.53 cm inner diameter is employed as a fixed-bed column. The column is packed with the nANB in a stepwise manner. Primarily, a known quantity of nANB is filled into the column and is shaken manually in order to have intense packing. The pattern is extended till the total amount of the adsorbent is packed into the column. Later, 500 mL of distilled water passes through

the bed to ensure an added dense packing. The aqueous solution of different metals is passed through the fixed-bed column in the down flow mode. In the present study, the effect of various parameters such as the mass of adsorbent, the inlet flow rate and the inlet metal concentration on the continuous metal ion removal are studied. The range of different parametric values used in the present study are given in Table 3.5. An optimum pH value (≈2.2) obtained from the batch experiments is maintained throughout the continuous experiments. The selected value of pH is also justified by the fact that the industrial effluent streams such as chromium plating effluent (pH=1) (Selvaraj et al., 2003), tannery (=2) (Aksu and Gönen, 2004), electroplating (= 2.2) (Kumar et al., 2008) and other literatures (Malkoc and Nuhoglu, 2007) are having low pH.

Continuous experiments are also performed for the synthetically prepared multiple metal ions solution [50 mg L^{-1} each of Cr(VI), Cu(II) and Zn(II)] to check the performance of the developed nANB. Although the batch studies are conducted out at actual chrome plating industrial effluent sample, however, due to its unavailability, continuous studies are not performed with this sample. Therefore, the nANB is utilized for the treatment of synthetically prepared pulp & paper industry effluent which contains multiple metal ions [Cd(II), Cr(VI), Cu(II), Ni(II), Pb(II) and Zn(II)]. The composition of the synthetically prepared multiple metal ions solution is given in Table 3.6. The flow rate and mass of the adsorbent is maintained as 10 mL min^{-1} and 75 g respectively during the experiment.

3.6 Analysis of Metal Ions

The concentration of total metal ions left in the liquid phase is determined spectro-photometrically using the Atomic Absorption Spectrophotometer (AA-7000, Shimadzu) shown in Plate 3.4 (Memon et al., 2009). Subsequently, the amount of metal ions

adsorbed by the nANB is calculated using the following Eq. 3.1 (Babu and Gupta, 2008b; 2009a).

$$q_e = \frac{(C_o - C_e)V}{W} \quad (3.1)$$

where q_e is the adsorption capacity (solid phase concentration of metal ion on the adsorbent) (mg g^{-1}), C_0 is the initial concentration of metal ion (mg L^{-1}), C_e is the concentration of metal ion at equilibrium (mg L^{-1}), V initial volume of metal solution (L) and W weight of the adsorbent (g).

3.7 Regeneration

In the present study, two types of desorption techniques have been applied. In the first technique, a simple thermal approach is considered. In this technique, the used adsorbent is kept for the shaking in a distilled water at 70°C. It is a well known fact that the adsorption of metals is favored at low pH. Therefore, the other technique is based on the base and acid treatment (Gupta and Babu, 2009b; Kapur and Mondal, 2013). The regeneration process is carried out by treating the saturated nANB with 1 N NaOH for 24 h and followed by 1N HCl treatment for 24 h. After the treatment, the regenerated nANB is washed thoroughly with distilled water to remove the traces of acid from the nANB surface (Gupta and Babu, 2009a).

Table 3.3: Different salts and their respective amounts used to prepare 1000 mg L^{-1} metal stock solutions.

Metal	Complex Salt	Formulae	Mol. Wt. (g)	Amount Used (g)
Cd(II)	Cadmium nitrate tetra-hydrate	$Cd(NO_3)_2.\ 4H_2O$	236.4208	2.7442
Cr(VI)	Potassium dichromate	$K_2Cr_2O_7$	294.1846	2.8287
Cu(II)	Copper sulphate penta-hydrate	$CuSO_4.5H_2O$	249.685	3.9293
Ni(II)	Nickel nitrate hexa-hydrate	$(NiNO_3)_2.\ 6H_2O$	290.79	4.9545
Pb(II)	Lead nitrate	$Pb(NO_3)_2$	331.2	1.608
Zn(II)	Zinc sulphate hepta-hydrate	$ZnSO_4.7H_2O$	287.54956	4.397

Table 3.4: Various parameters considered during the batch experimental study.

Parametric Study	Initial Metal Concentration (mg L^{-1})	Adsorbent Dosage (g L^{-1})	Contact Time (h)	pH	Temp. (°C)
Initial metal concentration	5-200	6	48	2.70	35
Adsorbent dosage	100	4-28	48	2.70	35
Contact time	100	6	0-48	2.70	35
pH	100	6	48	1.2-12	35
Temperature	100	6	48	2.70	35-70

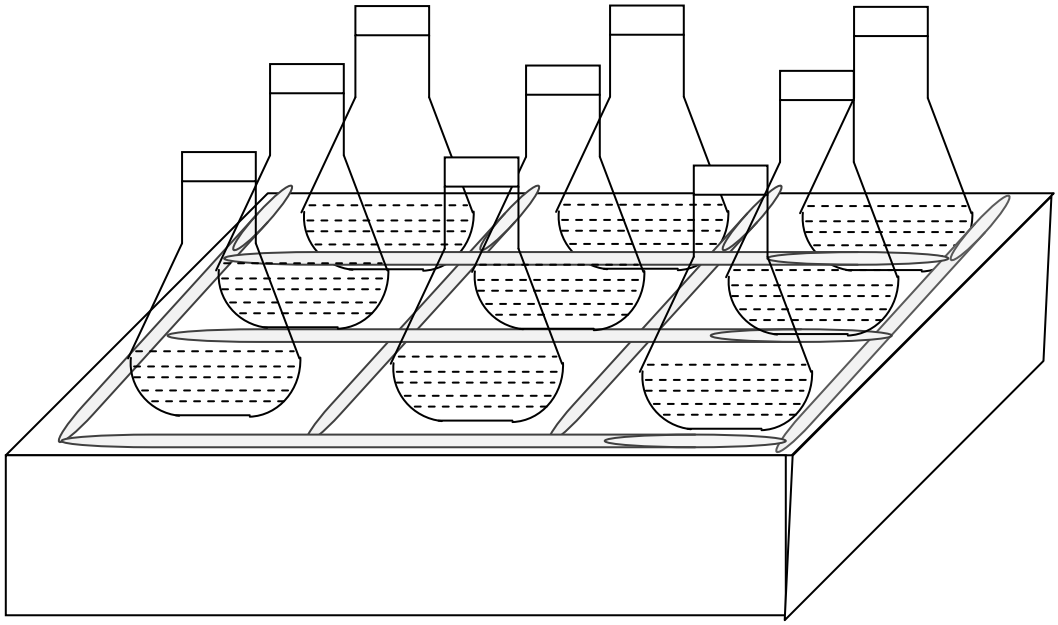

Fig 3.1: Batch experimental setup.

Plate 3.2: Photograph of Batch Experimental setup.

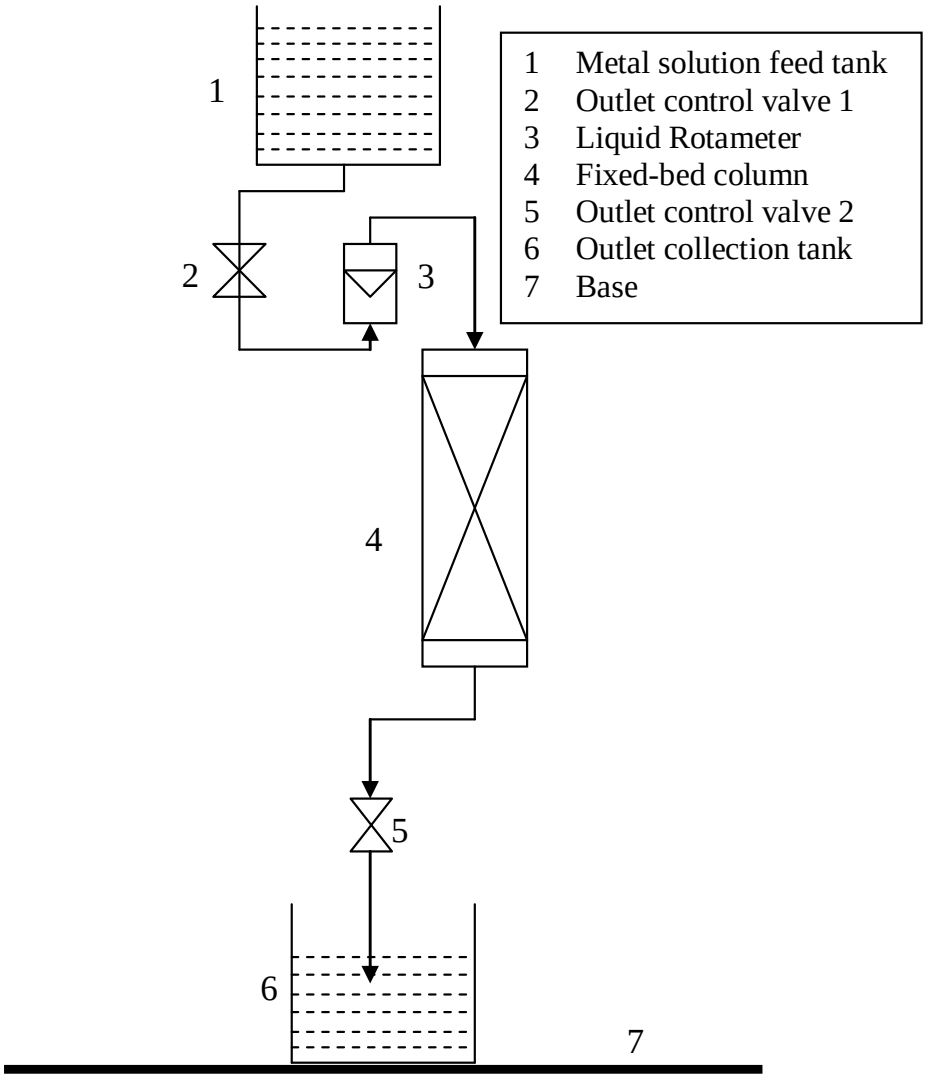

Fig 3.2: Fixed-bed experimental setup for continuous adsorption process.

Plate 3.3: Photograph of experimental setup for continuous adsorption process.

Table 3.5: Various parameters considered during the column study.

Parametric Study	Initial Metal Concentration ($mg\ L^{-1}$)	Adsorbent Amount (g)	Inlet Flowrate ($mL\ min^{-1}$)	pH
Initial metal concentration	50, 100	75	10	2.20
Adsorbent amount	50	25-175	10	2.20
Inlet flow rate	50	75	5 - 15	2.20

Table 3.6: Composition of synthetically developed pulp & paper industrial effluent (Thippeswamy et al., 2012).

Metals	Concentration ($mg\ L^{-1}$)
Cr(VI)	59.02
Cu(II)	7.72
Zn(II)	2.9
Pb(II)	1.54
Ni(II)	3.49
Cd(II)	1.44

Plate 3.4: Photograph of Atomic Absorption Spectrophotometer (AA-7000).

CHAPTER 4
MATHEMATICAL MODELING

The batch adsorption experimental data are used to evaluate various parameters with the help of different isotherm and kinetic models available in the literature. Batch experiments are not suitable for large scale treatment processes, however, the parameters evaluated from this study are helpful in designing the column for continuous experiments. The mathematical models available for the fixed-bed columns are also useful to estimate the design parameters by validating them using laboratory scale continuous experimental results. In the following sections, various available adsorption isotherm, kinetic and mass transfer models are described. Development of a generalized mathematical equation using the batch experimental data to estimate the optimum parametric values is also discussed. Mathematical equations to calculate various design parameters of adsorption column are also presented in the subsequent sections.

4.1 Adsorption Isotherm Models

In order to understand the distribution of the metal ions in the liquid and solid phases at equilibrium, there is a need to fit the different isotherm models with experimental equilibrium data. In the present work, the data are fitted with the Langmuir, Freundlich and Tempkin isotherm models. The linear form of these isotherm models are given in Table 4.1. These are applied to the equilibrium experimental data to estimate the different parameters of isotherms.

4.1.1 Langmuir Isotherm

The Langmuir isotherm model (Table 4.1) is one of the basic isotherm models which has been extensively used for the adsorption of heavy metals, dyes, organic pollutants, etc. (Gupta and Babu, 2009b). This isotherm model is principally valid for the mono molecular layer adsorption. It supports the homogeneous adsorption which states that all the adsorption sites are equally capable of adsorbing pollutants irrespective of the status of the adjacent sites. The Langmuir isotherm is also utilized to evaluate the maximum adsorption capacity (q_m) which represents the capacity produced from the complete single layer coverage of adsorbent surface. Another parameters evaluated using Langmuir isotherm models are b and R_L. The b is an adsorption equilibrium constant representing the adsorption energy while R_L represents the dimentionless equilibrium parameter and is calculated using Eq. 4.1 (Langmuir, 1916; 1918; Božić et al., 2009; Gupta and Babu, 2009a; 2009b; Huang et al., 2009).

$$R_L = \frac{1}{1 + bC_0} \tag{4.1}$$

4.1.2 Freundlich Isotherm

The Freundlich isotherm (Table 4.1) model which supports the heterogeneous adsorption process. This isotherm model illustrates that the ratio of the amount of solute adsorbed onto a given mass of adsorbent to the concentration of solute in the solution is not constant at different concentrations. For many systems, the heat of adsorption decreases in magnitude with increasing the extent of adsorption. This aspect has been incorporated in the Freundlich isotherm. K_F and n_F represents the Freundlich isotherm constants where K_F indicates the relative adsorption capacity of the adsorbent related to the bonding

energy and n_F is the representation of the heterogeneity of the process (Freundlich, 1932; Bhattacharya et al., 2008; Gupta and Babu, 2009a; 2009b; Wang and Li, 2009; Al-Ghouti et al., 2010).

4.1.3 Tempkin Isotherm

The Tempkin isotherm model (Table 4.1) contains a factor that takes into account of the adsorbent–adsorbate interactions. It is based on the assumption that the heat of adsorption of all the molecules in the layer decreases linearly with the coverage of molecules due to the adsorbate–adsorbate repulsions. It also assumes that the adsorption of adsorbate is uniformly distributed. The fall in the heat of adsorption is more linear rather than logarithmic, as implied in the Freundlich isotherm. The applicability of the Tempkin isotherm plot can be validated with the plot of q_e vs. ln C_e. The slope and intercept of this plot provide the Tempkin isotherm constants, A_T and B_T. Here, A_T represents the equilibrium binding constants and B_T is related with the value of b_T ($B_T = RT/b_T$) which provides the information of the heat of adsorption (Tempkin and Pyzhev, 1940; Gupta and Babu, 2009a; 2009b; Mittal et al., 2009).

4.2 Adsorption Kinetic Models

The kinetic experimental data are used to evaluate the rate and kinetic behavior of the adsorption process. The kinetic parameters are useful in predicting the rate of adsorption which is an important information in designing and modeling of the adsorption process. The various rate models used to study the kinetic behavior of the metals adsorption are pseudo-first order, second order and Elovich model. The linear forms of these models

(Table 4.2) are utilized to estimate the rate kinetic parameters and constants by the use of experimental data.

In the pseudo-first order kinetic model, the Lagergren (1898) showed that the adsorption capacity is an important factor affecting the adsorption of the solute on the adsorbent. The variation of true first order with the pseudo-first order are having two major consensus: (1) the parameter $k_1(q_e - q_t)$ does not represent the number of available sites; (2) the parameter log q_e which is an adjustable parameter and often found not to be equal to the intercept of the plot of $\log(q_e - q_t)$ versus t. While, it should be equal to the intercept when the true first order model is considered (Ho and McKay, 1998; Gupta and Babu, 2009a). The applicability of pseudo-first order kinetic model is evaluated by plotting graphs of log $(q_e - q_t)$ vs t. The obtained slope and intercept from the linear fit are used to estimate the value of q_e and k_{ad}. The second order rate kinetic model is used to calculate the value of q_e. The applicability of the second order kinetic model is evaluated by plotting a graph of $1/(q_e - q_t)$ vs. t. The best fit straight line helps in estimating the value of q_e and k_2. A graph of q_t vs. ln t is plotted to check the applicability of Elovich model. The slope and intercept of the best fit straight line would be used to estimate the Elovich model constants, α and β.

Table 4.1: Isotherm models along with their linear representative equations.

Isotherm Model	Linear Equation	Reference
Langmuir	$\frac{C_e}{q_e} = \frac{1}{bq_m} + \frac{C_e}{q_m}$	Langmuir (1916)
Freundlich	$\log(q_e) = \log(K_F) + n_F \log(C_e)$	Freundlich (1906)
Tempkin	$q_e = B_T \ln A_T + B_T \ln C_e$	Tempkin and Pyzhev (1940)

Table 4.2: Kinetic models along with their linear representative equations.

Kinetic Model	Linear Equation	Reference
Pseudo-first order	$\log(q_e - q_t) = \log q_e - k_{ad}\left(\frac{t}{2.303}\right)$	Lagergren (1898)
Second order	$\frac{1}{(q_e - q_t)} = \frac{1}{q_e} + k_2 t$	Ho and McKay (1998); Ho (2006)
Elovich model	$q_t = \frac{1}{\beta}\ln(\alpha\beta) + \frac{1}{\beta}\ln(t)$	Zeldowitsch (1934)

4.3 Mass Transfer Model

In the adsorption process, the movements of the adsorbate molecules occur from the fluid phase to the solid phase via different mechanisms. Initially, the molecules of the adsorbate transport from the bulk phase of the liquid to the surface of the adsorbent which is called as the Film diffusion. Further, molecules transport from the surface to the interior of the particle which is termed as the intraparticle diffusion. The molecule is finally adsorbed in the interstitial sites of the porous adsorbent. In the present study, the Weber & Moris (Weber and Morris, 1963; Malash and El-Khaiary, 2010; Kapur and Mondal, 2013) and the Boyd (Boyd et al., 1947; Malash and El-Khaiary, 2010; Kapur and Mondal, 2013) models are used to study the rate-limiting mechanism for the metal adsorption on nANB adsorbent.

4.3.1 Weber & Morris Model

In the adsorption process, the rate of mass transfer of adsorbate molecules is controlled by the film diffusion or intraparticle diffusion or both. Weber & Moris (Weber and Morris, 1963) proposed the intraparticle diffusion model and is given by Eq. 4.2:

$$q_t = K_{id} t^{1/2} + I \qquad (4.2)$$

where K_{id} (mg g^{-1} $min^{-1/2}$) and I represents the intraparticle diffusion rate constant and thickness of the boundary layer respectively. According to this model, a straight line passing through the origin for a plot of solute adsorbed versus the square root of time represents the perfect intraparticle diffusion. However, if the line does not pass through the origin, then there is a possibility of film diffusion mass transfer mechanism.

4.3.2 Boyd Model

An apparent differentiation between the intraparticle and film diffusion has to be made for the clear understanding of the adsorption mechanism. Boyd model is used for the film diffusion and is represented by Eqs. 4.3 and 4.4 (Boyd et al., 1947).

$$F = 1 - \frac{6}{\pi^2} \exp\ (-Bt) \tag{4.3}$$

$$F = \frac{q_t}{q_e} \tag{4.4}$$

where, the F is the fraction of solute adsorbed at a time t, and B is a function of F. Eq. 4.3 can be rearranged in the linear form and is given by Eq. 4.5.

$$Bt = [-0.4977 - \ln(1 - F)] \tag{4.5}$$

The applicability of the Boyd model can be confirmed by fitting the experimental data linearly for [-0.4977 - ln(1-F)] versus time. If the linear plot of the graph is not passing through the origin, then it confirms that the process is film diffusion controlled.

4.4 Conceptualization of the Model

In process analysis, modeling is of great interest. It is essential for forecasting the response and behavior of the system on the basis of reliant input parameters. Any experimental data can be well fitted by a suitable polynomial function. In the present study, the initial concentration, contact time, pH and the adsorbent dosage are being considered as input parameters for the modeling of the system. The experimental data are utilized to obtain 1^{st}, 2^{nd}, 3^{rd}, 4^{th}, 5^{th} order polynomial equation. It is observed that the regression correlation coefficient (R^2) value increases with the order of the polynomial,

while it is found unchanged after the 4th order polynomial. Therefore, the polynomial of fourth order (Eq. 4.6) is utilized to anticipate the response of the system in terms of the adsorption capacity of the adsorbent.

$$q_{\text{pre}} = a_0 + \sum a_{\text{i1}} X_{\text{i}} + \sum a_{\text{i2}} X_{\text{i}}^2 + \sum a_{i3} X_i^3 + \sum a_{i4} X_i^4 \text{s} \qquad (4.6)$$

where i represents the number of independent variables and can vary from 1 to n depending on the number of parameters, q_{pre} represents the predicted adsorption capacity, a_0 represents the intercept coefficient and a_{i1}, a_{i2}, a_{i3} *and* a_{i4} are the constants for 1st, 2nd, 3rd and 4th order variables and X_{i} represents the normalized value of i^{th} dependent variable.

The experimental data obtained during the various experiments for each parameter are normalized on the basis of maximum parametric value considered in all the experimentations for that parameter. The normalized experimental values of all parameters are regressed using Microsoft Excel 2007 to fit the fourth order polynomial (Eq. 4.6). The generalized form of obtained regressed equation is represented by Eq. 4.7.

$$\begin{aligned} q_{\text{pre}} = {} & a_0 + \text{a}_{11}\text{X}_1 + \text{a}_{21}\text{X}_2 + \text{a}_{31}\text{X}_3 + \text{a}_{41}\text{X}_4 + a_{12}X_1^2 + a_{22}X_2^2 + a_{32}X_3^2 + a_{42}X_4^2 \\ & + a_{13}Z_1^3 + a_{23}X_2^3 + a_{33}X_3^3 + a_{43}X_4^3 + a_{14}X_1^4 + a_{24}X_2^4 + a_{34}X_3^4 + a_{44}X_4^4 \end{aligned} \qquad (4.7)$$

where X_1, X_2, X_3 and X_4 are representing the inlet concentration, pH, contact time and adsorbent dosage respectively. Also the a_0 is the intercept coefficient and $a_{1\text{i}}$, $a_{2\text{i}}$, $a_{3\text{i}}$ and $a_{4\text{i}}$ are the coefficients for the first order, second order, third order and fourth order variables respectively. This equation leads to a mathematical model which can be used to predict the adsorption capacity of the adsorbent on substituting the various independent parameters.

4.5 Optimization

In the last few decades, there has been an increase in the interest towards the optimization of the parameters to make the process more efficient. There are various optimization algorithms available in the literature which can be used to solve the mathematical modeling equations and to obtain the optimum values for the dependent parameters. These algorithms are being examined on the belief of evolution, which states the survival of the fittest. The various algorithms available are Differential Evolution, Microsoft Excel Solver, Genetic Algorithm, Genetic Programming, Evolutionary Programming and Evolution Strategies (Nath and Das, 2011; Datta and Kumar, 2012; Fakhri, 2014). A conceptualized description of the evolutionary computation procedures is being presented by Babu (2007).

Differential Evolution (DE) is one of the most robust technique which utilizes the population based technique and is very much competent with other processes (Kumar et al., 2011a). The DE is having various advantages such as it is bare and straight forward to use arrangement, high speed and rugged nature (Storn and Price, 1997; Babu, 2007).

In the present study, the focus is to optimize a single equation with a single objective function. DE is used to solve the modeled equation. An algorithm is developed using the basic aspects of DE (Fig 4.1) and a code is developed to implement the developed algorithm using the platform of MATLAB 7 (Kumar et al., 2011b; Buehren, 2012). A minimization approach is taken for the optimization process. The function utilized here for the optimization is given in Eq. 4.8.

$$Z = q_{calc} - q_{pre} \tag{4.8}$$

where q_{calc} is the adsorption capacity obtained by varying individual parameters in DE and q_{pre} is the value obtained using the Eq. 4.7.

4.6 Mathematical Modeling of Fixed-bed Adsorption Column

The design of fixed-bed adsorption column is very complicated. The proper understanding and suitable design could be proposed by having the better understanding of the mathematical models. The behavior of the adsorption column can be explained in terms of the effluent concentration and the time profile, which is seldom termed as the breakthrough curve. The response of the column is very well explained by important parameters like breakthrough time and the shape of the curve. Breakthrough time corresponds to the time required to reach the outlet concentration of pollutant to its permissible limit. In most of the cases, the breakthrough concentration is in the range of 1-5 % of the feed concentration. Generally, the primary factors affecting the breakthrough time are the mass of adsorbent or the column height, the flow rate and the feed concentration. With the passage of time, the effluent concentration will suddenly increase from zero/low metal concentration to the inlet concentration. These results would be helpful in estimating the column adsorption capacity (Aksu and Gönen, 2004; Chu, 2004; Keshtkar et al., 2012). The data obtained from the laboratory scale continuous adsorption experiments are helpful in estimating the important design parameters which are discussed in the following paragraphs.

The total amount (stoichiometric) of metal adsorbed (q_t, mg) for a given initial metal concentration and flow rate for the column is obtained using Eq. 4.9.

$$q_t = \frac{QA_c}{1000} = \frac{Q}{1000}\int_{t=0}^{t=t_{total}} C_{ad}\,dt \text{ s} \tag{4.9}$$

The quantity of A_c, i.e. the area underneath the curve is acquired by plotting a graph of the adsorbed concentration (C_{ad}, mg L^{-1}) with respect to the time (t, min). The Q in the Eq. 4.8 is representing the flow rate during the process in mL min^{-1}. The amount of the total metal ion passed through the column (m_t) can be evaluated using Eq. 4.10.

$$m_t = \frac{C_{bo} Q t_t}{1000} \tag{4.10}$$

where, t_t is the time equivalent to the total stoichiometric capacity of the fixed-bed column and is given by Eq. 4.11.

$$t_t = \frac{q_t t_f}{m_t} \tag{4.11}$$

where t_f is representing the total time of the process. The amount of total metal removed in terms of percentage removal is calculated using Eq. 4.12.

$$\text{Total percentage removal of metal ion } (S) = \frac{q_t}{m_t} \times 100 \tag{4.12}$$

The total time needed to reside in the empty column is determined as the empty bed residence time (EBRT) and is calculated using Eq. 4.13.

$$EBRT = \frac{\text{Bed volume}}{\text{Volumetric flow rate of liquid}} \tag{4.13}$$

An additional parameter determined in the continuous experiments is the adsorbent exhaustion rate (R_a) which indicates the amount of the adsorbent (W) utilized on the basis of a unit volume of liquid treated till the breakthrough time. It is estimated by Eq. 4.14.

$$\text{Adsorbent exhaustion rate} (R_a) = \frac{\text{mass of adsorbent in column}}{\text{volume treated at breakthrough}} \tag{4.14}$$

The fraction of the unused bed length (y) is evaluated using Eq. 4.15.

$$y = 1 - \frac{t_b}{t_t} \tag{4.15}$$

where t_b is the breakthrough time of the process.

Due to the complex nature of the fixed-bed adsorption process, Yoon-Nelson and Yan mathematical models are utilized for predicting the dynamic behavior of the column (Aksu and Gönen, 2004; Salamatinia et al., 2008; Keshtkar et al., 2012).

4.6.1 The Yoon-Nelson Model

A simple model was developed by Yoon-Nelson (Yoon and Nelson, 1984) which addresses the adsorption and the breakthrough process of the vapors or gases on the activated carbon. The probability of adsorption is directly proportional to the solution breakthrough on the developed adsorbent (Calero et al., 2009). The Yoon-Nelson equation with respect to a single component system is expressed as Eq. 4.16.

$$\frac{C_i}{C_{0,i}} = \frac{\exp(K_{YN,i} \times t - K_{YN,i} \times \tau_i)}{1 + \exp(K_{YN,i} \times t - K_{YN,i} \times \tau_i)} \tag{4.16}$$

where $K_{YN,i}$ represents the Yoon-Nelson rate constant of i^{th} component (h^{-1}), τ_i represents the time required for 50% of i^{th} adsorbate breakthrough (h), and t is the sampling time (h). The analysis of the breakthrough curves with the help of the model requires the evaluation of the model parameters $K_{YN,i}$ and τ_i.

4.6.2 The Yan Model

The basis of the Yan model is the statistical analysis of the experimental results along with some of the simplifications (Yan et al., 2001). Yan model is more realistic than other

models as it explains the entire breakthrough curve with more precision. The model can be represented by Eq. 4.17.

$$\frac{C_i}{C_{0,i}} = 1 - \frac{1}{1 + \left(\left(\frac{0.001 \times C_{o,i} \times Q}{q_{o,i} \times M} \right) \times t \right)^{a_i}} \tag{4.17}$$

where, a_i and $q_{0,i}$ are the Yan model parameters. Here, the relation between the model parameters with the experimental condition is impossible which leads to an impossible scaling up of the process (Keshtkar et al., 2012).

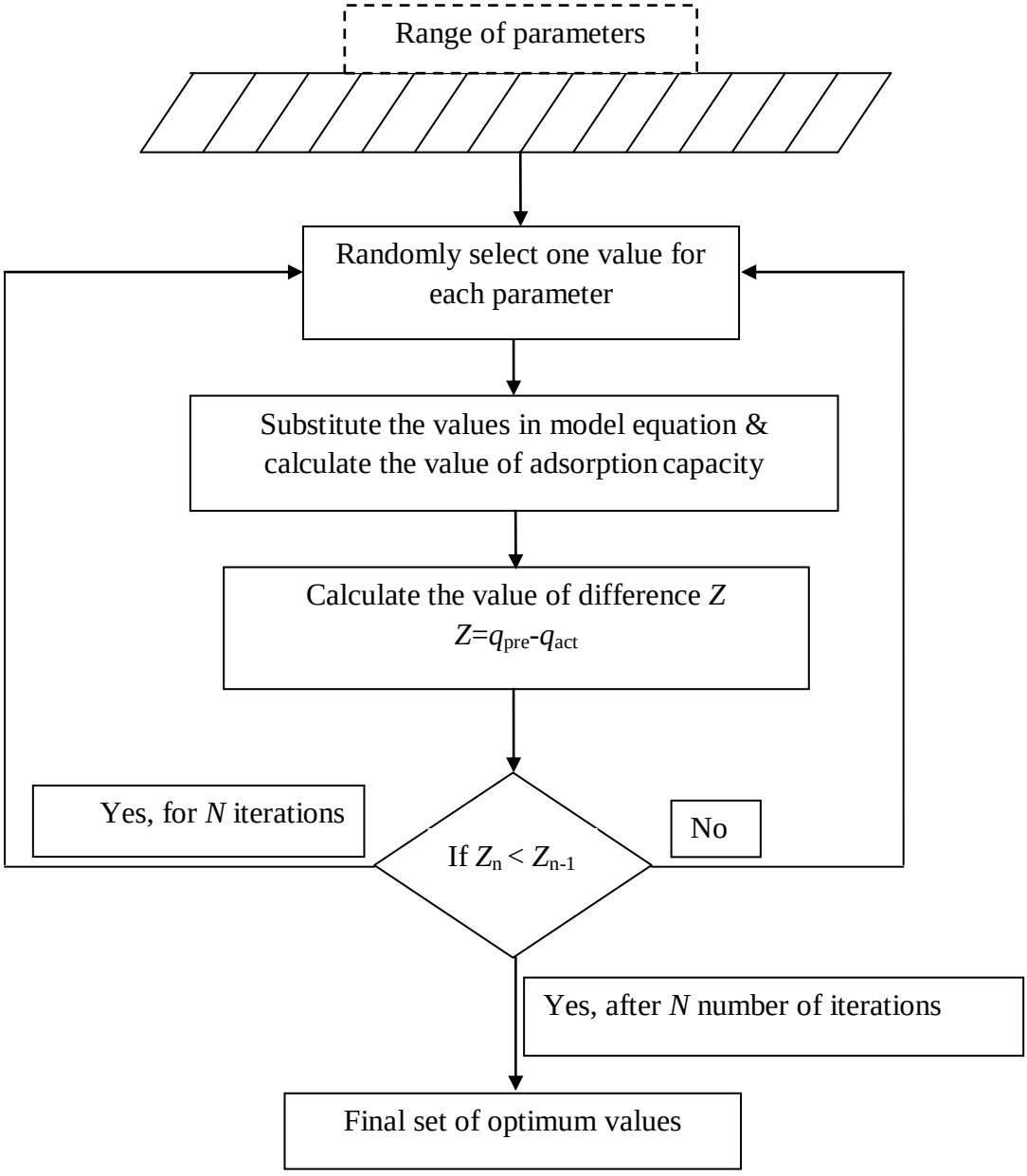

Fig 4.1: Algorithm for the evaluation of optimum parameters.

CHAPTER 5
RESULTS AND DISCUSSION

In the present study, the neem bark is activated by different activation procedures. The performance of six developed ANBs are evaluated for the removal of Cr(VI), Cu(II) and Zn(II) by performing equilibrium batch experiments. The ANB, which has shown a better adsorption capacity for the Cr(VI), Cu(II) and Zn(II) adsorption has been considered for further characterization and experimental studies. The results obtained for batch and continuous experimental studies are discussed in detail in the following sections.

5.1 Selection of nANB

The equilibrium experiments are performed to evaluate the performance of six (ANB1 to ANB6) developed adsorbents for the removal of Cr(VI), Cu(II) and Zn(II) using neem bark as the raw material. The inlet concentration is varied from 5 to 200 mg L^{-1} for all the experiments while keeping other parameters constant (Table 3.3). The results obtained for the Cr(VI), Cu(II) and Zn(II) removal using six ANBs are plotted as q_e vs. C_e (Figs 5.1, 5.3 and 5.5) and percentage removal vs. C_e (Figs 5.2, 5.4 and 5.6). The solid phase concentration of ANB1 for Cr(VI) adsorption is approximately double to that calculated for the other ANBs (Fig 5.1). The percentage removal of Cr(VI) using ANB1 is also found significantly higher than other ANBs (Fig 5.2). The solid phase concentration with the use of ANB2 and ANB6 is observed to be higher than that obtained by ANB1 for the removal of Cu(II), however, the obtained value for the ANB1 is nearly same to the ANB2 and ANB6 (Fig 5.3). Similar results are obtained for the removal of Cu(II) using ANB2, ANB5 and ANB6 in comparison to that of ANB1 (Fig 5.4). Similarly, ANB2, ANB5 and

ANB6 are showing higher solid phase concentration of Zn(II) as compared to ANB1, ANB3 and ANB4 (Fig 5.5). However, ANB1 shows better capacity for Zn(II) adsorption as compared to ANB3 and ANB4. Likewise, percentage removal is higher for Zn(II) removal using ANB2, ANB5 and ANB6 as compared to that for ANB1 (Fig 5.6). In the real scenario, the industrial effluent streams contain several metal ions, hence, the adsorbent employed must have significant capacity to simultaneously adsorb multiple metal ions. On a whole, ANB1 is found to have better adsorption capacity for Cr(VI), comparatively good for Cu(II) and significant for Zn(II) as compared to other developed ANBs. The maximum adsorption capacity obtained during equilibrium experiments using ANB1 to ANB6 for the removal of Cr(VI), Cu(II) and Zn(II) are tabulated in Table 5.1. It is observed that the overall adsorption capacity of ANB1, ANB2 and ANB6 are very close. However, the adsorption capacity of ANB1 for Cr(VI) adsorption is significantly higher (≈ 50%) as compared to ANB2 and ANB6. Cr(VI) is more harmful as compared to other metals [Cu(II) and Zn(II)]. Hence, the selection of suitable adsorbent is mainly dominated by the adsorption capacity for Cr(VI). Although the adsorption capacities of ANB2 and ANB6 are better for Cu(II) and Zn(II) adsorption, however, based on the above mentioned fact, ANB1 is selected for different heavy metals adsorption. The equilibrium data obtained for ANB1 to ANB6 for the removal of Cr(VI), Cu(II) and Zn(II) are fitted with Langmuir isotherm and the estimated isotherm parameters are reported in Table 5.2. The maximum adsorption capacity of ANB1 for the adsorption of Cr(VI), Cu(II) and Zn(II) are found to be 26.95, 21.23 and 11.904 mg g^{-1} respectively which are maximum among all the ANBs. Based on the experimental and theoretical

evaluation of developed ANBs, ANB1 is considered as suitable adsorbent for the single and multiple metal ions adsorption from wastewater streams.

The ANB1 is also tested for the removal of other metal ions such as Cd(II), Ni(II) and Pb(II) to check its wider industrial applicability. The equilibrium experiments are performed for Cd(II), Ni(II) and Pb(II) removal and results are plotted in Fig 5.7. The solid phase concentration for Cd(II), Ni(II) and Pb(II) adsorption using ANB1 are found to be 13.43, 22.28 and 8.42 mg g^{-1} respectively for the initial concentration of 200 mg L^{-1}. The maximum adsorption capacity parameter of Langmuir isotherm is also estimated and is obtained as 20.833, 29.412 and 26.316 mg g^{-1} for Cd(II), Ni(II) and Pb(II) adsorption respectively (Table 5.2). Thus, this study supports the capability of ANB1 to be used for the adsorption of Cr(VI), Cu(II), Cd(II), Ni(II), Pb(II) and Zn(II) and is considered for further experimental studies and is termed as nANB.

5.2 Characterization

The developed ANBs (ANB1 to ANB6) are characterized using FTIR and the analysis is shown in Fig 5.8. It is observed that the ANB1 is showing two extra peaks in comparison to the ANB 2 to ANB6. The specific peaks which are making ANB1 different than others are at 3300 and 1027 cm^{-1} which are corresponding to the O-H and C-O bond respectively. The presence of O-H and C-O bonds on the adsorbent surface confirms the acidic nature of the surface, which favors the metal adsorption (Depci et al., 2012; Kaya et al., 2014). This also supports the applicability of ANB1 as compared to the other ANBs for the multiple metals adsorption. The FTIR analysis of ANB1(nANB) is separately shown in Fig 5.9 for better understanding of the available functional groups on the surface.

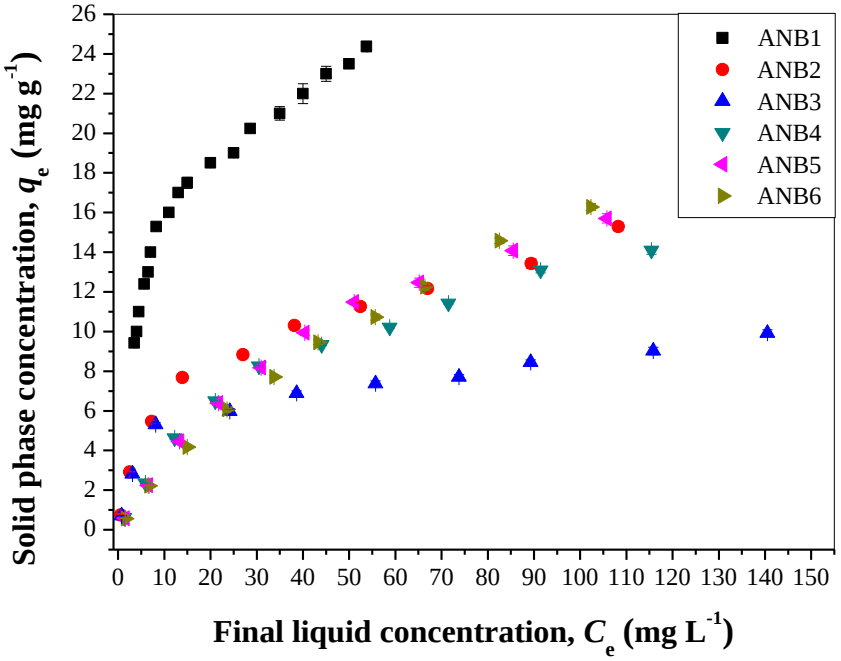

Fig 5.1: q_e vs. C_e for the removal of Cr(VI) using various ANBs.

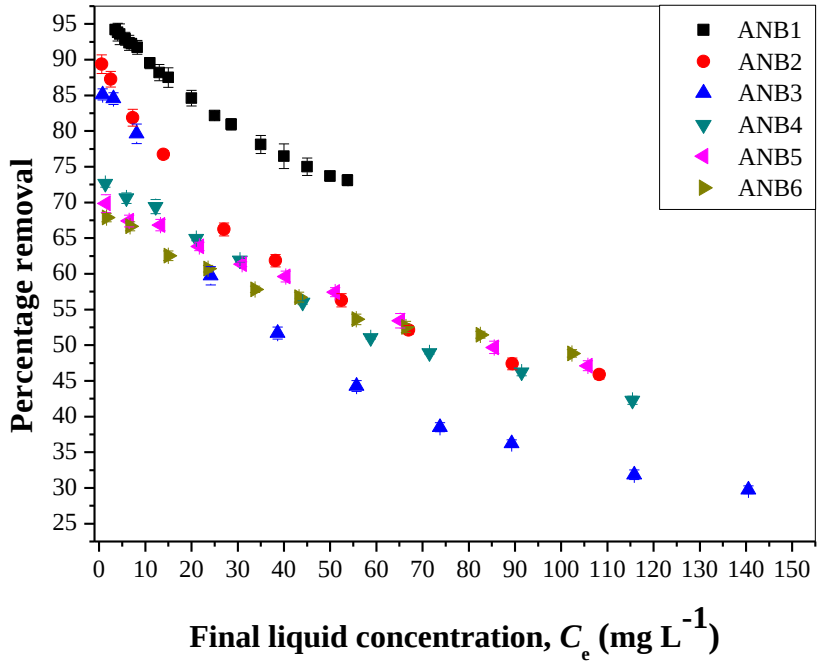

Fig 5.2: Percentage removal vs. C_e for the removal of Cr(VI) using various ANBs.

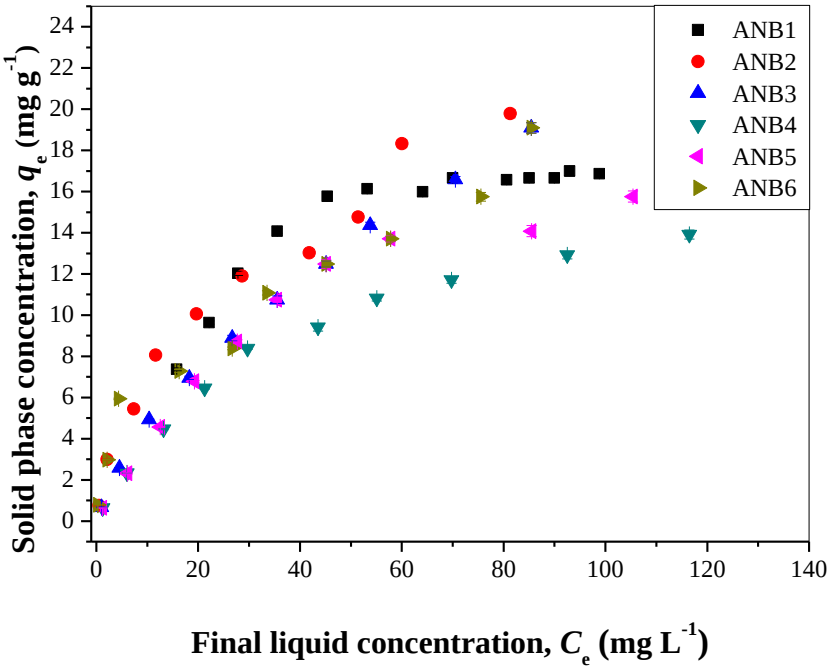

Fig 5.3: q_e vs. C_e for the removal of Cu(II) using various ANBs.

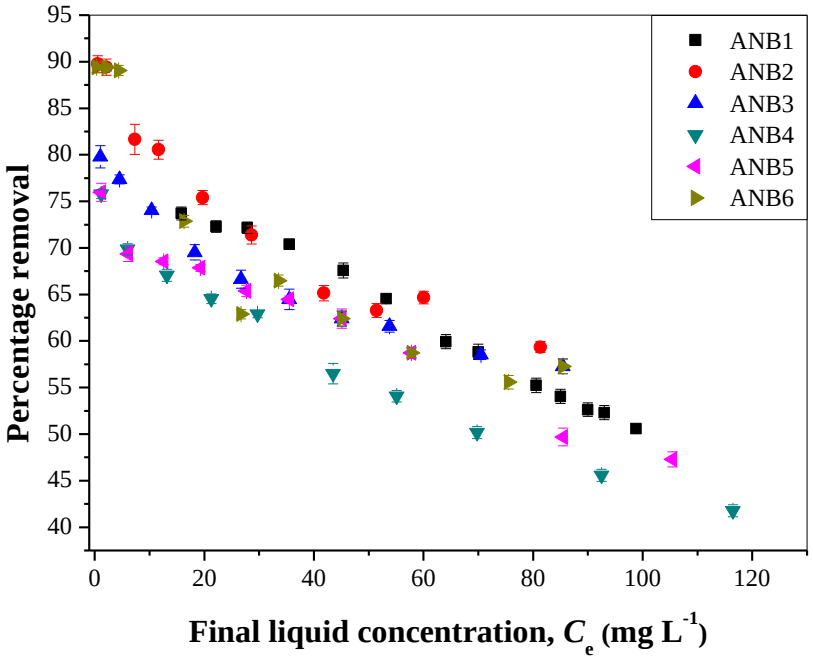

Fig 5.4: Percentage removal vs. C_e for the removal of Cu(II) using various ANBs.

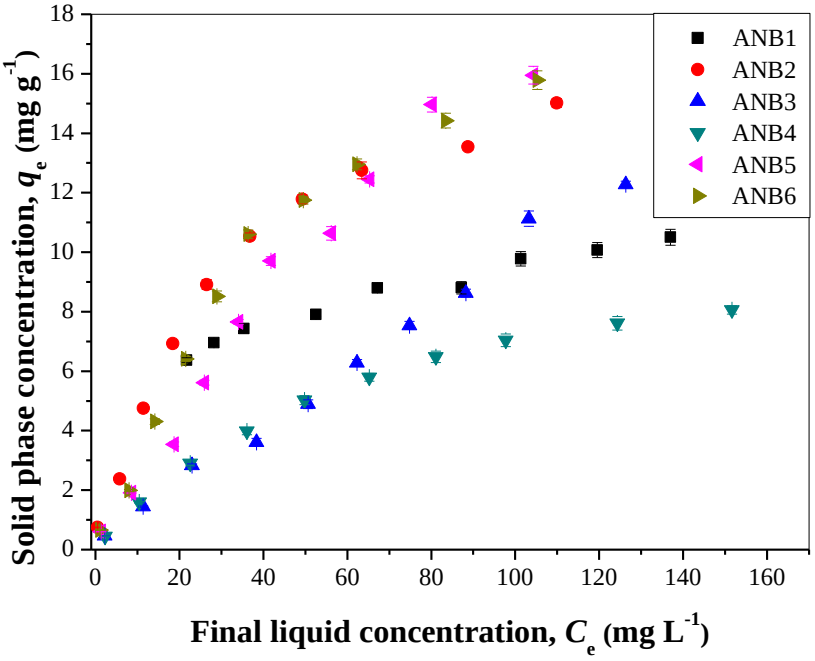

Fig 5.5: q_e vs. C_e for the removal of Zn(II) using various ANBs.

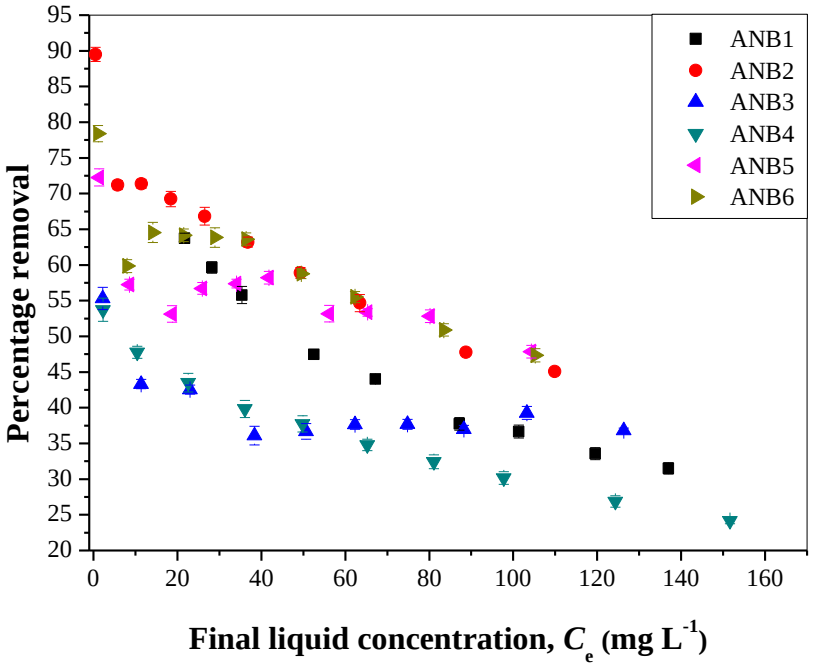

Fig 5.6: Percentage removal vs. C_e for the removal of Zn(II) using various ANBs.

Table 5.1: Maximum solid phase capacity obtained from equilibrium experiments.

Adsorbent	Maximum q_e from Experiments (mg g^{-1})			
	Cr(VI)	**Cu(II)**	**Zn(II)**	**Total**
ANB1	24.37	16.87	10.50	51.74
ANB2	15.29	19.78	15.02	50.09
ANB3	9.92	19.10	12.28	41.30
ANB4	14.09	13.92	8.06	36.07
ANB5	15.71	15.76	15.95	47.42
ANB6	16.28	19.10	15.76	51.14

Table 5.2: Langmuir isotherm parameters for the removal of Cd(II), Cr(VI), Cu(II) Ni(II), Pb(II) and Zn(II).

Metal	Adsorbent	Langmuir Parameters			R^2
		b	q_m (mg g^{-1})	R_L	
Cr(VI)	ANB1	0.144	26.95	0.034 - 0.104	0.995
	ANB2	0.113	13.158	0.042 - 0.639	0.999
	ANB3	0.105	9.901	0.045 - 0.656	0.995
	ANB4	0.040	14.286	0.111 - 0.833	0.997
	ANB5	0.016	25.000	0.238 - 0.926	0.999
	ANB6	0.015	23.810	0.250 - 0.930	0.999
Cu(II)	ANB1	0.045	21.23	0.100 - 0.270	0.976
	ANB2	0.089	17.241	0.053 - 0.692	0.997
	ANB3	0.130	20.001	0.037 - 0.606	0.999
	ANB4	0.022	19.231	0.185 - 0.901	0.995
	ANB5	0.030	17.857	0.143 - 0.870	0.996
	ANB6	0.230	11.628	0.021 - 0.465	0.992
Zn(II)	ANB1	0.045	11.904	0.100 - 0.270	0.991
	ANB2	0.166	9.174	0.029 - 0.546	0.963
	ANB3	0.023	9.346	0.179 - 0.897	0.987
	ANB4	0.016	11.494	0.238 - 0.926	0.996
	ANB5	0.032	11.495	0.135 - 0.862	0.978
	ANB6	0.009	11.364	0.357 - 0.957	0.969
Cd(II)	ANB1	0.0153	20.833	0.246 - 0.521	0.995
Ni(II)	ANB1	0.0386	29.412	0.115 - 0.302	0.982
Pb(II)	ANB1	0.0037	26.316	0.575 - 0.818	0.989

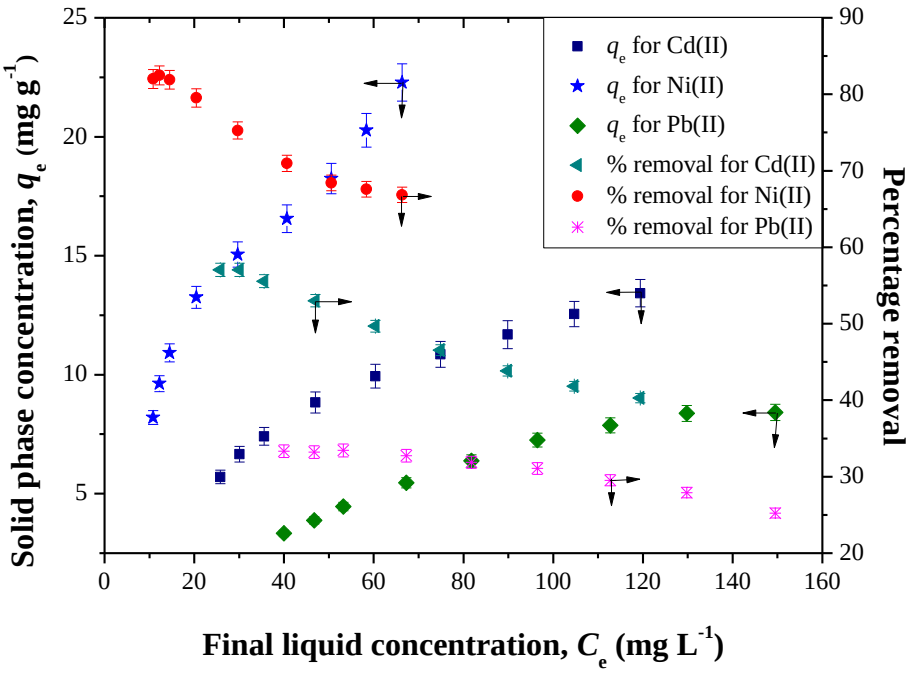

Fig 5.7: q_e vs. C_e for the removal of Cd(II), Ni(II) and Pb(II) using ANB1.

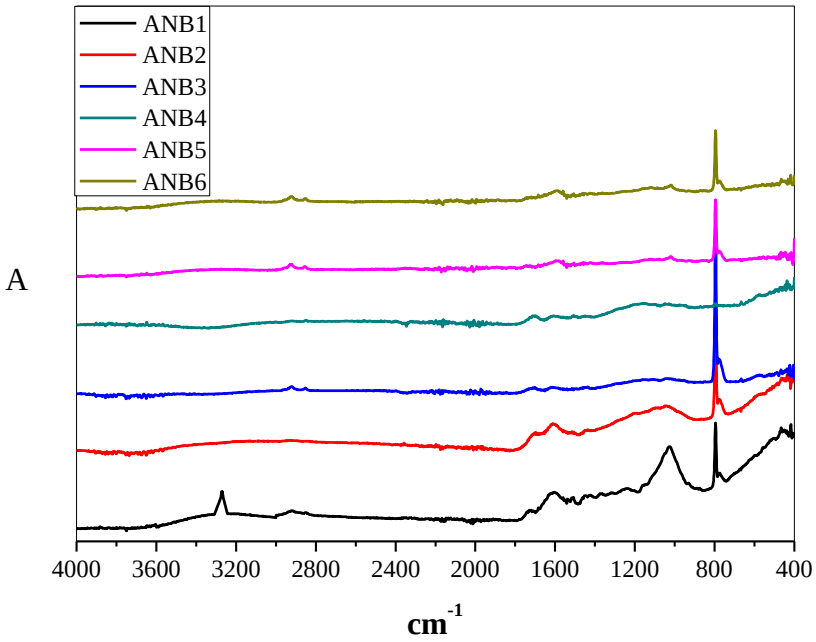

Fig 5.8: FTIR spectra for ANB1 to ANB6 from 4000 to 400 cm^{-1} wavelength.

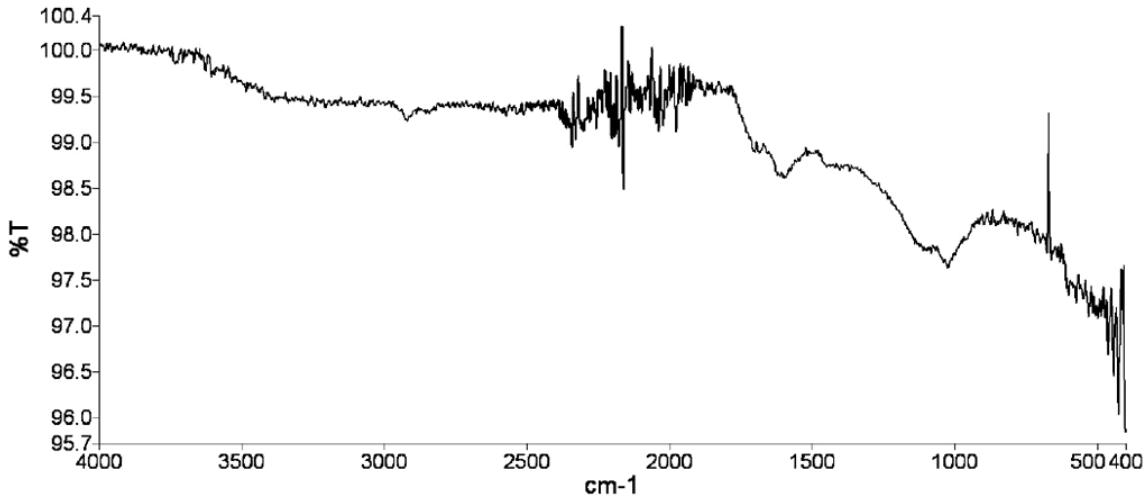

Fig 5.9: FTIR for fresh nANB for 4000 to 400 cm^{-1} wavelength.

A wavy spectrum is obtained in place of a smooth one which confirms the amorphous nature of the developed ANB1. According to the peaks identified at 670 & 2900, 1120, 1540, 1620 and 2152 cm^{-1} confirms the presence of C-H, C-O, C=O, C=C and C≡C stretching vibrations respectively. The availability of water molecules (i.e. O-H stretching mode of hydroxyl groups) is supported by the presence of a peak at 3300 cm^{-1} (Bakiler et al., 1999; Kaya et al., 2014). The presence of C-O and C=O suggests the existence of various acidic groups on the surface of ANB1 (Depci et al., 2012; Kaya et al., 2014).

In the present study, the selected nANB is further characterized by SEM, EDS, BET Surface area, XRD and TGA to study the characteristic behavior of the developed nANB. SEM and EDS analysis of fresh nANB is shown in Fig 5.10. The SEM image in Fig 5.10(a) provides the morphology of the surface of the fresh nANB. The presence of different size of the pores on the surface of fresh nANB are clearly visible [Fig. 5.10(a)]. The comparison of the size of the pores with image resolution, confirms the presence of significant number of 10-100 nm size pores along with other pores. This supports the nano-porous characteristics of the nANB adsorbent. The heavy metals selected for the adsorption in the present have ionic diameter less than 20 nm which is lesser then the pore size of developed adsorbent. This confirms the possible utilization of these pores for the heavy metals adsorption.

The SEM and EDS analysis of used nANB for Cr(VI), Cu(II) and Zn(II) removal are shown in Figs 5.11, 5.12 and 5.13 respectively. The surface morphology of the used nANB shows clearly the utilization of the nano-pores for the metal adsorption while comparing with the surface morphology of the fresh nANB [Figs 5.10(a) to 5.13(a)]. The EDS analysis of fresh nANB [Fig. 5.10(b)] confirms the absence of any metal at the

surface of the fresh adsorbent. The highest peak is observed for carbon (C), which is approximately 55.35% of the total adsorbent by weight. This may be due to the utilization of the carbonaceous material (neem bark) for the preparation of the adsorbent. The EDS analysis of the surface of the used nANB shows the presence of Cr(VI), Cu(II) and Zn(II) [Figs 5.11(b) to 5.13(b)]. The EDS analysis of used nANB suggests the presence of 10, 3 and 2 wt.% of Cr(VI), Cu(II) and Zn(II) respectively. This also supports the significant adsorption of Cr(VI), Cu(II) and Zn(II) on the nANB. The presence of Potassium (K) (1 wt%) can be clearly seen in the Cr(VI) saturated adsorbent [Fig 5.11(b)] which may be due to the use of Potassium dichromate as a preparatory chemical for Cr(VI) stock solution.

The surface area of the developed nANB is analyzed using the BET surface area analyzer. The measured value of specific surface area of nANB is found as 36.64 m^2 g^{-1} which is higher in comparison with some of the other adsorbents reported in Table 5.3. Higher surface area of the adsorbent supports higher adsorption capacity for metal removal (Hossain et al., 2010).

The phase of the developed nANB is also characterized using XRD. In the present study, diffractometer uses Cu-K_α radiation. The wavelength considered is 1.54 Å and angle 2θ has varied in a range of 10 to 90° at a step size of 0.01°. The XRD pattern for the nANB is shown in Fig 5.14. There is no sharp peak observed in the spectrum and therefore, the particle size of developed adsorbent cannot be estimated using the Scherrer's formula. This also confirms the amorphous nature of the adsorbent. Taha and Ibrahim (2014) also reported the similar FTIR analysis for the Nano zero-valent iron particles.

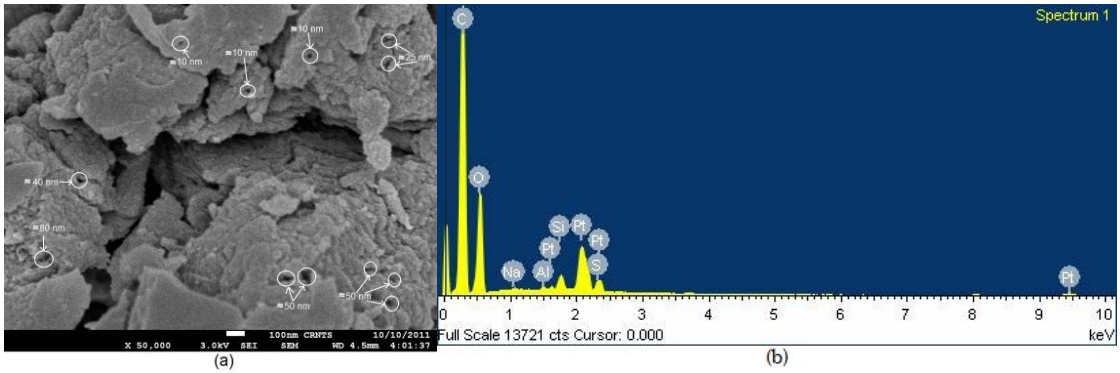

Fig 5.10: (a)SEM and (b)EDS for fresh nANB.

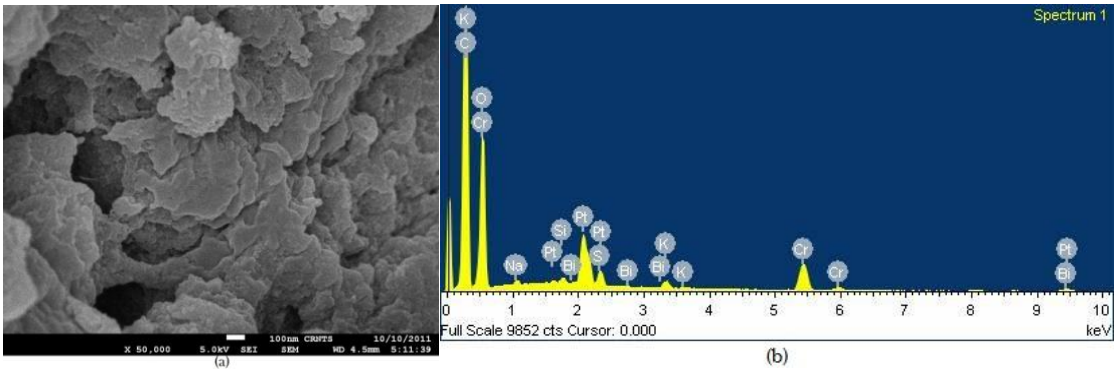

Fig 5.11: (a)SEM and (b)EDS for used nANB on pure Cr(VI) solution.

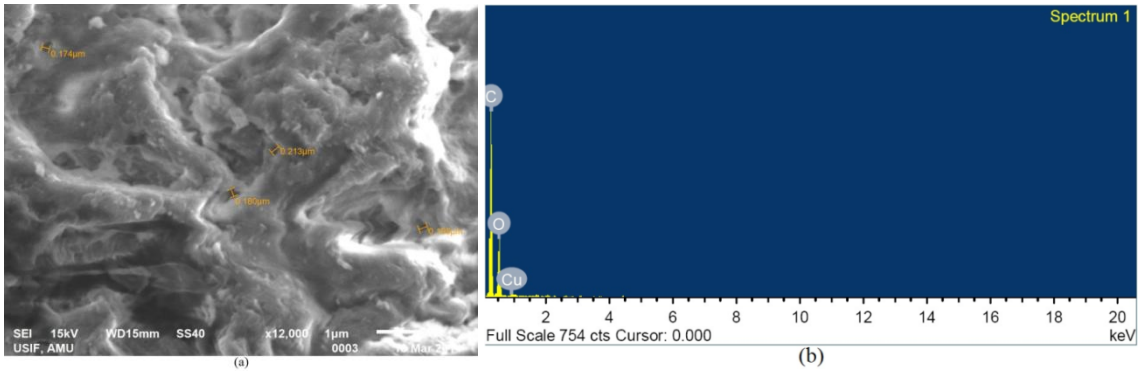

Fig 5.12: (a) SEM and (b) EDS for saturated nANB on Cu(II) solution.

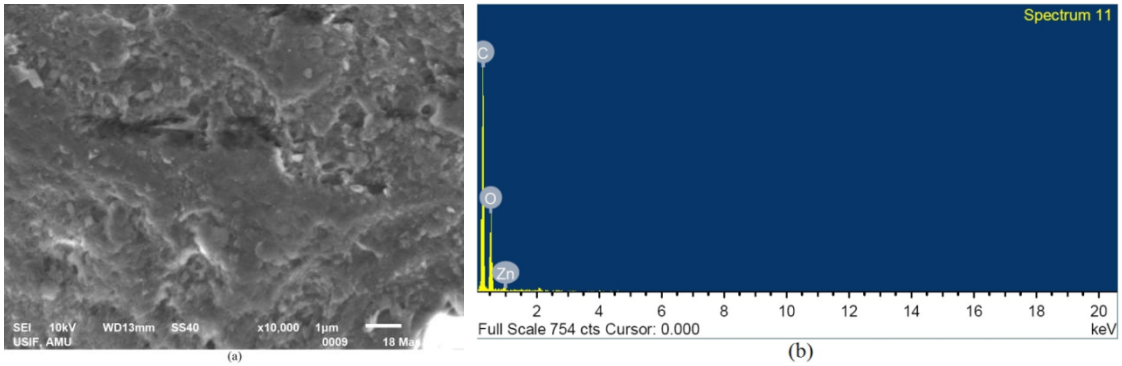

Fig 5.13: (a) SEM and (b) EDS for saturated nANB on Zn(II) solution.

TGA analysis of the developed nANB is shown in Fig 5.15. It can be seen that there is a slow decrease upto 90 wt.% by increasing the temperature upto 100°C and further decrease to 82 wt.% when the temperature rises upto 240°C. The initial dip in the weight percent may be due to the removal of surface moisture. Further increase in the temperature (>240°C) results in the slow rate of pyrolysis and burning of the adsorbent. Finally, nANB completely converts into ash, when the temperature has reached to approximately 550°C. Further increase in temperature will not affect the weight of nANB as there will be only ash left in the analysis chamber. The result of TGA analysis indicates that the developed adsorbent is thermally stable up to 200^{o}C. TGA results also suggests that the saturated adsorbent can be regenerated at higher temperatures (upto 200°C) without any degradation of adsorbent.

Table 5.3: Surface area of various developed low-cost adsorbents.

S.No.	Adsorbent	Surface Area (m^2 g^{-1})	References
1	nANB	36.64	**Present Study**
2	Alkaline-activated montmorillonite	30.7	Akpomie and Dawodu (2014)
3	Oak bark char	25.4	Mohan et al. (2014)
4	Rice husk biochar	25.161	Samsuri et al. (2013)
5	Montmorillonite	23.2	Akpomie and Dawodu (2014)
6	Activated Neem Leaves	15.284	Babu and Gupta (2008b)
7	Magnetic oak bark char	8.8	Mohan et al. (2014)
8	Tamarind seeds	2.61	Gupta and Babu (2009a)
9	Coir pith	2.3	Namasivayam and Sureshkumar (2008)
10	Empty fruit bunch biochar	1.89	Samsuri et al. (2013)
11	Water bamboo husk	1.87	Asberry et al. (2014)
12	Formosa papaya seed powder	1.38	Pavan et al. (2014)
13	Kolubara lignite	1	Milicevic et al. (2012)
14	Sawdust	0.86	Gupta and Babu (2009b)

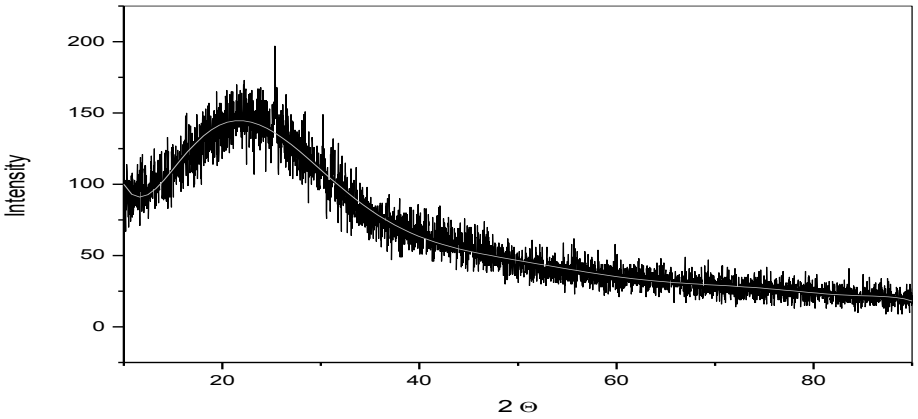

Fig 5.14: Powder X-ray diffraction pattern for nANB.

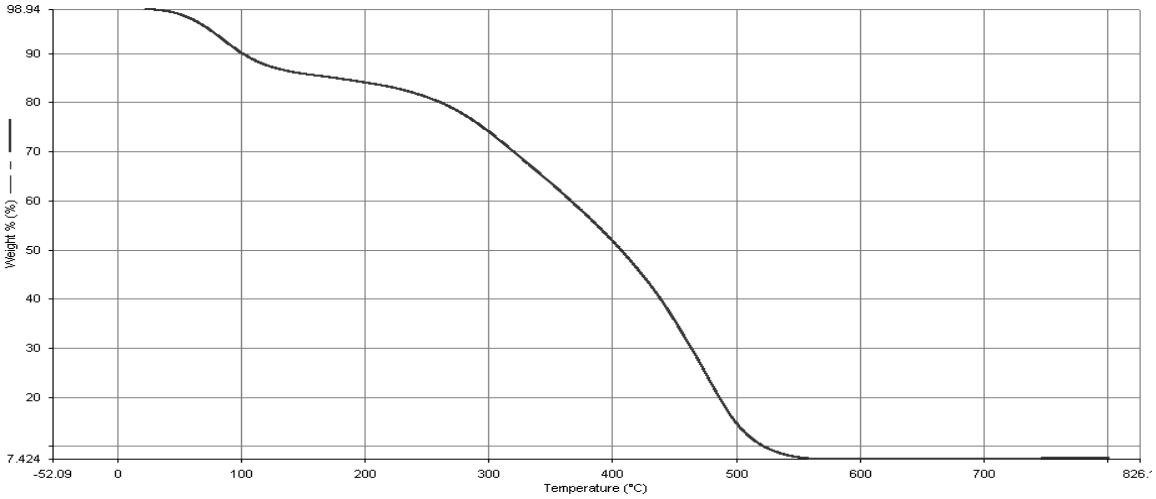

Fig 5.15: Thermo gravimetric analysis of nANB.

5.3 Batch Experiments

5.3.1 Effect of Contact Time

The effect of contact time will be helpful to acquire the kinetic parameters and to propose the rate kinetics for the metal removal. The effect of contact time is evaluated by performing kinetic experiments for the removal of Cr(VI), Cu(II) and Zn(II). Fig 5.16 shows the effect of contact time on the percentage removal and adsorption capacity for the Cr(VI), Cu(II) and Zn(II) removal using nANB.

It is observed that for the removal of Cr(VI), Cu(II) and Zn(II), the percentage removal rapidly increases with the increase in contact time up to 4 h and later it increases gradually with the further increase in contact time. With an increase in the contact time from 0 to 40 h, the percentage removal increases and reaches to a stable value of approximately 35.3, 54.6 and 65.3% for the removal of Cu(II), Zn(II) and Cr(VI) respectively. In 40 h of contact time, the solid phase concentration increases and reaches to 11.604, 5.91 and 9.146 mg g^{-1} for the adsorption of Cr(VI), Cu(II) and Zn(II) respectively. Increase in contact time from 40 to 48 h shows a little change in the solid phase concentration and percentage removal. Therefore, 48 h is considered as the equilibrium time for further studies.

In the initial stages, the metal adsorption rate is faster due to the large concentration gradient between the bulk fluid and the solid surface metal concentration. This may be due to the availability of free active sites for adsorption in the initial period. In later stages, the rate of metal adsorption onto nANB decreases, as the intraparticle diffusion becomes more dominant. This leads to an increase in mass transfer resistances for solute

transfer from the solid surface to the internal adsorption sites. In the later part of the adsorption, the active sites get saturated with time leading to the decrease in the adsorption rate.

5.3.2 Effect of Adsorbent Dosage

The effect of nANB dosage on the Cr(VI), Cu(II) and Zn(II) ion removal is studied to obtain the optimal value of adsorbent dosage (Fig 5.17). The solid phase concentration decreases from 10.54 to 2.22, 6.01 to 1.20 and 5.69 to 1.61 mg g^{-1} for the removal of Cr(VI), Cu(II) and Zn(II) respectively with an increase in adsorbent dosage from 4 to 40 g L^{-1}. The percentage removal increases from 42.15 to 88.98, 24.02 to 45.53 and 22.76 to 50.25% with an increase in the adsorbent dosage from 4 to 40 g L^{-1} for the removal of Cr(VI), Cu(II) and Zn(II) respectively. The decrease in adsorption capacity may be due to the increase in the adsorbent amount, which leads to the increase in the number of active sites available for the adsorption process. As the amount of metal ions to be adsorbed is fixed, an increase in number of active sites results to an increase in percentage removal. There is a trade-off between solid phase concentration and percent removal with an increase in the adsorbent dosage for metal adsorption. The trade-off curves provide that 6, 8 and 10.5 g L^{-1} are obtained as the optimal adsorbent dosage for the removal of Cr(VI), Cu(II) and Zn(II) adsorption.

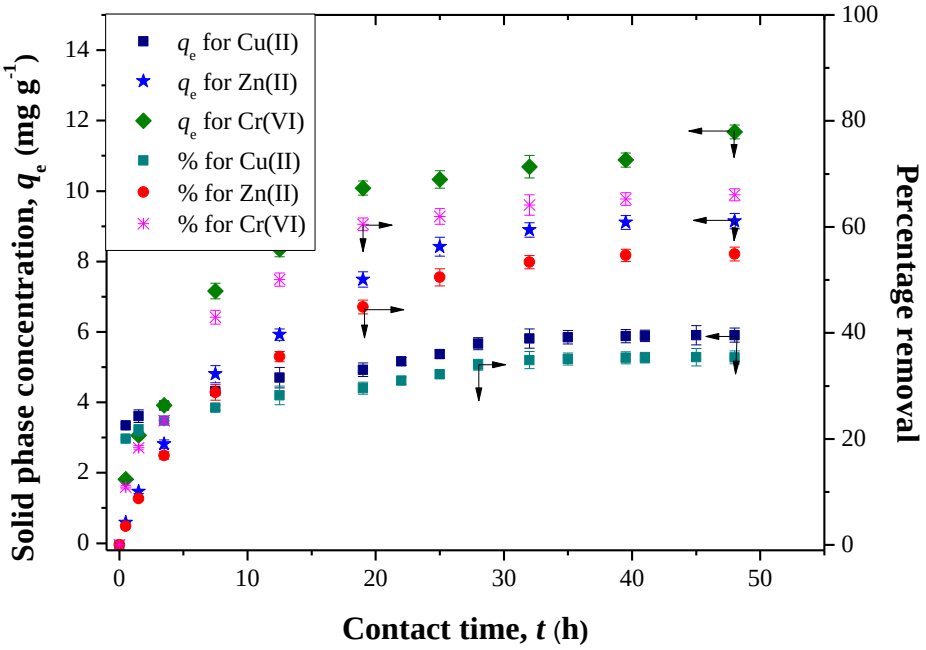

Fig. 5.16: Effect of contact time on the removal of Cr(VI), Cu(II) and Zn(II).

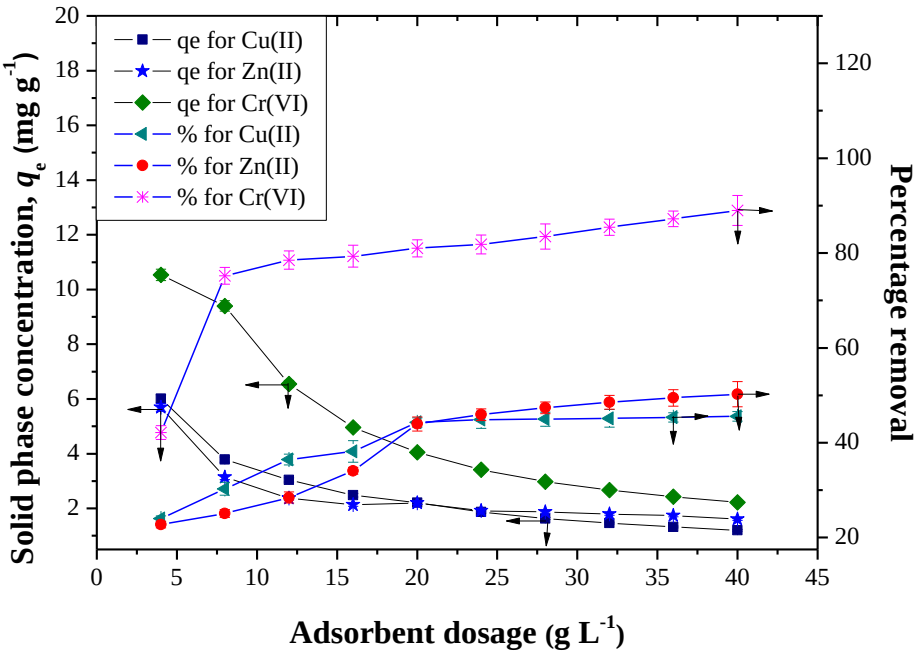

Fig 5.17: Effect of adsorbent dosage on the removal of Cr(VI), Cu(II) and Zn(II).

5.3.3 Effect of Initial Concentration

The effect of inlet concentration on the performance of the developed nANB for the removal of Cr(VI), Cu(II) and Zn(II) is already discussed in Sec. 5.1 and shown in Fig 5.18. It is observed from Fig 5.18 that the percentage removal decreases while the solid phase concentration increases with an increase in the inlet concentration. The trade-off between solid phase concentration and percentage removal suggests the optimum intial concentration as 174, 148 and 106 mg L^{-1} for Cr(VI), Cu(II) and Zn(II) adsorption respectively.

The increase in the solid phase concentration may be due to the utilization of the more active sites available for adsorption at higher initial metal concentration. The decrease in the percent removal may be due to the availability of insufficient active sites for adsorption. These active sites become saturated beyond a certain concentration limit of adsorbate. On further increasing the metal concentration, no adsorption takes place and will remain in the final solution.

5.3.4 Effect of pH

The other significant parameter studied is the effect of pH on the removal of Cr(VI), Cu(II) and Zn(II). The range of pH values considered during the study are 1.2 to 12. The effect of pH on the Cr(VI), Cu(II) and Zn(II) removal is shown in Fig 5.19.

It is observed that the solid phase concentration decreases from 16.26 to 1, 15.83 to 2.13 and 9.99 to 1.05 mg g^{-1} for the removal of Cr(VI), Cu(II) and Zn(II) with an increase in the pH value from 1.2 to 12 (Fig. 5.19). This supports the adsorption of metal ions at lower pH.

It is also observed that during the Cr(VI) adsorption, the pH of the different solutions increases from 2.16 to 4.62, 4.04 to 5.39 and 6.14 to 6.38. During the removal of Cu(II), the pH of the solutions decreases from 2.04 to 1.41, 3.05 to 2.37, 5.09 to 3.89. Similarly, for the removal of Zn(II), the pH of the solutions decreases from 1.16 to 1, 2.77 to 2.48, 5.28 to 3.16, 6.96 to 3.46, 9.2 to 4.61.

The chromium ion exists in various forms at different solution pH as represented in Eq. 5.1 (Gupta and Babu, 2009b).

$$2H^{+} + 2HCrO_4^{-} \xleftrightarrow{2H^{+}} 2HCrO_4 \leftrightarrow 2H_2O + Cr_2O_7^{2-} \xleftrightarrow{2H^{+}} 2CrO_3 + H_2O \qquad (5.1)$$

The dominating form of Cr(VI) at lower pH (pH ≈ 2) is $HCrO_4^-$ (Gupta and Babu, 2009b; Kapur and Mondal, 2013). The surface of the adsorbent is positively charged at low pH value of the solution. This favors the adsorption of negatively charged $HCrO_4^-$ molecules onto the positively charged adsorbent surface. A decline in the adsorption capacity is observed with increase in the solution pH value. This may be due to the shifting of $HCrO_4^-$ in other forms like CrO_4^{2-} and $Cr_2O_7^{2-}$. Furthermore, this can also be attributed to the dual competition between CrO_4^{2-} and OH^- ions available for adsorption, out of which OH^- predominates (Babu and Gupta, 2008b; Muthukumaran and Beulah, 2011).

The copper is present in different ionic forms in the solution during the adsorption process. At lower pH, the active sites for adsorption are positively charged. The neutralization of these active sites are completed with the adsorption of negatively charged copper ions [$Cu(OH)_3^-$] at low pH. At higher pH, the copper is present in hydroxide form which gets precipitated as per Eq. 5.2 (Kim et al., 2008; Eloussaief et al., 2009; Wang et al., 2014).

$$Cu^{2+} + 2OH^{-} \Leftrightarrow Cu(OH)_2 \quad (5.2)$$

In the aqueous solution, the zinc ions exist in various forms. The stability of these forms is very much dependent on the pH of the solution. It is reported that, at pH value above 6, there is a chance of metal precipitation over the surface of the nANB due to nucleation reaction (Eq. 5.3). This decreases the tendency of the Zn(II) adsorption to occur on the adsorbent surface (Agrawal et al., 2004). The lower pH favors the Zn(II) adsorption which might be due to the replacement of the metal ion with the hydrogen ions available on the nANB surface (Gabaldón et al., 1996; Wasewar, 2010).

$$Zn^{2+} + 2OH^{-} \Leftrightarrow Zn(OH)_2 \quad (5.3)$$

The critical pH of Cu(II) and Zn(II) precipitation can be evaluated using the following Eqs. 5.4, 5.5 and 5.6.

$$c(OH^{-}) = \sqrt{K_{sp} / c(Cu^{2+})} \quad (5.4)$$

$$c(OH^{-}) = \sqrt{K_{sp} / c(Zn^{2+})} \quad (5.5)$$

$$pH = -\log c(H^{+}) = \log(1 \times 10^{-14} / c(OH^{-})) \quad (5.6)$$

To estimate the critical pH for Cu(II) and Zn(II) precipitation, the initial concentration of Cu(II) and Zn(II) is taken as 1.563 and 1.539 mmol L^{-1} respectively which is equivalent to 100 mg L^{-1} of initial concentration of both ions. The solubility (K_{sp}) at 25°C of $Cu(OH)_2$ and $Zn(OH)_2$ are considered as 2.2×10^{-20} and 6.8×10^{-17} respectively.

The critical values of pH for Cu(II) and Zn(II) precipitation are found to be 5.57 and 7.32 respectively. Hence, for the adsorption of Cu(II) and Zn(II), the pH of the solution should be maintained lower than the critical value of precipitation.

5.3.5 Effect of Temperature

The effect of the temperature on the adsorption of heavy metals is evaluated by performing equilibrium batch experiments at 35, 50 and 60°C. The effect of temperature for the removal of Cr(VI), Cu(II) and Zn(II) is shown in Fig. 5.20, 5.21 and 5.22 respectively.

For the initial Cr(VI) concentration of 60 mg L^{-1}, there is a reduction in solid phase concentration (q_e) and percentage removal from 9.42 to 7.39 and 94.2 to 73.85% respectively by increasing the temperature from 35 to 60°C. The q_e and percentage removal decreases from 7.37 to 4.55 and 73.7 to 45.5% respectively as the process temperature increases from 35 to 60°C for the initial Cu(II) concentration of 60 mg L^{-1}. Likewise, with the change in the adsorption temperature from 35 to 60°C, there is a decrease in q_e and percentage removal from 6.38 to 5.78 and 63.75 to 57.59%, respectively for the 60 mg L^{-1} of initial Zn(II) concentration. Similar results are obtained for the different initial metal concentration ranging from 80 - 200 mg L^{-1}.

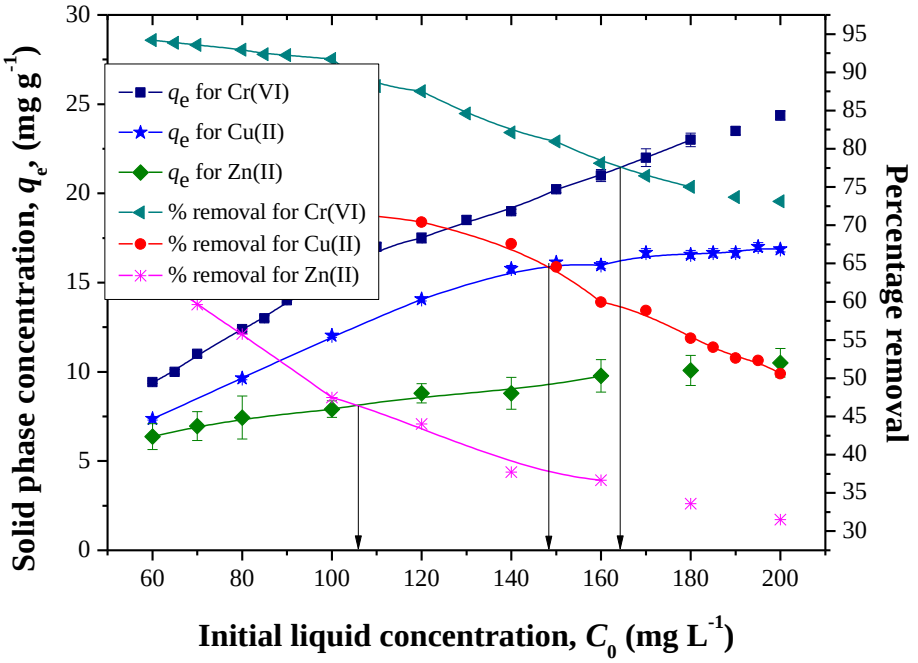

Fig 5.18: Effect of inlet concentration on the removal of Cr(VI), Cu(II) and Zn(II) using nANB.

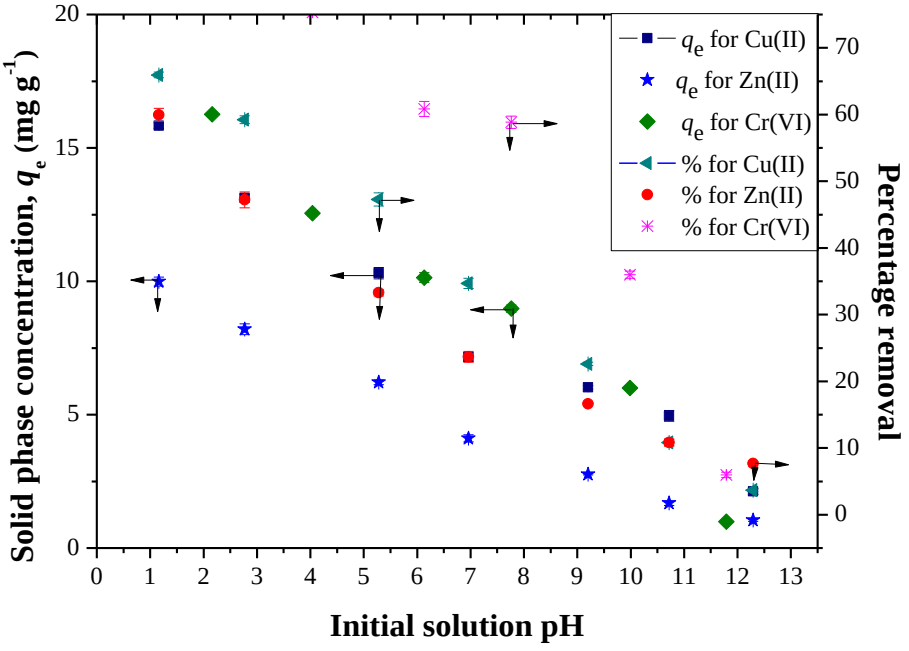

Fig 5.19: Effect of pH on the removal of Cr(VI), Cu(II) and Zn(II) using nANB.

The equilibrium experimental data at different temperature are also fitted with the Langmuir isotherm model. There is a decrease in the maximum adsorption capacity from 26.95 to 12.87, 21.23 to 9.43 and 11.9 to 7.19 mg g^{-1} for the removal of Cr(VI), Cu(II) and Zn(II) respectively with an increase in temperature from 35 to 60°C.

The mechanism of adsorption can be well understood by the thermodynamic behavior of the operation. The thermodynamic parameters such as ΔG, ΔH and ΔS are evaluated using Eq. 5.7, 5.8 and 5.9 (Liang et al., 2013).

$$K_c = \frac{C_{ad}}{C_e} \tag{5.7}$$

$$\Delta G = -RT \ln K_c \tag{5.8}$$

$$\ln K_c = \frac{\Delta S}{R} - \frac{\Delta H}{RT} \tag{5.9}$$

The values of ΔH and ΔS are evaluated by calculating the slope and intercept from the plot of ln K_c vs. $1/T$ (Figs 5.23 to 5.24). The estimated values of ΔH, ΔG and ΔS for the removal of Cr(VI), Cu(II) and Zn(II) are given in Table 5.4.

The values of ΔG are found to be negative at 308 K. This suggests the spontaneous nature of the adsorption process. The values of ΔG are increasing from negative to positive values with an increase in the temperature. This increase in ΔG values also supports the decrease in the metal adsorption capacity. The adsorption of metals on nANB is confirmed to be an exothermic process by the obtained negative values of ΔH. The negative values of ΔS support less randomness of the adsorption process at the solid liquid interface (Liang et al., 2013; Rajamohan et al., 2014; Wang et al., 2014).

5.3.6 Regeneration Studies

In the present study, there are two techniques considered for the regeneration of the utilized adsorbent. The first technique is based on the thermal approach. The Cr(VI), Cu(II) and Zn(II) utilized adsorbents are thoroughly stirred in hot water at 70°C. It is observed that approximately 40, 36, 33% of the Cr(VI), Cu(II) and Zn(II) are desorbed respectively from the corresponding saturated nANB.

The other technique followed is the base and acid treatment. The utilized nANB is treated for 24 h with 1N NaOH followed by 24 h treatment with 1N HCL. The recovery of Cr(VI), Cu(II) and Zn(II) are found to be 91.4, 86 and 72% respectively from the used nANB for respective metal ions.

The EDS analysis of regenerated nANB by base and acid treatment is shown in Fig 5.26. This confirms a significant reduction in the Cr(VI) amount as compared to that present in saturated nANB [Fig 5.11(b)]. Approximately 1.14 % of Cr(VI) is remaining on the regenerated nANB surface which supports the recovery of 91.4% of Cr(VI). This also shows the regenerability and re-usability of the nANB.

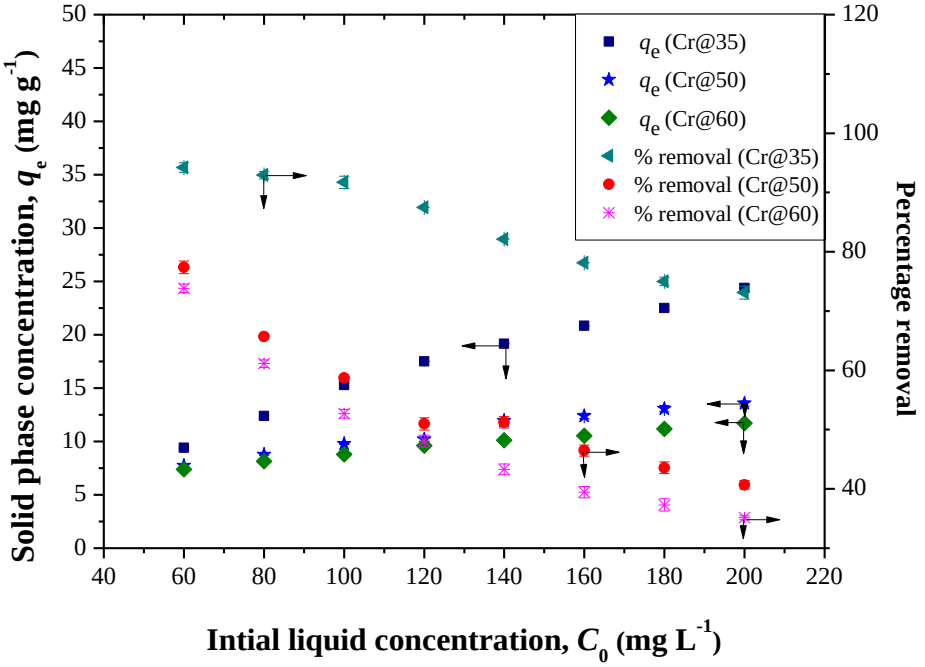

Fig 5.20: Effect of temperature on the removal of Cr(VI) using nANB.

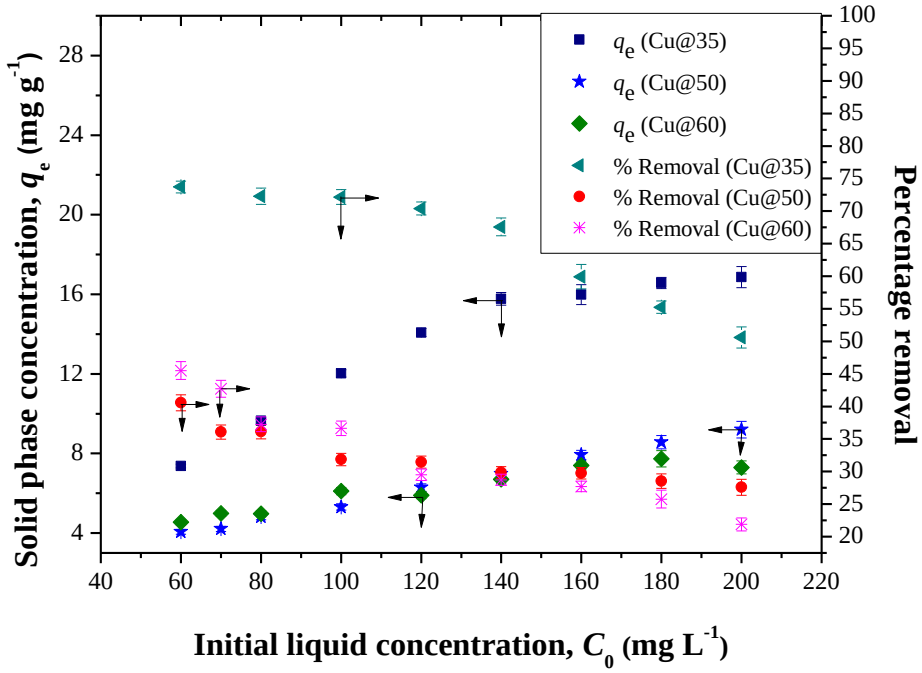

Fig 5.21: Effect of temperature on the removal of Cu(II) using nANB.

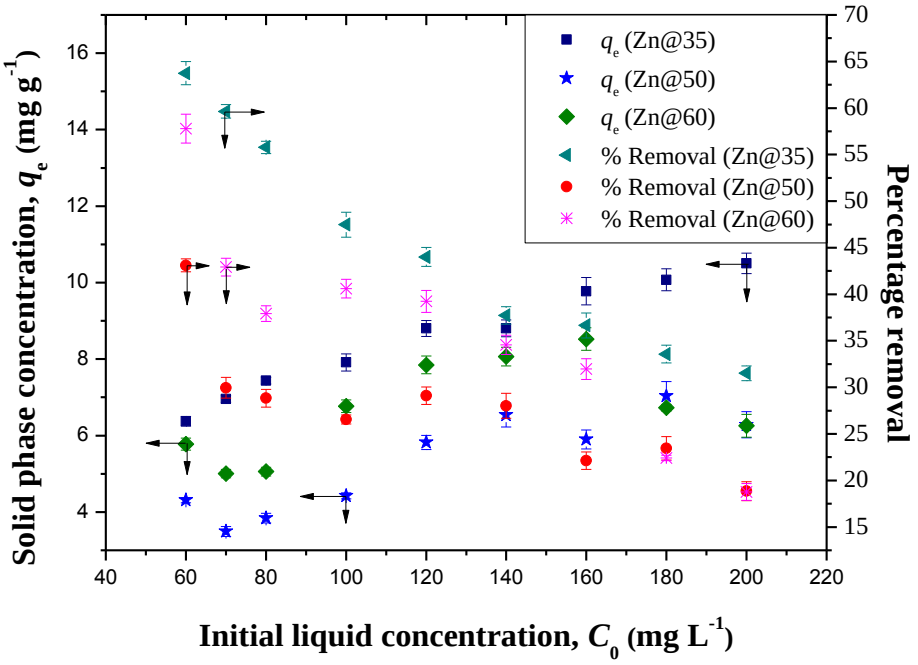

Fig 5.22: Effect of temperature on the removal of Zn(II) using nANB.

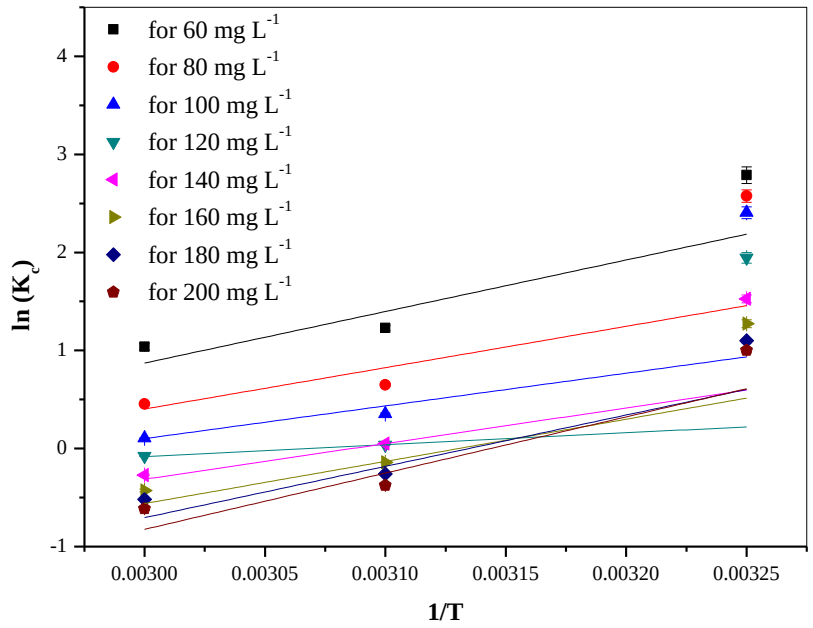

Fig 5.23: Plot for thermodynamic calculations for Cr(VI) removal.

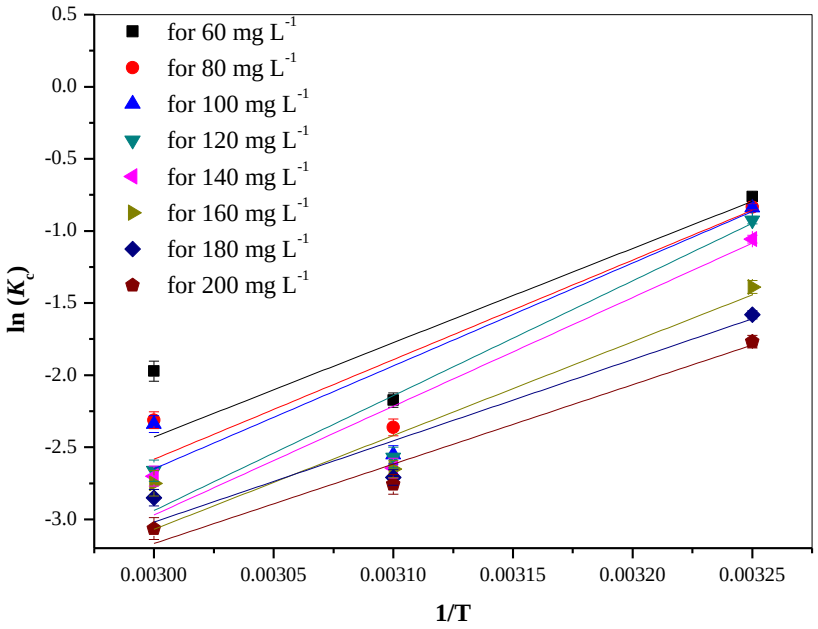

Fig 5.24: Plot for thermodynamic calculations for Cu(II) removal.

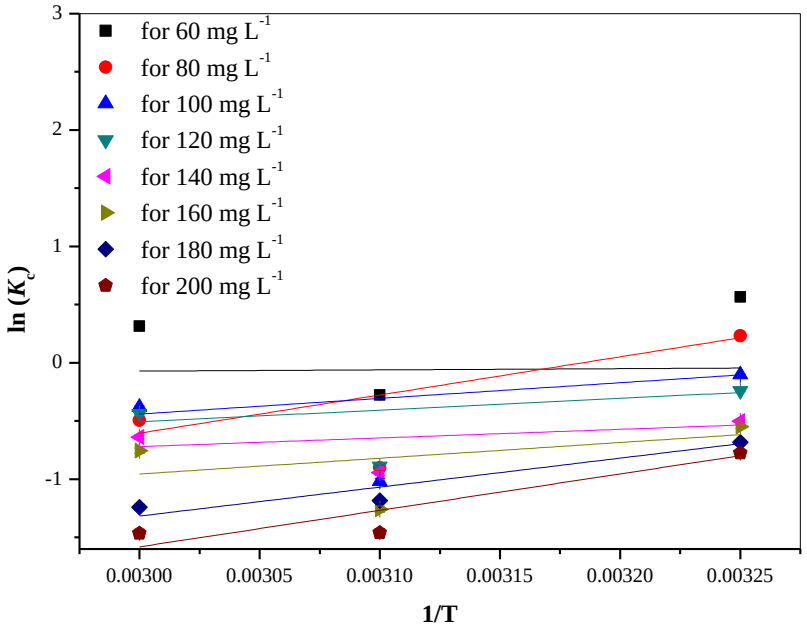

Fig 5.25: Plot for thermodynamic calculations for Zn(II) removal.

Table 5.4: Thermodynamic parameters for the removal of Cr(VI), Cu(II) and Zn(II).

		For Cr(VI)				For Cu(II)				For Zn(II)			
C_0	T	Kc	ΔG	ΔH	ΔS	Kc	ΔG	ΔH	ΔS	Kc	ΔG	ΔH	ΔS
60	308	16.26	-7.14	-62.19	-179.72	2.80	-2.64	-49.94	-154.23	1.76	-1.45	-27.27	-83.27
	323	3.42	-3.30			0.84	0.48			1.37	-0.84		
	333	2.82	-2.87			0.68	1.06			0.76	0.77		
80	308	13.14	-6.59	-75.61	-225.34	2.61	-2.45	-53.67	-167.53	1.14	-0.34	-35.19	-113.10
	323	1.92	-1.75			0.57	1.53			0.61	1.32		
	333	1.57	-1.25			0.59	1.44			0.41	2.50		
100	308	11.09	-6.16	-81.70	-246.58	2.59	-6.63	-55.28	-173.18	0.90	0.26	-29.72	-96.73
	323	1.42	-0.95			0.47	-1.26			0.68	1.02		
	333	1.11	-0.30			0.58	-1.60			0.36	2.82		
120	308	7	-4.98	-72.47	-220.48	2.38	-2.22	-62.24	-196.03	0.79	0.62	-21.05	-69.92
	323	1.04	-0.10			0.46	2.09			0.65	1.17		
	333	0.93	0.22			0.42	2.41			0.41	2.46		
140	308	4.6	-3.91	-63.16	-193.13	2.08	-1.88	-59.03	-186.73	0.61	1.28	-14.37	-50.53
	323	1.05	-0.13			0.43	2.29			0.53	1.71		
	333	0.76	0.75			0.40	2.51			0.39	2.61		

		For Cr(VI)				For Cu(II)				For Zn(II)			
C_0	T	Kc	ΔG	ΔH	ΔS	Kc	ΔG	ΔH	ΔS	Kc	ΔG	ΔH	ΔS
160	308	3.57	-3.26	-59.91	-184.69	1.50	-1.03	-48.62	-155.40	0.58	1.40	-23.02	-78.81
	323	0.87	0.38			0.42	2.31			0.47	2.03		
	333	0.65	1.19			0.38	2.65			0.28	3.48		
180	308	3	-2.81	-57.04	-176.80	1.23	-0.54	-45.05	-145.18	0.51	1.75	-18.39	-65.91
	323	0.77	0.69			0.40	2.46			0.29	3.33		
	333	0.60	1.44			0.35	2.93			0.31	3.27		
200	308	2.72	-2.56	-57.01	-177.56	1.02	-0.06	-45.17	-146.84	0.46	1.99	-24.71	-87.17
	323	0.69	1.01			0.38	2.59			0.23	3.93		
	333	0.54	1.70			0.28	3.52			0.23	4.04		

5.3.7 Interference Studies

The performance of the developed nANB is also evaluated for the removal of synthetically developed multiple metal ion aqueous solution. The aqueous solution contains equal amounts of Cr(VI), Cu(II) and Zn(II). It is observed that the solid phase concentration for the simultaneous adsorption of Cr(VI), Cu(II) and Zn(II) is less than the one obtained from the respective pure aqueous solutions (Fig. 5.27). This decrease in the solid phase concentration may be a result of the utilization of the active sites for the removal of other metal ions. It is also observed that the total solid phase concentration of developed nANB for the simultaneous removal of all the metal ions is coming to be 38.95 mg g^{-1}. This solid phase concentration value is much higher than the one evaluated for the removal of any individual metal ions. The EDS image (Fig 5.28) of the used nANB for the simultaneous adsorption of Cr(VI), Cu(II) and Zn(II) confirms their presence on the surface of the saturated nANB. The increase in the adsorption capacity may be also a result of some of the active sites which are not having affinity towards specific metal ion, however, has good adsorption characteristics for other metal ions. For example, in the adsorption of Cr(VI), there may be some active sites which are not utilized for the adsorption of Cr(VI) may be occupied by either Cu(II) or Zn(II) during multiple metal adsorption.

5.3.8 Utilization on Actual Chrome Plating Industrial Effluent

The developed nANB is also utilized for the treatment of actual chrome plating industrial effluent. The chrome plating industry effluent is mainly contaminated with large amount of Cr(VI) along with the traces of other metal ions. Hence, in this study, Cr(VI) is targeted to be removed from plating industry wastewater using

nANB as an adsorbent. The concentration of Cr(VI) in the industrial sample is measured and is found as 1850 mg L^{-1} which is further diluted to maintain 100 mg L^{-1} of Cr(VI) concentration. The diluted sample is treated for a contact time of 48 h with an adsorbent dosage of 18 g L^{-1}.

The removal of Cr(VI) from the industrial sample is found as 62.77%, while it is 79.33% for 100 mg L^{-1} of initial concentration of pure Cr(VI) aqueous solution. The adsorption capacity of nANB for Cr(VI) removal from plating industry sample is found as 3.49 mg g^{-1} while that of an aqueous solution is 4.53 mg g^{-1}. This decrease in adsorption capacity may be due to the presence of other metal ions (Aluminum, Nickel, etc.) along with other impurities (Chlorine, etc.) in the industrial effluent. These ions and impurities occupy the active sites available for Cr(VI) adsorption. This may be one of the reasons for decreased adsorption capacity. This is also supported by the EDS analysis of used nANB utilized for the treatment of industrial sample [Fig 5.29(b)]. The SEM image of used nANB [Fig 5.29(a)] confirms the utilization of all the pores available for Cr(VI) adsorption. Hence, the results obtained from this study established the fact that the developed nANB can be successfully utilized for the treatment of industrial wastewater which contain Cr(VI) along with other metal ions and impurities.

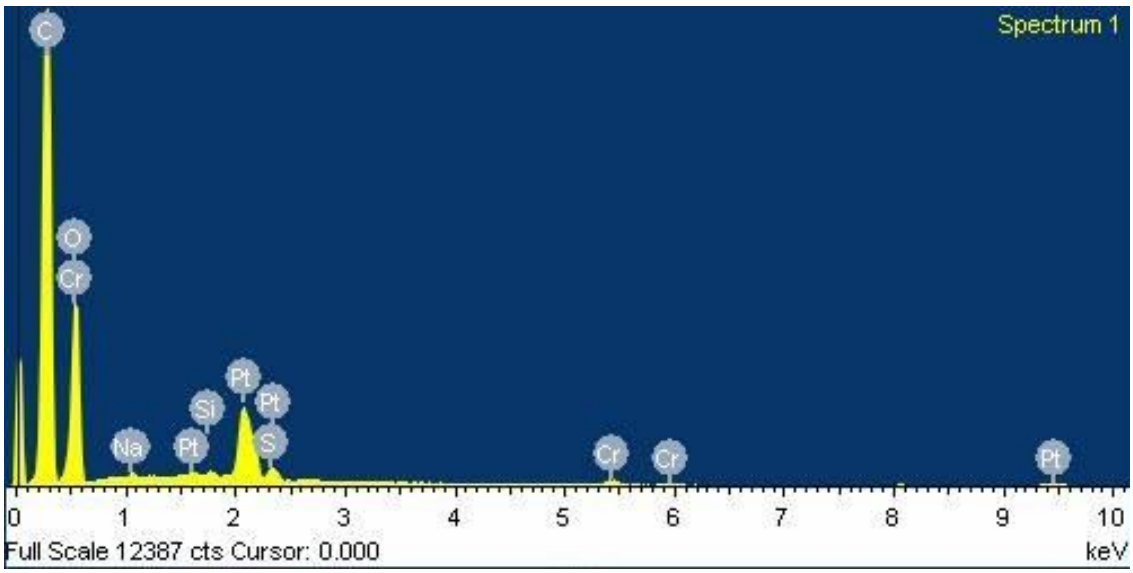

Fig 5.26: EDS for regenerated nANB utilized on Cr(VI).

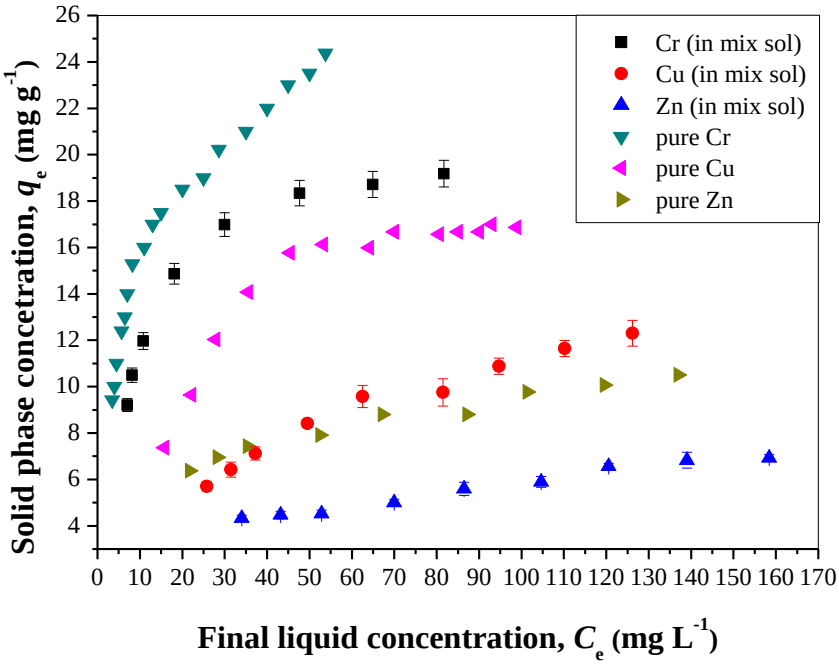

Fig 5.27: Effect of interference of other ions on the removal of Cr(VI), Cu(II) and Zn(II).

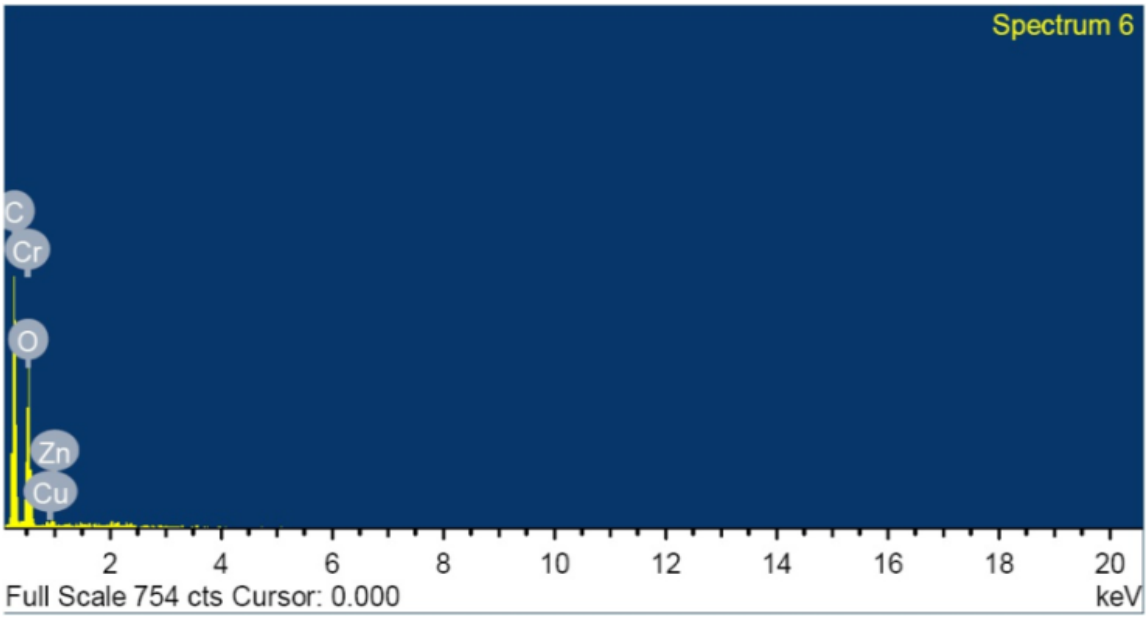

Fig 5.28: EDS for saturated nANB on synthetic industrial solution [Cr(VI), Cu(II) & Zn(II)].

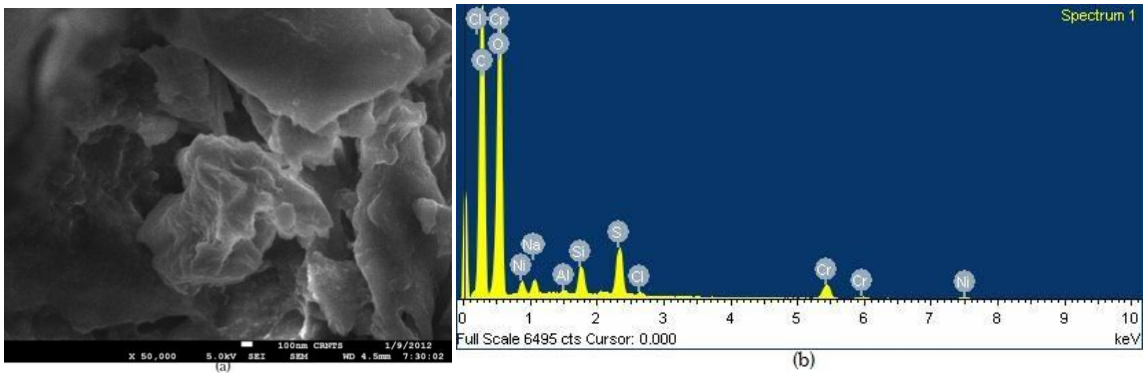

Fig 5.29: (a)SEM and (b)EDS for used nANB on actual chrome plating industrial effluent.

5.3.9 Adsorption Isotherms

Adsorption isotherms are an important tool in adsorption process which helps in understanding the adsorption mechanism in term of the interaction of the metal ions with the solid adsorbent surface. The applicability of the various isotherm models help in evaluating different isotherm constants that provide the information about the surface property and affinity of the adsorbent towards the metal removal. The obtained equilibrium experimental results are fitted with the isotherm models available in the literature. In the present work, Langmuir, Freundlich and Tempkin isotherm models are considered and are discussed in the subsequent sections. The various isotherm parameters are estimated and tabulated in Table 5.5.

5.3.9.1 Langmuir Isotherm

The linearized Langmuir isotherm model (Table 4.1) is utilized to fit the experimentally obtained q_e and C_e for the removal of Cr(VI), Cu(II) and Zn(II) using nANB and are shown in Fig 5.30. The Langmuir parameters, i.e. q_m, b and R_L are estimated and are given in Table 5.5. The maximum adsorption capacity estimated for nANB is 26.95, 21.23 and 11.904 mg g^{-1} for the removal of Cr(VI), Cu(II) and Zn(II) respectively. The value of q_m obtained from Langmuir isotherm model for the removal of Cr(VI), Cu(II) and Zn(II) using nANB is also in accordance with the maximum q_e obtained from the experimental results (Table 5.5). Similarly, the value of *b*, which represents the adsorption energy is found in the range of 0.045 to 0.144 for the metal removal. The dimensionless equilibrium parameter, R_L is also calculated. The minimum and maximum value of R_L are estimated as 0.034 and 0.27 respectively for the metals removal. The values of R_L are lying between 0 and 1 which also confirms the favorable adsorption of

different metal ions using nANB. The regression correlation coefficient (R^2) values for fitting of the Langmuir isotherm model on all the equilibrium adsorption studies is found to be in the range of 0.976 to 0.995. The high R^2 value supports the agreement of experimental values with Langmuir isotherm model. This also suggests the monolayer adsorption of metal ions on the surface of nANB.

5.3.9.2 Freundlich Isotherm

The equilibrium experimental data for the removal of Cr(VI), Cu(II) and Zn(II) using nANB are fitted with the linearized form of the Freundlich isotherm model (Table 4.1). The Freundlich isotherm parameters K_F and n_F are obtained using the linear plot of log q_e vs. log C_e (Fig 5.31) and are tabulated in Table 5.5. The regression correlation coefficients (R^2) obtained for Cr(VI), Cu(II) and Zn(II) adsorption using Freundlich model are estimated as 0.961, 0.8404 and 0.982 respectively. The obtained value of R^2 for Cr(VI) and Cu(II) adsorption do not support the possibility of heterogeneous adsorption. However, the heterogeneity cannot be ignored in case of Zn(II) adsorption (R^2 = 0.982). The value of n_F is found as 0.324, 0.401 and 0.26 for the Cr(VI), Cu(II) and Zn(II) adsorption respectively. The obtained values of n_F are obtained to be less than 1 which supports the chemisorption phenomena during metal adsorption on nANB (Daneshvar et al., 2002; Gupta, 2008b).

5.3.9.3 Tempkin Isotherm

The equilibrium studies for the removal of Cr(VI), Cu(II) and Zn(II) using nANB are also fitted with the Tempkin isotherm model. The linear plot of q_e vs. ln C_e (Fig 5.32) helps in estimating the Tempkin adsorption isotherm parameters, A_T & b_T. The estimated values of A_T and b_T are given in Table 5.5. The Tempkin isotherm model takes the adsorbent–

adsorbate interactions in consideration (Foo and Hameed, 2010). The regression coefficient of Tempkin isotherm model is found to be 0.989, 0.889 and 0.973 for the removal of Cr(VI), Cu(II) and Zn(II) respectively. The R^2 values obtained are less than that for the Langmuir model while values are more when compared with Freundlich isotherm model. The Tempkin isotherm model is found suitable for describing the behaviour of equilibrium experiments in comparison to that of the Freundlich isotherm model.

The q_e values obtained from the experiment and from the three isotherm models for the removal of Cr(VI), Cu(II) and Zn(II) are plotted and compared in Figs 5.33, 5.34 and 5.35 respectively.

5.3.9.4 Concluding Remarks

The calculated values of regression correlation coefficient (R^2) of the three isotherm models for the adsorption of Cr(VI), Cu(II) and Zn(II) indicate that the equilibrium experimental data are best fitted with the Langmuir isotherm model (Table 5.5). This also supports the monolayer adsorption of Cr(VI), Cu(II) and Zn(II) on nANB surface.

Table 5.5: Isotherm constants for removal of Cr(VI), Cu(II) & Zn(II) using nANB.

Metal	Max $q_{e(exp)}$ (mg g^{-1})	Langmuir Isotherm				Freundlich Isotherm			Tempkin Isotherm		
		Constants			R^2	Constants		R^2	Constants		R^2
		q_m (mg g^{-1})	b	R_L		K_F	n		A_T	b_T	
Cr(VI)	24.37	26.95	0.144	0.034-0.104	0.995	6.896	0.324	0.961	1.906	490.89	0.989
Cu(II)	17	21.23	0.045	0.1-0.27	0.976	2.942	0.401	0.840	0.380	519.67	0.890
Zn(II)	10.51	11.90	0.045	0.1-0.27	0.991	2.877	0.260	0.982	0.849	1186.09	0.973

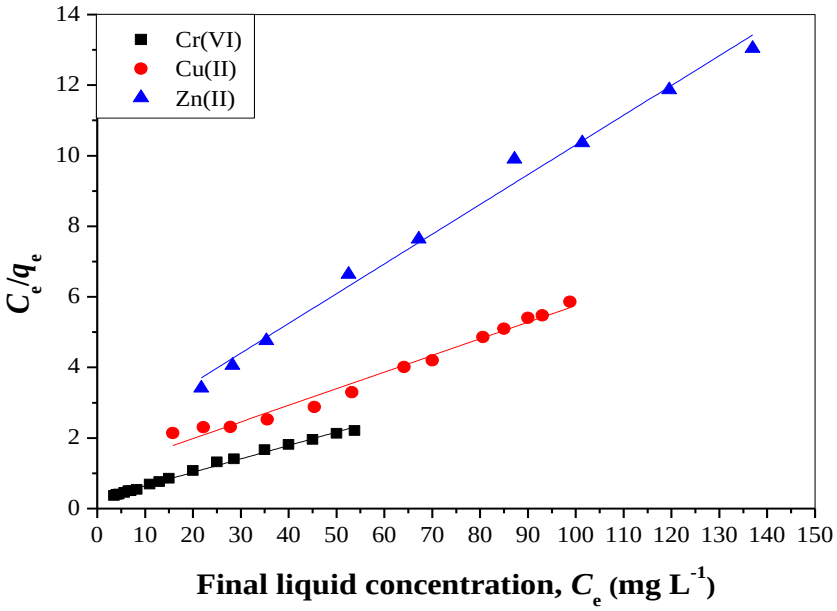

Fig 5.30: Applicability of Langmuir isotherm model for the removal Cr(VI), Cu(II) and Zn(II) using ANBs.

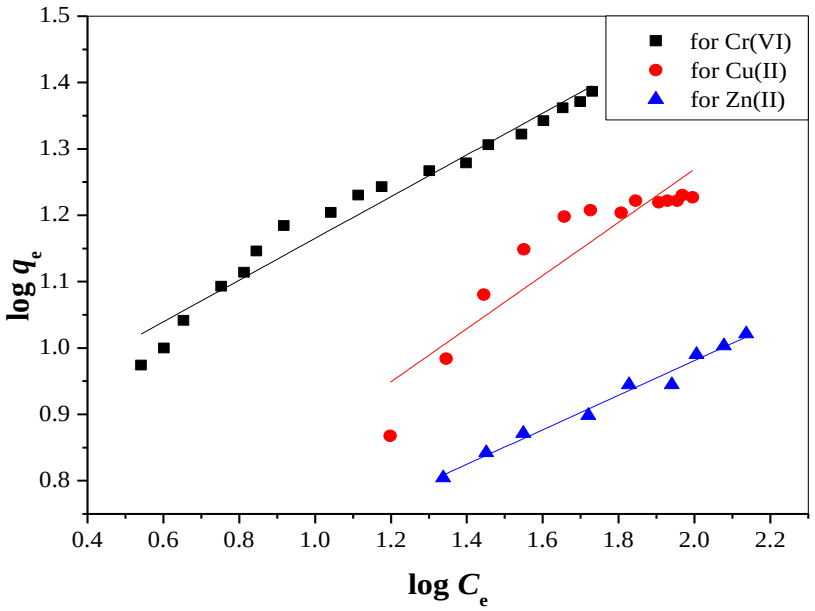

Fig 5.31: Applicability of Freundlich isotherm model for the removal Cr(VI), Cu(II) and Zn(II).

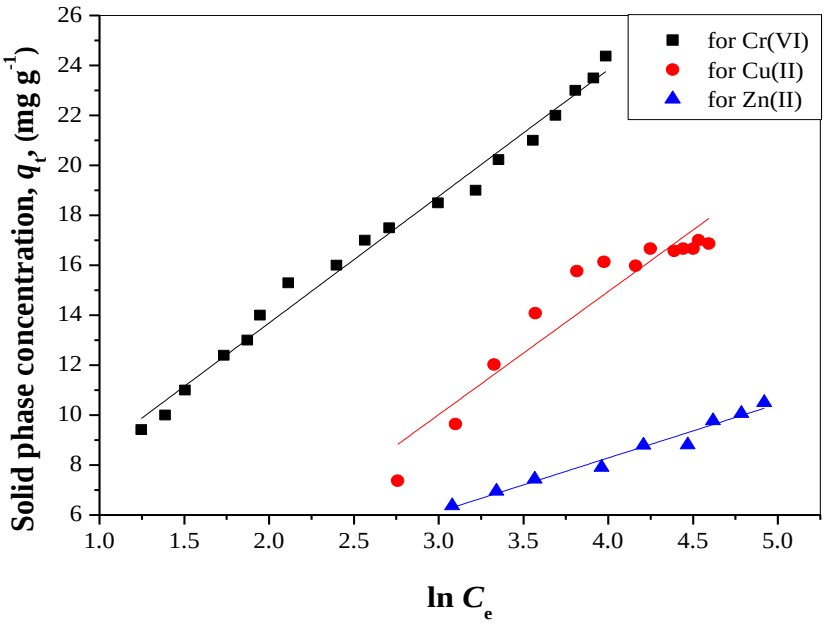

Fig 5.32: Applicability of Tempkin isotherm model for the removal Cr(VI), Cu(II) and Zn(II).

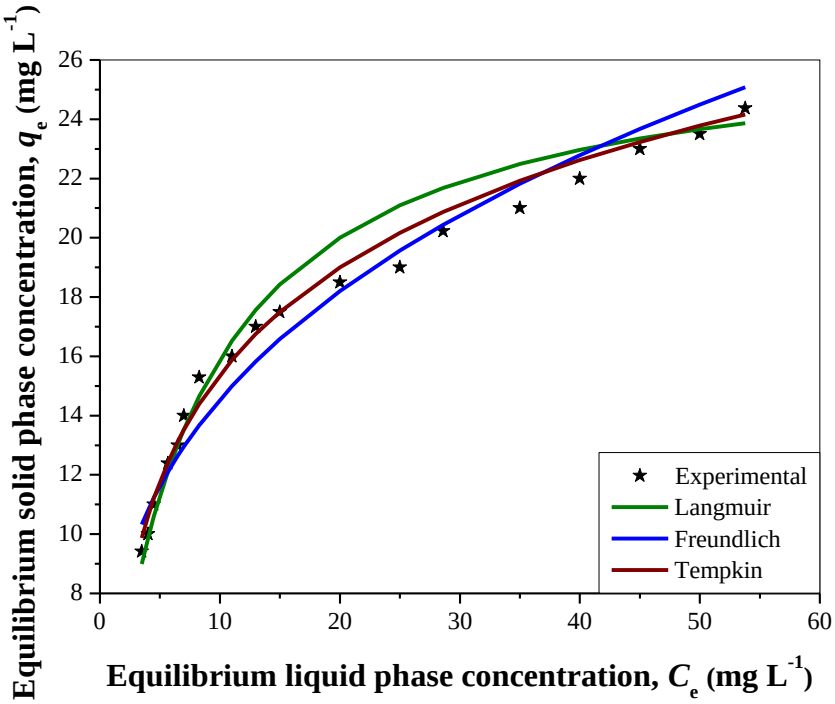

Fig 5.33: Comparison of various isotherm models on the removal of Cr(VI) using nANB.

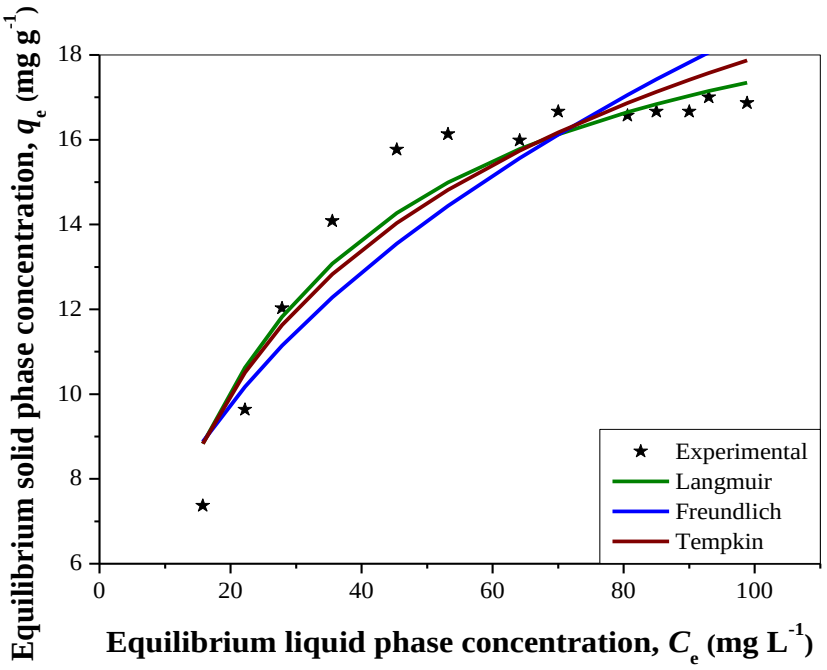

Fig 5.34: Comparison of various isotherm models on the removal of Cu(II) using nANB.

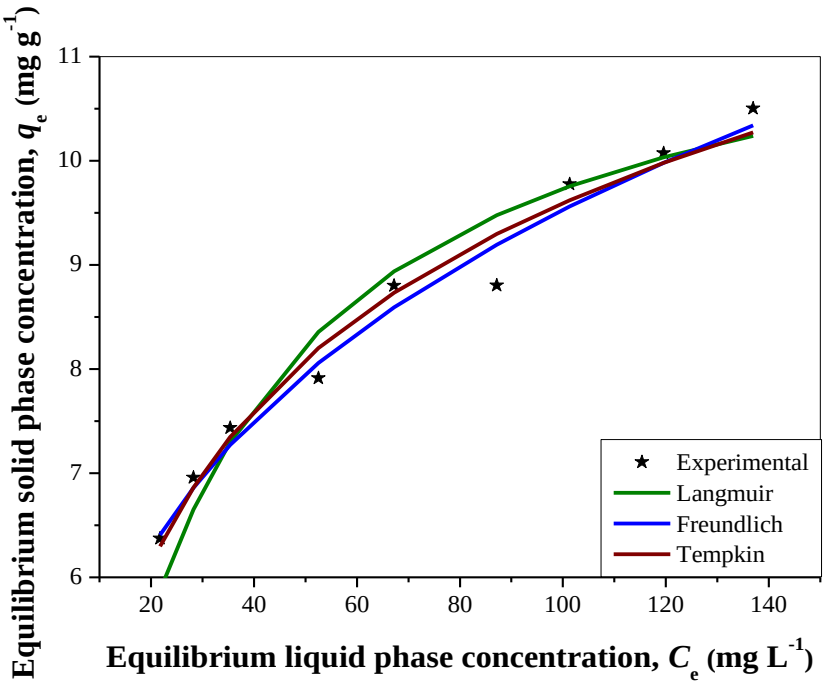

Fig 5.35: Comparison of various isotherm models on the removal of Zn(II) using nANB.

5.3.10 Adsorption Kinetics

In order to understand the kinetic behavior of the adsorption process for the removal of Cr(VI), Cu(II) and Zn(II) using nANB, the pseudo-first order, second order and Elovich models are considered to fit the kinetic experimental data. The different parameters are evaluated and tabulated in Table 5.6.

5.3.10.1 Pseudo-first Order Kinetic Model

The applicability of the pseudo-first order kinetic model (Lagergren, 1898) to the experimental data are tested by plotting a graph of log (q_e-q_t) vs. t (Fig 5.36). The estimated values of the pseudo-first order kinetic parameters, k_{ad} and q_e along with the regression correlation coefficient (R^2) are tabulated in Table 5.6. The values of R^2 are estimated as 0.953, 0.922 and 0.956 for the removal of Cr(VI), Cu(II) and Zn(II) respectively using pseudo-first order kinetic model. These values indicate the non-agreement of the pseudo-first order kinetic model with the experimental data. The obtained values of the equilibrium adsorption capacity for Cr(VI) and Cu(II) are 9.099 and 4.454 mg g^{-1} respectively. The predicted values of adsorption capacities for Cr(VI) and Cu(II) are approximately half of the value obtained from the experimental results. The predicted adsorption capacity for Zn(II) adsorption is estimated as 11.04 mg g^{-1} which is better than the obtained experimental values (9.15 mg g^{-1}), however, the R^2 = 0.956 is not supporting the applicability of pseudo-first order kinetic model for the Zn(II) adsorption. This also suggests that the pseudo-first order kinetic model cannot explain the kinetic behavior of the metals adsorption on nANB.

5.3.10.2 Second Order Kinetic Model

The kinetic experimental data are also fitted with the second order kinetic model (Ho and McKay, 1998; Ho, 2006). The second order kinetic parameter, k_2 and q_e are calculated using the slope and intercept of the plot between t/q_t and t (Fig 5.37). The obtained values of k_2, q_e and R^2 for Cr(VI), Cu(II) and Zn(II) adsorption are given in Table 5.6. The predicted equilibrium adsorption capacity is close to the one obtained from the experimental data. The values of k_2 obtained are 0.0102, 0.07 and 0.01363 for the removal of Cr(VI), Cu(II) and Zn(II) respectively. The estimated values of k_2 are found to be less than 1 which suggests the higher rate of adsorption of metal at initial stage and further decreases with the lapse of time. High values of R^2 (0.992-0.996) obtained for the removal of Cr(VI), Cu(II) and Zn(II) using nANB show the agreement between experimental data and the second order kinetic model. This also confirms the chemisorption of Cr(VI), Cu(II) and Zn(II) on nANB during the adsorption process.

5.3.10.3 Elovich Kinetic Model

The kinetic experimental data are also fitted with the Elovich kinetic model (Zeldowitsch, 1934). The experimental data are plotted as q_t vs. ln t and the Elovich constants, α and β are estimated from the slope and intercept of the plot (Fig 5.38). The evaluated constants along with R^2 are tabulated in Table 5.6. The R^2 for the Elovich model are found as 0.966, 0.933 and 0.967 for the removal of Cr(VI), Cu(II) and Zn(II) respectively. These correlation coefficient values are higher than the values obtained from pseudo-first order kinetic models, however, these values are less than the values obtained for the second order kinetic model. The values of β are obtained as 0.425, 1.5576 and 0.4697 for the removal of Cr(VI), Cu(II) and Zn(II) respectively. The lower value of β (<5) supports the

higher adsorption capacity for the metal adsorption using nANB (Chien and Clayton, 1980; Gupta, 2008b; Kumar and Kirthika, 2009).

The comparison of the solid phase concentration obtained from experimental results and by using the three models is shown in Figs 5.39, 5.40 and 5.41 for the removal of Cr(VI), Cu(II) and Zn(II) respectively.

5.3.10.4 Concluding Remarks

Comparison of solid phase concentration (Figs 5.39, 5.40 and 5.41) and the correlation coefficients for the removal of Cr(VI), Cu(II) and Zn(II) (Table 5.6) supports the applicability of the second order kinetic model during the adsorption process. The results suggest that the chemisorption is the primary rate-limiting step in the process which leads to the possibility of covalent bond formation between adsorbent surface and metal ions.

The kinetic relationship is also important to predict the rate at which the adsorption is taking place. This prediction is helpful in designing the fixed-bed adsorption column. The mass transfer coefficients and the equilibrium capacity of the adsorbent are estimated using the adsorption rate kinetics. The design parameters for the fixed-bed adsorption process such as the shape of breakthrough curve and breakthrough time also depend on the rate of adsorption (Babu and Gupta, 2008b; Gupta and Babu, 2009a; 2009b; Kumar and Kirthika, 2009).

Table 5.6: Kinetic parameters for the removal of Cr(VI), Cu(II) and Zn(II) using nANB.

	Pseudo-first Order			Second Order			Elovich Model		
	k_{ad} (h^{-1})	q_e (mg g^{-1})	R^2	k_2 (h^{-1})	q_e (mg g^{-1})	R^2	α	β	R^2
Cr(VI)	0.07	9.10	0.95	0.01	12.67	0.99	6.71	0.43	0.97
Cu(II)	0.12	4.45	0.92	0.07	6.10	0.99	121.11	1.56	0.93
Zn(II)	0.13	11.04	0.96	0.01	11.31	0.99	3.46	0.47	0.97

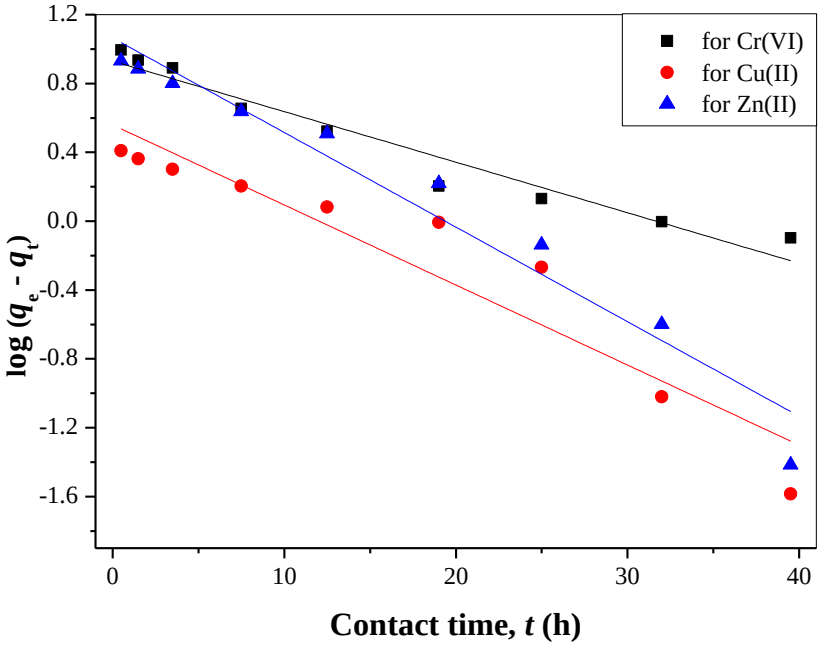

Fig 5.36: Applicability of pseudo-first order kinetic model for Cr(VI), Cu(II) and Zn(II) removal.

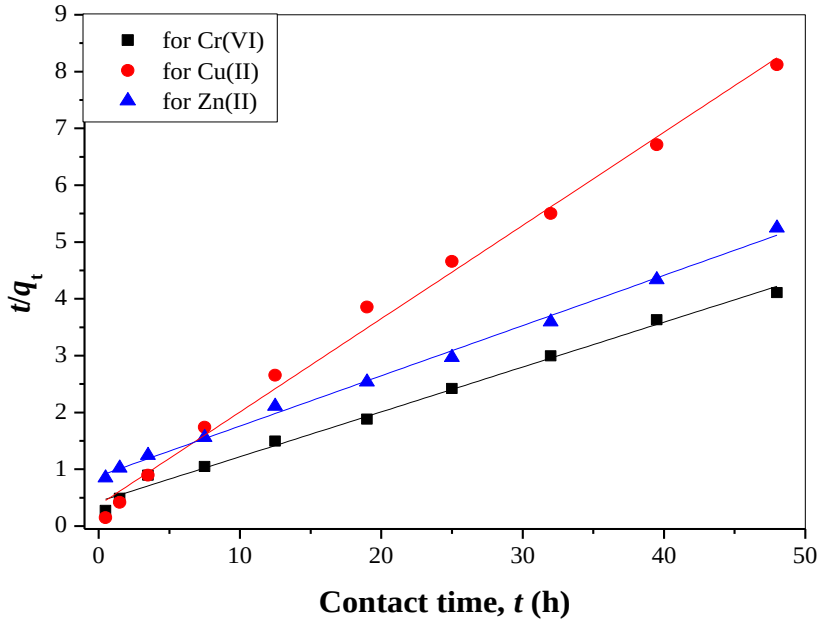

Fig 5.37: Applicability of second order kinetic model for Cr(VI), Cu(II) and Zn(II) removal.

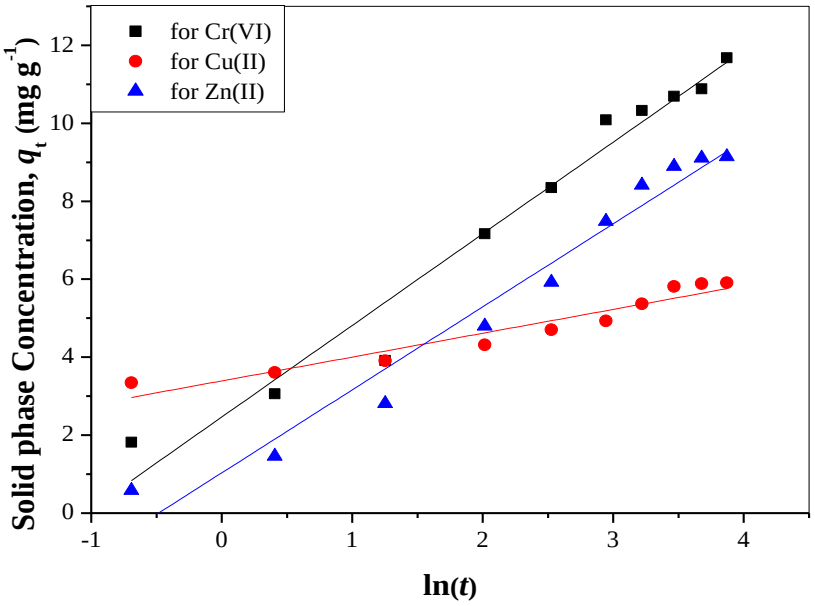

Fig 5.38: Applicability of Elovich kinetic model for Cr(VI), Cu(II) and Zn(II) removal

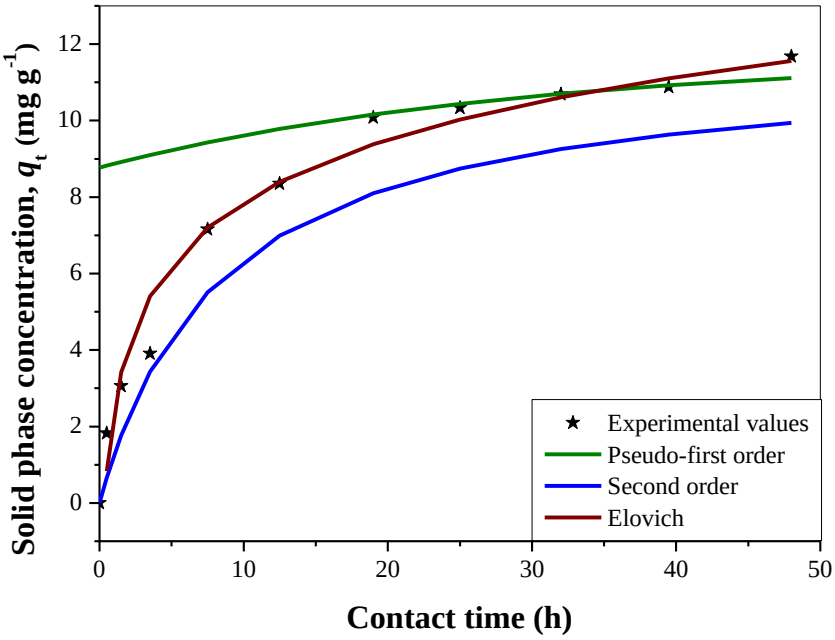

Fig 5.39: Comparison of kinetic models for the removal of Cr(VI) using nANB.

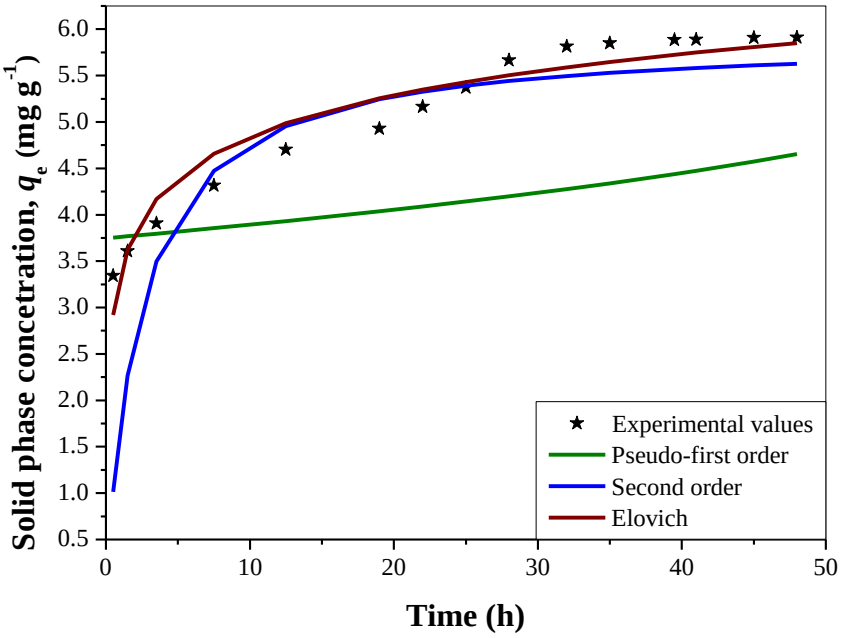

Fig 5.40: Comparison of kinetic models for the removal of Cu(II) using nANB.

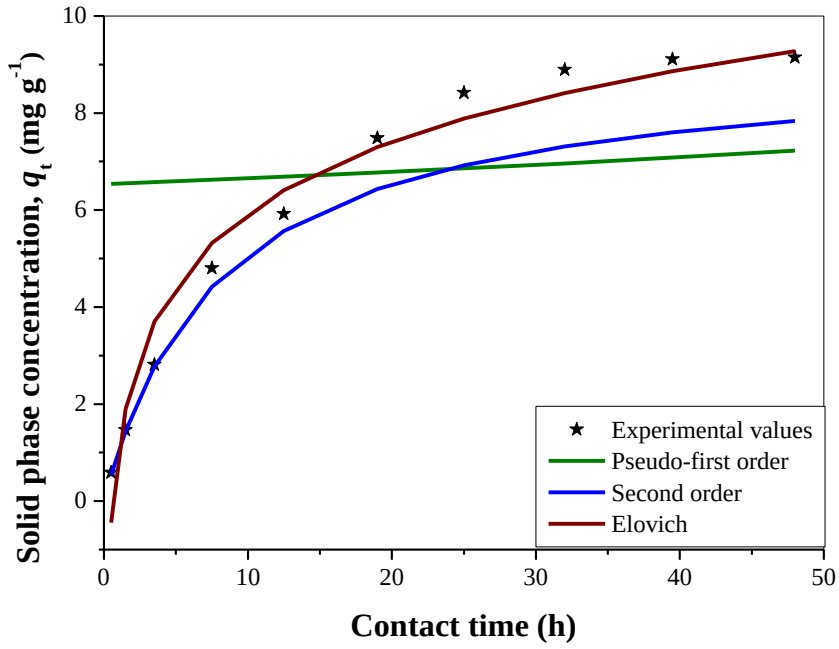

Fig 5.41: Comparison of kinetic models for the removal of Zn(II) using nANB.

5.3.11 Mass Transfer Mechanism

Adsorption is a mass transfer process, hence, it is very important to understand its mechanism of metal transfer from liquid phase to nANB surface. The movement of the solute from bulk fluid to surface can be supported by either the film diffusion or intraparticle diffusion or maybe both. Weber & Moris and Boyd models are applied in the present study to establish the mechanism of metal transfer (Figs 5.42 and 5.43).

5.3.11.1 Weber & Morris Model

Kinetic experimental data are further utilized to study the mass transfer mechanism using the Weber & Morris mass transfer model (Weber and Morris, 1963). The experimental data considered for the evaluation are those which are showing a high mass transfer rate i.e. the initial experimental data i.e. till t = 19, 32 and 25 h for Cr(VI), Cu(II) and Zn(II) respectively. Rate of adsorption becomes very slow in the later part of the adsorption process. The applicability of the Weber & Morris model is evaluated using a plot of q_t vs. $t^{1/2}$ (Fig 5.42). The slope and intercept of the linear fit helps in calculating the value of K_{id} and I (Table 5.7). The Weber & Morris model supports the intraparticle diffusion mechanism of mass transfer, if the best fit line passes through the origin. The best fit linear plots when passed through the origin are giving the R^2 value as 0.996, 0.889 and 0.995 for Cr(VI), Cu(II) and Zn(II) removal. The values of R^2 are very near to 1 for Cr(VI) and Zn(II) removal confirming that the adsorption of these metals on nANB is controlled by the intraparticle diffusion. The data for Cu(II) adsorption data are not showing good agreement with the linear fit, which indicates the possibility of other mass transfer mechanism for Cu(II) adsorption on nANB (Bhatnagar et al., 2010). The value of I which corresponds to the boundary layer thickness is obtained as 0.137, 3.003 and 0.656

for the Cr(VI), Cu(II) and Zn(II) adsorption respectively. The value of *I* also confirms the absence of boundary layer which supports that the film diffusion is not a controlling mechanism for adsorption of Cr(VI) and Zn(II). However, the thickness of boundary layer is reasonable in case of Cu(II) adsorption which suggests the possibility of film diffusion along with intraparticle diffusion as controlling mechanism for adsorption (Ogata and Kawasaki, 2013; Chatterjee and Schiewer, 2014).

5.3.11.2 Boyd Model

Boyd model (Boyd et al., 1947) is also utilized to evaluate the mass transfer mechanism during the adsorption process. The same set of experimental data considered for Weber & Morris model are used to fit the Boyd model. The applicability of the Boyd model is evaluated by plotting a graph of [-0.4977-ln(1-(q_t/q_e))] vs. *t* (Fig 5.43). The slope of the linear fit curve passing through the zero is used to evaluate the value of Boyd constant *B* (Table 5.7) (Chatterjee and Schiewer, 2014). The value of the Boyd constant, *B* is obtained as 0.069, 0.094 and 0.067 for Cr(VI), Cu(II) and Zn(II) adsorption respectively. The values of the R^2 using Boyd model for the removal of Cr(VI), Cu(II) and Zn(II) adsorption are obtained as 0.856, 0.941 and 0.849 respectively. The value of R^2 for Cu(II) adsorption also supports the presence of film diffusion along with intraparticle diffusion. However, Boyd model is not found suitable for describing the mechanism of Cr(VI) and Zn(II) adsorption (Boyd et al., 1947).

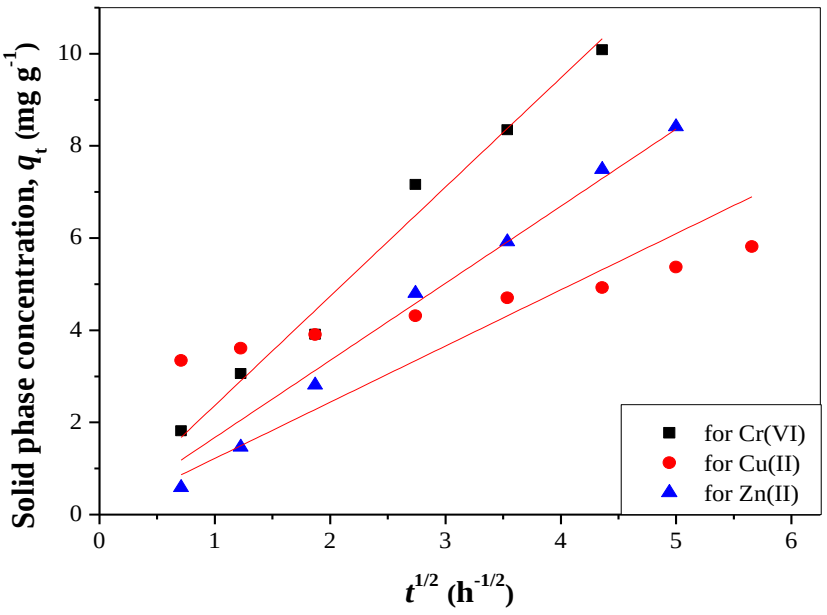

Fig 5.42: Applicability of Weber & Moris model for the removal of Cr(VI), Cu(II) and Zn(II) using nANB.

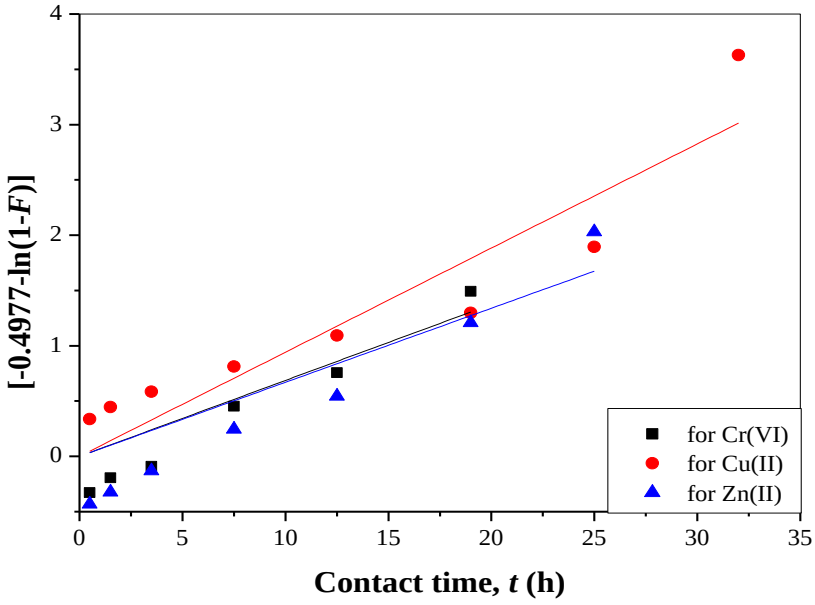

Fig 5.43: Applicability of Boyd model for the removal of Cr(VI), Cu(II) and Zn(II) using nANB.

Table 5.7: Mass transfer coefficients and correlation coefficients for the removal of Cr(VI), Cu(II) and Zn(II).

Metals	Boyd Model		Weber & Morris Model		
	B	R^2	K_{id}	I	R^2
Cr(V)	0.069	0.856	2.324	0.137	0.996
Cu(II)	0.094	0.941	0.477	3.003	0.889
Zn(II)	0.067	0.849	1.856	0.656	0.995

5.3.11.3 Concluding Remarks

The applicability of the Weber & Morris and Boyd mass transfer models (Figs 5.42 & 5.43 and Table 5.7) are tested in the present work. It is observed that the adsorption of Cr(VI) and Zn(II) using nANB are intraparticle diffusion controlled whereas the Cu(II) adsorption on nANB is due to the both, film diffusion and intraparticle diffusion.

5.3.12 Modeling and Optimization

5.3.12.1 Model Development

The batch experimental data for the removal of Cr(VI), Cu(II) and Zn(II) are utilized to develop the model for the prediction of the optimum parameter values for attaining maximum adsorption capacity. The maximum values of individual parameters are identified by tabulating all the related experimental studies of that parameter for a particular metal ion. In all the experiments of three metal ions, the maximum values of contact time, initial concentration, pH and adsorbent dosage are obtained as 48 h, 200 mg L^{-1}, 12.3 and 40 g L^{-1} respectively. The independent parameters along with the adsorption capacity (q_e) are normalized using their respective maximum values. Furthermore, the normalized values of experimental data are calculated according to the Eq. 4.7 and are regressed using the Microsoft Excel 2007 software. The modeled equations obtained for the removal of Cr(VI), Cu(II) and Zn(II) are provided in Eq. 5.10, 5.11 and 5.12 respectively.

$$\begin{aligned}\left(q_{\text{pre}}\right)_{\text{Cr}} = {} & 1.6031 - 6.7863\,X_1 - 11.9281\,X_2 + 1.7652\,X_3 + 6.8039\,X_4 + 17.0896\,X_1^2 \\ & + 34.8511\,X_2^2 - 2.803\,X_3^2 - 25.4028\,X_4^2 - 15.4701\,X_1^3 - 41.1095\,X_2^3 + 1.3957\,X_3^3 \\ & + 32.6020\,X_4^3 + 4.8622\,X_1^4 + 16.3088\,X_2^4 + 0.1264\,X_3^4 - 13.8564\,X_4^4\end{aligned}$$

(5.10)

$$\left(q_{\text{pre}}\right)_{\text{Cu}} = 5.1154 - 26.6715\,X_1 - 9.1814\,X_2 - 0.2065\,X_3 - 0.886\,X_4 + 64.5636\,X_1^2 + 26.6576\,X_2^2 + 3.0046\,X_3^2 - 4.5693\,X_4^2 - 62.096\,X_1^3 - 31.5315\,X_2^3 - 6.1278\,X_3^3 + 10.3155X_4^3 + 21.0209\,X_1^4 + 12.6430\,X_2^4 + 3.6425\,X_3^4 - 5.5455\,X_4^4$$

(5.11)

$$\left(q_{\text{pre}}\right)_{\text{Zn}} = 1.7632 - 4.0155\,X_1 - 5.3391\,X_2 + 3.7152\,X_3 - 3.5182\,X_4 + 7.5819\,X_1^2 + 14.3923\,X_2^2 - 8.282\,X_3^2 + 2.2237\,X_4^2 - 4.0253\,X_1^3 - 18.0854\,X_2^3 + 10.148\,X_3^3 + 3.2327X_4^3 + 0.1755\,X_1^4 + 7.8070\,X_2^4 - 4.9397\,X_3^4 - 2.9448\,X_4^4$$

(5.12)

The regression correlation coefficient coefficients for Eqs. 5.10, 5.11 and 5.12 are obtained as 0.957, 0.921 and 0.927 respectively. This indicates the better fit of the developed equation with the experimental results. The values of predicted q_e from developed model are compared with the experimental q_e in the Fig 5.44 as most of the values are well aligned with the 45° line, this also shows the better agreement between model and experimental data.

5.3.12.2 Optimization

The modeled equations presented in Eqs. 5.10, 5.11 and 5.12 are optimized using the Differential Evolution (DE) method. The range of parameters selected for the optimization study are based on the experimental study of present work. The range of parameters considered are 5 to 200 mg L^{-1} for initial Cr(VI) concentration, 4 to 40 g L^{-1} for adsorbent dosage, 0.17 to 48 h for contact time and 2 to 12 for pH value of the solution. The values of each parameter are normalized using the same maximum values of the experimental parameters.

The convergence plots obtained during the optimization of the models given by Eqs. 5.10, 5.11 and 5.12 are provided in Figs 5.45(a-d), 5.46(a-d) and 5.47(a-d) for the removal of Cr(VI), Cu(II) and Zn(II) respectively. From Figs 5.45 - 5.47, it is evident that the parameters (1) and (3), i.e. initial concentration and contact time must be maximized to attain the maximum adsorption capacity. Whereas the parameters (2) and (4), i.e. pH and mass of adsorbent must be minimized to attain maximum adsorption capacity. The similar results are also obtained from the batch experimental studies for the removal of Cr(VI), Cu(II) and Zn(II).

The optimum values of the initial concentration, contact time, pH and mass of adsorbent for Eq. 5.10 are 200 mg L^{-1}, 48 h, 2.04 and 8.24 g L^{-1}, respectively. These values are in accordance with the optimum values obtained from the experimental results for the individual parameters (Table 5.8). The experimental result shows that the maximum adsorption capacity is obtained when the inlet concentration and contact time is maximized while the pH of the solution and adsorbent dosage is minimized. The optimization results are in alignment with the experimental outcomes. Similarly, the models obtained for the removal of Cu(II) and Zn(II) presented in Eqs. 5.11 and 5.12 are optimized and the optimized values of parameters are tabulated in Table 5.8 along with the optimum values of respective parameter obtained from experimental study.

The sensitivity analysis is also carried out to find the dominant parameters for the adsorption process. The optimum values of parameters are made as twice and a half to see the effect of these changes in the adsorption capacity. For the Cr(VI) adsorption model equation, when the initial concentration increases from 100 to 200 mg L^{-1} and decreases from 100 to 50 mg L^{-1}, the q_e value increases by 62.31% and decreases by

14.05% respectively. Similarly, when the contact time increases from 24 to 48 h, the q_e value increases by 11.99 %. However, q_e decreases by 7.31% when the contact time decreases to 12 h. Also, when the pH of the solution is made double and half from the initial value of pH = 4, the q_e value decreases by 1.11% and increases by 22.79% respectively. Likewise, with the increase in the adsorbent dosage from 16 to 32 g L^{-1}, the q_e value decreases by 19.33% whereas it decreases by 20.1% when the adsorbent dosage is decreased from 16 to 8 g L^{-1}. Similar results are obtained for the Cu(II) and Zn(II) adsorption model equations. Based on the sensitivity analysis of four independent parameters for Cr(VI), Cu(II) and Zn(II) adsorption, it is concluded that the adsorption capacity highly depends on the inlet concentration and is more or less equally dependent on the other three parameters. The order of sensitivity for four parameters is initial concentration > adsorbent dosage > pH > contact time.

5.3.13 Mechanism of Adsorption

It is very important to understand the mechanism of metal adsorption onto the surface of developed adsorbent. The adsorbent used in the present study is prepared from neem bark as raw material. The neem bark is activated by acid and thermal treatment which develop the acidic oxides groups on the surface of prepared nANB adsorbent (Gupta and Babu, 2009b). The surface of nANB is positively charged due to the presence of these groups. This is also supported by the fact that the nANB is a carbonaceous substance and forms positively charged hydroxides ($C_xOH_2^{2+}$) on the surface when it comes in contact with an aqueous solution (Eq. 5.13) (Gupta and Babu, 2009b; 2010a).

$$C_xO_2 + 2H_2O \Leftrightarrow C_xOH_2^{2+} + 2OH^- \qquad (5.13)$$

The FTIR spectra of nANB (Fig 5.6) also confirms the presence of acidic groups on the adsorbent surface. The solution pH and the pH_{zpc} (Zero Point Charge) value of the adsorbent can also be related to the type and ionic state of the functional groups present on the adsorbent surface. The pH_{zpc} value of nANB is found to be 2.80. The surface of the adsorbent is positively charged by maintaining the pH of the solution lower than the value of pH_{zpc} (Gupta and Babu, 2009c; Kapur and Mondal, 2013).

The FTIR of the used adsorbent for the removal of Cr(VI), Cu(II) and Zn(II) are performed to establish the mechanism of metal adsorption and is shown in Fig 5.48 along with the FTIR of the fresh nANB.

While comparing the FTIR spectrum (Fig 5.48) of the fresh nANB and the used nANB for Cr(VI), Cu(II) and Zn(II) adsorption, it is observed that the intensity of the peaks at 1120, 1620 and 3300 cm^{-1} are reduced. This indicate the utilization of C-O, C=C and O-H bonds for metal bonding on the surface of adsorbent during the metal adsorption process. There is no change observed in other peaks present in the spectrums. This also supports the better metal adsorption capability of nANB due to the presence of acidic groups on the surface.

Adsorption of Cr(VI) is more favorable for an acid treated adsorbent (Gupta and Babu, 2009b; 2010a). At a lower pH, the more stable form of Cr is $HCrO_4^-$ which is favorable for adsorption (Kapur and Mondal, 2013). The applicability of nANB for the adsorption of Cr(VI) may be due to the electrostatic attraction between the $HCrO_4^-$ and the positively charged surface of the nANB as per the reaction given by Eq. 5.14:

$$C_XOH_2^{2+} + HCrO_4^- \Rightarrow C_XO_2H_3CrO_3^- \qquad (5.14)$$

Eqs. 5.13 and 5.14 are combined to get Eq. 5.15 as follows:

$$C_XO_2 + 2H_2O + HCrO_4^- \Leftrightarrow C_XO_2H_3CrO_3^- + 2OH^- \quad (5.15)$$

As per Eq. 5.15, the adsorption of one mole of $HCrO_4^-$, liberates two moles of hydroxyl ions which further raises the pH of the solution (Babu and Gupta, 2008b; Gupta and Babu, 2009c; 2010b). In the present study, the increase in pH of the solution is observed after the adsorption of Cr(VI) on the surface of nANB (Section 5.3.4). This also supports the proposed mechanism of Cr(VI) adsorption on nANB surface.

The mechanism of Cu (II) and Zn (II) adsorption on nANB can be commonly represented by Eqs. 5.16, 5.17, and 5.18 (Wasewar, 2010; Zhao et al., 2012; Jellouli Ennigrou et al., 2014):

$$RCOOH \rightarrow RCOO^- + H^+ \quad (5.16)$$

$$2\,RCOO^- + M^{2+} \rightarrow (RCOO)_2\,M \quad (5.17)$$

$$2\,RCOOH + M^{2+} \rightarrow (RCOO)_2\,M + 2H^+{}_S \quad (5.18)$$

As per the above reactions, the adsorption of each metal ion liberates the two H^+ ions in the solution. This results in the decrease of the pH of the solution. The results discussed in Sec. 5.3.4 indicate that the pH of solution is decreased after the adsorption of Cu(II) and Zn(II) ions on nANB surface. This also supports the above described mechanism for Cu(II) and Zn(II) adsorption on nANB surface.

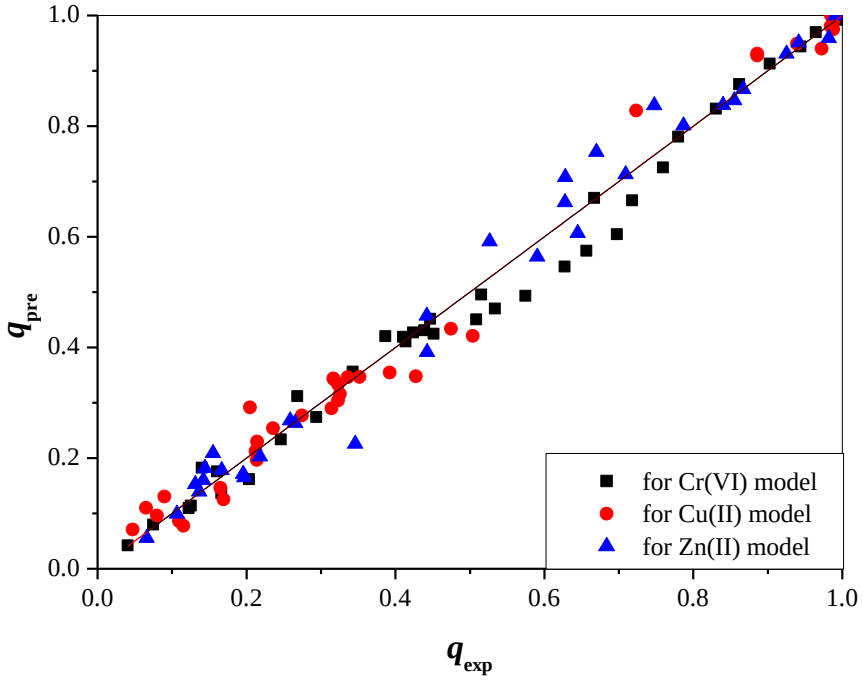

Fig 5.44: Comparison of modeled q_{pre} vs. q_{exp} for the removal of Cr(VI), Cu(II) and Zn(II) using nANB.

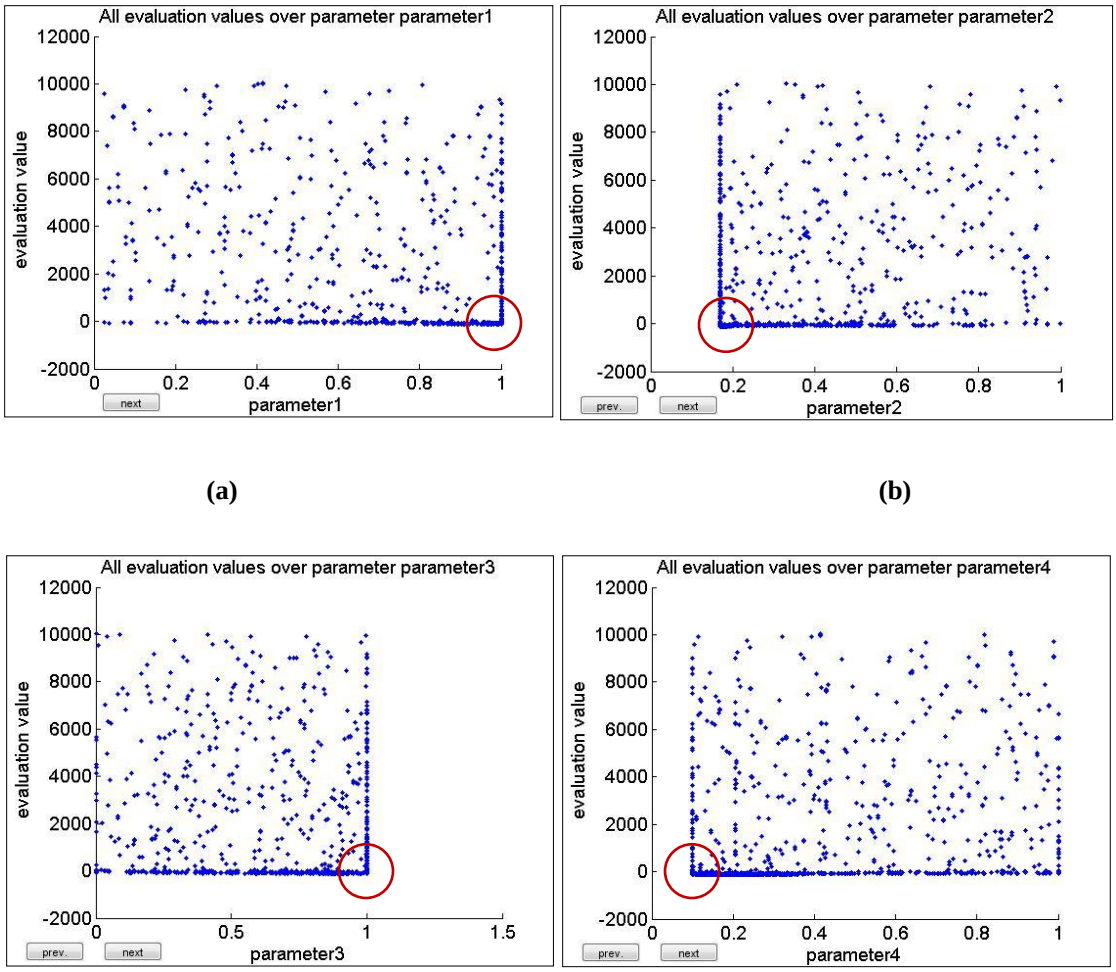

(a) **(b)**

(c) **(d)**

Fig 5.45: Convergence plot for various parameters versus the evaluated value of q. (a) Parameter 1 (Initial concentration), (b) Parameter 2 (pH), (c) Parameter 3 (contact time) and (d) Parameter 4 (mass of adsorbent) for the removal of Cr(VI) using nANB.

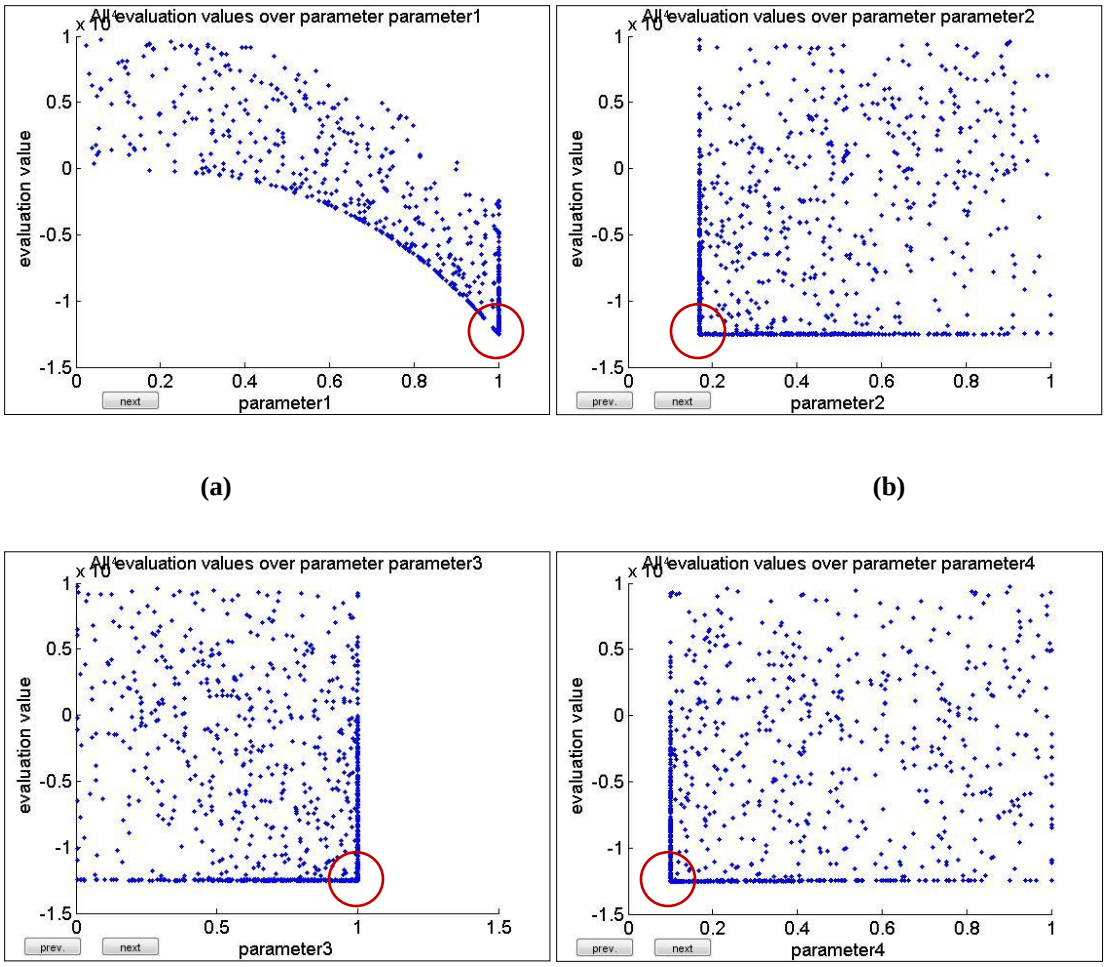

(a) **(b)**

(c) **(d)**

Fig 5.46: Convergence plot for various parameters versus the evaluated value of q. (a) Parameter 1 (Initial concentration), (b) Parameter 2 (pH), (c) Parameter 3 (contact time) and (d) Parameter 4 (mass of adsorbent) for the removal of Cu(II) using nANB.

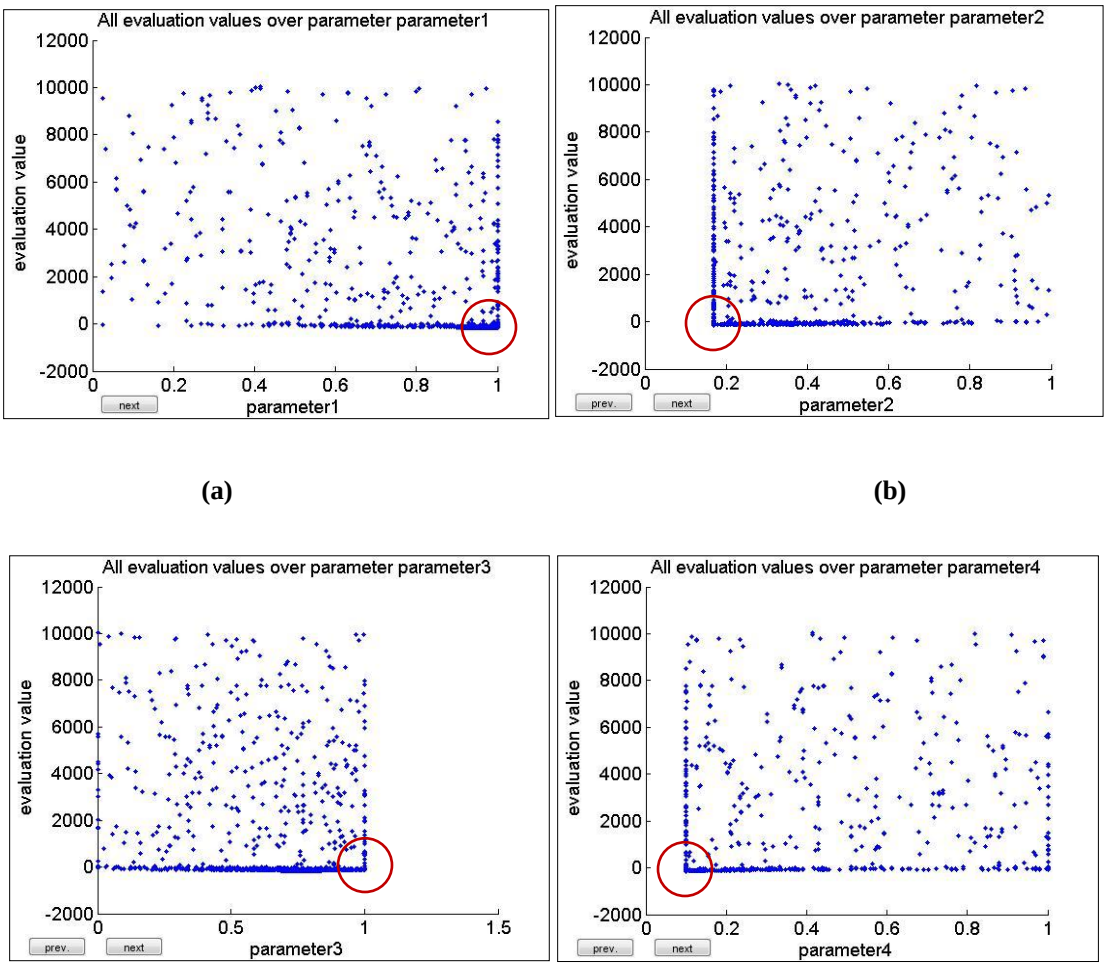

(a) **(b)**

(c) **(d)**

Fig 5.47: Convergence plot for various parameters versus the evaluated value of q. (a) Parameter 1 (Initial concentration), (b) Parameter 2 (pH), (c) Parameter 3 (contact time) and (d) Parameter 4 (mass of adsorbent) for the removal of Zn(II) using nANB.

Table 5.8: Optimum parameter values obtained from the optimization of obtained model for maximizing the adsorption capacity for removal of specific metals

Metal	Optimum Parameters							
	Initial Conc. (mg L^{-1})		pH		Contact Time (h)		Mass of Adsorbent (g L^{-1})	
	Exp.	Model	Exp.	Model	Exp.	Model	Exp.	Model
Cr(VI)	200	200	2	2.04	48	48	4	8.24
Cu(II)	200	200	2	2.04	48	48	4	4
Zn(II)	200	193	2	2.04	48	36.88	4	4

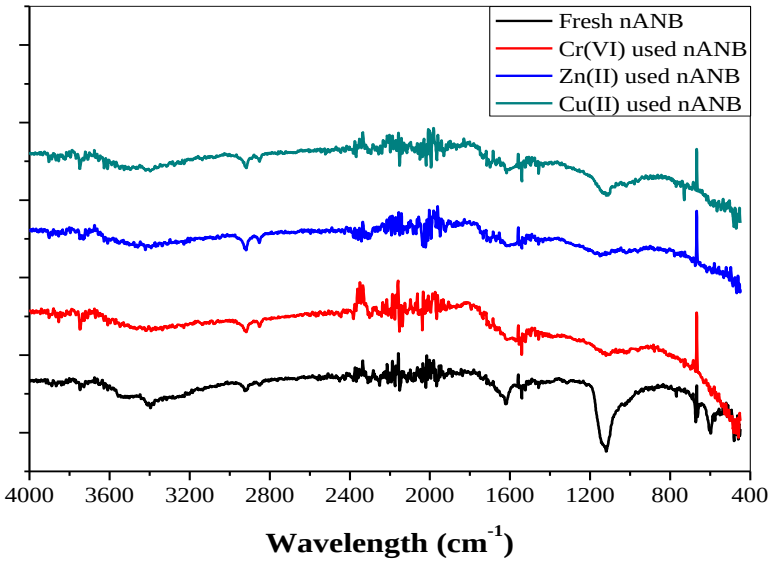

Fig 5.48: FTIR of fresh and used nANB on Cr(VI), Cu(II)and Zn(II).

5.3.14 Comparison of Adsorption Capacity

The Langmuir isotherm model is considered to evaluate the maximum adsorption capacity of nANB for the individual removal of Cr(VI), Cu(II) and Zn(II). It is observed that the adsorption capacity of nANB is sufficiently high as compared to other low-cost adsorbents reported in the literature. A comparison of the maximum adsorption capacity of developed adsorbent for the Cr(VI), Cu(II) and Zn(II) adsorption with other reported low-cost adsorbents are given in Tables 5.9, 5.10 and 5.11 respectively. The total adsorption capacity of developed nANB for the simultaneous removal of Cr(VI), Cu(II) and Zn(II) ions is obtained as 38.95 mg g^{-1}. This adsorption capacity value is approximately 1.5 times of the one evaluated for the removal of any individual metal ions. This also supports the utilization of developed nANB for the simultaneous removal of multiple metals ions which is an additional advantage of developed adsorbent over other reported low-cost adsorbents.

Table 5.9: Comparison of adsorption capacity for the removal of Cr(VI) using various adsorbents.

S.No.	Adsorbent	Capacity q_m (mg g^{-1})	References
1	Saw dust	41.9	Gupta and Babu (2009b)
2	Activated tamarind seeds	28.9	Gupta and Babu (2009a)
3	**nANB**	**26.95**	**Present Study**
4	Leaf mould	25.9	Sharma and Forster (1996)
5	Pine needles	21.50	Dakiky et al. (2002)
6	Coconut shell based activated carbon	20.0	Alaerts et al. (1989)
7	Sugar beet pulp	17.2	Sharma and Forster (1994)
8	Palm pressed-fibers	15.0	Tan et al. (1993)
9	Maize cob	13.8	Sharma and Forster (1994)
10	Sugar cane bagasse	13.4	Sharma and Forster (1994)
11	Almond	10.0	Dakiky et al. (2002)
12	Maple saw dust	8.2	Yu et al. (2003)
13	Cactus	7.08	Dakiky et al. (2002)
14	Coal	6.78	Dakiky et al. (2002)
15	Biomass residual slurry	5.87	Namasivayam and Yamuna (1995)
16	Distillery sludge	5.7	Selvaraj et al. (2003)
17	Waste tea	1.55	Orhan and Büyükgüngör (1993)
18	Fe(III)/Cr(III) hydroxide	1.43	Namasivayam and Ranganathan (1993)
19	Walnut shell	1.33	Orhan and Büyükgüngör (1993)
20	Soya cake	0.28	Daneshvar et al. (2002)

Table 5.10: Comparison of adsorption capacity for the removal of Cu(II) using various adsorbents.

S.No.	Adsorbent	Capacity q_m (mg g^{-1})	References
1	Green Clay	28.3	Eloussaief et al. (2009)
2	Activated red clay	26.8	Eloussaief et al. (2009)
3	Chemically activated carbon residue	23	Runtti et al. (2014)
4	Chemical activated pomegranate peel	21.78	El-Ashtoukhy et al. (2008)
5	**nANB**	**21.6**	**Present Study**
6	Granulated activated carbon	20.833	Senthil Kumar et al. (2010)
7	Cashew nut shell	20.00	Senthil Kumar et al. (2011)
8	Cellulose-g-acrylic acid copolymer	17.16	Güçlü et al. (2003)
9	Starch-graft-acrylic acid copolymer	16.52	Keleş and Güçlü (2006)
10	Wheat bran	15.00	Farajzadeh and Monji (2004)
11	MMT-modified with Hexa-decyl-trimethyl-ammonium ions /2-mercapto-5-amino-1,3,4-thiadiazole	≈15	Filho et al. (2006)
12	SiaL2(0.38)	12.7	Bou-Maroun et al. (2006)
13	Zeolite	11.3	Egashira et al. (2012)
14	Kaolinite	10.79	Yavuz et al. (2003)
15	Clay	10.53	Sheikhhosseini et al. (2013)
16	Grape stalks wastes	10.10	Villaescusa et al. (2004)
17	MMT modified with sodium dodecylsulfate	8.3	Lin and Juang (2002)
18	Hazelnut shell	6.65	Altun and Pehlivan (2007)
19	Walnut shell	6.64	Altun and Pehlivan (2007)
20	Chestnut shell	5.47	Vázquez et al. (2009)
21	Red mud	5.3493	Nadaroglu et al. (2010)
22	Barley straw	4.64	Pehlivan et al. (2009)
23	Lignite	4.045	Milicevic et al. (2012)
24	Almond shell	3.62	Altun and Pehlivan (2007)
25	Quinalizarin-functionalized XAD-2	3.15	Kumar et al. (2001)

Table 5.11: Comparison of adsorption capacity for the removal of Zn(II) using various adsorbents.

S.No.	Adsorbent	Capacity q_m (mg g^{-1})	References
1	Saw dust	14.1	Naiya et al. (2009)
2	Activated carbon prepared from Van apple pulp	12.91	Depci et al. (2012)
3	**nANB**	**11.904**	**Present Study**
4	Active carbon	11.24	Mishra and Patel (2009)
5	Penicillium chrysogenum	11.11	Üçer et al. (2006)
6	Fly ash	11	Pehlivan et al. (2006)
7	Saw dust	10.96	Shukla and Pai (2005)
8	Low-grade phosphate	10.32	Kandah (2004)
9	Groundnut shells (dyed with C.I. Reactive Orange 13)	9.57	Shukla and Pai (2005)
10	Streptoverticillium cinnamoneum	9.15	Puranik and Paknikar (1999)
11	Bentonite	9.12	Mishra and Patel (2009)
12	Groundnut shells	7.62	Shukla and Pai (2005)
13	Zeolite	3.7	Egashira et al. (2012)
14	Clay	3.6	Sheikhhosseini et al. (2013)
15	Fly ash	5.82	Mishra and Patel (2009)
16	BFS	3.25	
17	Kaolin	3.05	
18	Chestnut shell	2.5	Vázquez et al. (2009)
19	Low rank Turkish coal	1.66	Karabulut et al. (2000)
20	Tannic acid immobilized activated carbon	1.23	Üçer et al. (2006)
21	Carbon aerogel	1.183	Meena et al. (2005)
22	Sugar beat pulp	0.176	Pehlivan et al. (2006)

5.3.15 Cost Analysis

Cost analysis is an important influential factor for the selection of any heavy metal removal process. The economics of the adsorption process is primarily dependent on the cost of the adsorbent utilized for the removal of heavy metals from wastewater. The most utilized adsorbent is the activated carbon which is expensive. Therefore, in the developing countries like India, a low-cost adsorbent is a more affordable option if it is easily available and environmental friendly. In the present work, an effort is made to estimate the cost of the developed nANB. The cost of the development of 1 kg of nANB is calculated on the basis of the cost of chemical, crushing energy and heating energy utilized during the process as discussed in Sec. 3.1. The breakup cost of the all the physical and chemical components involved are provided in Table 5.12. The commercial activated carbon developed from coconut shell is available at 75.86 Rs/kg (Fan, 2015). Based on the adsorption capacity obtained using batch experiments for all the metal ions, the cost of adsorbent for the removal of 1 g of each metal ion is calculated (Table 5.13).

It is observed that the removal of 1 g of Ni(II) is 1.73 Rs which is least in comparison to the removal of other the metal ions. This low-cost of the removal process is a result of the higher adsorption capacity i.e. 29.412 mg g^{-1} of nANB for the removal of Ni(II). The cost of the removal of other metal ions i..e. Cr(VI), Pb(II), Cu(II), Cd(II) and Zn(II) are obtained as Rs. 1.89, 1.94, 2.36, 2.44 and 4.59 respectively. The cost removal of 1 g of Cr(VI) using activated carbon developed from coconut shell is coming to be Rs. 3.79 which is approximately double than that for the nANB (Rs.1.89). Although the surface area of the developed adsorbent is less in comparison to the commercial adsorbents (Table 5.3), however, the raw material used for the development of adsorbent is biodegradable and low-cost. This makes the overall metal removal process cost effective as compared to that for the commercial adsorbent. This supports the economic viability of the developed nANB and as an alternate of the commercial adsorbent for metal removal.

Table 5.12: Breakup and total cost for preparing 1 kg of nANB from neem bark.

Materials	**Amount Used for 1 Kg production**	**Unit price**	**Net price (Rs.)**
Sulfuric Acid (kg)	0.555 kg	12.8 Rs. kg^{-1}	7.104
Cost of Crushing 1 (Rs. kg^{-1})	0.1 h	21 Rs. h^{-1}	2.1
Cost of Crushing 2(Rs. kg^{-1})	0.2 h	7 Rs. h^{-1}	1.4
Cost of Crushing 3(Rs. kg^{-1})	0.1 h	21 Rs. h^{-1}	2.1
Cost of heating (Rs. kg^{-1})	24 h	1.4 Rs. h^{-1}	33.6
Net Cost			**46.30**
Overhead (10% of net cost)			4.63
Total cost (Rs.)			**50.93**

Table 5.13: Cost of adsorbent for the removal of 1 g of metal ions.

Metal	**Capacity (mg g^{-1})**	**Adsorbent Required for 1 g Metal Removal**	**Cost of Adsorbent (Rs.)**
Cd(II)	20.83	48.00	2.44
Cr(VI)	26.9	37.17	1.89
Cu(II)	21.6	46.30	2.36
Ni(II)	29.41	34.00	1.73
Pb(II)	26.32	37.99	1.94
Zn(II)	11.1	90.09	4.59
Cr(VI) by Activated carbon (Fan, 2015)	20	50.00	3.79

5.4 Continuous Experiments

The batch study results established the fact that the nANB is a suitable adsorbent for the removal of Cd(II), Cr(VI), Cu(II), Ni(II), Pb(II) and Zn(II). Hence, the continuous experiments are performed in the laboratory scale fixed-bed adsorption column for the removal of individual as well as multiple metal ions from wastewater. In the succeeding sections, the effect of various parameters such as the mass of adsorbent, the inlet flow rate, the inlet metal ion concentration and interference of other ions on the continuous removal of Cr(VI), Cu(II) and Zn(II) is discussed. The applicability of nANB is also checked for the simultaneous removal of multiple metal ions from the synthetically prepared pulp & paper industrial effluent solution. The various kinetic parameters such as the breakthrough time (t_b), the stoichiometric capacity of the column (q_t), time equivalent to the stoichiometric capacity of the column (t_t), total percentage removal (S), the empty bed residence time (EBRT) and the fraction of the unused bed length (y) are also evaluated (Tables 5.14 to 5.16) . The experimental data are also fitted with the Yoon-Nelson and Yan models.

5.4.1 Effect of Inlet Flowrate

The effect of inlet flow rate on the breakthrough curve for the removal of Cr(VI), Cu(II) and Zn(II) is studied by varying the flow rate from 5 to 15 mL min^{-1} while keeping the mass of the adsorbent and initial metal ion concentration constant as 75 g and 50 mg L^{-1} respectively. The obtained breakthrough curves for Cr(VI), Cu(II) and Zn(II) removal at different flow rates are shown in Figs 5.49, 5.50 and 5.51 respectively.

With an increase in the flow rate from 5 to 15 mL min^{-1}, there is a decrease in the breakthrough time from 35.09 to 8.26 h, 31.93 to 13.46 h and 32.07 to 25.06 h for the removal of Cr(VI), Cu(II) and Zn(II) respectively (Tables 5.14, 5.15 and 5.16). This decrease in the breakthrough time may be due to availability of more amount of metal for adsorption in the same time duration for the same number of active sites. The total amount of the Cr(VI), Cu(II) and Zn(II) adsorbed increases from 1246 to 1907, 1086 to 1656 and 841 to 1810 mg respectively with an increase in the flowrate from 5 to 15 mL min^{-1}. It is observed that the steepness of breakthrough curve increases with an increase in the flowrate. This increase in the amount adsorbed and the steepness may be due to the better mixing at high flow rate which reduces the film thickness over the adsorbent. This subsequently reduces the film mass transfer resistance for metal transfer from bulk to adsorbent surface (Gupta, 2008b) and leads to higher rate of mass transfer. With an increase in the flow rate from 5 to 15 mL min^{-1}, there is a decrease in residence time from 30.41 to 10.14 sec. The decrease in the contact time affect the proper utilization of the adsorbent. The fraction of the unused bed length increases from 57.79 to 80.33 and 56.27 to 64.17% with an increase in the inlet flowrate from 5 to 15 mL min^{-1} for the removal of Cr(VI) and Cu(II) respectively. The percentage removal of Cr(VI), Cu(II) and Zn(II) decreases from 61.17 to 58.94, 57.10 to 54.93 and 61.10 to 57.90% respectively with an increase in the flowrate from 5 to 15 mL min^{-1}. The total time required corresponding to the stoichiometric capacity of the column decreases from 135.8 to 71.9 h, 126.8 to 67.0 h and 91.7 to 69.5 h for the removal of Cr(VI), Cu(II) and Zn(II) respectively with an increase in the flow rate from 5 to 15 mL min^{-1}. This may be due to the presence of more amount of adsorbate in per unit time for the adsorbent to get saturated. The average

saturation loading (q_s) for Cr(VI), Cu(II) and Zn(II) are found as 22.53, 18.99 and 18.5 mg g^{-1} respectively. The saturation loading values estimated from continuous studies for Cr(VI) and Cu(II) removal are less than the values obtained from batch studies [26.95 mg g^{-1} for Cr(VI) and 21.23 mg g^{-1} for Cu(II)]. However, the saturation loading value for Zn(II) removal estimated from continuous studies is significantly higher than the values obtained from the batch studies (11.904 mg g^{-1}).

5.4.2 Effect of Mass of Adsorbent

The effect of the mass of the adsorbent on the breakthrough curve for Cr(VI), Cu(II) and Zn(II) removal is studied. The breakthrough curves for variable mass i.e. 25, 50, 75, 100, 125, 150 and 175 g are shown in Figs 5.52, 5.53 and 5.54 respectively. The other parameters such as the inlet flow rate and initial metal ion concentration are maintained constant as 10 mL min^{-1} and 50 mg L^{-1} respectively. The various adsorption parameters for fixed-bed adsorption are evaluated and tabulated in Tables 5.14, 5.15 and 5.16 for Cr(VI), Cu(II) and Zn(II) adsorption respectively.

With an increase in the mass of the adsorbent from 25 to 175 g, the breakthrough time is increased from 9.25 to 111.66 h, 6.03 to 69.32 h and 8.75 to 79.03 h for the removal of Cr(VI), Cu(II) and Zn(II) respectively (Figs 5.52, 5.53 and 5.54). The increase in the breakthrough time may be due to the longer bed length (Rout et al., 2014). It is observed that with an increase in the mass of the adsorbent, the total amount of Cr(VI), Cu(II) and Zn(II) adsorbed is increased from 868 to 5069, 824 to 4113 and 645 to 3570 mg respectively. The increase in the adsorbed amount and breakthrough time may be due to the availability of more number of active sites for the adsorption of the metal ions (Deng et al., 2014). This also leads to an increase in the overall percentage removal of the

Cr(VI), Cu(II) and Zn(II) from 38.23 to 72.89, 38.73 to 65.45 and 48.89 to 62.98 % respectively with an increase in the mass of the adsorbent from 25 to 175 g. The residence time increases from 5.07 to 35.48 sec with an increase in the mass of adsorbent from 25 to 175 g. Stoichiometric capacity for the removal of Cr(VI), Cu(II) and Zn(II) are obtained as 28.30, 24.41 and 20.65 mg g^{-1} respectively. The obtained stoichiometric capacity values from the fixed-bed adsorption experiments are better than the values obtained from the batch experiments. The total time required corresponding to the stoichiometric capacity of the column increases from 75.7 to 231.8 h, 70.9 to 209.4 h and 44 to 188.9 h for the removal of Cr(VI), Cu(II) and Zn(II) respectively when the mass of adsorbent increases from 25 to 175 g. This may be due to the presence of more amount of adsorbent for the adsorption of metal ions. The fraction of the unused bed length decreases from 73.83 to 33.74, 78.28 to 49.48 and 60.31 to 34.86% for the removal of Cr(VI), Cu(II) and Zn(II) respectively with an increase in the mass of the adsorbent from 25 to 175 g (Tables 5.14, 5.15 and 5.16). The unused bed length is constant for a given particle size of adsorbent and fluid velocity. With an increase in the bed height, the length of unused bed remains constant. Hence the fraction of the unused bed length decreases with an increase in the bed height (McCabe et al., 2007). With an increase in the mass of the adsorbent from 25 to 175 g, the adsorbent exhaustion rate decreases from 7.284 to 2.612, 6.90 to 4.21 and 4.76 to 3.69 g L^{-1} for the removal of Cr(VI), Cu(II) and Zn(II) respectively. This decrease with an increase in mass of adsorbent is due to the increase in the time required for the saturation of the bed (Gupta, 2008b).

Table 5.14: Different parameters for the removal of Cr(VI) from aqueous solution in a fixed-bed adsorption column.

S. No.	C_0	Q	W	t_t	t_f	t_b	q_s	q_t	m_t	S	EBRT	R_a	y
	mg L^{-1}	mL min^{-1}	g	h	h	h	mg g^{-1}	mg	mg	%	sec	g L^{-1}	
1	50	10	75	110.7	198	24.78	25.75	1858	3321	55.92	15.21	5.04	0.6151
2	100	10	75	57.4	150	13.88	35.08	1316	3442	38.24	15.21	9.01	0.6836
3	50	5	75	135.8	222	35.09	16.62	1246	2036	61.17	30.41	7.13	0.5779
4	50	15	75	71.9	122	8.26	25.21	1907	3236	58.94	10.14	10.09	0.8034
5	50	10	25	75.7	198	9.25	34.57	868	2270	38.23	5.07	4.50	0.6789
6	50	10	50	93.2	198	11.44	26.23	1316	2795	47.06	10.14	7.28	0.7383
7	50	10	100	147.7	246	50.24	26.61	2659	4429	60.02	20.28	3.32	0.4337
8	50	10	125	176.9	270	74.15	27.65	3478	5307	65.52	25.35	2.81	0.3563
9	50	10	150	204.8	294	98.23	28.42	4282	6145	69.68	30.41	2.55	0.3086
10	50	10	175	231.8	318	111.6	28.89	5069.	6954	72.89	35.48	2.61	0.3374

Table 5.15: Different parameters for the removal of Cu(II) from aqueous solution in a fixed-bed adsorption column.

S.No.	C_o	Q	W	t_t	t_f	t_b	q_s	q_t	m_t	S	EBRT	R_a	y
	mg L^{-1}	mL min^{-1}	gm	h	h	h	mg g^{-1}	mg	mg	%	sec	gm L^{-1}	%
1	50	10	75	99.1	198	19.8148	19.82	1488.6	2973.60	50.06	15.21	6.31	0.6001
2	100	10	75	75.9	150	8.875	30.83	2305.02	4554.69	50.61	15.21	14.08	0.7697
3	50	5	75	126.8	222	31.9266	14.60	1085.7	1901.42	57.10	30.41	7.83	0.5627
4	50	15	75	67.0	122	13.4595	22.54	1656.45	3015.61	54.93	10.14	6.19	0.6417
5	50	10	25	70.9	183	6.0357	33.35	823.5	2126.27	38.73	5.07	6.90	0.7828
6	50	10	50	85.1	185	11.3097	23.62	1173.6	2552.15	45.98	10.14	7.37	0.7128
7	50	10	100	134.5	246	23.608	22.18	2205.12	4034.08	54.66	20.28	7.06	0.6807
8	50	10	125	163.6	270	46.075	24.15	2973.33	4907.54	60.59	25.35	4.52	0.5421
9	50	10	150	189.7	298	53.9158	24.23	3621.15	5689.73	63.64	30.41	4.64	0.5549
10	50	10	175	209.4	320	69.317	23.52	4112.55	6283.35	65.45	35.48	4.21	0.4948

Table 5.16: Different parameters for the removal of Zn(II) from aqueous solution in a fixed-bed adsorption column.

S.No.	C_o	Q	W	t_t	t_f	t_b	q_s	q_t	m_t	S	EBRT	R_a	y
	mg L^{-1}	mL min^{-1}	gm	h	h	h	mg g^{-1}	mg	mg	%	sec	gm L^{-1}	%
1	50	10	75	75.0	120	27.5	19.16	1405.5	2249.40	62.48	15.21	4.55	0.4258
2	100	10	75	72.6	130	20.37	32.93	2432.85	4356.17	55.85	15.21	6.14	0.5051
3	50	5	75	91.7	150	32.069	11.54	840.075	1374.83	61.10	30.41	7.80	0.4444
4	50	15	75	69.5	120	25.0575	24.80	1810.35	3126.64	57.90	10.14	3.33	0.3938
5	50	10	25	44.0	90	8.748	26.45	645.3	1319.97	48.89	5.07	4.76	0.6031
6	50	10	50	47.4	100	13.889	18.47	675	1423.02	47.43	10.14	6.00	0.5488
7	50	10	100	109.1	190	36.273	19.09	1879.5	3273.09	57.42	20.28	4.59	0.4301
8	50	10	125	145.3	270	49.94	19.30	2346.3	4359.48	53.82	25.35	4.17	0.3790
9	50	10	150	171.1	280	70.136	21.30	3135.6	5132.16	61.10	30.41	3.56	0.3416
10	50	10	175	188.9	300	79.032	20.80	3569.85	5668.21	62.98	35.48	3.69	0.3486

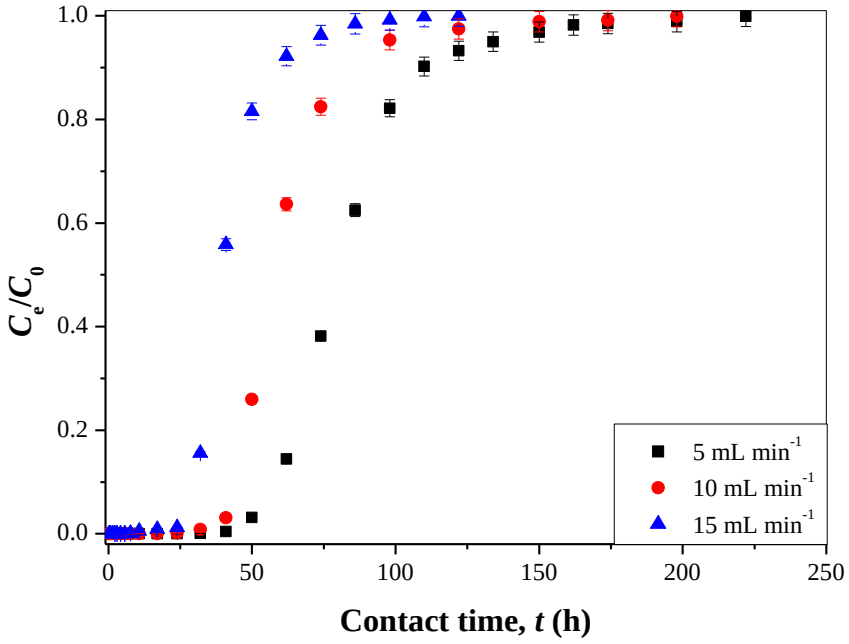

Fig 5.49: Effect of inlet flow rate on the removal of Cr(VI) using nANB.

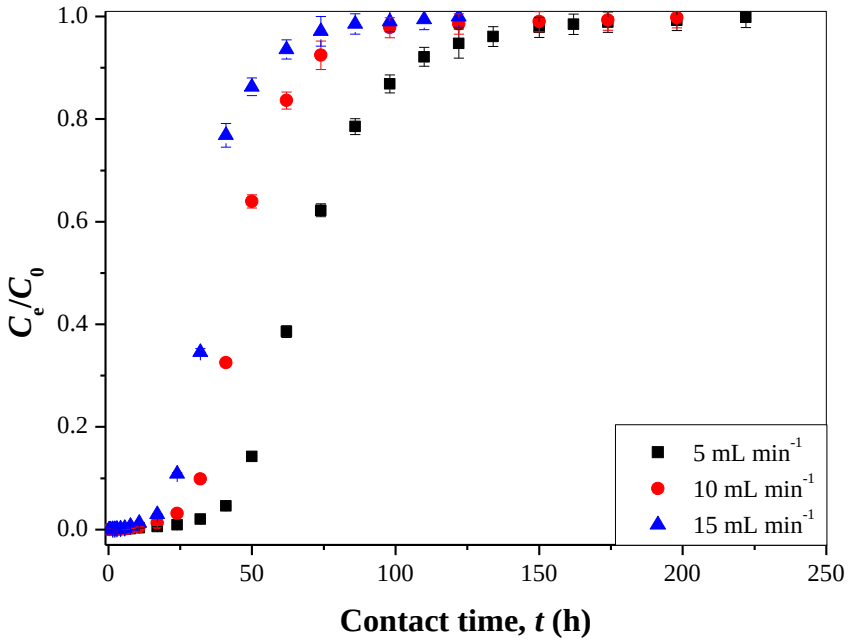

Fig 5.50: Effect of inlet flow rate on the removal of Cu(II) using nANB.

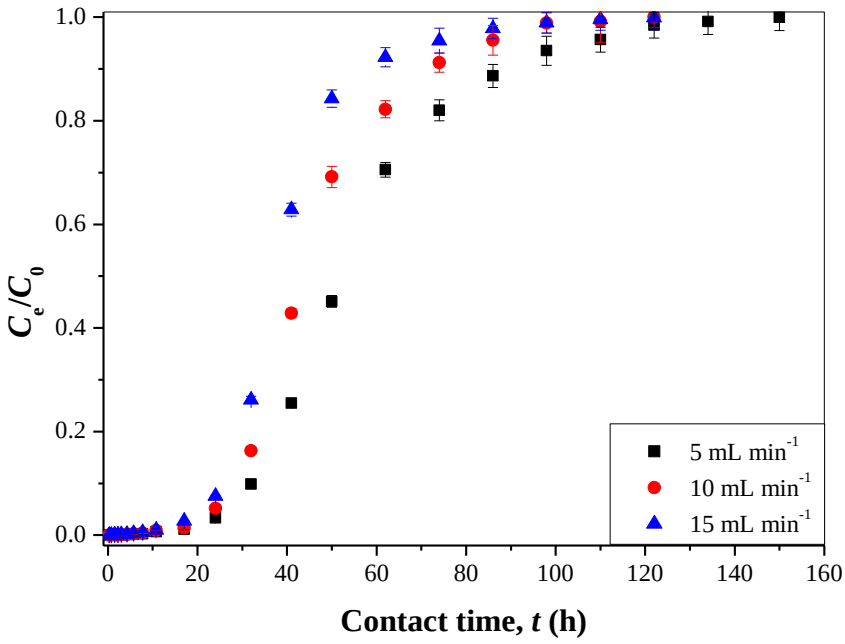

Fig 5.51: Effect of inlet flow rate on the removal of Zn(II) using nANB.

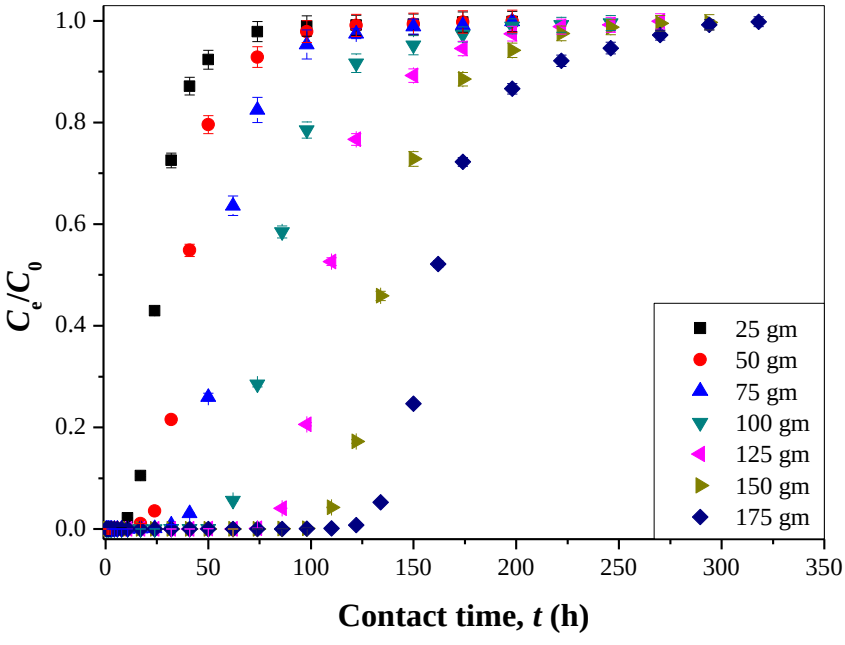

Fig 5.52: Effect of mass of adsorbent on the continuous removal of Cr(VI) using nANB.

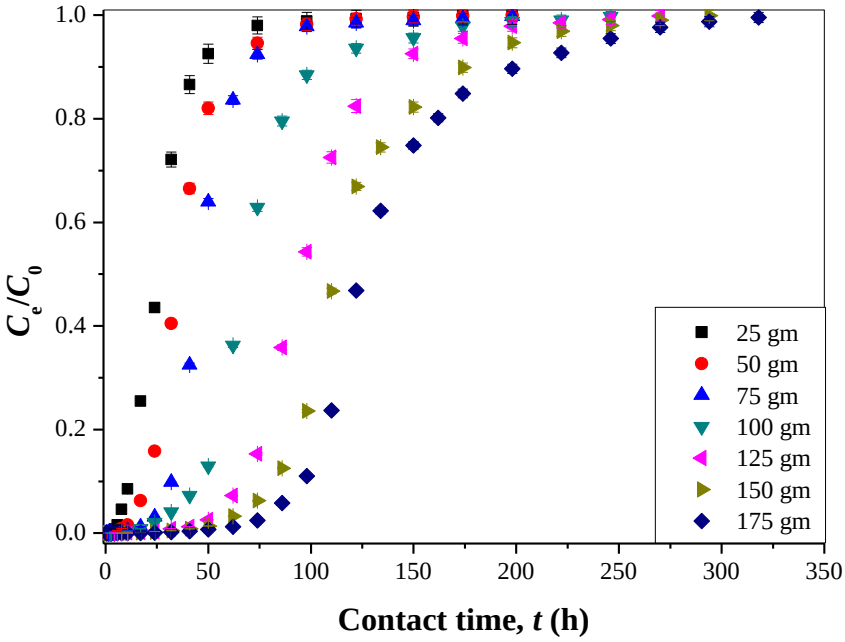

Fig 5.53: Effect of mass of adsorbent on the continuous removal of Cu(II) using nANB.

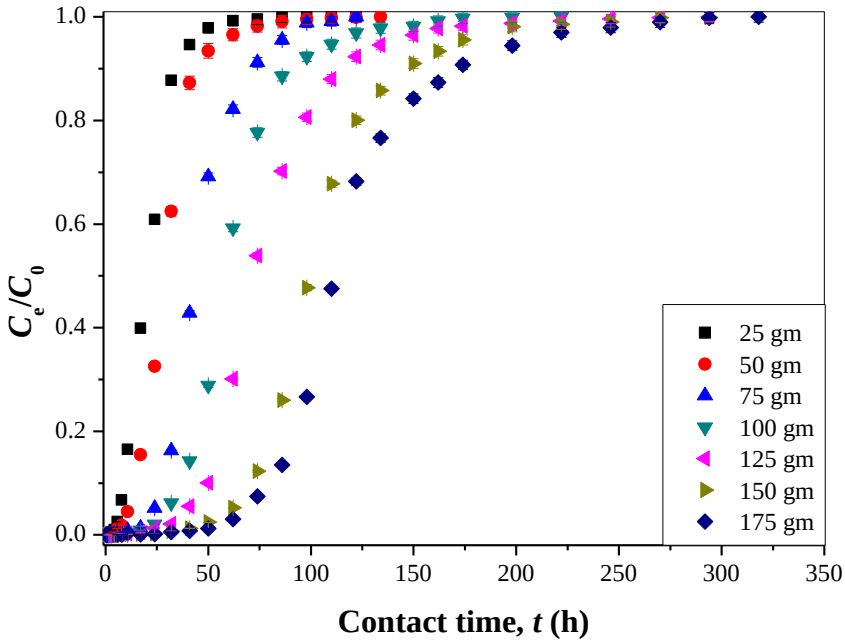

Fig 5.54: Effect of mass of adsorbent on the continuous removal of Zn(II) using nANB.

5.4.3 Effect of Inlet Concentration

The effect of the initial concentrations (50 mg L^{-1} and 100 mg L^{-1}) on the breakthrough curve for Cr(VI), Cu(II) and Zn(II) adsorption from aqueous solution is shown in Figs 5.55, 5.56 and 5.57 respectively. The parameters for Cr(VI), Cu(II) and Zn(II) adsorption are calculated for each experimental run and are reported in Tables 5.14, 5.15 and 5.16 respectively.

It is observed that, with an increase in the initial concentration from 50 to 100 mg L^{-1}, there is a decrease in breakthrough time from 24.78 to 13.88, 27.5 to 20.37 and 19.81 to 8.88 h for the removal of Cr(VI), Cu(II) and Zn(II) respectively. This may be due to the fact that more amount of metal ions are passed through the fixed-bed in per unit time. This leads to the faster saturation of the bed and further decrease in breakthrough time. The adsorption exhaustion rate for the removal of Cr(VI), Cu(II) and Zn(II) increases from 5.04 to 9.01, 6.31 to 14.08 and 4.55 to 6.14 g L^{-1} respectively with an increase in the inlet concentration from 50 to 100 mg L^{-1}. The increase in the concentration in bulk liquid phase increases the driving force (concentration difference) for mass transfer which further increases the rate of diffusion. This also results in the increase of diffusion and mass transfer coefficients for metal transport from liquid to solid phase. This leads to the relatively faster transport of the molecules from the bulk phase to solid surface of nANB (Aksu and Gönen, 2004; Gupta and Babu, 2009c)

The fraction of the unused bed length increases from 61.51 to 68.36, 60.01 to 76.97 and 42.58 to 50.51% for the removal of Cr(VI), Cu(II) and Zn(II) respectively with an increase in inlet concentration. The total percentage removal of Cr(VI) and Zn(II) decreases from 55.92 to 38.24 and 62.48 to 55.85% with an increase in the inlet metal

concentration from 50 to 100 mg L^{-1}. The total time required for the adsorption is analogous to the stoichiometric capacity of the column and is found to be decreased from 110.7 to 57.4, 99.1 to 75.9 and 75.0 to 72.6 h for the removal of Cr(VI), Cu(II) and Zn(II) respectively when the inlet concentration is increased from 50 to 100 mg L^{-1}. This is due to the availability of more molecules of metal ions in the solution for the same amount of adsorbent to get saturated (Gupta and Babu, 2009c; Riazi et al., 2014).

5.4.4 Effect of Interference of Other Metal Ions

It is very important to study the performance of nANB for the removal of individual metal ions from wastewater in the presence of other metal ions. This study would indicate the applicability of nANB to treat industrial effluents. In this study, the inlet concentration of 50 mg L^{-1} of each metal [Cr(VI), Cu(II) and Zn(II)] is maintained. The flow rate and mass of adsorbent are maintained as 10 mL min^{-1} and 75 g respectively. The breakthrough curves for the simultaneous removal of Cr(VI), Cu(II) and Zn(II) are shown in Fig 5.58. To compare the results of individual metal ion removal with multiple metal ion, the breakthrough curves for individual metal ions are also shown in Fig 5.58. The adsorption parameters are evaluated and tabulated in Table 5.17.

The breakthrough time is obtained as 9.25, 14.3 and 6.83 h for the removal of Cr(VI), Cu(II) and Zn(II) respectively for mixed metal adsorption. The breakthrough time obtained for Cr(VI), Cu(II) and Zn(II) from mixed solution is lesser than the breakthrough time obtained from the pure aqueous solution of metal ions (Fig 5.58). This decrease in the breakthrough time is due to the simultaneous utilization of the active sites available on the nANB surface for the adsorption of Cr(VI), Cu(II) and Zn(II) from the solution. The simultaneous adsorption of Cr(VI), Cu(II) and Zn(II) on the surface of the

nANB can also be confirmed from the EDS analysis (Fig 5.28). The saturation loading capacity of Cr(VI), Cu(II) and Zn(II) in the mixed solution is obtained as 20.64, 16.29 and 17.02 mg g^{-1} respectively. The saturation loading capacity for the pure Cr(VI), Cu(II) and Zn(II) are obtained as 25.75, 35.30 and 18.40 mg g^{-1} respectively, which are higher than the saturation capacity obtained from the mixed solution for each metal ion. Further, the percentage removal of individual metal ions in the presence of multiple metal ions decreases by approximately 11.81% in comparison to their pure adsorption runs.

The maximum average saturation loading for either of the metal ions [Cr(VI), Cu(II) and Zn(II)] is found as 26.485 mg g^{-1}. However, the saturation loading for the simultaneous adsorption of Cr(VI), Cu(II) and Zn(II) is obtained as 53.95 mg g^{-1} which is approximately double to that of the maximum saturation capacity of either of the metal ions. This indicates that the developed adsorbent, nANB, is more suitable to treat the wastewater containing multiple metal ions i.e. more efficient and economical to treat the industrial effluent.

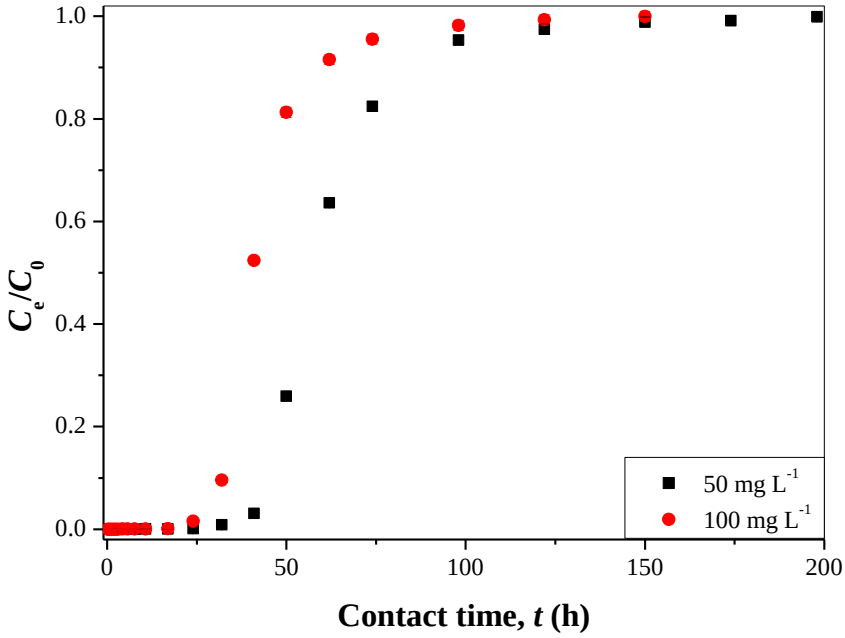

Fig 5.55: Effect of inlet concentration on the continuous removal of Cr(VI) using nANB.

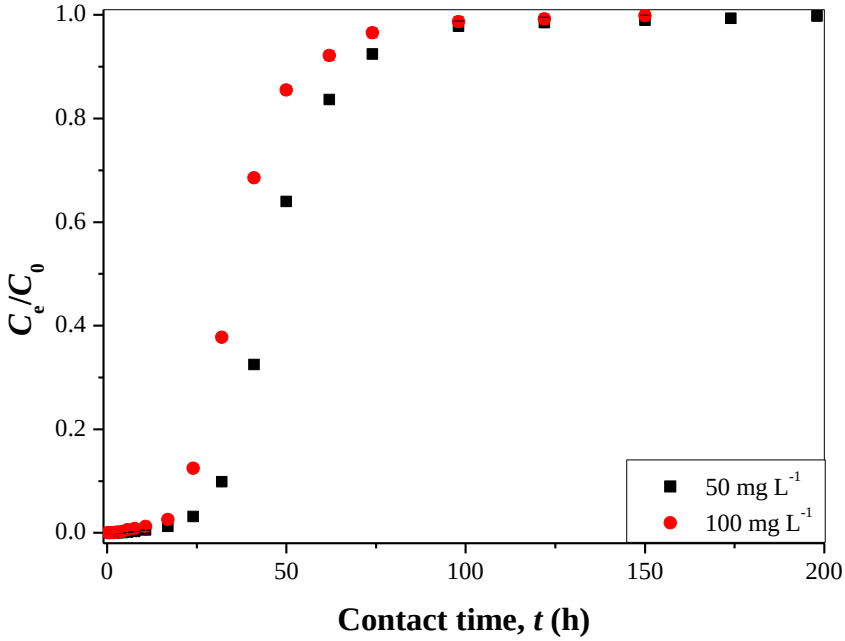

Fig 5.56: Effect of inlet concentration on the continuous removal of Cu(II) using nANB.

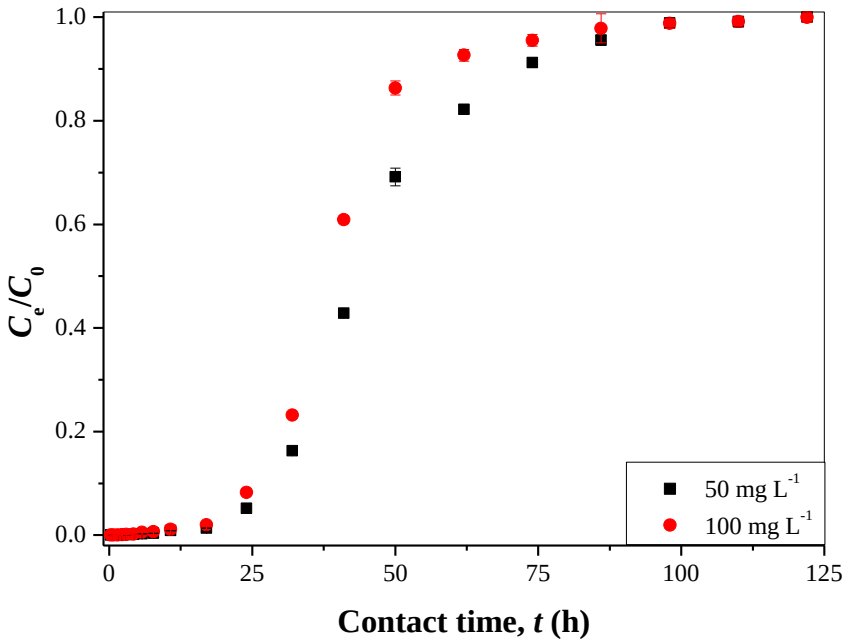

Fig 5.57: Effect of inlet concentration on the continuous removal of Zn(II) using nANB.

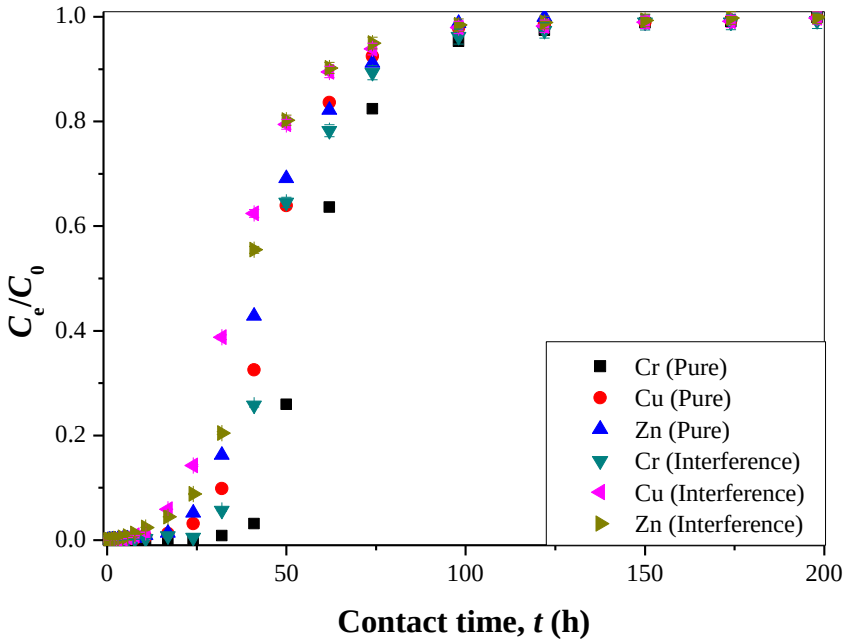

Fig 5.58: Interference study of Cr(VI), Cu(II) and Zn(II) in a fixed-bed adsorption column.

Table 5.17: Parameters for the removal of various metal ions from aqueous solution in a fixed-bed adsorption column.

(P: Pure sample; I: Interference Sample)

S. No.	Metal	C_0	Q	W	t_t	t_f	t_b	q_s	q_t	m_t	S	EBRT	R_a	y
		mg L^{-1}	mL min^{-1}	g	h	h	h	mg g^{-1}	mg	mg	%	sec	g L^{-1}	
1	Cr(VI)(P)	50	10	75	111	198	24.8	25.75	1857.6	3321.77	55.92	15.21	5.04	0.6151
2	Cr(VI) (I)	50	10	75	97.6	198	9.25	20.64	1443.6	2928.31	49.30	15.21	13.51	0.8207
3	Cu(II) (P)	50	10	75	98.9	198	25	35.30	1482	2967.00	49.95	15.21	4.99	0.7163
4	Cu(II) (I)	50	10	75	89.3	198	14.3	16.29	1207.8	2678.49	45.09	15.21	8.73	0.6485
5	Zn(II) (P)	50	10	75	95.6	198	12.3	18.40	1383.84	2867.06	48.27	15.21	10.20	0.7336
6	Zn(II) (I)	50	10	75	82.3	198	6.83	17.02	1026.84	2469.70	41.58	15.21	18.31	0.8395

5.4.5 Utilization on Pulp & Paper Industrial Effluent

The applicability of the developed nANB on the simultaneous removal of multiple metal ions present in the synthetically developed pulp & paper industrial effluent is evaluated. A continuous experiment is performed by maintaining the initial concentration of different metal ions in aqueous solution as provided in Table 3.6. The breakthrough curves for the simultaneous removal of all the metal ions are shown in Fig 5.59. The fixed-bed adsorption parameters for different metal ions are evaluated by considering their individual permissible limits and are being tabulated in Table 5.18. It is observed that the breakthrough time for the individual metal ions (considering individual breakpoint concentration) are obtained as 4.393, 6.397, 9.425, 22.136, 34.34 and 34.96 h for Cd(II), Ni(II), Cr(VI), Pb(II), Zn(II) and Cu(II) respectively. The percentage removal is estimated as 30.61, 32.78, 38.14, 50.26, 52.80 and 78.52% for Ni(II), Cd(II), Zn(II), Cr(VI), Cu(II) and Pb(II) respectively when the fixed-bed column is allowed to reach the saturation till 198 h. The saturated loading capacity for Cr(VI), Cu(II), Zn(II), Pb(II), Ni(II) and Cd(II) are obtained as 24.73, 16.52, 0.99, 0.71, 0.50 and 0.25 mg g^{-1} respectively which is reducing according to the inlet concentration of each metal ion. The saturated adsorbent contains all the metal ions and the overall saturation loading capacity of the adsorbent is evaluated as 43.71 mg metals per g of adsorbent.

The effluent containing multiple metal ions is allowed to be released into the environment, when each of the pollutants present in the effluent must be in their permissible limit. The fixed-bed adsorption is required to be stopped, if the concentration of any metal ion in the effluent exceeds their permissible limit. Due to this reason, the parameters are re-estimated by considering the lower value of breakthrough time i.e.

4.393 h among all metal ions and are reported in Table 5.19. The overall unused bed length of the column is obtained as 16.56%, which is very less in comparison to any of the column studies considering individual metal ions. The saturation loading capacity also reduces to 24.73, 3.42, 0.72, 0.68, 0.50 and 0.28 mg g^{-1} for Cr(VI), Cu(II), Pb(II), Zn(II), Ni(II) and Cd(II) respectively. The overall saturation loading capacity of nANB is obtained as 30.30 mg metals per g of adsorbent. On comparing with the adsorption capacity of nANB for individual metal ions, it is found that the adsorption capacity increases for the simultaneous removal of multiple metal ions. This supports the utilization of the developed nANB for the removal of multiple pollutants from industrial effluent streams.

The saturated nANB utilized on the synthetically developed pulp & paper industry effluent is also characterized using SEM and EDS. The SEM and EDS image of used nANB are shown in Fig 5.60(a) and (b) respectively. It is observed that the nano pores available on the surface of fresh nANB [Fig 5.10(a)] are not visible on the surface of saturated nANB [Fig 5.60(a)] which confirms the utilization of the active sites available for adsorption. The EDS analysis [Fig 5.60(b)] confirms the adsorption of multiple metal ions on the surface of the developed nANB. This EDS analysis also supports the higher adsorption of Pb and Cr in comparison to other metal ions. The presence of other impurities such as Sulphur, Magnesium, Cobolt, Chlorine, Silicon, etc. is due to the salts utilized for the preparation of stock solution and the EDS coating & analysis procedure.

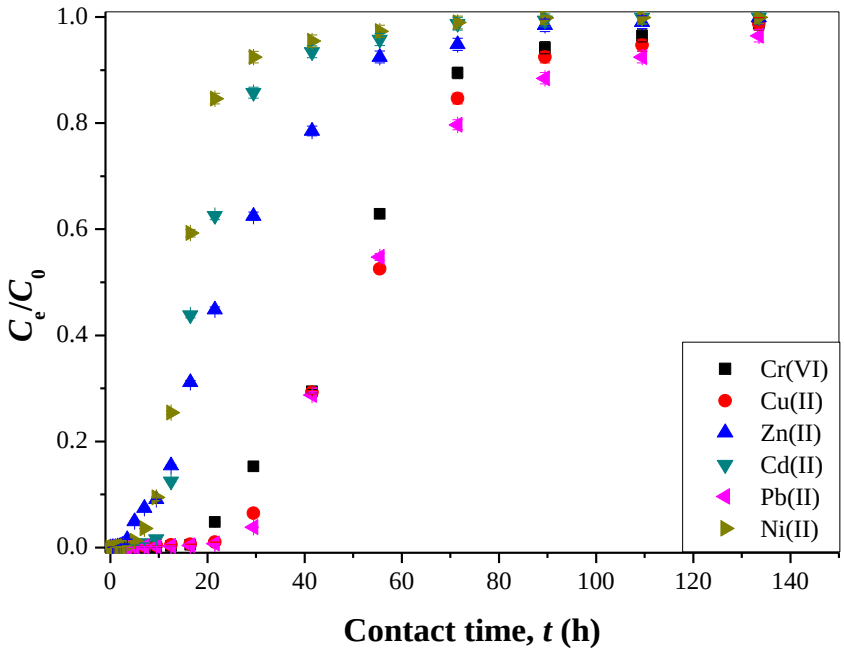

Fig 5.59: Breakthrough curve for the simultaneous removal of multiple metal ions.

Table 5.18: Parameters for the removal of various metal ions from synthetically prepared pulp & paper industry effluent solution in a fixed-bed adsorption column.

S. No.	Metal	C_0	Q	W	t_t	t_f	t_b	q_s	q_t	m_t	S	EBRT	R_a	y
		mg L^{-1}	mL min^{-1}	g	h	h	h	mg g^{-1}	mg	mg	%	sec	g L^{-1}	
1	Cr(VI)	59.2	10	75	99.52	198	9.425	24.73	1776.84	3535.03	50.26	15.21	13.26	0.8195
2	Cu(II)	7.72	10	75	104.55	198	34.96	16.52	255.72	484.28	52.80	15.21	3.58	0.8693
3	Zn(II)	2.9	10	75	75.52	198	34.342	0.99	50.118	131.40	38.14	15.21	3.64	0.1986
4	Cd(II)	1.44	10	75	64.90	198	4.393	0.25	18.378	56.07	32.78	15.21	28.45	0.7995
5	Pb(II)	1.54	10	75	155.47	198	22.136	0.71	112.8	143.66	78.52	15.21	5.65	0.6182
6	Ni(II)	3.49	10	75	60.61	198	6.397	0.50	38.856	126.93	30.61	15.21	19.54	0.6427

Table 5.19: Parameters for the removal of various metal ions from synthetically prepared pulp & paper industry effluent solution in a fixed-bed adsorption column at overall breakpoint.

S. No.	Metal	C_0	Q	W	t_t	t_f	t_b	q_s	q_t	m_t	S	EBRT	R_a	y
		mg L^{-1}	mL min^{-1}	g	h	h	h	mg g^{-1}	mg	mg	%	sec	g L^{-1}	
1	Cr(VI)	59.2	10	75	99.52	198	4.393	24.73	1776.84	3535.03	50.26	15.21	28.45	0.9159
2	Cu(II)	7.72	10	75	104.55	198	4.393	3.42	255.72	484.28	52.80	15.21	28.45	0.9206
3	Zn(II)	2.9	10	75	75.52	198	4.393	0.68	50.118	131.40	38.14	15.21	28.45	0.8506
4	Cd(II)	1.44	10	75	64.90	198	4.393	0.25	18.378	56.07	32.78	15.21	28.45	0.7995
5	Pb(II)	1.54	10	75	155.47	198	4.393	0.72	112.8	143.66	78.52	15.21	28.45	0.9251
6	Ni(II)	3.49	10	75	60.61	198	4.393	0.50	38.856	126.93	30.61	15.21	28.45	0.7539

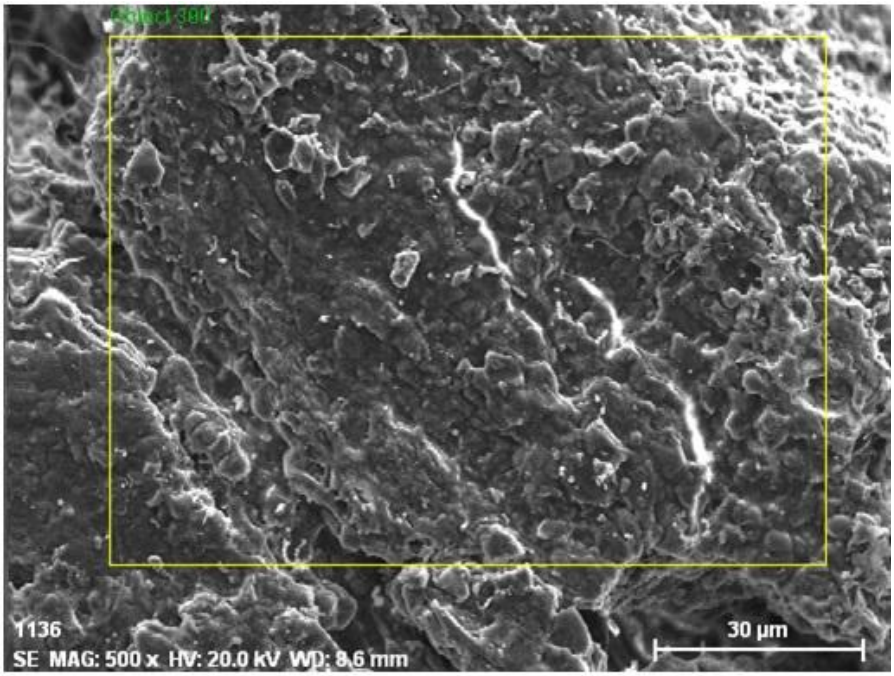

(a)

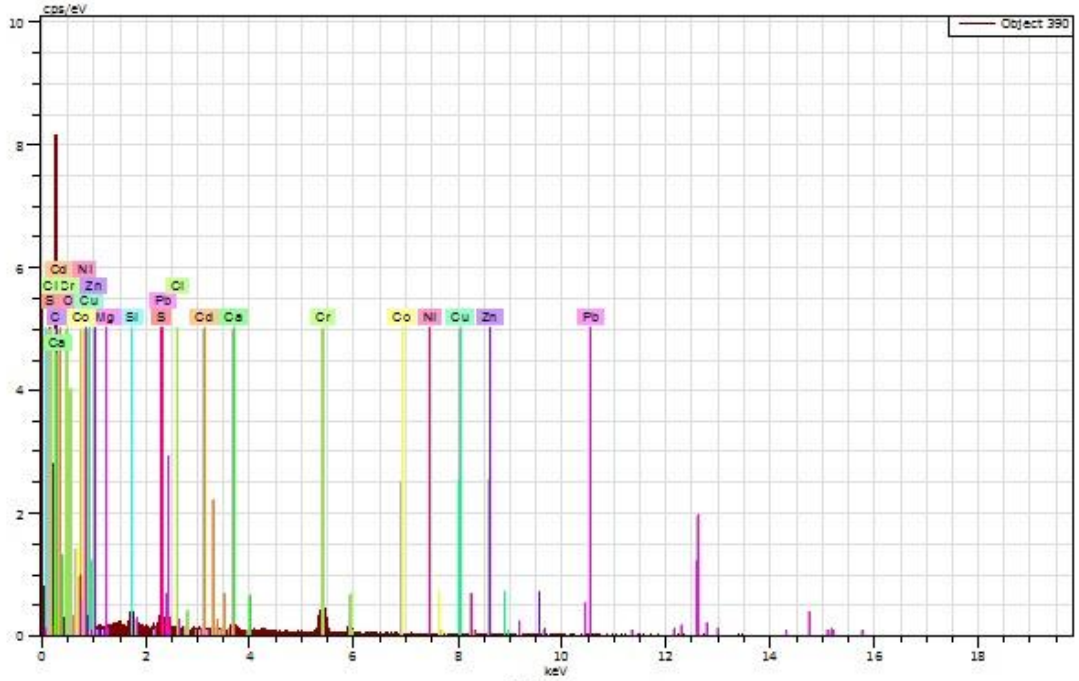

(b)

Fig 5.60: (a) SEM & (b)EDS analysis of the used adsorbent on the multiple metal ions from synthetically prepared pulp & paper industry effluent solution.

5.4.6 Evaluation of Kinetic Parameters from Column Data Modeling

The experimental data of the breakthrough curves are fitted with the Yoon-Nelson and Yan models using the non-linear regression method of Origin 6.0 software. The values of the different parameters for the Yoon-Nelson and Yan models for the removal of Cr(VI), Cu(II) and Zn(II) are being tabulated in Tables. 5.20, 5.21 and 5.22 respectively.

5.4.6.1 The Yoon-Nelson Model

It is observed that the increase in the inlet concentration from 50 to 100 mg L^{-1}, the value of, a Yoon-Nelson rate constant ($K_{YN,i}$) increases from 7.842 to 11.547 h^{-1}, 0.129 to 0.146 h^{-1} and 0.116 to 0.165 h^{-1} for the removal of Cr(VI), Cu(II) and Zn(II) respectively. It also increases from 5.272 to 10.703, 0.082 to 0.174 and 0.088 to 0.156 h^{-1} for the removal of Cr(VI), Cu(II) and Zn(II) respectively (Tables 5.20, 5.21 and 5.22), with an increase in the flow rate from 5 min^{-1} to 15 ml min^{-1}. The value of τ_i, the time required for 50% of i^{th} adsorbate breakthrough is decreased from 0.980 to 0.690, 46.824 to 36.165 and 44.584 to 38.765 h for the removal of Cr(VI), Cu(II) and Zn(II) with an increase in inlet concentration from 50 to 100 mg L^{-1} respectively. The increase in the $K_{YN,i}$ with increase in inlet concentration and flowrate may be due to the increase in the driving force for adsorption and decrease in mass transfer resistance respectively. The decrease in τ_i with an increase in the inlet concentration is a result of the rapid saturation of the nANB adsorbent in the fixed-bed column (Aksu and Gönen, 2006; Sugashini and Begum, 2013).

With the increases in the mass of the adsorbent from 25 to 175 g, the value of τ_i increases from 0.446 to 2.704, 25.94 to 129.451 h and 20.797 to 113.716 h for the removal of Cr(VI), Cu(II) and Zn(II) respectively. This increase in the τ_i is a result of the availability

of more number of active sites for the same driving force. This leads to the delay in saturation of the nANB surface (Aksu and Gönen, 2006).

5.4.6.2 The Yan Model

The Yan model is applied to the obtained experimental results and estimated parameters for the adsorption of Cr(VI), Cu(II) and Zn(II) are reported in Tables 5.20, 5.21 and 5.22 respectively.

The Yan model parameter, a_i, increases with an increase in the inlet flow rate and the mass of adsorbent for the removal of Cu(II) and Zn(II) while it remains unchanged for the removal of Cr(VI). The a_i increases from 4.419 to 12.427, 3.287 to 6.376 and 3.218 to 6.231 for the removal of Cr(VI), Cu(II) and Zn(II) with an increase in the mass of adsorbent from 25 to 175 g respectively.

5.4.6.3 Concluding Remarks

The R^2 value is better for the Yan model, however the trends for the model parameters are very irregular with the variation of parameter values. Also, the R^2 value for Yoon-Nelson model is close to Yan model. Hence, in the present study, the applicability of Yoon-Nelson model for the scaling up the existing process is more suitable. For these models, the constants are estimated using the laboratory scale experimental data of breakthrough curve. Further, these model equations could be utilized to get the breakthrough curve at different operating conditions (pilot scale and commercial scale) which could be helpful in designing of the scaled-up fixed-bed adsorption column.

Table 5.20: Different parameters for the Yoon-Nelson and Yan models for Cr(VI) removal.

Inlet Conc. C_o (mg L^{-1})	Flowrate (mL min^{-1})	Mass of Adsorbent (g)	Yoon-Nelson Model				Yan Model			
			$K_{YN,i}$ (h^{-1})	τ_i (h)	R^2	Chi^2	$q_{0,i}$	a_i	R^2	Chi^2
50	10	75	7.842	0.980	0.997	0.00057	0.00039	7.230	0.999	0.00023
100	10	75	11.547	0.690	0.997	0.00068	0.00055	7.547	0.998	0.00031
50	5	75	5.272	1.345	0.998	0.00035	0.00027	6.837	0.999	0.00008
50	15	75	10.703	0.676	0.998	0.0005	0.0004	6.855	0.999	0.00015
50	10	25	11.026	0.446	0.996	0.00084	0.00052	4.419	0.999	0.00012
50	10	50	9.474	0.673	0.998	0.00043	0.0004	5.793	0.999	0.00015
50	10	100	6.113	1.396	0.997	0.00053	0.00042	7.983	0.999	0.00024
50	10	125	6.394	1.836	0.997	0.00062	0.00044	10.940	0.998	0.00043
50	10	150	5.162	2.305	0.997	0.00054	0.00046	11.310	0.998	0.00031
50	10	175	4.868	2.714	0.996	0.00067	0.00046	12.427	0.997	0.00046

Table 5.21: Different parameters for the Yoon-Nelson and Yan models for Cu(II) removal.

Inlet Conc. C_o (mg L^{-1})	Flow rate (mL min^{-1})	Mass of Adsorbent (g)	Yoon-Nelson Model				Yan Model			
			$K_{YN,i}$ (h^{-1})	τ_i (h)	R^2	Chi^2	$q_{0,i}$	a_i	R^2	Chi^2
50	10	75	0.129	46.824	0.998	0.00039	0.00031	5.780	0.999	0.00009
100	10	75	0.146	36.165	0.998	0.00046	0.00047	4.936	0.999	0.00005
50	5	75	0.082	69.540	0.997	0.00054	0.00023	5.400	0.999	0.00006
50	15	75	0.174	35.431	0.997	0.00058	0.0035	5.848	0.998	0.00033
50	10	25	0.150	25.940	0.997	0.00066	0.00049	3.284	0.999	0.00027
50	10	50	0.131	36.058	0.998	0.00041	0.00035	4.191	0.999	0.00005
50	10	100	0.085	69.310	0.998	0.00041	0.00034	5.578	0.999	0.0002
50	10	125	0.068	96.323	0.998	0.00032	0.00038	6.159	0.999	0.00008
50	10	150	0.059	114.772	0.995	0.00082	0.00038	6.379	0.998	0.00039
50	10	175	0.052	129.451	0.993	0.00116	0.00037	6.376	0.997	0.00052

Table 5.22: Different parameters for the Yoon-Nelson and Yan models for Zn(II) removal.

Inlet Conc. C_o (mg L^{-1})	Flow rate (mL min^{-1})	Mass of Adsorbent (g)	Yoon-Nelson Model				Yan Model			
			$K_{YN,i}$ (h^{-1})	τ_i (h)	R^2	Chi^2	$q_{0,i}$	a_i	R^2	Chi^2
50	10	75	0.116	44.584	0.996	0.00076	0.00029	4.862	0.999	0.00014
100	10	75	0.165	38.765	0.998	0.00032	0.00051	6.103	0.999	0.00022
50	5	75	0.088	53.738	0.996	0.00072	0.00017	4.426	0.999	0.00006
50	15	75	0.156	38.413	0.998	0.00038	0.00038	5.695	0.999	0.00013
50	10	25	0.184	20.797	0.997	0.00079	0.00039	3.218	0.998	0.00047
50	10	50	0.158	28.795	0.999	0.00022	0.00028	4.196	0.999	0.00028
50	10	100	0.090	59.757	0.998	0.00038	0.00029	5.103	0.999	0.00008
50	10	125	0.071	74.868	0.997	0.00058	0.00029	5.034	0.999	0.00007
50	10	150	0.065	100.958	0.998	0.00043	0.00033	6.371	0.999	0.00012
50	10	175	0.057	113.716	0.996	0.00078	0.00032	6.231	0.998	0.00032

CHAPTER 6
SUMMARY AND CONCLUSIONS

In the present study, a low-cost nano-porous adsorbent, activated neem bark (nANB) is developed using a neem bark as the raw material. The developed adsorbent is utilized to remove individual [Cr(VI), Cu(II), Zn(II)] and simultaneous removal of multiple metal ions from wastewater. Batch and continuous adsorption experiments are successfully performed. The various adsorption isotherm, kinetic and mass transfer models are validated using the batch experimental data to understand the adsorption behavior of the developed nANB. A generalized mathematical equation is proposed which can be utilized to provide an optimal set of parameter values resulting in the maximum removal efficiency or adsorption capacity. The model is further optimized using Differential Evolution (DE) to obtain the optimum parametric values for maximum adsorption capacity. Furthermore, continuous fixed-bed adsorption experiments are performed to see the effect of independent parameters on the breakthrough curve. This part of the thesis presents a brief summary of the present study followed by the conclusions, major contributions and future scope for the research.

6.1 Summary

6.1.1 Introduction

Adsorption is a promising method for the removal of heavy metals in a simple, efficient and economical manner. A number of researchers have reported the use of different solid materials as the adsorbent for the removal of heavy metals and other impurities. The effluents from the industries are containing multiple metal ions. Very few adsorbents are

reported in the literature for the adsorption of multiple metal ions. Therefore, there is a need to identify a low-cost material which can be utilized effectively for the adsorption of multiple metal ions from effluent streams. A higher adsorption capacity of the adsorbent can be achieved by undergoing proper physical and chemical activation procedures. Nano-porous materials can meet the requirements for a good adsorbent due to the availability of large surface area for adsorption. The selection of the adsorbent is the foremost important objective which can be accomplished by analyzing the different activation procedures.

The performance of the adsorbent is characterized by the adsorption capacity, which is estimated using the batch adsorption experiments. The applicability of the developed adsorbent for the industrial use can be checked by performing continuous experiment. The design of the column depends on various factors such as flow rate, initial concentration, bed height, etc. These studies will help in evaluating the various design parameters required to scale up the process.

The completion of the adsorption process leads to the metal loaded saturated adsorbent. This saturated adsorbent is considered to be toxic and hazardous when released into the environment. Hence, the prior treatment of saturated adsorbent is necessary to recover the adsorbed metal ions before it discharge into the environment. The environmental constraints further emphasize the need to develop a suitable method for regeneration of the saturated adsorbent.

6.1.2 Gaps in Literature

The literature survey in the proposed research area revealed that in the present industrial era, the presence of toxic metals in the effluent streams of different industries is a

growing environmental concern. There are various physical and chemical methods available for the removal of toxic metals from these effluent streams. It is also observed that few adsorption studies were reported for the purification of industrial effluent streams. However, economical treatment of effluent streams is the most important criteria. The reported low-cost materials used as adsorbents do not possess the higher adsorption capacity for the metal adsorption. In addition to that, most of the reported adsorbents were utilized for the removal of single metal ion. Very few adsorbents have been reported for the simultaneous removal of two metal ions. However, the actual industrial effluents contain multiple metal ions which are also required to be treated before discharging the effluent streams to the outer water bodies. Therefore, there is a need to develop a low-cost adsorbent prepared from biodegradable material capable of simultaneous adsorption of multiple metal ions with higher metal uptake. The removal of single metal ion, with the use of specific adsorbent in the presence of other metals affects the adsorbent performance.

Very few studies have reported the regeneration of metal loaded adsorbent for the reutilization of adsorbent. The regeneration is very much required to make the adsorption process more economical and environmental friendly. The literature survey also revealed that very few studies have reported the continuous adsorption experiments using the low-cost adsorbents. The lab/pilot scale continuous experiments are required to design/scale up the process to the industrial scale. The studies related to the removal of multiple metal ions using fixed-bed column are scarce. The mathematical models are used to scale-up the adsorption process from laboratory scale to pilot scale and subsequent to the industrial scale. A significant number of batch studies reported the use of various

isotherm and kinetic model to fit the obtained experimental data and the estimation of model parameters. However, very few studies attempted the validation of available mathematical for the fixed-bed adsorption by the continuous experimental data.

Most of the researchers follow a common trend of performing batch experiments to study the effect of a single parameter on the adsorption removal efficiency keeping the other parameters constant. Only few studies have been reported for the estimation of the maximum removal efficiency as a function of all the dependent parameters. Whereas, no study is found where the researchers have performed experiments at the optimum parametric condition.

6.1.3 Scope of Work

There is a need to develop a low-cost adsorbent from the naturally available waste material which can be utilized as a potential adsorbent for the removal of multiple metal ions. It is required to find the optimum activation conditions for the development of the suitable low-cost adsorbent having more surface area and higher adsorption capacity for the multiple metal ions. The batch experiments are needed to be performed at different parametric values to evaluate the performance of developed adsorbent. There is an ample scope of performing the continuous experiments using the developed low-cost adsorbent for the removal of Cu(II), Cr(VI) and Zn(II) to demonstrate the use of the developed adsorbent for the treatment of industrial effluent streams. A suitable method for the regeneration of metal loaded adsorbent is required to be developed to make the adsorption process more environmental friendly.

The industrial effluents from pulp & paper and plating industries are mainly containing multiple metal ions ranging from Cu(II), Cr(VI), Cd(II), Pb(II), Ni(II) and Zn(II). Hence,

there is a need to evaluate the application of the developed low-cost adsorbent for the simultaneous removal of multiple metal ions in a continuous column.

There is a need to propose a generalized mathematical equation which can be used by most of the reported studies in the literature to find an optimal set of parameters which results in the maximum removal efficiency or adsorption capacity. Batch and continuous experimental results are required to be analyzed by the use of appropriate mathematical models available in the literature. The obtained design parameters from the model validation can be further utilized to propose a design of adsorption column in pilot and industrial scale.

6.1.4 Experimental Studies

The present work focuses on the development of a nano-porous adsorbent using neem bark as the low-cost raw material. The neem bark particles are activated by six different chemical and physical activation procedures. The performance of all the six developed ANBs is tested for the removal of Cr(VI), Cu(II) and Zn(II) by performing equilibrium experiments. The six developed ANBs (ANB1 to ANB6) are characterized using the Fourier Transform Infrared (FTIR) Spectroscopy. Out of the six developed adsorbents, the one which is having the relevant functional groups on the surface and shows the maximum adsorption capacity for the removal of Cr(VI), Cu(II) and Zn(II) is being utilized for the further study and is termed as nANB. The nANB is further characterized using five more techniques. The performance of the nANB is also studied for the removal of Cd(II), Ni(II) and Pb(II).

The effect of other parameters such as pH, adsorbent dosage, contact time, temperature and interference of other metals is evaluated for the removal of Cr(VI), Cu(II) and Zn(II).

Later on, continuous experiments are performed to study the effect of various parameters such as the inlet concentration, inlet flowrate, adsorbent dosage and presence of other ions on the continuous removal of Cr(VI), Cu(II) and Zn(II) individually. The performance of nANB is also tested for the removal of multiple metal ions [Cd(II), Cr(VI), Cu(II), Ni(II), Pb(II) and Zn(II)] from the synthetically developed pulp & paper industry effluent in a continuous experiment. The saturated adsorbent is further being regenerated by thermal and chemical treatment to study the possibility of re-utilization of the developed nANB.

6.1.5 Mathematical Modeling

The batch adsorption experimental data are used to evaluate various parameters with the help of different isotherm and kinetic models available in the literature. In the present work, the data are fitted with the Langmuir, Freundlich and Tempkin isotherm models. The rate kinetic models used in this study are pseudo-first order, second order and Elovich model. The Weber & Moris and the Boyd models are also used to determine the rate-limiting mechanism for the metal adsorption on nANB adsorbent.

It is essential for forecasting the response and behavior of the system on the basis of reliant input parameters. Any experimental data can be well fitted by a suitable polynomial function. In the present study, the initial concentration, contact time, pH and the adsorbent dosage are being considered as input parameters for the modeling of the system. The obtained model is further optimized using the Differential Evolution (DE) technique to find the optimum parametric values required to attain maximum adsorption capacity.

Batch experiments are not suitable for large scale treatment processes, however, the parameters evaluated from this study are helpful in designing the column for continuous experiments. The mathematical models available for the fixed-bed columns are also useful to estimate the design parameters by validating them using laboratory scale continuous experimental results. The experimental data are also fitted with the Yoon-Nelson and Yan model.

6.1.6 Results and Discussion

The results obtained from experimental, modeling and optimization studies are summarized in the following sections.

6.1.6.1 Selection of nANB

The equilibrium experiments are performed to evaluate the performance of six (ANB1 to ANB6) developed adsorbents for the removal of Cr(VI), Cu(II) and Zn(II) using neem bark as the raw material. In the real scenario, the industrial effluent streams contain several metal ions, hence, the adsorbent employed must have significant capacity to simultaneously adsorb multiple metal ions. Based on the experimental and theoretical evaluation of developed ANBs, ANB1 is considered as suitable adsorbent for the single and multiple metal ions adsorption from wastewater streams.

The ANB1 is also tested for the removal of other metal ions such as Cd(II), Ni(II) and Pb(II) to check its wider industrial applicability. This study supports the capability of ANB1 to be used for the adsorption of Cr(VI), Cu(II), Cd(II), Ni(II), Pb(II) and Zn(II) and is considered for further experimental studies and is termed as nANB.

6.1.6.2 Characterization

The developed ANBs (ANB1 to ANB6) are characterized using FTIR. It is observed that the ANB1 is showing two extra peaks in comparison to the ANB 2 to ANB6. A wavy spectrum is obtained in place of a smooth one which confirms the amorphous nature of the developed ANB1. The presence of C-O and C=O suggests the existence of various acidic groups on the surface of ANB1(nANB).

In the present study, the selected nANB is further characterized by SEM, EDS, BET Surface area, XRD and TGA to study the characteristic behavior of the developed nANB. The presence of different size of the pores on the surface of fresh nANB are clearly visible. The comparison of the size of the pores with image resolution, confirms the presence of significant number of 10-100 nm size pores along with other pores. This supports the nano-porous characteristics of the developed nANB adsorbent. The SEM of the used nANB shows clearly the utilization of the nano pores for the metal adsorption while comparing with the surface morphology of the fresh nANB. The EDS analysis of the surface of the used nANB shows the presence of Cr(VI), Cu(II) and Zn(II). The surface area of the developed nANB is analyzed using the BET surface area analyzer. The phase of the developed nANB is also characterized using XRD. There is no sharp peak observed in the spectrum and therefore, the particle size of developed adsorbent cannot be estimated. This also supports the amorphous nature of the adsorbent as confirmed by FTIR analysis. TGA analysis of the developed nANB is also performed. The result of TGA analysis indicates that the developed adsorbent is thermally stable up to 200^{o}C. TGA results also suggests that the saturated adsorbent can be regenerated at higher temperatures (upto 200°C) without any degradation of adsorbent.

6.1.6.3 Batch Experiments

The effect of contact time will be helpful to acquire the kinetic parameters and to propose the rate kinetics for the metal removal. The effect of contact time is evaluated by performing kinetic experiments for the removal of Cr(VI), Cu(II) and Zn(II). It is observed that for the removal of Cr(VI), Cu(II) and Zn(II), the percentage removal rapidly increases with the increase in contact time up to 4 h and later it increases gradually with the further increase in contact time. Increase in contact time from 40 to 48 h shows a little change in the solid phase concentration and percentage removal. Therefore, 48 h is considered as the equilibrium time for further studies.

The effect of nANB dosage on the Cr(VI), Cu(II) and Zn(II) ion removal is studied to obtain the optimal value of adsorbent dosage. There is a trade-off between solid phase concentration and percent removal with an increase in the adsorbent dosage for metal adsorption. The optimal adsorbent dosage for the removal of Cr(VI), Cu(II) and Zn(II) adsorption is obtained as 6, 8 and 10.5 g L^{-1} respectively from the trade-off between adsorption capacity and percentage removal.

The effect of inlet concentration on the performance of the developed nANB for the removal of Cr(VI), Cu(II) and Zn(II) is also studied. It is observed that the percentage removal decreases while the solid phase concentration increases with an increase in the inlet concentration.

The other significant parameter studied is the effect of pH on the removal of Cr(VI), Cu(II) and Zn(II). The range of pH values considered during the study are 1.2 to 12. It is observed that the solid phase concentration decreases from 16.26 to 1, 15.83 to 2.13 and 9.99 to 1.05 mg g^{-1} for the removal of Cr(VI), Cu(II) and Zn(II) respectively with an

increase in the pH value from 1.2 to 12. This supports the adsorption of metal ions at lower pH.

The effect of the temperature on the adsorption of heavy metals is evaluated by performing equilibrium batch experiments at 35, 50 and 60°C. The equilibrium experimental data at different temperature are also fitted with the Langmuir isotherm model. The adsorption of metals on nANB is confirmed to be an exothermic process by the obtained negative values of ΔH. The negative values of ΔS support less randomness of the adsorption process at the solid liquid interface.

In the present study, there are two techniques considered for the regeneration of the utilized adsorbent. The first technique is based on the thermal approach. The Cr(VI), Cu(II) and Zn(II) utilized adsorbents are thoroughly stirred in hot water at 70°C. The other technique followed is the base and acid treatment. The utilized nANB is treated for 24 h with 1N NaOH followed by 24 h treatment with 1N HCL. The results support the regenerability and re-usability of the nANB.

The performance of the developed nANB is also evaluated for the removal of synthetically developed multiple metal ion aqueous solution. The aqueous solution contains equal amounts of Cr(VI), Cu(II) and Zn(II). It is observed that the solid phase concentration for each metal ion during the simultaneous adsorption of Cr(VI), Cu(II) and Zn(II) is less than the one obtained from the respective pure aqueous solutions. However, the total solid phase concentration of developed nANB for the simultaneous removal of all metal ions is much higher than the individual ones.

The developed nANB is also utilized for the treatment of actual chrome plating industrial effluent. The chrome plating industry effluent is mainly contaminated with large amount

of Cr(VI) along with the traces of other metal ions. Hence, in this study, Cr(VI) is targeted to remove from plating industry wastewater using nANB as an adsorbent. The results obtained from this study established the fact that the developed nANB can be successfully utilized for the treatment of industrial wastewater which contain Cr(VI) along with other metal ions and impurities.

Adsorption isotherms are an important tool in adsorption process which helps in understanding the adsorption mechanism in term of the interaction of the metal ions with the solid adsorbent surface. The applicability of the various isotherm models help in evaluating different isotherm constants that provide the information about the surface property and affinity of the adsorbent towards the metal removal. The obtained equilibrium experimental results are fitted with the isotherm models available in the literature. In the present work, Langmuir, Freundlich and Tempkin isotherm models are considered and are discussed. The calculated values of regression correlation coefficient (R^2) of the three isotherm models for the adsorption of Cr(VI), Cu(II) and Zn(II) indicate that the equilibrium experimental data are best fitted with the Langmuir isotherm model. This also supports the monolayer adsorption of Cr(VI), Cu(II) and Zn(II) on nANB surface.

In order to understand the kinetic behavior of the adsorption process for the removal of Cr(VI), Cu(II) and Zn(II) using nANB, the pseudo-first order, second order and Elovich models are considered to fit the kinetic experimental data. Comparison of solid phase concentration and the correlation coefficients for the removal of Cr(VI), Cu(II) and Zn(II) supports the applicability of second order kinetic model during the adsorption process. The results suggest the chemisorption is the primary rate-limiting step in the process

which leads to the possibility of covalent bond formation between adsorbent surface and metal ions.

Adsorption is a mass transfer process, hence, it is very important to understand its mechanism of metal transfer from liquid phase to nANB surface. The movement of the solute from bulk fluid to nANB surface can be supported by either the film diffusion or intraparticle diffusion or maybe both. Weber & Moris and Boyd models are applied in the present study to establish the mechanism of metal transfer. It is observed that the adsorption of Cr(VI) and Zn(II) using nANB are intraparticle diffusion controlled whereas the Cu(II) adsorption on nANB is due to the both, film diffusion and intraparticle diffusion.

The batch experimental data for the removal of Cr(VI), Cu(II) and Zn(II) are utilized to develop the model for the prediction of the optimum parameter values for attaining maximum adsorption capacity. The maximum values of individual parameters are identified by tabulating all the related experimental studies of that parameter for a particular metal ion. The independent parameters along with the adsorption capacity (q_e) are normalized using their respective maximum values and are regressed using the Microsoft Excel 2007 software to formulate the model. The modeled equations are optimized using the Differential Evlolution (DE) method.

The sensitivity analysis is also carried out to find the dominant parameters for the adsorption process. The optimum values of parameters are made as twice and a half to see the effect of these changes in the adsorption capacity. It is confirmed from the analysis that the adsorption capacity highly depends on the inlet concentration and is

more or less equally dependent on the other three parameters. The order of sensitivity is initial concentration > adsorbent dosage > pH > contact time.

It is very important to understand the mechanism of metal adsorption onto the surface of developed adsorbent. The adsorbent used in the present study is prepared from neem bark as raw material. The neem bark is activated by acid and thermal treatment which develop the acidic oxides groups on the surface of prepared nANB adsorbent. The surface of nANB is positively charged due to the presence of these groups. The FTIR of the used adsorbent for the removal of Cr(VI), Cu(II) and Zn(II) are performed to establish the mechanism of metal adsorption.

The Langmuir isotherm model is considered to evaluate the maximum adsorption capacity of nANB for the individual removal of Cr(VI), Cu(II) and Zn(II). It is observed that the adsorption capacity of nANB is sufficiently high as compared to other low-cost adsorbents reported in the literature.

Cost analysis is an important influential factor for the selection of any heavy metal removal process. The economics of the adsorption process is primarily dependent on the cost of the adsorbent utilized for the removal of heavy metals from wastewater. The cost analysis supports the economic viability of the developed nANB and as an alternate of the commercial adsorbent for metal removal.

6.1.6.4 Continuous Experiments

The batch study results established the fact that the nANB is a suitable adsorbent for the removal of Cd(II), Cr(VI), Cu(II), Ni(II), Pb(II) and Zn(II). Hence, the continuous

experiments are performed in the laboratory scale fixed-bed adsorption column for the removal of individual as well as multiple metal ions from wastewater.

The effect of inlet flow rate on the breakthrough curve for the removal of Cr(VI), Cu(II) and Zn(II) is studied by varying the flow rate from 5 to 15 mL min^{-1}. With an increase in the flow rate, there is a decrease in the breakthrough time for the removal of metal ions. This decrease in the breakthrough time may be due to availability of more amount of metal for adsorption in the same time duration for the same number of active sites.

The effect of the mass of the adsorbent on the breakthrough curve for Cr(VI), Cu(II) and Zn(II) removal is studied. With an increase in the mass of the adsorbent, the breakthrough time is increased. The increase in the breakthrough time may be due to the longer bed length. The effect of the initial concentrations (50 and 100 mg L^{-1}) on the breakthrough curve for metal adsorption from aqueous solution is studied. It is observed that, with an increase in the initial concentration, there is a decrease in breakthrough time.

It is very important to study the performance of nANB for the removal of individual metal ions from wastewater in the presence of other metal ions. This study would indicate the applicability of nANB to treat industrial effluents. In this study, the inlet concentration of 50 mg L^{-1} of each metal [Cr(VI), Cu(II) and Zn(II)] is maintained.

The applicability of the developed nANB on the simultaneous removal of multiple metal ions present in the synthetically developed pulp & paper industrial effluent is evaluated. A continuous experiment is performed by maintaining the initial concentration of different metal ions in aqueous solution as provided in literature. On comparing with the adsorption capacity of nANB for individual metal ions, it is found that the adsorption capacity increases for the simultaneous removal of multiple metal ions. This supports the

utilization of the developed nANB for the removal of multiple pollutants from industrial effluent streams.

The experimental data of the breakthrough curves are fitted with the Yoon-Nelson and Yan models using the non-linear regression method of Origin 6.0 software. The applicability of Yoon-Nelson model for the scaling up the existing process is more suitable.

6.2 Conclusions

Based on the results obtained in the present study, the following conclusions are drawn:

1) A low-cost nano-porous adsorbent using Neem bark as raw material is successfully developed.

2) The optimum conditions for the activation of neem bark are obtained as 1:1 wt. % H_2SO_4 and 70°C.

3) The equilibrium contact time for metals removal using nANB is found to be 48 h.

4) Optimum values of adsorbent dosages are obtained as 6, 8 and 10.5 g L^{-1} for the removal of Cr(VI), Cu(II) and Zn(II) respectively.

5) Optimum values of initial concentration are found for the optimum adsorption capacity and percentage removal of all metal ions.

6) Metal adsorption capacity of nANB is found decreasing with an increase in the solution pH and temperature of the process.

7) The equilibrium adsorption of metal ions on nANB are well explained by Langmuir isotherm model which confirms the monolayer adsorption of metals on nANB surface.

8) The maximum adsorption capacity of individual metal ions is obtained as 20.83, 26.95, 21.23, 29.41, 26.32 and 11.90 mg g^{-1} for the removal of Cd(II), Cr(VI), Cu(II), Ni(II), Pb(II) and Zn(II) respectively.

9) The adsorption capacity of nANB for the simultaneous removal of Cr(VI), Cu(II) and Zn(II) is found to be approximately 1.5 times (38.95 mg g^{-1}) the capacity of the either of the metal ions.

10) The desorption efficiency of 91.4% is obtained for nANB adsorbent using acid and base treatment.

11) The rate kinetics of Cr(VI), Cu(II) and Zn(II) adsorption is well explained by second order kinetic model.

12) The Weber & Morris and Boyd models suggest that intraparticle diffusion is found as the controlling mass transfer mechanism for Cr(VI) and Zn(II) adsorption, whereas Cu(II) adsorption is due to both, film diffusion and intraparticle diffusion.

13) The presence of positive charged surface developed by the activation of the nANB supports the adsorption of Cr(VI), Cu(II) and Zn(II).

14) A generalized mathematical equation is successfully developed for the evaluation of maximum adsorption capacity as a function of independent parameters using Microsoft Excel 2007 regression tool.

15) DE is successfully applied in the developed mathematical equation to obtain the optimum parametric values for the maximum adsorption capacity for Cr(VI), Cu(II) and Zn(II) adsorption on nANB.

16) The cost analysis concludes that the nANB is a better possible alternative for the adsorption of multiple ions as compared to commercial and other low-cost adsorbents.

17) The fixed-bed adsorption studies carried out for different metals removal from wastewater suggests the suitability of nANB as an adsorbent for the treatment of metal contaminated effluent streams.

18) The breakthrough time for metal removal is found increasing with an increase in the mass of the adsorbent while it is found decreasing with an increase in the inlet concentration, inlet flowrate and presence of other metal ions in a fixed-bed adsorption column.

19) The nANB is found suitable for the removal of multiple metal ions from the plating industry and synthetically prepared pulp & paper industrial effluent.

20) The Yoon-Nelson model is found suitable for the scaling up of the fixed-bed adsorption process.

21) The adsorption capacity for the removal of multiple metal ions (six) in a fixed-bed adsorption column is found to be 43.71 mg g^{-1} which is approximately double to the individual adsorption capacity of any of the metal ions.

6.3 Major Contributions

1) A nano-porous adsorbent is developed using neem bark as a low-cost material for the removal of multiple metal ions

2) Various properties and characteristics of the developed adsorbent are found by different characterization techniques.

3) The developed nANB is tested for the removal of six metal ions [Cd(II), Cr(VI), Cu(II), Ni(II), Pb(II) and Zn(II)] by performing an extensive batch and continuous experiments.

4) The methods for the desorption of metal ions from saturated nANB are proposed.

5) The mechanism for the Cr(VI), Cu(II) and Zn(II) adsorption is proposed based on the characterization and experimental studies results.

6) A generalized mathematical equation is developed using batch experimental data and further utilized to obtain optimum parametric values of independent parameters.

7) The optimum values of independent parameters are found for Cr(VI), Cu(II) and Zn(II) adsorption using DE as an optimization technique.

8) The cost analysis is carried out to check the economic viability of the adsorption process using nANB.

9) The developed adsorbent is successfully tested for the simultaneous removal of multiple metal ions from the plating industry effluent and synthetically prepared pulp & paper industry effluent.

6.4 Future Scope

The present work can be extended to further studies. The future scope of the present study can be:

1) The developed adsorbent can be further utilized for the adsorption of other metal ions.

2) The effect of particle size on the removal of metal ions can be studied.

3) The developed nANB has positive charge on the surface due to which it can also be tested for the removal of dyes from effluent streams.

4) The proposed mathematical equation can also be modified for other independent parameters such as temperature, particle size etc. to get the optimum parametric values.

5) Life cycle analysis of developed adsorbent can be carried out.

REFERENCES

Aggarwal, S. C. and Kumar, S., 2011. Industrial Water Demand in India: Challenges and Implications for Water Pricing. India Infrastructure Report 2011. IDFC. New Delhi, Oxford University Press**:** 274-281.

Agrawal, A., Sahu, K. K. and Pandey, B. D., 2004. Removal of zinc from aqueous solutions using sea nodule residue. *Colloids and Surfaces A: Physicochemical and Engineering Aspects* 237(1–3): 133-140.

Ahmadi, A., Heidarzadeh, S., Mokhtari, A. R., Darezereshki, E. and Harouni, H. A., Optimization of heavy metal removal from aqueous solutions by maghemite (γ-Fe2O3) nanoparticles using response surface methodology. *Journal of Geochemical Exploration*.

Ahmaruzzaman, M., 2011. Industrial wastes as low-cost potential adsorbents for the treatment of wastewater laden with heavy metals. *Advances in Colloid and Interface Science* 166(1–2): 36-59.

Ajmal, M., Ali Khan Rao, R., Anwar, S., Ahmad, J. and Ahmad, R., 2003. Adsorption studies on rice husk: removal and recovery of Cd(II) from wastewater. *Bioresource Technology* 86(2): 147-149.

Akbal, F. and Camcı, S., 2011. Copper, chromium and nickel removal from metal plating wastewater by electrocoagulation. *Desalination* 269(1–3): 214-222.

Akpomie, K. G. and Dawodu, F. A., 2014. Efficient abstraction of nickel(II) and manganese(II) ions from solution onto an alkaline-modified montmorillonite. *Journal of Taibah University for Science* 8(4): 343-356.

Aksu, Z. and Gönen, F., 2004. Biosorption of phenol by immobilized activated sludge in a continuous packed bed: prediction of breakthrough curves. *Process Biochemistry* 39(5): 599-613.

Aksu, Z. and Gönen, F., 2006. Binary biosorption of phenol and chromium(VI) onto immobilized activated sludge in a packed bed: Prediction of kinetic parameters and breakthrough curves. *Separation and Purification Technology* 49(3): 205-216.

Al-Asheh, S., Banat, F. and Mohai, F., 1999. Sorption of copper and nickel by spent animal bones. *Chemosphere* 39(12): 2087-2096.

Al-Ghouti, M. A., Li, J., Salamh, Y., Al-Laqtah, N., Walker, G. and Ahmad, M. N. M., 2010. Adsorption mechanisms of removing heavy metals and dyes from aqueous solution using date pits solid adsorbent. *Journal of Hazardous Materials* 176(1–3): 510-520.

Al-Qodah, Z., 2000. Adsorption of dyes using shale oil ash. *Water Research* 34(17): 4295-4303.

Alaerts, G. J., Jitjaturant, V. and Kelderman, P., 1989. Use of coconut shell based activated carbon for chromium (VI) removal. *Water Science and Technology* 21: 1701–1704.

Ali Khan Rao, R., Rehman, F. and Kashifuddin, M., 2012. Removal of Cr(VI) from electroplating wastewater using fruit peel of Leechi (Litchi chinensis). *Desalination and Water Treatment* 49(1-3): 136-146.

Aliabadi, M., Morshedzadeh, K. and Soheyli, H., 2006. Removal of hexavalent chromium from aqueous solution by lignocellulosic solid wastes. *International Journal of Environmental Science & Technology* 3(3): 321-325.

Altun, T. and Pehlivan, E., 2007. Removal of Copper(II) Ions from Aqueous Solutions by Walnut-, Hazelnut- and Almond-Shells. *CLEAN – Soil, Air, Water* 35(6): 601-606.

Argun, M. E., Dursun, S. and Karatas, M., 2009. Removal of Cd(II), Pb(II), Cu(II) and Ni(II) from water using modified pine bark. *Desalination* 249(2): 519-527.

Argun, M. E., Dursun, S., Ozdemir, C. and Karatas, M., 2007. Heavy metal adsorption by modified oak sawdust: Thermodynamics and kinetics. *Journal of Hazardous Materials* 141(1): 77-85.

Arshadi, M., Amiri, M. J. and Mousavi, S., 2014. Kinetic, equilibrium and thermodynamic investigations of Ni(II), Cd(II), Cu(II) and Co(II) adsorption on barley straw ash. *Water Resources and Industry* 6: 1-17.

Arulkumar, M., Thirumalai, K., Sathishkumar, P. and Palvannan, T., 2012. Rapid removal of chromium from aqueous solution using novel prawn shell activated carbon. *Chemical Engineering Journal* 185–186: 178-186.

Asberry, H. B., Kuo, C.-Y., Gung, C.-H., Conte, E. D. and Suen, S.-Y., 2014. Characterization of water bamboo husk biosorbents and their application in heavy metal ion trapping. *Microchemical Journal* 113: 59-63.

Auta, M. and Hameed, B. H., 2014. Chitosan–clay composite as highly effective and low-cost adsorbent for batch and fixed-bed adsorption of methylene blue. *Chemical Engineering Journal* 237: 352-361.

Avila, M., Burks, T., Akhtar, F., Göthelid, M., Lansåker, P. C., Toprak, M. S., Muhammed, M. and Uheida, A., 2014. Surface functionalized nanofibers for the removal of chromium(VI) from aqueous solutions. *Chemical Engineering Journal* 245: 201-209.

Awual, M. R., Rahman, I. M. M., Yaita, T., Khaleque, M. A. and Ferdows, M., 2014. pH dependent Cu(II) and Pd(II) ions detection and removal from aqueous media by an efficient mesoporous adsorbent. *Chemical Engineering Journal* 236: 100-109.

Babel, S. and Kurniawan, T. A., 2003. Low-cost adsorbents for heavy metals uptake from contaminated water: a review. *Journal of Hazardous Materials* 97(1–3): 219-243.

Babu, B. V., 2007. Process Plant Simulation. New Delhi, Oxford University Press.

Babu, B. V. and Gupta, S., 2008a. Removal of Cr(VI) from wastewater using activated tamarind seeds as an adsorbent. *Journal of Environmental Engineering and Science* 7(5): 553-557.

Babu, B. V. and Gupta, S., 2008b. Adsorption of Cr(VI) using activated neem leaves: kinetic studies. *Adsorption* 14(1): 85-92.

Bailey, S. E., Olin, T. J., Bricka, R. M. and Adrian, D. D., 1999. A review of potentially low-cost sorbents for heavy metals. *Water Research* 33(11): 2469-2479.

Bakiler, M., Maslov, I. V. and Akyüz, S., 1999. Theoretical study of the vibrational spectra of 2-chloropyridine metal complexes II. Calculation and analysis of the IR spectra of Cd– and Ni–2-Chloropyridine complexes. *Journal of Molecular Structure* 476(1–3): 21-26.

Baral, S. S., Das, N., Ramulu, T. S., Sahoo, S. K., Das, S. N. and Chaudhury, G. R., 2009. Removal of Cr(VI) by thermally activated weed Salvinia cucullata in a fixed-bed column. *Journal of Hazardous Materials* 161(2–3): 1427-1435.

Benaïssa, H. and Elouchdi, M. A., 2007. Removal of copper ions from aqueous solutions by dried sunflower leaves. *Chemical Engineering and Processing: Process Intensification* 46(7): 614-622.

Bhatnagar, A., Minocha, A. K. and Sillanpää, M., 2010. Adsorptive removal of cobalt from aqueous solution by utilizing lemon peel as biosorbent. *Biochemical Engineering Journal* 48(2): 181-186.

Bhattacharya, A. K., Naiya, T. K., Mandal, S. N. and Das, S. K., 2008. Adsorption, kinetics and equilibrium studies on removal of Cr(VI) from aqueous solutions using different low-cost adsorbents. *Chemical Engineering Journal* 137(3): 529-541.

Bou-Maroun, E., Goetz-Grandmont, G. J. and Boos, A., 2006. Sorption of europium(III) and copper(II) by a mesostructured silica doped with acyl-hydroxypyrazole derivatives: Extraction, kinetic and capacity studies. *Colloids and Surfaces A: Physicochemical and Engineering Aspects* 287(1–3): 1-9.

Bouhamed, F., Elouear, Z. and Bouzid, J., 2012. Adsorptive removal of copper(II) from aqueous solutions on activated carbon prepared from Tunisian date stones: Equilibrium, kinetics and thermodynamics. *Journal of the Taiwan Institute of Chemical Engineers* 43(5): 741-749.

Boyd, G. E., A.W.Adamson and Jr.L.S.Myers, 1947. The exchange adsorption of ions from aqueous solutions by organic zeolites, II: kinetics. *Journal of the American Chemical Society* 69: 2836–2848.

Božić, D., Stanković, V., Gorgievski, M., Bogdanović, G. and Kovačević, R., 2009. Adsorption of heavy metal ions by sawdust of deciduous trees. *Journal of Hazardous Materials* 171(1–3): 684-692.

Buehren, M. (2012). "Optimization using the evolutionary algorithm of Differential Evolution." Retrieved 13-12-2012, from http://in.mathworks.com/matlabcentral/fileexchange/18593-differential-evolution/content/rosenbrocksaddle.m.

Bulut, Y. and Baysal, Z., 2006. Removal of Pb(II) from wastewater using wheat bran. *Journal of Environmental Management* 78(2): 107-113.

Cai, X., Gao, Y., Sun, Q., Chen, Z., Megharaj, M. and Naidu, R., 2014. Removal of co-contaminants Cu (II) and nitrate from aqueous solution using kaolin-Fe/Ni nanoparticles. *Chemical Engineering Journal* 244: 19-26.

Calero, M., Hernáinz, F., Blázquez, G., Tenorio, G. and Martín-Lara, M. A., 2009. Study of Cr (III) biosorption in a fixed-bed column. *Journal of Hazardous Materials* 171(1–3): 886-893.

Camarillo, R., Pérez, Á., Cañizares, P. and de Lucas, A., 2012. Removal of heavy metal ions by polymer enhanced ultrafiltration: Batch process modeling and thermodynamics of complexation reactions. *Desalination* 286: 193-199.

Cechinel, M. A. P., Ulson de Souza, S. M. A. G. and Ulson de Souza, A. A., 2014. Study of lead (II) adsorption onto activated carbon originating from cow bone. *Journal of Cleaner Production* 65: 342-349.

Charerntanyarak, L., 1999. Heavy metals removal by chemical coagulation and precipitation. *Water Science and Technology* 39(10–11): 135-138.

Chatterjee, A. and Schiewer, S., 2014. Multi-resistance kinetic models for biosorption of Cd by raw and immobilized citrus peels in batch and packed-bed columns. *Chemical Engineering Journal* 244: 105-116.

Chien, S. H. and Clayton, W. R., 1980. Application of Elovich Equation to the Kinetics of Phosphate Release and Sorption in Soils. *Soil Science Society of America Journal* 44(2): 265-268.

Chu, K. H., 2004. Improved fixed bed models for metal biosorption. *Chemical Engineering Journal* 97(2–3): 233-239.

Cooney, D. O., 1999. Adsorption Design for Wastewater Treatment. Florida, Lewis Publishers.

Cooper, C. A., Lin, Y. S. and Gonzalez, M., 2004. Separation properties of surface modified silica supported liquid membranes for divalent metal removal/recovery. *Journal of Membrane Science* 229(1–2): 11-25.

Cruz-Olivares, J., Pérez-Alonso, C., Barrera-Díaz, C., López, G. and Balderas-Hernández, P., 2010. Inside the removal of lead(II) from aqueous solutions by De-Oiled Allspice Husk in batch and continuous processes. *Journal of Hazardous Materials* 181(1–3): 1095-1101.

Cutillas-Barreiro, L., Ansias-Manso, L., Fernández-Calviño, D., Arias-Estévez, M., Nóvoa-Muñoz, J. C., Fernández-Sanjurjo, M. J., Álvarez-Rodríguez, E. and Núñez-Delgado, A., 2014. Pine bark as bio-adsorbent for Cd, Cu, Ni, Pb and Zn: Batch-type and stirred flow chamber experiments. *Journal of Environmental Management* 144: 258-264.

Dąbrowski, A., Hubicki, Z., Podkościelny, P. and Robens, E., 2004. Selective removal of the heavy metal ions from waters and industrial wastewaters by ion-exchange method. *Chemosphere* 56(2): 91-106.

Dakiky, M., Khamis, M., Manassra, A. and Mer'eb, M., 2002. Selective adsorption of chromium(VI) in industrial wastewater using low-cost abundantly available adsorbents. *Advances in Environmental Research* 6(4): 533-540.

Daneshvar, N., Salari, D. and Aber, S., 2002. Chromium adsorption and Cr(VI) reduction to trivalent chromium in aqueous solutions by soya cake. *Journal of Hazardous Materials* 94(1): 49-61.

Das, D., Basak, G., Lakshmi, V. and Das, N., 2012. Kinetics and equilibrium studies on removal of zinc(II) by untreated and anionic surfactant treated dead biomass of yeast: Batch and column mode. *Biochemical Engineering Journal* 64: 30-47.

Datta, D. and Kumar, S., 2012. Modeling and Optimization of Recovery Process of Glycolic Acid using Reactive Extraction. *International Journal of Chemical Engineering and Applications* 3(2): 141-146.

Dawodu, F. A. and Akpomie, K. G., 2014. Simultaneous adsorption of Ni(II) and Mn(II) ions from aqueous solution unto a Nigerian kaolinite clay. *Journal of Materials Research and Technology* 3(2): 129-141.

Deliyanni, E. A., Peleka, E. N. and Matis, K. A., 2007. Removal of zinc ion from water by sorption onto iron-based nanoadsorbent. *Journal of Hazardous Materials* 141(1): 176-184.

Demirbas, A., 2008. Heavy metal adsorption onto agro-based waste materials: A review. *Journal of Hazardous Materials* 157(2–3): 220-229.

Demopoulos, G. P. and Gefvert, D. L., 1984. Iron(III) removal from base-metal electrolyte solutions by solvent extraction. *Hydrometallurgy* 12(3): 299-315.

Deng, L., Shi, Z., Li, B., Yang, L., Luo, L. and Yang, X., 2014. Adsorption of Cr(VI) and Phosphate on Mg–Al Hydrotalcite Supported Kaolin Clay Prepared by Ultrasound-Assisted Coprecipitation Method Using Batch and Fixed-Bed Systems. *Industrial & Engineering Chemistry Research* 53(18): 7746-7757.

Depci, T., Kul, A. R. and Önal, Y., 2012. Competitive adsorption of lead and zinc from aqueous solution on activated carbon prepared from Van apple pulp: Study in single- and multi-solute systems. *Chemical Engineering Journal* 200–202: 224-236.

Dong, Y., Täffner, T., Fernández, J. F. and Niemeyer, B., 2012. Off-Gas-Treatment by Application of Selective Adsorbents. *Procedia Engineering* 42: 1260-1269.

Egashira, R., Tanabe, S. and Habaki, H., 2012. Adsorption of heavy metals in mine wastewater by Mongolian natural zeolite. *Procedia Engineering* 42: 49-57.

El-Ashtoukhy, E. S. Z., Amin, N. K. and Abdelwahab, O., 2008. Removal of lead (II) and copper (II) from aqueous solution using pomegranate peel as a new adsorbent. *Desalination* 223(1–3): 162-173.

Eloussaief, M., Jarraya, I. and Benzina, M., 2009. Adsorption of copper ions on two clays from Tunisia: pH and temperature effects. *Applied Clay Science* 46(4): 409-413.

Escudero, C., Poch, J. and Villaescusa, I., 2013. Modelling of breakthrough curves of single and binary mixtures of Cu(II), Cd(II), Ni(II) and Pb(II) sorption onto grape stalks waste. *Chemical Engineering Journal* 217: 129-138.

Ewecharoen, A., Thiravetyan, P. and Nakbanpote, W., 2008. Comparison of nickel adsorption from electroplating rinse water by coir pith and modified coir pith. *Chemical Engineering Journal* 137(2): 181-188.

Fakhri, A., 2014. Application of response surface methodology to optimize the process variables for fluoride ion removal using maghemite nanoparticles. *Journal of Saudi Chemical Society* 18(4): 340-347.

Fan, M. (2015). "Coconut shell activated carbon price." 2015, from http://www.alibaba.com/product-detail/coconut-shell-activated-carbon-price_60221228484.html.

Farajzadeh, M. A. and Monji, A. B., 2004. Adsorption characteristics of wheat bran towards heavy metal cations. *Separation and Purification Technology* 38(3): 197-207.

Filho, N. L. D., Carmo, D. R. d. and Rosa, A. H., 2006. Selective Sorption of Mercury(II) from Aqueous Solution with an Organically Modified Clay and its Electroanalytical Application. *Separation Science and Technology* 41(4): 733-746.

Foo, K. Y. and Hameed, B. H., 2010. Insights into the modeling of adsorption isotherm systems. *Chemical Engineering Journal* 156(1): 2-10.

Freundlich, H., 1932. Of the adsorption of gases. Section II. Kinetics and energetics of gas adsorption. Introductory paper to section II. *Transactions of the Faraday Society* 28: 195-201.

Freundlich, H. M. F., 1906. Over the adsorption in solution. *Journal of Physical Chemistry* 57: 385–471.

Gabaldón, C., Marzal, P., Ferrer, J. and Seco, A., 1996. Single and competitive adsorption of Cd and Zn onto a granular activated carbon. *Water Research* 30(12): 3050-3060.

Gandhi, M. R., Kousalya, G. N. and Meenakshi, S., 2011. Removal of copper(II) using chitin/chitosan nano-hydroxyapatite composite. *International Journal of Biological Macromolecules* 48(1): 119-124.

Garg, U. K., Kaur, M. P., Garg, V. K. and Sud, D., 2007. Removal of hexavalent chromium from aqueous solution by agricultural waste biomass. *Journal of Hazardous Materials* 140(1–2): 60-68.

Gode, F. and Moral, E., 2008. Column study on the adsorption of Cr(III) and Cr(VI) using Pumice, Yarıkkaya brown coal, Chelex-100 and Lewatit MP 62. *Bioresource Technology* 99(6): 1981-1991.

Goel, J., Kadirvelu, K., Rajagopal, C. and Kumar Garg, V., 2005. Removal of lead(II) by adsorption using treated granular activated carbon: Batch and column studies. *Journal of Hazardous Materials* 125(1–3): 211-220.

Gong, J.-L., Wang, X.-Y., Zeng, G.-M., Chen, L., Deng, J.-H., Zhang, X.-R. and Niu, Q.-Y., 2012. Copper (II) removal by pectin–iron oxide magnetic nanocomposite adsorbent. *Chemical Engineering Journal* 185–186: 100-107.

Güçlü, G., Gürdağ, G. and Özgümüş, S., 2003. Competitive removal of heavy metal ions by cellulose graft copolymers. *Journal of Applied Polymer Science* 90(8): 2034-2039.

Gundogdu, A., Ozdes, D., Duran, C., Bulut, V. N., Soylak, M. and Senturk, H. B., 2009. Biosorption of Pb(II) ions from aqueous solution by pine bark (Pinus brutia Ten.). *Chemical Engineering Journal* 153(1–3): 62-69.

Guo, H., Zhang, S., Kou, Z., Zhai, S., Ma, W. and Yang, Y., 2015. Removal of cadmium(II) from aqueous solutions by chemically modified maize straw. *Carbohydrate Polymers* 115: 177-185.

Gupta, K. R., Ed. 2008a. Water Crisis in India. New Delhi, Atlantic Publishers & Distributors (P) Ltd.

Gupta, S., 2008b. Theoretical & Experimental Investigations for Removal of Pollutants using Adsorption. Department of Chemical Engineering. Pilani, Birla Institute of Technology & Science(BITS)- Pilani, Pilani Campus. Doctor of Philosophy**:** 223.

Gupta, S. and Babu, B. V., 2009a. Utilization of waste product (tamarind seeds) for the removal of Cr(VI) from aqueous solutions: Equilibrium, kinetics, and regeneration studies. *Journal of Environmental Management* 90(10): 3013-3022.

Gupta, S. and Babu, B. V., 2009b. Removal of toxic metal Cr(VI) from aqueous solutions using sawdust as adsorbent: Equilibrium, kinetics and regeneration studies. *Chemical Engineering Journal* 150(2–3): 352-365.

Gupta, S. and Babu, B. V., 2009c. Modeling, simulation, and experimental validation for continuous Cr(VI) removal from aqueous solutions using sawdust as an adsorbent. *Bioresource Technology* 100(23): 5633-5640.

Gupta, S. and Babu, B. V., 2010a. Experimental, kinetic, equilibrium and regeneration studies for adsorption of Cr(VI) from aqueous solutions using low cost adsorbent (activated flyash). *Desalination and Water Treatment* 20(1-3): 168-178.

Gupta, S. and Babu, B. V., 2010b. Experimental investigations and theoretical modeling aspects in column studies for removal of Cr(VI) from aqueous solutions using activated tamarind seeds. *Jornal of Water Resource and Protection* 2: 706-716.

Gupta, V. K., Suhas, Nayak, A., Agarwal, S., Chaudhary, M. and Tyagi, I., 2014. Removal of Ni (II) ions from water using scrap tire. *Journal of Molecular Liquids* 190: 215-222.

Hashmat, I., Azad, H. and Ahmed, A., 2012. Neem (Azadirachta indica A. Juss) - A Nature's Drugstore: An overview. *International Research Journal of Biological Sciences* 1(6): 76-79.

Ho, Y.-S., 2006. Review of second-order models for adsorption systems. *Journal of Hazardous Materials* 136(3): 681-689.

Ho, Y. S. and McKay, G., 1998. The kinetics of sorption of basic dyes from aqueous solution by sphagnum moss peat. *The Canadian Journal of Chemical Engineering* 76(4): 822-827.

Hossain, M. A., Kumita, M. and Mori, S., 2010. SEM Characterization of the mass transfer of Cr(VI) during the adsorption on used black tea leaves. *African Journal of Pure and Applied Chemistry* 4(7): 135-141.

Huang, G., Shi, J. X. and Langrish, T. A. G., 2009. Removal of Cr(VI) from aqueous solution using activated carbon modified with nitric acid. *Chemical Engineering Journal* 152(2–3): 434-439.

Isaac, C. P. J. and Sivakumar, A., 2013. Removal of lead and cadmium ions from water using Annona squamosa shell: kinetic and equilibrium studies. *Desalination and Water Treatment* 51(40-42): 7700-7709.

Issabayeva, G., Aroua, M. K. and Sulaiman, N. M., 2008. Continuous adsorption of lead ions in a column packed with palm shell activated carbon. *Journal of Hazardous Materials* 155(1–2): 109-113.

Itankar, N. and Patil, Y., 2014. Management of Hexavalent Chromium from Industrial Waste Using Low-cost Waste Biomass. *Procedia - Social and Behavioral Sciences* 133: 219-224.

Jellouli Ennigrou, D., Ben Sik Ali, M. and Dhahbi, M., 2014. Copper and Zinc removal from aqueous solutions by polyacrylic acid assisted-ultrafiltration. *Desalination* 343: 82-87.

Jha, R. C. (2010). Water and Related Statistics, Central Water Comission.

Juang, R.-S., Lin, S.-H. and Wang, T.-Y., 2003. Removal of metal ions from the complexed solutions in fixed bed using a strong-acid ion exchange resin. *Chemosphere* 53(10): 1221-1228.

Kalmykova, Y., Strömvall, A.-M. and Steenari, B.-M., 2008. Adsorption of Cd, Cu, Ni, Pb and Zn on Sphagnum peat from solutions with low metal concentrations. *Journal of Hazardous Materials* 152(2): 885-891.

Kandah, M. I., 2004. Zinc and cadmium adsorption on low-grade phosphate. *Separation and Purification Technology* 35(1): 61-70.

Kapur, M. and Mondal, M. K., 2013. Mass transfer and related phenomena for Cr(VI) adsorption from aqueous solutions onto Mangifera indica sawdust. *Chemical Engineering Journal* 218: 138-146.

Karabulut, S., Karabakan, A., Denizli, A. and Yürüm, Y., 2000. Batch removal of copper(II) and zinc(II) from aqueous solutions with low-rank Turkish coals. *Separation and Purification Technology* 18(3): 177-184.

Kausar, A., Bhatti, H. N., Sarfraz, R. A. and Shahid, M., 2013. Prediction of optimum equilibrium and kinetic models for U(VI) sorption onto rice husk: comparison of linear and nonlinear regression methods∗. *Desalination and Water Treatment* 52(7-9): (ix)-(ix).

Kaya, K., Pehlivan, E., Schmidt, C. and Bahadir, M., 2014. Use of modified wheat bran for the removal of chromium(VI) from aqueous solutions. *Food Chemistry* 158: 112-117.

Kazemipour, M., Ansari, M., Tajrobehkar, S., Majdzadeh, M. and Kermani, H. R., 2008. Removal of lead, cadmium, zinc, and copper from industrial wastewater by carbon developed from walnut, hazelnut, almond, pistachio shell, and apricot stone. *Journal of Hazardous Materials* 150(2): 322-327.

Keleş, S. and Güçlü, G., 2006. Competitive Removal of Heavy Metal Ions by Starch-Graft-Acrylic Acid Copolymers. *Polymer-Plastics Technology and Engineering* 45(3): 365-371.

Keshtkar, A., Kafshgari, F. and Mousavian, M., 2012. Binary biosorption of uranium(VI) and nickel(II) from aqueous solution by Ca-pretreated Cystoseira indica in a fixed-bed column. *Journal of Radioanalytical and Nuclear Chemistry* 292(2): 501-512.

Kim, D.-H., Shin, M.-C., Choi, H.-D., Seo, C.-I. and Baek, K., 2008. Removal mechanisms of copper using steel-making slag: adsorption and precipitation. *Desalination* 223(1–3): 283-289.

Kumar, M. and Puri, A., 2012. A review of permissible limits of drinking water. *Indian Journal of Occupational & Environmental Medicine* 16(1): 40-44.

Kumar, M., Rathore, D. P. and Singh, A. K., 2001. Quinalizarin anchored on Amberlite XAD-2. A new matrix for solid-phase extraction of metal ions for flame atomic absorption spectrometric determination. *Fresenius J Anal Chem* 370(4): 377-382.

Kumar, P. S. and Kirthika, K., 2009. Equilibrium and kinetic study of adsorption of nickel from aqueous solution onto bael tree leaf powder. *Journal of Engineering Science and Technology* 4(4): 351 - 363.

Kumar, R., Bishnoi, N. R., Garima and Bishnoi, K., 2008. Biosorption of chromium(VI) from aqueous solution and electroplating wastewater using fungal biomass. *Chemical Engineering Journal* 135(3): 202-208.

Kumar, S., Datta, D. and Babu, B. V., 2011a. Differential Evolution Approach for Reactive Extraction of Propionic Acid Using Tri-n-Butyl Phosphate (TBP) in Kerosene and 1-Decanol. *Materials and Manufacturing Processes* 26(9): 1222-1228.

Kumar, S., Datta, D. and Babu, B. V., 2011b. Estimation of equilibrium parameters using differential evolution in reactive extraction of propionic acid by tri-n-butyl phosphate. *Chemical Engineering and Processing: Process Intensification* 50(7): 614-622.

Kyzas, G. Z., Siafaka, P. I., Pavlidou, E. G., Chrissafis, K. J. and Bikiaris, D. N., 2015. Synthesis and adsorption application of succinyl-grafted chitosan for the simultaneous removal of zinc and cationic dye from binary hazardous mixtures. *Chemical Engineering Journal* 259: 438-448.

Labor, U. S. D. o. (2006). "Health Effects of Hexavalent Chromium." OSHA Fact Sheet Retrieved 1st October, 2014, from https://www.osha.gov/OshDoc/data_General_Facts/hexavalent_chromium.pdf.

Labor, U. S. D. o. (2014). "Chromium." Safety and Health Topics Retrieved 3rd September, 2014, from https://www.osha.gov/SLTC/chromium/index.html.

Lagergren, S., 1898. Zur theorie der sogenannten adsorption geloster stoffe. *K. Sven. Vetenskapsakad. Handl.* 24: 1–39.

Langmuir, I., 1916. The constitution and fundamental properties of solids and liquids. Part I. Solids. *Journal of the American Chemical Society* 38(11): 2221-2295.

Langmuir, I., 1918. The Adsorption of Gases on Plane Surfaces of Glass, Mica and Platinum. *Journal of the American Chemical Society* 40(9): 1361-1403.

Lassonde, K. (2013). "possible Harmful or Dangerous side effects of Zinc." Retrieved 8th November, 2014, from http://www.pwnfitness.com/harmful-dangerous-side-effects-zinc/.

Li, C.-W., Chen, Y.-M. and Hsiao, S.-T., 2008a. Compressed air-assisted solvent extraction (CASX) for metal removal. *Chemosphere* 71(1): 51-58.

Li, X., Tang, Y., Cao, X., Lu, D., Luo, F. and Shao, W., 2008b. Preparation and evaluation of orange peel cellulose adsorbents for effective removal of cadmium, zinc, cobalt and nickel. *Colloids and Surfaces A: Physicochemical and Engineering Aspects* 317(1–3): 512-521.

Li, Y., Liu, F., Xia, B., Du, Q., Zhang, P., Wang, D., Wang, Z. and Xia, Y., 2010. Removal of copper from aqueous solution by carbon nanotube/calcium alginate composites. *Journal of Hazardous Materials* 177(1–3): 876-880.

Liang, F.-B., Song, Y.-L., Huang, C.-P., Zhang, J. and Chen, B.-H., 2013. Adsorption of hexavalent chromium on a lignin-based resin: Equilibrium, thermodynamics, and kinetics. *Journal of Environmental Chemical Engineering* 1(4): 1301-1308.

Liang, S., Guo, X., Feng, N. and Tian, Q., 2010. Isotherms, kinetics and thermodynamic studies of adsorption of Cu2+ from aqueous solutions by Mg2+/K+ type orange peel adsorbents. *Journal of Hazardous Materials* 174(1–3): 756-762.

Liang, S., Guo, X., Lautner, S. and Saake, B., 2014. Removal of Hexavalent Chromium by Different Modified Spruce Bark Adsorbents. *Journal of Wood Chemistry and Technology* 34(4): 273-290.

Liao, H.-T. and Shiau, C.-Y., 2000. Analytical solution to an axial dispersion model for the fixed-bed adsorber. *AIChE Journal* 46(6): 1168-1176.

Lim, H. K., Teng, T. T., Ibrahim, M. H., Ahmad, A. and Chee, H. T., 2012. Adsorption and Removal of Zinc (II) from Aqueous Solution Using Powdered Fish Bones. *APCBEE Procedia* 1: 96-102.

Lin, S.-H. and Juang, R.-S., 2002. Heavy metal removal from water by sorption using surfactant-modified montmorillonite. *Journal of Hazardous Materials* 92(3): 315-326.

Liu, T., Wang, Z.-L., Yan, X. and Zhang, B., 2014. Removal of mercury (II) and chromium (VI) from wastewater using a new and effective composite: Pumice-supported nanoscale zero-valent iron. *Chemical Engineering Journal* 245: 34-40.

Lugo-Lugo, V., Barrera-Díaz, C., Ureña-Núñez, F., Bilyeu, B. and Linares-Hernández, I., 2012. Biosorption of Cr(III) and Fe(III) in single and binary systems onto pretreated orange peel. *Journal of Environmental Management* 112: 120-127.

Maher, A., Sadeghi, M. and Moheb, A., 2014. Heavy metal elimination from drinking water using nanofiltration membrane technology and process optimization using response surface methodology. *Desalination* 352: 166-173.

Mahmoud, M. R., Lazaridis, N. K. and Matis, K. A., 2014. Study of flotation conditions for cadmium(II) removal from aqueous solutions. *Process Safety and Environmental Protection*.

Malash, G. F. and El-Khaiary, M. I., 2010. Piecewise linear regression: A statistical method for the analysis of experimental adsorption data by the intraparticle-diffusion models. *Chemical Engineering Journal* 163(3): 256-263.

Malkoc, E. and Nuhoglu, Y., 2007. Potential of tea factory waste for chromium(VI) removal from aqueous solutions: Thermodynamic and kinetic studies. *Separation and Purification Technology* 54(3): 291-298.

McCabe, W. L., Smith, J. M. and Harriott, P., 2007. Unit operations of Chemical Engineering, Mc-Graw Hill International Edition.

Meena, A. K., Kadirvelu, K., Mishra, G. K., Rajagopal, C. and Nagar, P. N., 2008. Adsorptive removal of heavy metals from aqueous solution by treated sawdust (Acacia arabica). *Journal of Hazardous Materials* 150(3): 604-611.

Meena, A. K., Mishra, G. K., Rai, P. K., Rajagopal, C. and Nagar, P. N., 2005. Removal of heavy metal ions from aqueous solutions using carbon aerogel as an adsorbent. *Journal of Hazardous Materials* 122(1–2): 161-170.

Memon, J. R., Memon, S. Q., Bhanger, M. I., El-Turki, A., Hallam, K. R. and Allen, G. C., 2009. Banana peel: A green and economical sorbent for the selective removal of Cr(VI) from industrial wastewater. *Colloids and Surfaces B: Biointerfaces* 70(2): 232-237.

Metcalf and Eddy, I., 2005. Wastewater Engineering, Treatment and Reuse. New Delhi, Tata McGraw-Hill Publishing Company.

Meunier, N., Drogui, P., Montané, C., Hausler, R., Mercier, G. and Blais, J.-F., 2006. Comparison between electrocoagulation and chemical precipitation for metals removal from acidic soil leachate. *Journal of Hazardous Materials* 137(1): 581-590.

Milicevic, S., Boljanac, T., Martinovic, S., Vlahovic, M., Milosevic, V. and Babic, B., 2012. Removal of copper from aqueous solutions by low cost adsorbent-Kolubara lignite. *Fuel Processing Technology* 95: 1-7.

Mishra, P. C. and Patel, R. K., 2009. Removal of lead and zinc ions from water by low cost adsorbents. *Journal of Hazardous Materials* 168(1): 319-325.

Mittal, A., Mittal, J., Malviya, A. and Gupta, V. K., 2009. Adsorptive removal of hazardous anionic dye "Congo red" from wastewater using waste materials and recovery by desorption. *Journal of Colloid and Interface Science* 340(1): 16-26.

Mohan, D., Kumar, H., Sarswat, A., Alexandre-Franco, M. and Pittman Jr, C. U., 2014. Cadmium and lead remediation using magnetic oak wood and oak bark fast pyrolysis bio-chars. *Chemical Engineering Journal* 236: 513-528.

Mohan, S. and Sreelakshmi, G., 2008. Fixed bed column study for heavy metal removal using phosphate treated rice husk. *Journal of Hazardous Materials* 153(1–2): 75-82.

Mor, S., Ravindra, K. and Bishnoi, N. R., 2007. Adsorption of chromium from aqueous solution by activated alumina and activated charcoal. *Bioresource Technology* 98(4): 954-957.

Morcali, M. H., Zeytuncu, B., Baysal, A., Akman, S. and Yucel, O., 2014. Adsorption of copper and zinc from sulfate media on a commercial sorbent. *Journal of Environmental Chemical Engineering* 2(3): 1655-1662.

Moreno-Piraján, J., Garcia-Cuello, V. and Giraldo, L., 2011. The removal and kinetic study of Mn, Fe, Ni and Cu ions from wastewater onto activated carbon from coconut shells. *Adsorption* 17(3): 505-514.

Muthukumaran, K. and Beulah, S., 2011. Removal of Chromium (VI) from wastewater using chemically activated Syzygium jambolanum nut carbon by batch studies. *Procedia Environmental Sciences* 4: 266-280.

Nadaroglu, H., Kalkan, E. and Demir, N., 2010. Removal of copper from aqueous solution using red mud. *Desalination* 251(1–3): 90-95.

Naiya, T. K., Chowdhury, P., Bhattacharya, A. K. and Das, S. K., 2009. Saw dust and neem bark as low-cost natural biosorbent for adsorptive removal of Zn(II) and Cd(II) ions from aqueous solutions. *Chemical Engineering Journal* 148(1): 68-79.

Namasivayam, C. and Ranganathan, K., 1993. Waste Fe(III)/Cr(III) hydroxide as adsorbent for the removal of Cr(VI) from aqueous solution and chromium plating industry wastewater. *Environmental Pollution* 82(3): 255-261.

Namasivayam, C. and Sureshkumar, M. V., 2008. Removal of chromium(VI) from water and wastewater using surfactant modified coconut coir pith as a biosorbent. *Bioresource Technology* 99(7): 2218-2225.

Namasivayam, C. and Yamuna, R. T., 1995. Adsorption of chromium (VI) by a low-cost adsorbent: Biogas residual slurry. *Chemosphere* 30(3): 561-578.

Nath, K. and Das, D., 2011. Modeling and optimization of fermentative hydrogen production. *Bioresource Technology* 102(18): 8569-8581.

Ofomaja, A. E., Unuabonah, E. I. and Oladoja, N. A., 2010. Competitive modeling for the biosorptive removal of copper and lead ions from aqueous solution by Mansonia wood sawdust. *Bioresource Technology* 101(11): 3844-3852.

Ogata, F. and Kawasaki, N., 2013. Adsorption of Pt(IV) and Pd(II) by calcined dried aluminum hydroxide gel from aqueous solution system. *Journal of Environmental Chemical Engineering* 1(4): 1013-1019.

Ogbuewu, I. P., Odoemenam, V. U., Obikaonu, H. O., Opara, M. N., Emenalom, O. O., Uchegbu, M. C., Okoli, I. C., Esonu, B. O. and Iloeje, M. U., 2011. The Growing Importance of Neem (Azadirachta indica A. Juss) in Agriculture, Industry, Medicine and Environment: A Review. *Research Journal of Medicinal Plant* 5(3): 230-245.

Orhan, Y. and Büyükgüngör, H., 1993. The Removal of Heavy Metals by Using Agricultural Wastes. *Water Science & Technology* 28(2): 247-255.

Orozco, A. M. F., Contreras, E. M. and Zaritzky, N. E., 2008. Modelling Cr(VI) removal by a combined carbon-activated sludge system. *Journal of Hazardous Materials* 150(1): 46-52.

Pandaya, A. B. (2013). Annual Report 2012-13, Central Water Commission.

Patel, K. P., Tank, S. K., Patel, K. M. and Patel, P., 2013. Removal of Cadmium and Zinc Ions From Aqueous Solution By Using Two Type of Husks. *APCBEE Procedia* 5: 141-144.

Patnukao, P., Kongsuwan, A. and Pavasant, P., 2008. Batch studies of adsorption of copper and lead on activated carbon from Eucalyptus camaldulensis Dehn. bark. *Journal of Environmental Sciences* 20(9): 1028-1034.

Pavan, F. A., Camacho, E. S., Lima, E. C., Dotto, G. L., Branco, V. T. A. and Dias, S. L. P., 2014. Formosa papaya seed powder (FPSP): Preparation, characterization and application as an alternative adsorbent for the removal of crystal violet from aqueous phase. *Journal of Environmental Chemical Engineering* 2(1): 230-238.

Pehlivan, E., Altun, T. and Parlayici, Ş., 2012. Modified barley straw as a potential biosorbent for removal of copper ions from aqueous solution. *Food Chemistry* 135(4): 2229-2234.

Pehlivan, E., Altun, T. and Parlayıcı, S., 2009. Utilization of barley straws as biosorbents for Cu2+ and Pb2+ ions. *Journal of Hazardous Materials* 164(2–3): 982-986.

Pehlivan, E., Cetin, S. and Yanık, B. H., 2006. Equilibrium studies for the sorption of zinc and copper from aqueous solutions using sugar beet pulp and fly ash. *Journal of Hazardous Materials* 135(1–3): 193-199.

Perlman, H. (2014). "How much water is there on, in, and above the Earth?" Retrieved 12/06/2014, 2014, from http://water.usgs.gov/edu/earthhowmuch.html.

Plum, L. M., Rink, L. and Haase, H., 2010. The Essential Toxin: Impact of Zinc on Human Health. *International Journal of Environmental Research and Public Health* 7(4): 1342-1365.

Polat, H. and Erdogan, D., 2007. Heavy metal removal from waste waters by ion flotation. *Journal of Hazardous Materials* 148(1–2): 267-273.

Puranik, P. R. and Paknikar, K. M., 1999. Influence of co-cations on biosorption of lead and zinc – a comparative evaluation in binary and multimetal systems. *Bioresource Technology* 70(3): 269-276.

Puri, H. S., 2006. Neem, Harwood academic publisher**:** 23-32.

Qiu, Y.-R. and Mao, L.-J., 2013. Removal of heavy metal ions from aqueous solution by ultrafiltration assisted with copolymer of maleic acid and acrylic acid. *Desalination* 329: 78-85.

Rafiq, Z., Nazir, R., Durr e, S., Shah, M. R. and Ali, S., 2014. Utilization of magnesium and zinc oxide nano-adsorbents as potential materials for treatment of copper electroplating industry wastewater. *Journal of Environmental Chemical Engineering* 2(1).

Rajamohan, N., Rajasimman, M., Rajeshkannan, R. and Saravanan, V., 2014. Equilibrium, kinetic and thermodynamic studies on the removal of Aluminum by modified Eucalyptus camaldulensis barks. *Alexandria Engineering Journal* 53(2): 409-415.

Rao, R. A. K. and Rehman, F., 2010. Adsorption studies on fruits of Gular (Ficus glomerata): Removal of Cr(VI) from synthetic wastewater. *Journal of Hazardous Materials* 181(1–3): 405-412.

Riazi, M., Keshtkar, A. and Moosavian, M., 2014. Batch and continuous fixed-bed column biosorption of thorium(IV) from aqueous solutions: equilibrium and dynamic modeling. *Journal of Radioanalytical and Nuclear Chemistry*: 1-11.

Rout, P. R., Dash, R. R. and Bhunia, P., 2014. Modelling and packed bed column studies on adsorptive removal of phosphate from aqueous solutions by a mixture of ground burnt patties and red soil. *Advances in Environmental Research* 3(3): 231-251.

Runtti, H., Tuomikoski, S., Kangas, T., Lassi, U., Kuokkanen, T. and Rämö, J., 2014. Chemically activated carbon residue from biomass gasification as a sorbent for iron(II), copper(II) and nickel(II) ions. *Journal of Water Process Engineering* 4: 12-24.

Saadat, S. and Karimi-Jashni, A., 2011. Optimization of Pb(II) adsorption onto modified walnut shells using factorial design and simplex methodologies. *Chemical Engineering Journal* 173(3): 743-749.

Salamatinia, B., Kamaruddin, A. H. and Abdullah, A. Z., 2008. Modeling of the continuous copper and zinc removal by sorption onto sodium hydroxide-modified oil palm frond in a fixed-bed column. *Chemical Engineering Journal* 145(2): 259-266.

Samsuri, A. W., Sadegh-Zadeh, F. and Seh-Bardan, B. J., 2013. Adsorption of As(III) and As(V) by Fe coated biochars and biochars produced from empty fruit bunch and rice husk. *Journal of Environmental Chemical Engineering* 1(4): 981-988.

Sankararamakrishnan, N., Jaiswal, M. and Verma, N., 2014. Composite nanofloral clusters of carbon nanotubes and activated alumina: An efficient sorbent for heavy metal removal. *Chemical Engineering Journal* 235: 1-9.

Seid, L., Chouder, D., Maouche, N., Bakas, I. and Barka, N., 2014. Removal of Cd(II) and Co(II) ions from aqueous solutions by polypyrrole particles: Kinetics, equilibrium and thermodynamics. *Journal of the Taiwan Institute of Chemical Engineers* 45(6): 2969-2974.

Selvaraj, K., Manonmani, S. and Pattabhi, S., 2003. Removal of hexavalent chromium using distillery sludge. *Bioresource Technology* 89(2): 207-211.

Senthil Kumar, P., SathyaSelvaBala, V., Ramakrishnan, K., Vijayalakshmi, P. and Sivanesan, S., 2010. Kinetics and adsorption equilibrium in the system aqueous solution of copper ions—granulated activated carbon. *Russian Chemical Bulletin* 59(10): 1859-1864.

Senthil Kumar, P., Ramalingam, S., Sathyaselvabala, V., Kirupha, S. D. and Sivanesan, S., 2011. Removal of copper(II) ions from aqueous solution by adsorption using cashew nut shell. *Desalination* 266(1–3): 63-71.

Shah, B. A., Mistry, C. B. and Shah, A. V., 2013. Sequestration of Cu(II) and Ni(II) from wastewater by synthesized zeolitic materials: Equilibrium, kinetics and column dynamics. *Chemical Engineering Journal* 220: 172-184.

Sharma, A. and Bhattacharyya, K. G., 2005. Azadirachta indica (Neem) leaf powder as a biosorbent for removal of Cd(II) from aqueous medium. *Journal of Hazardous Materials* 125(1–3): 102-112.

Sharma, D. C. and Forster, C. F., 1994. A preliminary examination into the adsorption of hexavalent chromium using low-cost adsorbents. *Bioresource Technology* 47(3): 257-264.

Sharma, D. C. and Forster, C. F., 1996. A comparison of the sorbtive characteristics of leaf mould and activated carbon columns for the removal of hexavalent chromium. *Process Biochemistry* 31(3): 213-218.

Sheela, T., Nayaka, Y. A., Viswanatha, R., Basavanna, S. and Venkatesha, T. G., 2012. Kinetics and thermodynamics studies on the adsorption of Zn(II), Cd(II) and Hg(II) from aqueous solution using zinc oxide nanoparticles. *Powder Technology* 217: 163-170.

Sheikhhosseini, A., Shirvani, M. and Shariatmadari, H., 2013. Competitive sorption of nickel, cadmium, zinc and copper on palygorskite and sepiolite silicate clay minerals. *Geoderma* 192: 249-253.

Sheikholeslami, R. and Bright, J., 2002. Silica and metals removal by pretreatment to prevent fouling of reverse osmosis membranes. *Desalination* 143(3): 255-267.

Shen, J., Zhu, S., Liu, X., Zhang, H. and Tan, J., 2010. The prediction of elemental composition of biomass based on proximate analysis. *Energy Conversion and Management* 51(5): 983-987.

Shukla, S. R. and Pai, R. S., 2005. Adsorption of Cu(II), Ni(II) and Zn(II) on dye loaded groundnut shells and sawdust. *Separation and Purification Technology* 43(1): 1-8.

Sikder, M. T., Mihara, Y., Islam, M. S., Saito, T., Tanaka, S. and Kurasaki, M., 2014. Preparation and characterization of chitosan–caboxymethyl-β-cyclodextrin entrapped nanozero-valent iron composite for Cu (II) and Cr (IV) removal from wastewater. *Chemical Engineering Journal* 236: 378-387.

Sousa, F. W., Oliveira, A. G., Ribeiro, J. P., Rosa, M. F., Keukeleire, D. and Nascimento, R. F., 2010. Green coconut shells applied as adsorbent for removal of toxic metal ions using fixed-bed column technology. *Journal of Environmental Management* 91(8): 1634-1640.

Srivastava, R. and Rupainwar, D. C., 2011. A comparative evaluation for adsorption of dye on Neem bark and Mango bark powder. *Indian Journal of Chemical Technology* 18(1): 67-75.

Storn, R. and Price, K., 1997. Differential Evolution – A Simple and Efficient Heuristic for global Optimization over Continuous Spaces. *Journal of Global Optimization* 11(4): 341-359.

Sugashini, S. and Begum, K. M. M. S., 2013. Performance of ozone treated rice husk carbon (OTRHC) for continuous adsorption of Cr (VI) ions from synthetic effluent. *Journal of Environmental Chemical Engineering* 1(1–2): 79-85.

Suksabye, P. and Thiravetyan, P., 2012. Cr(VI) adsorption from electroplating plating wastewater by chemically modified coir pith. *Journal of Environmental Management* 102: 1-8.

Suksabye, P., Thiravetyan, P. and Nakbanpote, W., 2008. Column study of chromium(VI) adsorption from electroplating industry by coconut coir pith. *Journal of Hazardous Materials* 160(1): 56-62.

Suksabye, P., Thiravetyan, P., Nakbanpote, W. and Chayabutra, S., 2007. Chromium removal from electroplating wastewater by coir pith. *Journal of Hazardous Materials* 141(3): 637-644.

Suopajärvi, T., Liimatainen, H., Karjalainen, M., Upola, H. and Niinimäki, J., 2014. Lead adsorption with sulfonated wheat pulp nanocelluloses. *Journal of Water Process Engineering*.

Taha, M. R. and Ibrahim, A. H., 2014. Characterization of nano zero-valent iron (nZVI) and its application in sono-Fenton process to remove COD in palm oil mill effluent. *Journal of Environmental Chemical Engineering* 2(1): 1-8.

Tan, G., Yuan, H., Liu, Y. and Xiao, D., 2010. Removal of lead from aqueous solution with native and chemically modified corncobs. *Journal of Hazardous Materials* 174(1–3): 740-745.

Tan, W. T., Ooi, S. T. and Lee, C. K., 1993. Removal of chromium(VI) from solution by coconut husk and palm pressed fibres. *Environmental Technology* 14(3): 277-282.

Tempkin, M. I. and Pyzhev, V., 1940. Kinetics of ammonia synthesis on promoted iron catalyst. *Acta Physico Chimica USSR* 12: 327–356.

Terdkiatburana, T., Wang, S. and Tade, M. O., 2009. Adsorption of heavy metal ions by natural and synthesised zeolites for wastewater treatment. *International Journal of Environment and Waste Management* 3(3): 327-335.

Thippeswamy, B., Shivakumar, C. K. and Krishnappa, M., 2012. Accumulation potency of heavy metals by saccharomyces sp. Indigenous to paper mill effluent. *Journal of Environmental Research And Development* 6(3): 439-445.

Üçer, A., Uyanik, A. and Aygün, Ş. F., 2006. Adsorption of Cu(II), Cd(II), Zn(II), Mn(II) and Fe(III) ions by tannic acid immobilised activated carbon. *Separation and Purification Technology* 47(3): 113-118.

Ujang, Z. and Anderson, G. K., 1996. Application of low-pressure reverse osmosis membrane for Zn2+ and Cu2+ removal from wastewater. *Water Science and Technology* 34(9): 247-253.

USEPA. (2009). "National Primary Drinking Water Regulations." Retrieved 10 September, 2013, from http://water.epa.gov/drink/contaminants/.

Vázquez, G., Calvo, M., Sonia Freire, M., González-Alvarez, J. and Antorrena, G., 2009. Chestnut shell as heavy metal adsorbent: Optimization study of lead, copper and zinc cations removal. *Journal of Hazardous Materials* 172(2–3): 1402-1414.

Villaescusa, I., Fiol, N., Martínez, M. a., Miralles, N., Poch, J. and Serarols, J., 2004. Removal of copper and nickel ions from aqueous solutions by grape stalks wastes. *Water Research* 38(4): 992-1002.

Vukčević, M., Pejić, B., Kalijadis, A., Pajić-Lijaković, I., Kostić, M., Laušević, Z. and Laušević, M., 2014. Carbon materials from waste short hemp fibers as a sorbent for heavy metal ions – Mathematical modeling of sorbent structure and ions transport. *Chemical Engineering Journal* 235: 284-292.

Walkowiak, W. and Kozlowski, C. A., 2009. Macrocycle carriers for separation of metal ions in liquid membrane processes—a review. *Desalination* 240(1–3): 186-197.

Wan Ngah, W. S. and Hanafiah, M. A. K. M., 2008. Removal of heavy metal ions from wastewater by chemically modified plant wastes as adsorbents: A review. *Bioresource Technology* 99(10): 3935-3948.

Wang, J., Ding, L., Wei, J. and Liu, F., 2014a. Adsorption of copper ions by ion-imprinted simultaneous interpenetrating network hydrogel: Thermodynamics, morphology and mechanism. *Applied Surface Science* 305: 412-418.

Wang, X., Sun, R. and Wang, C., 2014b. pH dependence and thermodynamics of Hg(II) adsorption onto chitosan-poly(vinyl alcohol) hydrogel adsorbent. *Colloids and Surfaces A: Physicochemical and Engineering Aspects* 441: 51-58.

Wang, X. S., Chen, L. F., Li, F. Y., Chen, K. L., Wan, W. Y. and Tang, Y. J., 2010. Removal of Cr (VI) with wheat-residue derived black carbon: Reaction mechanism and adsorption performance. *Journal of Hazardous Materials* 175(1–3): 816-822.

Wang, X. S. and Li, Z. Z., 2009. Removal of Cr (VI) from aqueous solution by newspapers. *Desalination* 249(1): 175-181.

Wang, Y.-H., Lin, S.-H. and Juang, R.-S., 2003. Removal of heavy metal ions from aqueous solutions using various low-cost adsorbents. *Journal of Hazardous Materials* 102(2–3): 291-302.

Wasewar, K. L., 2010. Adsorption Of Metals Onto Tea Factory Waste: A Review. *International Journal of Research and Reviews in Applied Sciences* 3(3).

Weber, W. J. J. and Morris, J. C., 1963. Kinetics of adsorption on carbon from solution. *Journal of the Sanitary Engineering Division* 89(2): 31-60.

Wen, Y., Ma, J., Chen, J., Shen, C., Li, H. and Liu, W., 2015. Carbonaceous sulfur-containing chitosan–Fe(III): A novel adsorbent for efficient removal of copper (II) from water. *Chemical Engineering Journal* 259: 372-380.

WHO, 2008. Chapter 12 - Chemical fact sheets. Guidelines for drinking-water quality - Volume 1: Recommendations, World Health Organization**:** 296-460.

Xu, P., Zeng, G. M., Huang, D. L., Feng, C. L., Hu, S., Zhao, M. H., Lai, C., Wei, Z., Huang, C., Xie, G. X. and Liu, Z. F., 2012. Use of iron oxide nanomaterials in wastewater treatment: A review. *Science of The Total Environment* 424: 1-10.

Yan, G., Viraraghavan, T. and Chen, M., 2001. A New Model for Heavy Metal Removal in a Biosorption Column. *Adsorption Science & Technology* 19(1): 25-43.

Yavuz, O., Altunkaynak, Y. and Guzel, F., 2003. Removal of copper, nickel, cobalt and manganese from aqueous solution by kaolinite. *Water Res* 37(4): 948-952.

Yoon, Y. H. and Nelson, J. H., 1984. Application of Gas Adsorption Kinetics I. A Theoretical Model for Respirator Cartridge Service Life. *American Industrial Hygiene Association Journal* 45(8): 509-516.

Yu, L. J., Shukla, S. S., Dorris, K. L., Shukla, A. and Margrave, J. L., 2003. Adsorption of chromium from aqueous solutions by maple sawdust. *Journal of Hazardous Materials* 100(1–3): 53-63.

Zeldowitsch, J., 1934. Uber den mechanismus der katalytischen oxidation von CO an MnO2. *Acta Physicochim. URSS* 1: 364-449.

Zeng, G., Liu, Y., Tang, L., Yang, G., Pang, Y., Zhang, Y., Zhou, Y., Li, Z., Li, M., Lai, M., He, X. and He, Y., 2015. Enhancement of Cd(II) adsorption by polyacrylic acid modified magnetic mesoporous carbon. *Chemical Engineering Journal* 259: 153-160.

Zhao, X.-T., Zeng, T., Li, X.-Y., Hu, Z. J., Gao, H.-W. and Xie, Z., 2012. Modeling and mechanism of the adsorption of copper ion onto natural bamboo sawdust. *Carbohydrate Polymers* 89(1): 185-192.

Zhong, Q.-Q., Yue, Q.-Y., Li, Q., Gao, B.-Y. and Xu, X., 2014. Removal of Cu(II) and Cr(VI) from wastewater by an amphoteric sorbent based on cellulose-rich biomass. *Carbohydrate Polymers* 111: 788-796.

Zhou, Y., Fu, S., Zhang, L., Zhan, H. and Levit, M. V., 2014. Use of carboxylated cellulose nanofibrils-filled magnetic chitosan hydrogel beads as adsorbents for Pb(II). *Carbohydrate Polymers* 101: 75-82.

LIST OF PUBLICATIONS

International Journals

1. **Maheshwari, U.** and Gupta, S., 2015. Removal of Cr(VI) from Wastewater Using a Natural Nanoporous Adsorbent: Experimental, Kinetic and Optimization Studies. *Adsorption Science & Technology* 33(1): 71-88.
2. **Maheshwari, U.** and Gupta, S., 2015. Removal of Cr(VI) from wastewater using activated neem bark in a fixed-bed column: interference of other ions and kinetic modelling studies. *Desalination and Water Treatment*.
3. **Maheshwari, U.** and Gupta, S., 2015. A novel method to identify optimized parametric values for adsorption of heavy metals from waste water. *Journal of Water Process Engineering*.
4. Gangadhar, G., **Maheshwari, U.** and Gupta, S., 2012. Application of Nanomaterials for the Removal of Pollutants from Effluent Streams. *Nanoscience & Nanotechnology-Asia* 2: 140-150.
5. **Maheshwari, U.** and Gupta, S., 2011. Kinetic and Equilibrium Studies of Cr(VI) Removal from Aqueous Solutions using Activated Neem Bark. *Research Journal of Chemistry and Environment* 15(2): 939-943.
6. **Maheshwari, U.**, Mathesan, B. and Gupta, S., Efficient Adsorbent for simultaneous removal of Cu(II), Zn(II) and Cr(VI): Kinetic, Thermodynamics and Mass Transfer Mechanism". (*Communicated*)
7. **Maheshwari, U.**, Kuhar, K. and Gupta, S., "Removal of multiple metal ions (Cd(II), Cr(VI), Cu(II), Ni(II), Pb(II) and Zn(II)) using Developed Activated Neem Barks at Different Activation Conditions: Batch and Continuous Experiments". (C*ommunicated*)
8. **Maheshwari, U.** and Gupta, S., Column studies for the removal of Cu(II) and Zn(II) using Activated Neem Bark as a low cost adsorbent. (*To be communicated*)

International Conference Proceedings

1. **Maheshwari, U.** and Gupta, S., 2015. Activated Neem Bark as a Potential Low-Cost adsorbent for the Removal of Cr(VI), Cu(II) and Zn(II) from Wastewater. International Conference on Biotechnology, Nanotechnology and Environmental Engineering (ICBNE'15), Bangkok, Thailand, International Academy of Arts, Science & Technology (IAAST), April 22 - 23, 2015, 43 - 45.
2. **Maheshwari, U.**, Kuhar, K. and Gupta, S., 2014. Equilibrium studies for the removal of Cr(VI), Cu(II) and Zn(II) Using activated neem bark. 67th Annual Session of IIChE (CHEMCON-2014) and Indo-Japanese Symposium, Chandigarh, India, December 27-30, 2014.
3. Gupta, S. and **Maheshwari, U.**, 2014. Copper (II) Removal Using Activated Neem Bark from Waste Water As a Low Cost Adsorbent: Column Studies. AIChE Annual Meeting, Atlanta, USA, AIChE, November 16-21, 2014, 346.
4. **Maheshwari, U.** and Gupta, S., 2013. Column studies for Chromium(VI) removal using Activated Neem Bark as a low cost adsorbent. 66th Annual Session of IIChE in association with International Partners (CHEMCON-2013) and Joint Indo-North American Symposium, Mumbai, India, December 27-30, 2013, 272.
5. Arun, **Maheshwari, U.** and Gupta, S., 2013. Removal of Zn(II) from Aqueous Solutions using Activated Neem Bark as an Adsorbent: Equilibrium Studies. 66th Annual Session of IIChE in association with International Partners (CHEMCON-2013) and Joint Indo-North American Symposium, Mumbai, India, December 27-30, 2013, 28.
6. **Maheshwari, U.**, Mathesan, B. and Gupta, S., 2013. Kinetic studies for the removal of copper from industrial wastewater using activated neem (Azadirachta indica) bark. 2013 AIChE Annual Meeting, San Francisco, CA, USA, AIChE, November 3 – 8, 2013, 276.
7. **Maheshwari, U.** and Gupta, S., 2012. Equilibrium studies for the removal of Copper (II) using Activated Neem Bark as a low cost adsorbent. 65th Annual Session of IIChE in association with International Partners (CHEMCON-2012) an

International Conference on Sustainable Technologies for Energy and Environment in Process Industries and Indo-US Joint International Conference on Energy and Environment, Jalandhar, India, December 27-30, 2012.

8. **Maheshwari, U.** and Gupta, S., 2011. Batch Studies for the Removal of Zinc from Aqueous Solution using Chemically Activated Neem Bark. International Symposium & 64th Annual Session of IIChE in association with International Partners (CHEMCON-2011), Bangalore, India, December 27-29, 2011.
9. **Maheshwari, U.** and Gupta, S., 2011. Kinetic and Equilibrium Studies of Cr (VI) Removal from Aqueous Solutions using Activated Neem Bark. 5th International Congress of Chemistry and Environment (ICCE-2011), Port Dickson, Negeri Senbilan, Malaysia, May 27-29, 2011.
10. **Maheshwari, U.** and Gupta, S., 2010. Kinetics and Equilibrium Studies of Chromium (VI) Removal from Aqueous Solutions using Neem Bark as a Low Cost Adsorbent. International Symposium & 63rd Annual Session of IIChE in association with International Partners (CHEMCON-2010), Chidambaram, Tamil Nadu, India, December 27-29, 2010.

BIOGRAPHIES

Biography of the Candidate

Utkarsh Maheshwari has completed his B. Tech. degree in Petrochemical Engineering from Zakir Hussain College of Engineering and Technology, Aligarh Muslim University in 2007. Later he had secured his M.E. degree in Chemical Engineering from Birla Institute of Technology and Science (BITS) Pilani in 2009. After his Masters degree, he had joined Department of Chemical Engineering, BITS Pilani, Pilani campus as Assistant Lecturer in October, 2009 and presently working as Lecturer in the department since November, 2009. He has 5+ years of teaching and research experience. He has taught various courses at undergraduate and graduate levels. He has also guided 3 B.E. thesis students and supervised more than 90 projects at various undergraduate and graduate levels. He has 6 journal publications and 54 national and international conference publications. He has successfully completed a UGC sponsored minor research project as the principal investigator. He is a member of several national and international professional associations. He presently also holds a post of "Honorary Regional Treasurer" for Pilani Regional Center, Indian Institute of Chemical Engineers from September, 2014. His biography is included in "Asian American Who's Who", vol. 7 in 2015. His research interest includes Separation Processes, Petrochemical Technology, Reservoir Engineering, Modeling, Simulation and Optimization.

Biography of the Supervisor

Prof. Suresh Gupta is Associate Professor and Head, Department of Chemical Engineering, Birla Institute of Technology and Science (BITS), Pilani, Pilani Campus. He had acquired his Ph.D. from BITS, Pilani in 2008. Prior to which he had completed his B.E. in Chemical Engineering from Government Engineering College, Ujjain and M. Tech. in Chemical Engineering from IIT Kanpur. He has an experience of 12+ years in teaching, research and consultancy. He has guided 10 ME Dissertation students, several BE Thesis and project students. He is presently supervising/co-supervising 6 Ph.D. and 4

ME dissertations. He has successfully completed research projects sponsored by UGC, MHRD and Birla Cellulosic, Kharach. He is currently having research projects sponsored from UGC, DST and BITS, Pilani. His research interests are Environmental Engineering & Separation Processes, Mathematical Modeling and Simulation of Chemical Processes, Computational Transport Phenomena, Environmental Management Systems (LCA, EIA) and Energy Integration. He has been a part of various academic and administrative committees at BITS, Pilani. He is the member of Senate, BITS Pilani.

He is recipient of travel grants from CSIR and INSA-CICS to attend international conferences in 2008 and 2013. He has also attended a day long workshop to critique the existing scheme of the Engineering Services Examination conducted by the Commission organized by UPSC at the International Management Development Centre (IMDC) Indian Institute of Management, Vastrapur, Ahmedabad on the 3rd of October, 2013 as an Invited Member. He has also been the reviewer for 16 journals of international repute. He is also having 25 Journal, 53 Conference and 7 Books/Book chapter publications. He has attended 18 workshops and conferences in India and abroad. He also acted as the Joint Organizing Secretary for the Student's Chemical Engineering Congress (SCHEMCON – 2012) organized by BITS, Pilani during September 21 - 22, 2012. He also acted as the Chairperson of Workshop on Analytical Instruments for Chemical and Environmental Engineers (WAICEE) organized by Department of Chemical Engineering, BITS Pilani in 2013 and 2015. He has also been the International Conference Committee member of the ICCBES -2013 at Taipei, Taiwan and ICCBES -2015 at Kyoto, Japan.

He is a member of several national and international professional associations such as American Institute of Chemical Engineers (AIChE), Life Member of Indian Institute of Chemical Engineers (IIChE), Fellow of International Congress of Chemistry and Environment (FICCE), Member of International Association of Engineers (IAENG) and Member of the Institute of Engineers (India) (IEI). He is also holding the post of Vice-Chairman of Pilani Regional Centre of Indian Institute of Chemical Engineers (IIChE). He had also delivered expert lectures on "Design of Experiments" in the Workshop on Analytical Instruments for Chemical and Environmental Engineers (WAICEE) at BITS, Pilani and "Computational Heat Transport" and "Separation Processes", Staff

Development Programme on Innovative Teaching Techniques for Transport Phenomena organized by ITM University, Gwalior. He has also delivered a lecture on "Bioremediation: Heavy Metals Removal from Wastewater" as an invited distinguished speaker in the Short Term Course on Water Pollution and Wastewater Treatment (WPWT – 2015) organized by Department of Chemical Engineering & Civil Engineering, MNNIT, Allahabad. He is also an Eternal Academic Expert Members in Board of Studies (BoS) Constitution for Chemical Engineering at Galgotia University, Noida. He is also Member of the Board of Studies of Faculty of Bio- and Chemical Engineering, at Sathyabama University, Jeppiaar Nagar, Chennai. He has been the external examiner for BTech (Chemical Engg.) students at Banasthali University and MTech Viva at ITM University Gwalior.

APPENDIX I

Raw Data for the batch and continuous experiments conducted in the present research work.

Table A1.1: Calibration curve for the determination of Cr(VI) using Atomic Absorption Spectrophotometer (AAS).

S.No.	Absorbance	Concentration (mg L^{-1})
1	0	0
2	0.1348	1
3	0.2492	2
4	0.3722	3
5	0.5016	4
6	0.6205	5
7	0.7533	6
8	0.8754	7
9	0.9995	8

Table A1.2: Calibration curve for the determination of Cu(II) using AAS.

S.No.	Absorbance	Concentration (mg L^{-1})
1	0	0
2	0.1268	0.5
3	0.2513	1
4	0.3721	1.5
5	0.4987	2
6	0.6292	2.5
7	0.7553	3
8	0.8768	3.5
9	0.9989	4

Table A1.3: Calibration curve for the determination of Zn(II) using AAS.

S.No.	Absorbance	Concentration (mg L^{-1})
1	0	0
3	0.0911	0.1
4	0.1823	0.2
5	0.3649	0.4
6	0.5469	0.6
7	0.7271	0.8
8	0.9092	1
9	1.0027	1.1

Table A1.4: Calibration curve for the determination of Cd(II) using AAS.

S.No.	Absorbance	Concentration (mg L^{-1})
1	0	0
2	0.0833	0.1
3	0.1676	0.2
4	0.3339	0.4
5	0.5011	0.6
6	0.6671	0.8
7	0.8322	1
8	0.9165	1.1
9	1.0012	1.2

Table A1.5: Calibration curve for the determination of Ni(II) using AAS.

S.No.	Absorbance	Concentration (mg L^{-1})
1	0	0
2	0.1232	1
3	0.2501	2
4	0.3715	3
5	0.5026	4
6	0.6221	5
7	0.7564	6
8	0.8752	7
9	1.0005	8

Table A1.6: Calibration curve for the determination of Pb(II) using AAS.

S.No.	Absorbance	Concentration (mg L^{-1})
1	0	0
2	0.1012	1
3	0.2007	2
4	0.2998	3
5	0.4012	4
6	0.5007	5
7	0.5986	6
8	0.7017	7
9	0.8066	8
10	0.9011	9
11	0.9979	10

Table A1.7: Effect of initial concentration on the removal of Cr(VI) using ANB1 (T=35°C, t_t = 48 h, pH=2.2 and M = 6 g L^{-1}) (10 times diluted).

S.No.	Initial Concentration (C_0) (mg L^{-1})	Absorbance	Final Concentration (C_e) (mg L^{-1})
1	60	0.0435	3.480
2	65	0.05	3.999
3	70	0.0563	4.503
4	80	0.0708	5.663
5	85	0.0813	6.503
6	90	0.0875	6.999
7	100	0.1034	8.271
8	105	0.1375	10.998
9	110	0.1625	12.998
10	120	0.1875	14.998
11	130	0.2501	20.005
12	140	0.3125	24.997
13	150	0.3576	28.604
14	160	0.4376	35.003
15	170	0.5001	40.002
16	180	0.5626	45.002
17	190	0.6251	50.001
18	200	0.6724	53.785

Table A1.8: Effect of initial concentration on the removal of Cr(VI) using ANB2 (T=35°C, t_t = 48 h, pH=2.2 and M = 6 g L^{-1}) (15 times diluted).

S.No.	Initial Concentration (C_0) (mg L^{-1})	Absorbance	Final Concentration (C_e) (mg L^{-1})
1	5	0.0044	0.528
2	20	0.0212	2.544
3	40	0.0605	7.259
4	60	0.1163	13.954
5	80	0.2252	27.020
6	100	0.318	38.155
7	120	0.437	52.433
8	140	0.5584	66.999
9	170	0.7454	89.436
10	200	0.9021	108.237

Table A1.9: Effect of initial concentration on the removal of Cr(VI) using ANB3 (T=35°C, t_t = 48 h, pH=2.2 and M = 6 g L^{-1}) (20 times diluted).

S.No.	Initial Concentration (C_0) (mg L^{-1})	Absorbance	Final Concentration (C_e) (mg L^{-1})
1	5	0.0047	0.752
2	20	0.0193	3.088
3	40	0.051	8.159
4	60	0.151	24.157
5	80	0.2415	38.635
6	100	0.3483	55.720
7	120	0.4612	73.782
8	140	0.5581	89.284
9	170	0.7242	115.856
10	200	0.8783	140.509

Table A1.10: Effect of initial concentration on the removal of Cr(VI) using ANB4 (T=35°C, t_t = 48 h, pH=2.2 and M = 6 g L^{-1}) (20 times diluted).

S.No.	Initial Concentration (C_0) (mg L^{-1})	Absorbance	Final Concentration (C_e) (mg L^{-1})
1	5	0.0085	1.360
2	20	0.0367	5.871
3	40	0.0765	12.238
4	60	0.1316	21.053
5	80	0.1905	30.476
6	100	0.2752	44.026
7	120	0.3674	58.776
8	140	0.4468	71.478
9	170	0.5715	91.427
10	200	0.7217	115.456

Table A1.11: Effect of initial concentration on the removal of Cr(VI) using ANB5 (T=35°C, t_t = 48 h, pH=2.2 and M = 6 g L^{-1}) (20 times diluted).

S.No.	Initial Concentration (C_0) (mg L^{-1})	Absorbance	Final Concentration (C_e) (mg L^{-1})
1	5	0.0094	1.503
2	20	0.0407	6.509
3	40	0.083	13.273
4	60	0.1357	21.701
5	80	0.1933	30.912
6	100	0.2523	40.347
7	120	0.3194	51.077
8	140	0.4075	65.166
9	170	0.5346	85.491
10	200	0.6611	105.720

Table A1.12: Effect of initial concentration on the removal of Cr(VI) using ANB6 (T=35°C, t_t = 48 h, pH=2.2 and M = 6 g L^{-1}) (20 times diluted).

S.No.	Initial Concentration (C_0) (mg L^{-1})	Absorbance	Final Concentration (C_e) (mg L^{-1})
1	5	0.0101	1.616
2	20	0.0417	6.671
3	40	0.0937	14.990
4	60	0.1473	23.565
5	80	0.2109	33.739
6	100	0.2705	43.274
7	120	0.3479	55.656
8	140	0.4153	66.439
9	170	0.5157	82.501
10	200	0.6396	102.322

Table A1.13: Effect of initial concentration on the removal of Cu(II) using ANB1 (T=35°C, t_t = 48 h, pH=2.2 and M = 6 g L^{-1}) (30 times diluted).

S.No.	Initial Concentration (C_0) (mg L^{-1})	Absorbance	Final Concentration (C_e) (mg L^{-1})
1	60	0.1317	15.775
2	80	0.1852	22.183
3	100	0.2324	27.836
4	120	0.2965	35.514
5	140	0.379	45.396
6	150	0.4442	53.205
7	160	0.5352	64.105
8	170	0.5844	69.998
9	180	0.6727	80.575
10	185	0.7096	84.994
11	190	0.7514	90.001
12	195	0.7764	92.996
13	200	0.8249	98.805

Table A1.14: Effect of initial concentration on the removal of Cu(II) using ANB2 (T=35°C, t_t = 48 h, pH=2.2 and M = 6 g L^{-1}) (30 times diluted).

S.No.	Initial Concentration (C_0) (mg L^{-1})	Absorbance	Final Concentration (C_e) (mg L^{-1})
1	5	0.0043	0.515
2	20	0.0177	2.120
3	40	0.0613	7.342
4	60	0.0975	11.678
5	80	0.1643	19.680
6	100	0.2389	28.615
7	120	0.3492	41.826
8	140	0.4293	51.421
9	170	0.5014	60.057
10	200	0.6789	81.317

Table A1.15: Effect of initial concentration on the removal of Cu(II) using ANB3 (T=35°C, t_t = 48 h, pH=2.2 and M = 6 g L^{-1}) (30 times diluted).

S.No.	Initial Concentration (C_0) (mg L^{-1})	Absorbance	Final Concentration (C_e) (mg L^{-1})
1	5	0.0084	1.006
2	20	0.0378	4.528
3	40	0.0867	10.385
4	60	0.1526	18.278
5	80	0.2229	26.699
6	100	0.2965	35.514
7	120	0.3766	45.108
8	140	0.449	53.780
9	170	0.5888	70.525
10	200	0.7133	85.438

Table A1.16: Effect of initial concentration on the removal of Cu(II) using ANB4 (T=35°C, t_t = 48 h, pH=2.2 and M = 6 g L^{-1}) (30 times diluted).

S.No.	Initial Concentration (C_0) (mg L^{-1})	Absorbance	Final Concentration (C_e) (mg L^{-1})
1	5	0.0101	1.210
2	20	0.0503	6.025
3	40	0.1101	13.188
4	60	0.1777	21.285
5	80	0.2479	29.693
6	100	0.3633	43.515
7	120	0.4601	55.110
8	140	0.5826	69.783
9	170	0.7724	92.517
10	200	0.9725	116.484

Table A1.17: Effect of initial concentration on the removal of Cu(II) using ANB5 (T=35°C, t_t = 48 h, pH=2.2 and M = 6 g L^{-1}) (30 times diluted).

S.No.	Initial Concentration (C_0) (mg L^{-1})	Absorbance	Final Concentration (C_e) (mg L^{-1})
1	5	0.0101	1.209758
2	20	0.0512	6.132634
3	40	0.105	12.57669
4	60	0.1611	19.29624
5	80	0.2312	27.69267
6	100	0.2965	35.51418
7	120	0.3766	45.10839
8	140	0.4824	57.78091
9	170	0.714	85.52149
10	200	0.8802	105.4286

Table A1.18: Effect of initial concentration on the removal of Cu(II) using ANB6 (T=35°C, t_t = 48 h, pH=2.2 and M = 6 g L^{-1}) (30 times diluted).

S.No.	Initial Concentration (C_0) (mg L^{-1})	Absorbance	Final Concentration (C_e) (mg L^{-1})
1	5	0.0044	0.527
2	20	0.0178	2.132
3	40	0.0366	4.384
4	60	0.136	16.290
5	80	0.2479	29.693
6	100	0.2798	33.514
7	120	0.3766	45.108
8	140	0.4824	57.781
9	170	0.6305	75.520
10	200	0.7133	85.438

Table A1.19: Effect of initial concentration on the removal of Zn(II) using ANB1 (T=35°C, t_t = 48 h, pH=2.2 and M = 6 g L^{-1}) (150 times diluted).

S.No.	Initial Concentration (C_0) (mg L^{-1})	Absorbance	Final Concentration (C_e) (mg L^{-1})
1	60	0.132	21.748
2	70	0.1715	28.256
3	80	0.2147	35.374
4	100	0.3188	52.525
5	120	0.4078	67.189
6	140	0.5291	87.175
7	160	0.6151	101.344
8	180	0.7257	119.566
9	200	0.8314	136.981

Table A1.20: Effect of initial concentration on the removal of Zn(II) using ANB2 (T=35°C, t_t = 48 h, pH=2.2 and M = 6 g L^{-1}) (100 times diluted).

S.No.	Initial Concentration (C_0) (mg L^{-1})	Absorbance	Final Concentration (C_e) (mg L^{-1})
1	5	0.0032	0.527
2	20	0.035	5.767
3	40	0.0696	11.467
4	60	0.112	18.453
5	80	0.1611	26.543
6	100	0.2234	36.807
7	120	0.2994	49.329
8	140	0.3852	63.466
9	170	0.5388	88.773
10	200	0.6669	109.878

Table A1.21: Effect of initial concentration on the removal of Zn(II) using ANB3 (T=35°C, t_t = 48 h, pH=2.2 and M = 6 g L^{-1}) (150 times diluted).

S.No.	Initial Concentration (C_0) (mg L^{-1})	Absorbance	Final Concentration (C_e) (mg L^{-1})
1	5	0.0136	2.241
2	20	0.0688	11.335
3	40	0.1395	22.984
4	60	0.2328	38.356
5	80	0.3074	50.647
6	100	0.3784	62.345
7	120	0.4539	74.785
8	140	0.5355	88.229
9	170	0.6266	103.239
10	200	0.7668	126.338

Table A1.22: Effect of initial concentration on the removal of Zn(II) using ANB4 (T=35°C, t_t = 48 h, pH=2.2 and M = 6 g L^{-1}) (150 times diluted).

S.No.	Initial Concentration (C_0) (mg L^{-1})	Absorbance	Final Concentration (C_e) (mg L^{-1})
1	5	0.014	2.307
2	20	0.0634	10.446
3	40	0.1372	22.605
4	60	0.2191	36.099
5	80	0.3024	49.823
6	100	0.3959	65.228
7	120	0.4922	81.095
8	140	0.5935	97.785
9	170	0.7547	124.344
10	200	0.9204	151.645

Table A1.23: Effect of initial concentration on the removal of Zn(II) using ANB5 (T=35°C, t_t = 48 h, pH=2.2 and M = 6 g L^{-1}) (150 times diluted).

S.No.	Initial Concentration (C_0) (mg L^{-1})	Absorbance	Final Concentration (C_e) (mg L^{-1})
1	5	0.0084	1.384
2	20	0.0519	8.551
3	40	0.1138	18.750
4	60	0.1576	25.966
5	80	0.2069	34.089
6	100	0.2536	41.783
7	120	0.3411	56.200
8	140	0.3964	65.311
9	170	0.4868	80.205
10	200	0.633	104.293

Table A1.24: Effect of initial concentration on the removal of Zn(II) using ANB6 (T=35°C, t_t = 48 h, pH=2.2 and M = 6 g L^{-1}) (150 times diluted).

S.No.	Initial Concentration (C_0) (mg L^{-1})	Absorbance	Final Concentration (C_e) (mg L^{-1})
1	5	0.0066	1.087
2	20	0.0487	8.024
3	40	0.0861	14.186
4	60	0.1306	21.518
5	80	0.1755	28.915
6	100	0.2208	36.379
7	120	0.3005	49.510
8	140	0.3781	62.296
9	170	0.5066	83.467
10	200	0.6391	105.298

Table A1.25: Effect of initial concentration on the removal of Cd(II) using nANB (T=35°C, t_t = 48 h, pH=2.2 and M = 6 g L^{-1}) (150 times diluted).

S.No.	Initial Concentration (C_0) (mg L^{-1})	Absorbance	Final Concentration (C_e) (mg L^{-1})
1	60	0.1433	25.783
2	70	0.1671	30.065
3	80	0.1976	35.553
4	100	0.2612	46.996
5	120	0.3356	60.383
6	140	0.416	74.849
7	160	0.4996	89.891
8	180	0.5819	104.698
9	200	0.6638	119.434

Table A1.26: Effect of initial concentration on the removal of Ni(II) using nANB (T=35°C, t_t = 48 h, pH=2.2 and M = 6 g L^{-1}) (10 times diluted).

S.No.	Initial Concentration (C_0) (mg L^{-1})	Absorbance	Final Concentration (C_e) (mg L^{-1})
1	60	0.1351	10.796
2	70	0.1535	12.266
3	80	0.1812	14.480
4	100	0.2563	20.481
5	120	0.3714	29.679
6	140	0.5088	40.659
7	160	0.6327	50.560
8	180	0.7302	58.352
9	200	0.8299	66.319

Table A1.27: Effect of initial concentration on the removal of Pb(II) using nANB (T=35°C, t_t = 48 h, pH=2.2 and M = 6 g L^{-1}) (20 times diluted).

S.No.	Initial Concentration (C_0) (mg L^{-1})	Absorbance	Final Concentration (C_e) (mg L^{-1})
1	60	0.2003	40.00191
2	70	0.2341	46.75211
3	80	0.2666	53.24269
4	100	0.3367	67.24236
5	120	0.4093	81.7413
6	140	0.4832	96.49987
7	160	0.5646	112.7563
8	180	0.6497	129.7516
9	200	0.7486	149.503

Table A 1.28: Effect of contact time on the removal of Cr(VI) using nANB (T=35°C, C_0 = 100 mg L^{-1}, pH=2.2 and M = 6 g L^{-1}) (15 times diluted).

S.No.	Time (h)	Absorbance	Final Concentration (C_e) (mg L^{-1})
1	0.0	0.8334	100.000
2	0.5	0.7425	89.088
3	1.5	0.6805	81.649
4	3.5	0.6378	76.525
5	7.5	0.4753	57.028
6	12.5	0.416	49.913
7	19.0	0.3292	39.499
8	25.0	0.31668	37.996
9	32.0	0.2989	35.863
10	39.5	0.2893	34.711
11	48.0	0.2493	29.912

Table A 1.29: Effect of contact time on the removal of Cu(II) using nANB (T=35°C, C_0 = 100 mg L^{-1}, pH=2.2 and M = 6 g L^{-1}) (30 times diluted).

S.No.	Time (h)	Absorbance	Final Concentration (C_e) (mg L^{-1})
1	0	0.8349	100
2	0.5	0.6674	79.940
3	1.5	0.6541	78.347
4	3.5	0.6391	76.550
5	7.5	0.6188	74.119
6	12.5	0.5992	71.771
7	19	0.5881	70.441
8	22	0.5761	69.004
9	25	0.5659	67.782
10	28	0.551	65.998
11	32	0.5436	65.111
12	35	0.5419	64.908
13	39.5	0.5401	64.692
14	41	0.5399	64.668
15	45	0.5389	64.548
16	48	0.5388	64.536

Table A 1.30: Effect of contact time on the removal of Zn(II) using nANB (T=35°C, C_0 = 100 mg L^{-1}, pH=2.2 and M = 6 g L^{-1}) (100 times diluted).

S.No.	Time (h)	Absorbance	Final Concentration (C_e) (mg L^{-1})
1	0	0.9104	100
2	0.5	0.8784	96.483
3	1.5	0.8304	91.211
4	3.5	0.7568	83.127
5	7.5	0.6482	71.198
6	12.5	0.5869	64.465
7	19	0.5014	55.074
8	25	0.4506	49.494
9	32	0.4246	46.638
10	39.5	0.4129	45.353
11	48	0.4108	45.122

Table A 1.31: Effect of adsorbent dosage on the removal of Cr(VI) using nANB (T=35°C, C_0 = 100 mg L^{-1}, pH=2.2 and t_t = 48 h) (15 times diluted).

S.No.	Mass of adsorbent M (g $L^{-1)}$	Absorbance	Final Concentration (C_e) (mg L^{-1})
1	0	0.8334	100
2	4	0.4822	57.856
3	8	0.2066	24.789
4	12	0.1791	21.489
5	16	0.1722	20.661
6	20	0.1584	19.005
7	24	0.1515	18.178
8	28	0.1378	16.534
9	32	0.1213	14.554
10	36	0.1066	12.790
11	40	0.0919	11.026

Table A 1.32 Effect of adsorbent dosage on the removal of Cu(II) using nANB (T=35°C, C_0 = 100 mg L^{-1}, pH=2.2 and t_t = 48 h) (30 times diluted).

S.No.	Mass of adsorbent M (g $L^{-1)}$	Absorbance	Final Concentration (C_e) (mg L^{-1})
1	0	0.8349	100.000
2	4	0.6343	75.975
3	8	0.5821	69.723
4	12	0.5305	63.542
5	16	0.5034	60.296
6	20	0.4652	55.721
7	24	0.4604	55.146
8	28	0.4529	54.247
9	32	0.4439	53.169
10	36	0.4377	52.427
11	40	0.4339	51.972

Table A 1.33: Effect of adsorbent dosage on the removal of Zn(II) using nANB (T=35°C, C_0 = 100 mg L^{-1}, pH=2.2 and t_t = 48 h) (100 times diluted).

S.No.	Mass of adsorbent M (g $L^{-1)}$	Absorbance	Final Concentration (C_e) (mg L^{-1})
1	0	0.9104	100
2	4	0.7032	77.239
3	8	0.6821	74.922
4	12	0.6515	71.561
5	16	0.6003	65.937
6	20	0.5102	56.040
7	24	0.4924	54.085
8	28	0.4337	47.638
9	32	0.3866	42.464
10	36	0.3417	37.532
11	40	0.3254	35.742

Table A 1.34: Effect of pH on the removal of Cr(VI) using nANB (T=35°C, C_0 = 100 mg L^{-1}, M = 6 g L^{-1} and t_t = 48 h) (15 times diluted).

S.No.	pH	Absorbance	Final Concentration (C_e) (mg L^{-1})	Final Solution pH
1	2.16	0.0204	2.448	4.62
2	4.038	0.2057	24.681	5.39
3	6.135	0.3264	39.163	6.28
4	7.762	0.3847	46.158	7.14
5	9.983	0.5334	63.999	7.39
6	11.789	0.7839	94.055	8.01

Table A 1.35: Effect of pH on the removal of Cu(II) using nANB (T=35°C, C_0 = 100 mg L^{-1}, M = 6 g L^{-1} and t_t = 48 h) (30 times diluted).

S.No.	pH	Absorbance	Final Concentration (C_e) (mg L^{-1})	Final Solution pH
1	2.04	0.042	5.031	1.41
2	3.05	0.1773	21.237	2.37
3	5.09	0.3188	38.185	3.89
4	6.89	0.4764	57.062	4.96
5	8.99	0.5332	63.866	6.38
6	11.04	0.5868	70.286	8.32
7	12.05	0.7283	87.234	9.36

Table A 1.36: Effect of pH on the removal of Zn(II) using nANB (T=35°C, C_0 = 100 mg L^{-1}, M=6 g L^{-1} and t_t = 48 h) (100 times diluted).

S.No.	pH	Absorbance	Final Concentration (C_e) (mg L^{-1})	Final Solution pH
1	1.16	0.3648	40.070	0.96
2	2.77	0.4623	50.779	2.48
3	5.28	0.571	62.719	3.16
4	6.96	0.6858	75.328	3.46
5	9.2	0.7592	83.391	4.61
6	10.72	0.8185	89.904	5.35
7	12.29	0.8532	93.715	9.39

Table A 1.37: Effect of temperature on the removal of Cr(VI) using nANB (C_0 = 100 mg L^{-1}, pH=2.2, M= 6 g L^{-1} and t_t = 48 h) (15 times diluted).

S.No.	Initial Concentration (C_0) (mg L^{-1})	@T = 50°C		@T = 60°C	
		Absorbance	Final Concentration (C_e) (mg L^{-1})	Absorbance	Final Concentration (C_e) (mg L^{-1})
1	60	0.1131	13.570	0.1308	15.694
2	80	0.2287	27.440	0.2592	31.100
3	100	0.3441	41.286	0.3944	47.321
4	120	0.4905	58.852	0.5196	62.343
5	140	0.5692	68.295	0.6616	79.381
6	160	0.7138	85.644	0.8074	96.875
7	180	0.8465	101.566	0.9405	112.844
8	200	0.9887	118.628	1.0812	129.726

Table A 1.38: Effect of temperature on the removal of Cu(II) using nANB (C_0 = 100 mg L^{-1}, pH=2.2, M= 6 g L^{-1} and t_t = 48 h) (30 times diluted).

S.No.	Initial Concentration (C_0) (mg L^{-1})	@T = 50°C		@T = 60°C	
		Absorbance	Final Concentration (C_e) (mg L^{-1})	Absorbance	Final Concentration (C_e) (mg L^{-1})
1	60	0.2977	35.658	0.273	32.699
2	70	0.3736	44.749	0.3348	40.102
3	80	0.4267	51.109	0.419	50.187
4	100	0.5689	68.142	0.5289	63.351
5	120	0.6868	82.264	0.7062	84.587
6	140	0.8198	98.194	0.833	99.775
7	160	0.9387	112.436	0.9655	115.646
8	180	1.0738	128.618	1.1156	133.624
9	200	1.2091	144.824	1.3042	156.214

Table A 1.39: Effect of temperature on the removal of Zn(II) using nANB (C_0 = 100 mg L^{-1}, pH=2.2, M= 6 g L^{-1} and t_t = 48 h) (150 times diluted).

S.No.	Initial Concentration (C_0) (mg L^{-1})	@T = 50°C		@T = 60°C	
		Absorbance	Final Concentration (C_e) (mg L^{-1})	Absorbance	Final Concentration (C_e) (mg L^{-1})
1	60	0.2072	34.138	0.1537	25.324
2	70	0.2976	49.033	0.2425	39.954
3	80	0.3455	56.925	0.3014	49.659
4	100	0.4458	73.450	0.3605	59.396
5	120	0.5164	85.082	0.4425	72.906
6	140	0.6116	100.767	0.556	91.607
7	160	0.7562	124.592	0.6606	108.840
8	180	0.8363	137.789	0.8475	139.634
9	200	0.9851	162.305	0.986	162.453

Table A 1.40: Effect of flowrate on the continuous removal of Cr(VI) using nANB (M=75g, C_0 = 50 mg L^{-1}) (7 times diluted).

S.No.	Time (h)	Q=5 ml min^{-1}		Q=15ml min^{-1}	
		Absorbance	Final Concentration (C_e) (mg L^{-1})	Absorbance	Final Concentration (C_e) (mg L^{-1})
1	0.25	0.0000	0.000	0.0000	0.000
2	0.75	0.0000	0.000	0.0000	0.000
3	1.5	0.0000	0.000	0.0000	0.000
4	2.25	0.0000	0.000	0.0001	0.005
5	3	0.0000	0.000	0.0001	0.005
6	4.25	0.0000	0.000	0.0003	0.015
7	5.75	0.0000	0.000	0.0004	0.025
8	7.75	0.0000	0.000	0.0012	0.065
9	10.75	0.0001	0.005	0.0048	0.270
10	17	0.0002	0.010	0.0079	0.445
11	24	0.0004	0.020	0.0112	0.625
12	32	0.0007	0.040	0.1391	7.790
13	41	0.0038	0.215	0.4986	27.920
14	50	0.0281	1.575	0.7281	40.770
15	62	0.1290	7.225	0.8234	46.105
16	74	0.3407	19.075	0.8595	48.125
17	86	0.5579	31.240	0.8791	49.225
18	98	0.7336	41.075	0.8861	49.615
19	110	0.8056	45.105	0.8918	49.935
20	122	0.8327	46.625	0.8927	49.985
21	134	0.8484	47.505		
22	150	0.8649	48.425		
23	162	0.8773	49.120		
24	174	0.8797	49.255		
25	198	0.8831	49.445		
26	222	0.8922	49.955		

Table A 1.41: Effect of flowrate on the continuous removal of Cu(II) using nANB (M=75g, C_0 = 50 mg L^{-1}) (15 times diluted).

S.No.	Time (h)	Q=5 ml min^{-1}		Q=15 ml min^{-1}	
		Absorbance	Final Concentration (C_e) (mg L^{-1})	Absorbance	Final Concentration (C_e) (mg L^{-1})
1	0.25	0	0	0	0
2	0.75	0	0	0	0
3	1.5	0	0	0.0001	0.005
4	2.25	0.0001	0.005	0.0004	0.025
5	3	0.0001	0.005	0.0008	0.045
6	4.25	0.0003	0.015	0.0015	0.090
7	5.75	0.0007	0.040	0.0023	0.140
8	7.75	0.0013	0.075	0.0057	0.340
9	10.75	0.0027	0.160	0.0104	0.625
10	17	0.0048	0.290	0.0249	1.490
11	24	0.0077	0.460	0.0906	5.425
12	32	0.0168	1.005	0.2886	17.285
13	41	0.0382	2.290	0.6416	38.425
14	50	0.1190	7.125	0.7203	43.140
15	62	0.3221	19.290	0.7813	46.790
16	74	0.5195	31.110	0.8108	48.560
17	86	0.6557	39.270	0.8228	49.275
18	98	0.7252	43.430	0.8268	49.515
19	110	0.7693	46.070	0.8303	49.725
20	122	0.7908	47.360	0.8342	49.960
21	134	0.8022	48.040		
22	150	0.8172	48.940		
23	162	0.8224	49.250		
24	174	0.8256	49.445		
25	198	0.8286	49.625		
26	222	0.8334	49.910		

Table A 1.42: Effect of flowrate on the continuous removal of Zn(II) using nANB (M=75g, C_0 = 50 mg L^{-1}) (50 times diluted).

S.No.	Time (h)	Q=5 ml min^{-1}		Q=15 ml min^{-1}	
		Absorbance	Final Concentration (C_e) (mg L^{-1})	Absorbance	Final Concentration (C_e) (mg L^{-1})
1	0.25	0.0000	0.000	0.0001	0.005
2	0.75	0.0000	0.000	0.0002	0.010
3	1.5	0.0001	0.005	0.0005	0.030
4	2.25	0.0003	0.015	0.0008	0.045
5	3	0.0005	0.025	0.0014	0.075
6	4.25	0.0006	0.035	0.0020	0.110
7	5.75	0.0016	0.090	0.0032	0.175
8	7.75	0.0023	0.125	0.0051	0.280
9	10.75	0.0060	0.330	0.0093	0.510
10	17	0.0100	0.550	0.0250	1.375
11	24	0.0302	1.660	0.0686	3.770
12	32	0.0899	4.940	0.2381	13.075
13	41	0.2321	12.745	0.5721	31.420
14	50	0.4107	22.555	0.7671	42.130
15	62	0.6422	35.270	0.8399	46.130
16	74	0.7467	41.010	0.8692	47.735
17	86	0.8072	44.330	0.8905	48.905
18	98	0.8514	46.760	0.9008	49.470
19	110	0.8709	47.830	0.9064	49.780
20	122	0.8963	49.225	0.9096	49.955
21	134	0.9024	49.560		
22	150	0.9098	49.965		

Table A 1.43: Effect of mass of adsorbent for the continuous removal of Cr(VI) using nANB (Q=10 ml min^{-1}, C_0 = 50 mg L^{-1}) (7 times diluted).

S.No.	Time (h)	*M*=25 g		*M*=50 g		*M*=100 g		*M*=125 g		*M*=150 g		*M*=175 g	
		Absor-bance	Final Concentration (C_e) (mg L^{-1})	Absor-bance	Final Concentration (C_e) (mg L^{-1})	Absor-bance	Final Concentration (C_e) (mg L^{-1})	Absor-bance	Final Concentration (C_e) (mg L^{-1})	Absor-bance	Final Concentration (C_e) (mg L^{-1})	Absor-bance	Final Concentration (C_e) (mg L^{-1})
1	0.25	0	0	0	0	0	0	0	0	0	0	0	0
2	0.75	0.0001	0.005	0.0001	0.005	0	0	0	0	0	0	0	0
3	1.5	0.0001	0.005	0.0001	0.005	0	0	0	0	0	0	0	0
4	2.25	0.0002	0.010	0.0001	0.005	0	0	0	0	0	0	0	0
5	3	0.0004	0.020	0.0001	0.005	0	0	0	0	0	0	0	0
6	4.25	0.0005	0.030	0.0002	0.010	0	0	0	0	0	0	0	0
7	5.75	0.0008	0.045	0.0004	0.020	0	0	0	0	0	0	0	0
8	7.75	0.0016	0.090	0.0005	0.030	0	0	0	0	0	0	0	0
9	10.75	0.0196	1.100	0.0008	0.045	0	0	0	0	0	0	0	0
10	17	0.0940	5.265	0.0096	0.540	0.0001	0.005	0	0	0	0	0	0
11	24	0.3834	21.470	0.0316	1.770	0.0002	0.010	0	0	0	0	0	0
12	32	0.6479	36.275	0.1925	10.780	0.0004	0.025	0.0001	0.005	0	0	0	0
13	41	0.7781	43.570	0.4899	27.428	0.0006	0.035	0.0002	0.010	0	0	0	0
14	50	0.8248	46.180	0.7106	39.790	0.0008	0.045	0.0004	0.025	0	0	0	0
15	62					0.0500	2.802	0.0001	0.004	0.0001	0.005	0	0
16	74	0.8741	48.945	0.8293	46.435	0.2547	14.260	0.0013	0.075	0.0003	0.015	0.0001	0.005
17	86					0.5219	29.225	0.0362	2.025	0.0007	0.040	0.0002	0.010
18	98	0.8840	49.495	0.8741	48.945	0.7012	39.260	0.1840	10.305	0.0011	0.060	0.0004	0.025
19	110							0.4699	26.310	0.0380	2.125	0.0010	0.055
20	122	0.8854	49.575	0.8849	49.550	0.8184	45.825	0.6847	38.340	0.1539	8.620	0.0068	0.383
21	134									0.4096	22.935	0.0468	2.620
22	150	0.8872	49.675	0.8871	49.670	0.8502	47.605	0.7969	44.621	0.6504	36.420	0.2204	12.340
23	162											0.4657	26.075

S.No.	Time (h)	*M*=25 g		*M*=50 g		*M*=100 g		*M*=125 g		*M*=150 g		*M*=175 g	
		Absor-bance	Final Concentration (C_e) (mg L^{-1})	Absor-bance	Final Concentration (C_e) (mg L^{-1})	Absor-bance	Final Concentration (C_e) (mg L^{-1})	Absor-bance	Final Concentration (C_e) (mg L^{-1})	Absor-bance	Final Concentration (C_e) (mg L^{-1})	Absor-bance	Final Concentration (C_e) (mg L^{-1})
24	174	0.8909	49.885	0.8910	49.890	0.8693	48.675	0.8442	47.270	0.7906	44.270	0.6452	36.125
25	198	0.8920	49.945	0.8922	49.955	0.8835	49.470	0.8705	48.740	0.8413	47.105	0.7738	43.325
26	222					0.8859	49.605	0.8829	49.435	0.8710	48.770	0.8229	46.075
27	246					0.8892	49.790	0.8859	49.605	0.8817	49.370	0.8452	47.325
28	270							0.8923	49.960	0.8889	49.770	0.8681	48.605
29	294									0.8905	49.860	0.8859	49.605
30	318											0.8916	49.920

Table A 1.44: Effect of mass of adsorbent for the continuous removal of Cu(II) using nANB (Q=10 ml min^{-1}, C_0 = 50 mg L^{-1}) (15 times diluted).

S.No.	Time (h)	M=25 g		M=50 g		M=100 g		M=125 g		M=150 g		M=175 g	
		Absor-bance	Final Concentration (C_e) (mg L^{-1})	Absor-bance	Final Concentration (C_e) (mg L^{-1})	Absor-bance	Final Concentration (C_e) (mg L^{-1})	Absor-bance	Final Concentration (C_e) (mg L^{-1})	Absor-bance	Final Concentration (C_e) (mg L^{-1})	Absor-bance	Final Concentration (C_e) (mg L^{-1})
1	0.25	0	0	0	0	0	0	0	0	0	0	0	0
2	0.75	0.0001	0.005	0.0001	0.005	0	0	0	0	0	0	0	0
3	1.5	0.0004	0.025	0.0003	0.015	0	0	0	0	0	0	0	0
4	2.25	0.0010	0.060	0.0007	0.040	0.0001	0.005	0	0	0	0	0	0
5	3	0.0027	0.160	0.0013	0.075	0.0001	0.005	0	0	0	0	0	0
6	4.25	0.0063	0.375	0.0023	0.140	0.0003	0.020	0.0001	0.005	0	0	0	0
7	5.75	0.0131	0.785	0.0047	0.280	0.0008	0.045	0.0001	0.005	0	0	0	0
8	7.75	0.0382	2.290	0.0077	0.460	0.0015	0.090	0.0004	0.025	0.000	0.005	0	0
9	10.75	0.0711	4.260	0.0132	0.790	0.0032	0.190	0.0008	0.045	0.000	0.005	0	0
10	17	0.2127	12.740	0.0523	3.135	0.0068	0.410	0.0013	0.075	0.001	0.045	0.0001	0.005
11	24	0.3636	21.775	0.1323	7.925	0.0173	1.035	0.0027	0.160	0.002	0.090	0.0007	0.040
12	32	0.6024	36.075	0.3380	20.240	0.0338	2.025	0.0072	0.430	0.004	0.230	0.0014	0.085
13	41	0.7228	43.290	0.5555	33.270	0.0607	3.635	0.0104	0.625	0.007	0.420	0.0032	0.190
14	50	0.7729	46.290	0.6847	41.005	0.1079	6.460	0.0215	1.290	0.012	0.690	0.0060	0.360
15	62					0.3026	18.125	0.0607	3.635	0.027	1.640	0.0104	0.625
16	74	0.8183	49.005	0.7896	47.290	0.5247	31.425	0.1276	7.640	0.052	3.125	0.0207	1.240
17	86					0.6641	39.770	0.2992	17.920	0.105	6.270	0.0486	2.910
18	98	0.8253	49.425	0.8202	49.120	0.7386	44.235	0.4532	27.140	0.197	11.785	0.0921	5.515
19	110							0.6056	36.270	0.390	23.375	0.1977	11.840
20	122	0.8288	49.635	0.8285	49.620	0.7814	46.795	0.6884	41.225	0.559	33.470	0.3912	23.430
21	134									0.622	37.245	0.5195	31.115
22	150	0.8311	49.775	0.8322	49.840	0.7982	47.805	0.7726	46.270	0.687	41.130	0.6249	37.425
23	162											0.6695	40.095
24	174	0.8334	49.910	0.8338	49.935	0.8169	48.925	0.7974	47.755	0.750	44.935	0.7086	42.435

S.No.	Time (h)	*M*=25 g		*M*=50 g		*M*=100 g		*M*=125 g		*M*=150 g		*M*=175 g	
		Absor-bance	Final Concentration (C_e) (mg L^{-1})	Absor-bance	Final Concentration (C_e) (mg L^{-1})	Absor-bance	Final Concentration (C_e) (mg L^{-1})	Absor-bance	Final Concentration (C_e) (mg L^{-1})	Absor-bance	Final Concentration (C_e) (mg L^{-1})	Absor-bance	Final Concentration (C_e) (mg L^{-1})
25	198	0.8343	49.965	0.8345	49.975	0.8244	49.375	0.8173	48.945	0.790	47.335	0.7484	44.820
26	222					0.8266	49.505	0.8227	49.270	0.809	48.445	0.7741	46.360
27	246					0.8327	49.870	0.8279	49.585	0.818	48.995	0.7971	47.740
28	270							0.8338	49.935	0.827	49.505	0.8151	48.815
29	294									0.834	49.960	0.8245	49.380
30	318											0.8313	49.785

Table A 1.45: Effect of mass of adsorbent for the continuous removal of Zn(II) using nANB (Q=10 ml min^{-1}, C_0 = 50 mg L^{-1}) (50 times diluted).

S.No.	Time (h)	*M*=25 g		*M*=50 g		*M*=100 g		*M*=125 g		*M*=150 g		*M*=175 g	
		Absor-bance	Final Concentration (C_e) (mg L^{-1})	Absor-bance	Final Concentration (C_e) (mg L^{-1})	Absor-bance	Final Concentration (C_e) (mg L^{-1})	Absor-bance	Final Concentration (C_e) (mg L^{-1})	Absor-bance	Final Concentration (C_e) (mg L^{-1})	Absor-bance	Final Concentration (C_e) (mg L^{-1})
1	0.25	0	0	0	0	0	0	0	0	0	0	0	0
2	0.75	0.0002	0.010	0.0002	0.010	0	0	0	0	0	0	0	0
3	1.5	0.0006	0.035	0.0005	0.025	0.0001	0.005	0	0	0	0	0	0
4	2.25	0.0015	0.085	0.0011	0.060	0.0001	0.005	0.0001	0.005	0	0	0	0
5	3	0.0047	0.260	0.0023	0.125	0.0002	0.010	0.0001	0.005	0	0	0	0
6	4.25	0.0093	0.510	0.0049	0.270	0.0006	0.035	0.0004	0.020	0.0001	0.005	0	0
7	5.75	0.0232	1.275	0.0114	0.625	0.0012	0.065	0.0007	0.040	0.0001	0.005	0.0001	0.005
8	7.75	0.0614	3.370	0.0171	0.940	0.0024	0.130	0.0011	0.060	0.0004	0.020	0.0002	0.010
9	10.75	0.1506	8.270	0.0407	2.235	0.0044	0.240	0.0025	0.135	0.0007	0.040	0.0036	0.200
10	17	0.3630	19.935	0.1409	7.740	0.0084	0.460	0.0047	0.260	0.0012	0.065	0.0008	0.045
11	24	0.5543	30.440	0.2963	16.275	0.0187	1.025	0.0120	0.660	0.0025	0.140	0.0011	0.060
12	32	0.7986	43.860	0.5686	31.225	0.0559	3.070	0.0192	1.055	0.0066	0.360	0.0051	0.280
13	41	0.8617	47.325	0.7945	43.635	0.1299	7.135	0.0503	2.760	0.0115	0.630	0.0070	0.385
14	50	0.8910	48.935	0.8507	46.720	0.2628	14.435	0.0913	5.015	0.0222	1.220	0.0111	0.610
15	62	0.9039	49.640	0.8789	48.270	0.5392	29.615	0.2741	15.055	0.0475	2.610	0.0275	1.510
16	74	0.9061	49.765	0.8942	49.110	0.7073	38.845	0.4904	26.935	0.1117	6.135	0.0678	3.725
17	86	0.9094	49.945	0.9020	49.540	0.8061	44.270	0.6395	35.120	0.2368	13.005	0.1232	6.765
18	98	0.9103	49.995	0.9064	49.780	0.8406	46.165	0.7342	40.320	0.4344	23.855	0.2428	13.335
19	110	0.9104	50.000	0.9087	49.905	0.8623	47.355	0.8010	43.990	0.6171	33.890	0.4329	23.775
20	122	0.9104	50.000	0.9097	49.960	0.8820	48.440	0.8404	46.155	0.7288	40.025	0.6211	34.110
21	134			0.9103	49.995	0.8905	48.905	0.8611	47.290	0.7808	42.880	0.6975	38.305
22	150					0.8939	49.095	0.8784	48.240	0.8284	45.495	0.7666	42.100
23	162					0.9032	49.605	0.8901	48.885	0.8501	46.690	0.7950	43.660
24	174					0.9079	49.860	0.8941	49.105	0.8700	47.780	0.8261	45.370

S.No.	Time (h)	*M*=25 g		*M*=50 g		*M*=100 g		*M*=125 g		*M*=150 g		*M*=175 g	
		Absor-bance	Final Concentration (C_e) (mg L^{-1})	Absor-bance	Final Concentration (C_e) (mg L^{-1})	Absor-bance	Final Concentration (C_e) (mg L^{-1})	Absor-bance	Final Concentration (C_e) (mg L^{-1})	Absor-bance	Final Concentration (C_e) (mg L^{-1})	Absor-bance	Final Concentration (C_e) (mg L^{-1})
25	198					0.9097	49.960	0.8990	49.375	0.8931	49.050	0.8600	47.230
26	222					0.9103	49.995	0.9033	49.610	0.8973	49.280	0.8832	48.505
27	246							0.9067	49.795	0.9015	49.510	0.8915	48.960
28	270							0.9088	49.910	0.9089	49.915	0.9012	49.495
29	294							0.9103	49.995	0.9096	49.955	0.9087	49.905
30	318											0.9103	49.995

Table A 1.46: Effect of inlet concentration on the continuous removal of Cr(VI) using nANB (M=75g, Q = 10 ml min^{-1}) (15 times diluted).

S.No.	Time (h)	C_0 = 50 mg L^{-1}		C_0 = 100 mg L^{-1}	
		Absorbance	Final Concentration (C_e) (mg L^{-1})	Absorbance	Final Concentration (C_e) (mg L^{-1})
1	0.25	0	0	0.0000	0.000
2	0.75	0	0	0.0000	0.000
3	1.5	0	0	0.0000	0.000
4	2.25	0	0	0.0001	0.010
5	3	0.0000	0.005	0.0001	0.010
6	4.25	0.0000	0.005	0.0002	0.020
7	5.75	0.0000	0.005	0.0002	0.020
8	7.75	0.0000	0.005	0.0003	0.040
9	10.75	0.0001	0.010	0.0006	0.070
10	17	0.0002	0.020	0.0011	0.130
11	24	0.0005	0.065	0.0132	1.580
12	32	0.0035	0.425	0.0798	9.580
13	41	0.0129	1.550	0.4368	52.410
14	50	0.1081	12.975	0.6772	81.250
15	62	0.2651	31.810	0.7628	91.520
16	74	0.3436	41.225	0.7963	95.540
17	98	0.3973	47.670	0.8185	98.210
18	122	0.4061	48.730	0.8278	99.320
19	150	0.4120	49.435	0.8332	99.970
20	174	0.4131	49.560		
21	198	0.4163	49.945		

Table A 1.47: Effect of inlet concentration on the continuous removal of Cu(II) using nANB (M=75g, Q = 10 ml min^{-1}) (30 times diluted).

S.No.	Time (h)	C_0 = 50 mg L^{-1}		C_0 = 100 mg L^{-1}	
		Absorbance	Final Concentration (C_e) (mg L^{-1})	Absorbance	Final Concentration (C_e) (mg L^{-1})
1	0.25	0	0	0	0
2	0.75	0	0	0.000	0.01
3	1.5	0.0000	0.005	0.000	0.03
4	2.25	0.0001	0.010	0.001	0.08
5	3	0.0001	0.010	0.001	0.12
6	4.25	0.0002	0.025	0.002	0.28
7	5.75	0.0005	0.060	0.005	0.58
8	7.75	0.0010	0.125	0.007	0.85
9	10.75	0.0022	0.260	0.010	1.25
10	17	0.0052	0.620	0.021	2.56
11	24	0.0131	1.565	0.104	12.48
12	32	0.0411	4.925	0.315	37.75
13	41	0.1357	16.255	0.572	68.51
14	50	0.2670	31.975	0.714	85.48
15	62	0.3491	41.810	0.769	92.15
16	74	0.3859	46.225	0.806	96.52
17	98	0.4084	48.920	0.824	98.66
18	122	0.4113	49.270	0.828	99.22
19	150	0.4132	49.495	0.834	99.87
20	174	0.4146	49.660		
21	198	0.4165	49.890		

Table A 1.48: Effect of inlet concentration on the continuous removal of Zn(II) using nANB (M=75g, Q = 10 ml min^{-1}) (100 times diluted).

S.No.	Time (h)	C_0 = 50 mg L^{-1}		C_0 = 100 mg L^{-1}	
		Absorbance	Final Concentration (C_e) (mg L^{-1})	Absorbance	Final Concentration (C_e) (mg L^{-1})
1	0.25	0	0	0	0
2	0.75	0.0000	0.005	0.0002	0.02
3	1.5	0.0001	0.015	0.0005	0.05
4	2.25	0.0002	0.025	0.0008	0.09
5	3	0.0003	0.035	0.0014	0.15
6	4.25	0.0005	0.060	0.0020	0.22
7	5.75	0.0011	0.125	0.0049	0.54
8	7.75	0.0017	0.190	0.0061	0.67
9	10.75	0.0040	0.435	0.0102	1.12
10	17	0.0061	0.675	0.0183	2.01
11	24	0.0236	2.590	0.0748	8.22
12	32	0.0740	8.130	0.2108	23.15
13	41	0.1951	21.425	0.5543	60.88
14	50	0.3148	34.575	0.7859	86.32
15	62	0.3742	41.105	0.8435	92.65
16	74	0.4152	45.610	0.8697	95.53
17	86	0.4350	47.775	0.8908	97.84
18	98	0.4500	49.425	0.8997	98.82
19	110	0.4512	49.560	0.9024	99.12
20	122	0.4552	49.995	0.9102	99.98

Table A 1.49: Effect of the presence of multiple metal ions (Cu(II) &Zn(II)) on the removal of Cr(VI) using nANB (M=75g, Q = 10 ml min^{-1} and C_0 for each = 50 g L^{-1}).

S.No.	Time (h)	Cr(VI) (7 times diluted)		Cu(II) (15 times diluted)		Zn(II) (50 times diluted)	
		Absor-bance	Final Concentration (C_e) (mg L^{-1})	Absor-bance	Final Concentration (C_e) (mg L^{-1})	Absor-bance	Final Concentration (C_e) (mg L^{-1})
1	0.25	0	0	0	0	0	0
2	0.75	0	0	0.0001	0.005	0.0001	0.005
3	1.5	0.0001	0.005	0.0003	0.015	0.0006	0.035
4	2.25	0.0003	0.015	0.0006	0.035	0.0011	0.060
5	3	0.0004	0.025	0.0010	0.060	0.0023	0.125
6	4.25	0.0007	0.040	0.0020	0.120	0.0043	0.235
7	5.75	0.0010	0.055	0.0042	0.250	0.0066	0.360
8	7.75	0.0013	0.075	0.0073	0.435	0.0113	0.620
9	10.75	0.0022	0.125	0.0124	0.745	0.0218	1.195
10	17	0.0068	0.380	0.0492	2.945	0.0402	2.210
11	24	0.0043	0.240	0.1190	7.125	0.0800	4.395
12	32	0.0502	2.810	0.3235	19.375	0.1862	10.225
13	41	0.2302	12.890	0.5214	31.225	0.5051	27.740
14	50	0.5764	32.270	0.6636	39.740	0.7307	40.130
15	62	0.6988	39.125	0.7470	44.740	0.8216	45.125
16	74	0.7980	44.680	0.7837	46.935	0.8650	47.505
17	98	0.8595	48.125	0.8180	48.990	0.8964	49.230
18	122	0.8699	48.705	0.8202	49.120	0.9008	49.470
19	150	0.8838	49.485	0.8263	49.485	0.9045	49.675
20	174	0.8843	49.510	0.8278	49.575	0.9086	49.900
21	198	0.8867	49.645	0.8334	49.910	0.9103	49.995

Table A1.50: Utilization of nANB on the removal of aqueous pulp and paper industrial effluent. (M=75g, Q = 10 ml min^{-1} and C_0 as in Table 3.5).

S.No.	Time (h)	Cr(VI) (8 times diluted)		Cu(II) (3 times diluted)		Zn(II) (3 times diluted)		Cd(II) (2 times diluted)		Pb(II) (No dilution)		Ni(II) (No dilution)	
		Absor-bance	Final Concentration (C_e) (mg L^{-1})	Absor-bance	Final Concentration (C_e) (mg L^{-1})	Absor-bance	Final Concentration (C_e) (mg L^{-1})	Absor-bance	Final Concentration (C_e) (mg L^{-1})	Absor-bance	Final Concentration (C_e) (mg L^{-1})	Absor-bance	Final Concentration (C_e) (mg L^{-1})
1	0.5	0	0	0	0.000	0.0002	0.001	0	0	0	0	0	0
2	1	0.0001	0.006	0.0001	0.001	0.0004	0.001	0	0	0	0	0.0000	0.000
3	1.5	0.0001	0.006	0.0001	0.001	0.0013	0.004	0.0001	0.000	0	0	0.0002	0.001
4	2	0.0002	0.012	0.0002	0.002	0.0023	0.008	0.0002	0.000	0	0	0.0003	0.003
5	2.5	0.0004	0.024	0.0005	0.004	0.0040	0.013	0.0005	0.001	0	0	0.0006	0.005
6	3	0.0006	0.035	0.0008	0.006	0.0056	0.019	0.0009	0.002	0.0000	0.000	0.0008	0.006
7	3.5	0.0008	0.053	0.0012	0.009	0.0136	0.045	0.0014	0.003	0.0001	0.001	0.0012	0.010
8	5	0.0011	0.071	0.0019	0.015	0.0430	0.142	0.0025	0.006	0.0001	0.001	0.0054	0.043
9	7	0.0014	0.089	0.0027	0.022	0.0656	0.216	0.0049	0.012	0.0002	0.002	0.0155	0.124
10	9.5	0.0016	0.100	0.0034	0.027	0.0802	0.264	0.0095	0.023	0.0003	0.003	0.0412	0.329
11	12.5	0.0026	0.165	0.0047	0.038	0.1361	0.448	0.0749	0.180	0.0004	0.004	0.1109	0.886
12	16.5	0.0045	0.289	0.0060	0.048	0.2741	0.903	0.2631	0.631	0.0006	0.006	0.2588	2.068
13	21.5	0.0443	2.833	0.0097	0.077	0.3944	1.300	0.3753	0.900	0.0011	0.011	0.3696	2.954
14	29.5	0.1408	9.012	0.0626	0.499	0.5499	1.812	0.5147	1.235	0.0059	0.059	0.4038	3.227
15	41.5	0.2713	17.364	0.2828	2.258	0.6912	2.278	0.5609	1.346	0.0443	0.442	0.4172	3.334
16	55.5	0.5799	37.106	0.5077	4.054	0.8139	2.682	0.5750	1.379	0.0845	0.844	0.4251	3.397
17	71.5	0.8252	52.805	0.8184	6.535	0.8347	2.751	0.5929	1.422	0.1229	1.228	0.4323	3.455
18	89.5	0.8692	55.620	0.8939	7.138	0.8666	2.856	0.5965	1.431	0.1364	1.362	0.4362	3.485
19	109.5	0.8898	56.942	0.9154	7.309	0.8717	2.872	0.5998	1.439	0.1426	1.424	0.4364	3.488
20	133.5	0.9108	58.282	0.9547	7.624	0.8793	2.897	0.6001	1.440	0.1488	1.486	0.4367	3.490

APPENDIX II

%**Code in Matlab for optimization of the model using Rosenbrock function (**Buehren 2012)

```
function val = rosenbrocksaddle(scale, params)
%ROSENBROCKSADDLE  Standard optimization function for demonstration.
%               VALUE = ROSENBROCKSADDLE(SCALE, PAR) returns the value of Rosenbrock's
%               saddle at (PAR.parameter1, PAR.parameters2) scaled with input parameter
%               SCALE. The absolute minimum of the function is at (1, 1).
%
%               Markus Buehren
%               Last modified 03.02.2008

x1 = params.parameter1(1);
x2 = params.parameter2(1);
x3 = params.parameter3(1);
x4 = params.parameter4(1);
y = params.parameter5(1);

z = (y - (1.6031 - 6.7863*x1 - 11.9281*x2 + 1.7652*x3 + 6.8039*x4 + 17.0896*x1.^2 + 34.8511*x2.^2 - 2.803*x3.^2 - 25.4028*x4.^2 - 15.4701*x1.^3 - 41.1095*x2.^3 + 1.3957*x3.^3 + 32.6020*x4.^3 + 4.8622*x1.^4 + 16.3088*x2.^4 + 0.1264*x3.^4 - 13.8564*x4.^4));

val = scale*(z);
pause(0.001);
```

%Code considered for calling the function (Buehren 2012)

```
function demo1
%DEMO1  Demo for usage of DIFFERENTIALEVOLUTION.
%               DEMO1 starts searching the minimum of Rosenbrock's saddle as a demo.
%               Modify this function for your first optimization.

optimInfo.title = 'Demo 1 (Rosenbrock"s saddle)';

% specify objective function
objFctHandle = @rosenbrocksaddle;

% define parameter names, ranges and quantization:
paramDefCell = {
        'parameter1', [0.05 5], 0.001
        'parameter2', [0.08 1], 0.001
   'parameter3', [0.04 1], 0.001
   'parameter4', [0.05 1.4286], 0.001
   'parameter5', [0 100], 0.5
};
% 1. column: parameter names
% 2. column: paramter ranges
% 3. column: paramter quantizations
% 4. column: initial values (optional)

% set initial parameter values in struct objFctParams
objFctParams.parameter1 = 0.414;
objFctParams.parameter2 = 0.35;
objFctParams.parameter3 = 0.414;
objFctParams.parameter4 = 0.414;
objFctParams.parameter5 = 100;

% set single additional function parameter
objFctSettings = 100;

% get default DE parameters
DEParams = getdefaultparams;

% set number of population members (often 10*D is suggested)
DEParams.NP = 50;

% do not use slave process here
DEParams.feedSlaveProc = 0;

% set times
DEParams.maxiter       = 100;
DEParams.maxtime       = 60;  % in seconds
```

```
DEParams.maxclock      = [];

% set display options
DEParams.refreshiter   = 1;
DEParams.refreshtime   = 10;  % in seconds
DEParams.refreshtime2  = 20;  % in seconds
DEParams.refreshtime3  = 40;  % in seconds

% do not send E-mails
emailParams = [];

% set random state in order to always use the same population members here
rand('state', 1);

% start differential evolution
[bestmem, bestval, bestFctParams] = ...
        differentialevolution(DEParams, paramDefCell, objFctHandle, ...
        objFctSettings, objFctParams, emailParams, optimInfo); %#ok

disp(' ');
disp('Best parameter set returned by function differentialevolution:');
disp(bestFctParams);
```